**UNIVERSITÀ DEGLI STUDI**
**DI MODENA E REGGIO EMILIA**

**Dottorato di ricerca in Neuroscienze**
**in convenzione con l'Università degli Studi di Parma**

Ciclo XXXIII

# Unraveling the physiological functions and pathological implications of HSPB3, the most deviating member of the HSPB family.

Candidato: Tatiana Sofia Pinheiro Tiago

Relatore (Tutor): Prof. Serena Carra

Coordinatore del Corso di Dottorato: Prof. Michele Zoli

# Acknowledgements

First, I would like to thank my supervisor Prof. Serena Carra for the precious support, advice and guidance during my PhD, and for sharing with me the exciting project that has been my motivation for the last 3 years. I also thank Prof. Michele Vendruscolo for the opportunity given to me to be able to learn in his lab, and for allowing me to carry on a promising collaborative project giving me all the support necessary.

I also thank enormously all the members of the Carra group who were always there for me and helped in unimageable ways during these 3 years. I specially thank to Federica for all the brainstorming sessions, for all the technical and Italian lessons, and most of all for being a wonderful friend and the best person I could have asked as lab partner; to Arianna for introducing me to the PhD and Italian life and for always being available to help whenever needed, life in Modena is not the same without you here; to Ilaria and Laura for the constant help in the lab and specially "mounting vitrini", I do not know what I would have done without your support. To Francesco and Veronica, thank you so much for all your support during this difficult 2020, you worked so hard this year and yet you did not hesitate even for a second in helping me with all the experiments over these last months, and were always there to support me. The lab would be very dull without your cheerfulness and our long talks. Last, but not least, I thank Dr. Jonathan Vinet (CIGS) for all the support with microscopy work and everyone from the CMD lab who have taught me everything they could, specially Roxine for not letting me get lost in mathematical equations and Swapan for having the patience to teach me over and over again how to purify proteins.

Finally, I express my heartfelt thanks to my family and loving boyfriend Giulio, without whom I would not be who I am. Thank you for always having my back and always encourage me forward.

# Contents

## Table of Figures

## Abstract English

HSPB3 is a small heat shock protein found predominantly in muscle cells. In contrast to other HSPBs, it is not upregulated upon heat-shock and it does not confer thermotolerance. In human myoblasts, HSPB3 is induced upon differentiation under the control of the myogenic regulatory factor MyoD. Yet whether HSPB3 plays a role in myogenic differentiation is unknown. The focus of this thesis was to assess whether HSPB3 participates in myogenic differentiation. Cell cycle exit and commitment to differentiation are regulated at the transcriptional level and require extensive chromatin remodeling. This process is modulated by the downregulation of Lamin B Receptor (LBR) and its detachment from chromatin and the nuclear envelope (NE). Immunofluorescence studies show that HSPB3 is enriched at the NE. This observation prompted the hypothesis that HSPB3 could act at the nuclear level facilitating the chromatin remodeling during muscle differentiation. Expression analysis and study of the subcellular localization of LBR in human myoblasts demonstrated that an interplay exists between HSPB3 and LBR. In particular, HSPB3 levels inversely correlate with LBR. Moreover, we demonstrate that HSPB3 directly interacts with LBR and promotes its detachment from the NE. Although we cannot exclude the possibility that, besides LBR, HSPB3 might also interact with other NE-associated proteins, our data clearly show that HSPB3 influences NE and chromatin remodeling, ultimately promoting the expression of pro-differentiating genes. In agreement, transcriptomic analysis links HSPB3 to changes in the expression of genes involved in extracellular matrix organization and skeletal muscle development. Four mutations in the HSPB3 gene were linked to neuromuscular pathologies. In this thesis we focused on the R116P mutation. R116P was unable to induce the expression of myogenic-specific genes, while including the Unfolded Protein Response. Thus, the R116P mutation may decrease the differentiation capacity and regenerative potential of muscles.

HSPB3 expression has also been detected in neuronal populations, but no physiological role has been identified so far. Of the best characterized function of HSPBs is the chaperone activity and prevention of irreversible aggregation. *In vitro* studies aimed at characterizing the chaperone activity of HSPB3 have demonstrated its ability to inhibit α-synuclein aggregation. In particular, the interaction between α-synuclein and lipid surfaces has been shown to trigger its conversion from a soluble state into the aggregated stated, associated to the development of Parkinson's disease. Of note, several HSPBs have been shown to interact with lipids but this function has not yet been linked to their anti-aggregation functions. The work presented in the first chapter indicates that HSPB3 affects LBR insertion into the NE opening the possibility that HSPB3 might interfere with protein-lipid binding. In the second chapter of this thesis, we sought to investigate whether HSPB3, and other better characterized HSPBs (HSPB5, HSPB6, HSPB7 and HSPB8) affect α-synuclein interaction with lipids and aggregation. Using a three-pronged approach developed in the laboratory of Prof. M. Vendruscolo, we find that all HSPBs studied have an impact on α-synuclein lipid-induced aggregation, elongation, and secondary nucleation. More specifically, HSPBs could bind α-synuclein in its monomeric, oligomeric and fibrillar forms, as well as to the lipid membranes themselves.

In summary, our findings pave the way for a better understanding of HSPB3 implication in the physiology and pathology of the neuromuscular system.

## Abstract Italiano

HSPB3 è una proteina da shock termico che si trova prevalentemente nelle cellule muscolari. A differenza di altre HSPB, HSPB3 non è sovraregolata in caso di shock termico e non conferisce termotolleranza. Nei mioblasti umani, HSPB3 è indotta al momento del differenziamento sotto il controllo del fattore regolatore miogenico MyoD. Tuttavia, non è noto se HSPB3 abbia un ruolo nel differenziamento miogenico, scopo di questa tesi. L'uscita dal ciclo cellulare e l'inizio del differenziamento sono regolati a livello trascrizionale e richiedono un rimodellamento della cromatina. Questo processo è modulato dalla sottoregolazione del recettore della lamina B (LBR) e dal suo distacco dalla cromatina e dall'involucro nucleare. Studi di immunofluorescenza mostrano un arricchimento di HSPB3 a livello dell'involucro nucleare. Questa osservazione ha suggerito l'ipotesi che HSPB3 possa agire a livello nucleare facilitando il rimodellamento della cromatina. L'analisi dell'espressione e lo studio della localizzazione subcellulare di LBR nei mioblasti dimostrano che esiste una connessione tra HSPB3 e LBR. In particolare, i livelli di mRNA di HSPB3 sono inversamente correlati a quelli di LBR. Inoltre, HSPB3 interagisce direttamente con LBR e promuove il suo distacco dall'involucro nucleare. Sebbene non possiamo escludere la possibilità che, oltre a LBR, HSPB3 possa anche interagire con altre proteine associate all'involucro nucleare, i nostri dati dimostrano che HSPB3 agisce su di esso e sul rimodellamento della cromatina, promuovendo l'espressione di geni specifici per il differenziamento. In accordo, l'analisi trascrittomica collega l'espressione di HSPB3 con cambiamenti nell'espressione dei geni coinvolti nell'organizzazione della matrice extracellulare e nello sviluppo del muscolo scheletrico. In questa tesi abbiamo poi studiato uno dei 4 mutanti nel gene HSPB3 associati a malattie neuromuscolari: R116P.- L'analisi trascrittomica su cellule esprimenti il mutante R116P dimostra una perdita di funzione sull'attivazione dei geni miogenici. Questi risultati suggeriscono che la mutazione R116P potrebbe diminuire la capacità di HSPB3 di indurre differenziamento e il potenziale rigenerativo dei muscoli.

HSPB3 è anche esspressa in popolazioni neuronali, ma finora non è stato identificato alcun ruolo fisiologico. Una delle funzioni delle HSPB è rappresentata dall'attività di chaperone e dalla prevenzione dell'aggregazione irreversibile. Studi *in vitro* volti a caratterizzare l'attività di chaperon di HSPB3 hanno dimostrato la sua capacità di inibire l'aggregazione dell'α-sinucleina, la cui aggregazione è associata alla malattia di Parkinson. In particolare, α-sinucleina interagisce con le superfici lipidiche e ciò innesca la sua conversione da uno stato solubile a uno stato aggregato. Nel primo capitolo di questo lavoro è stato dimostrato che HSPB3 influenza l'inserimento di LBR nel NE, aprendo la possibilità che HSPB3 possa interferire con il legame proteina-lipide. Nel secondo capitolo, abbiamo cercato di indagare se HSPB3 e altre HSPB meglio caratterizzate (HSPB5-B8) influenzano l'aggregazione di α-sinucleina e la sua interazione coi lipidi. Utilizzando un metodo sviluppato nel laboratorio del Prof. M. Vendruscolo, abbiamo dimostrato che tutti le HSPB studiate diminuiscono l'aggregazione di α-sinucleina indotta dai lipidi, il prolungamento e la nucleazione secondaria. Più specificamente, le HSPB legano α-sinucleina nelle sue forme monomerica, oligomerica, fibrillare, nonché associata alle membrane lipidiche stesse. In sintesi, i nostri risultati aprono la strada a una migliore comprensione dell'implicazione di HSPB3 nella fisiologia e patologia del sistema neuromuscolare.

# Introduction

## Heat Shock Proteins

Heat Shock Proteins (HSPs) belong to the superfamily of molecular chaperones, proteins that are essential for life and are involved in the regulation of the cellular stress response, cell survival and development. HSPs were first described as proteins involved in thermotolerance upon heat-shock, whose expression levels were strongly induced upon heat shock, hence the name (Ritossa, 1962). Following studies demonstrated that the expression of HSPs can be regulated by several insults including cold, hypoxia, oxidative stress, all conditions where HSP upregulation can provide protection against cytotoxicity (Ghosh et al., 2018). HSPs are classified into six major families based on their molecular weight: Hsp100/HSPH (100-110 kDa), Hsp90/HSPC (83-90 kDa), Hsp70/HSPA (66-78 kDa), Hsp60/HSPD (60 kDa), Hsp40/DNAJ (40 kDa) and small heat shock proteins (HSPBs)/HSPB (12-43 kDa). While some HSPs are constitutively expressed, others are induced upon stress and both constitutive and inducible members have been identified within the same family of molecular chaperones. For example, the 70 kDa group consists of the stress-inducible Hsp70s (e.g. HSPA1A, HSPA6) and the constitutively expressed heat shock cognate 70 (Hsc70) (Hartl and Hayer-Hartl 2002). Similarly, the 90-kDa group consists of two major isoforms, namely the inducible Hsp90α and the constitutively expressed Hsp90β (Sreedhar et al., 2004). Nevertheless, even the constitutive HSPs that are inherently transcribed can have their expression further induced upon stress. The transcription factors that regulate the expression of HSPs are known as Heat Shock Factors (HSFs) and the overall response is referred to as the heat shock response (HSR) (Morimoto, 1993).

HSPs are present in all kingdoms of life, from archaea to bacteria to eukarya and HSPs were initially named according to their molecular mass (Tavaria et al, 1996). As more proteins of the HSP family were uncovered in different species, several HSPs had the same molecular mass and, thus, the same name in different species, yet they were not necessarily sharing the same functions. For example, Drosophila melanogaster HSP22 is a mitochondrial small HSP that is different from human HSP22 (HSPB8), which is localized mainly in the cytoplasm (Morrow and Tanguay, 2015; Sun et al., 2003). Therefore, to avoid misunderstandings, a new nomenclature was drawn based on the systematic gene symbols that have been proposed by the HUGO Gene nomenclature Committee (HGNC). This nomenclature was then used as the primary identifier in databases such as Entrez Gene and

Ensemble (Kampinga et al, 2009). Nevertheless, the scientific literature still makes use of both nomenclatures, although scientists in the field often specify both names for a given HSP (e.g. alpha-B crystallin or HSPB5). Henceforth, for simplification all chaperones will be referred to by their new nomenclature.

The best characterized function of the HSPs is their role as molecular chaperones. Molecular chaperones assist the correct folding and assembly of other proteins, without being part of the final folded structure. Molecular chaperones are able to recognize the hydrophobic regions of misfolded or unfolded proteins. These hydrophobic regions are highly unstable in a hydrophilic cellular environment. Consequently, these regions are usually not accessible in properly folded proteins since they are buried in the "core" of the protein (Hartl and Hayer-Hartl 2002). In addition, molecular chaperones cooperate with degradative systems, such as the ubiquitin-proteasome system (UPS) and autophagy, to promote the clearance of damaged proteins or proteins that are no longer useful for the cells. The HSPs together with the degradative systems compose the so called "Protein Quality Control System" (PQC), which maintains protein homeostasis (or proteostasis) and is the primary defence of the cells against protein aggregation and related toxicity (Hartl et al., 2011). Proteostasis refers to the maintenance of the equilibrium between protein synthesis, folding and degradation and it is essential for life (Baltch et al., 2008; Klaips et al., 2017). It is thus not surprising that loss of a stable proteome has been linked to aging and to the development of neurodegenerative and neuromuscular disorders that are often referred to as protein conformational disorders or misfolding disorders (Stenoien et al. 1999; Cummings and Zoghbi 2000; Jana et al. 2000; Cummings et al. 2001; Sittler et al. 2001; Bailey et al. 2002; Chavez Zobel et al. 2003; Carra et al. 2005).

Molecular chaperones are able to switch between two conformational states, characterized by low or high affinity for misfolded substrates. The switch between the two states allows cycles of binding and release of the substrates, providing repeated opportunities for renaturation or degradation of the substrates. Based on the mechanisms that regulate the conformational changes of chaperones and their activity, we define two main families: ATP-dependent and ATP-independent molecular chaperones. For ATP-dependent HSPs (e.g. HSP70, HSP90, HSP100), the switch between the two states is regulated by the hydrolysis of ATP (Hartl and Hayer-Hartl 2002; Hessling et al., 2009). For small HSPs, which are ATP-independent, changes in the conformation of the proteins, changes in their oligomerization state and post-translational modifications have been proposed to play an important role in client binding (see "HSPB client interaction" for a detailed description).

By ensuring the correct folding of a large variety of proteins (referred to as substrates or clients), molecular chaperones are implicated in many cellular processes such as cellular differentiation, regulation of cell cycle, cell resistance to stress and modulation of apoptosis (Walsh et al., 1997; DeGeer et al., 2015; Li et al., 2015; Luo et al., 2006). By conferring stress resistance to cells and ensuring cell functionality, HSPs can prevent or delay the appearance of protein aggregates and may therefore be protective in protein misfolding diseases; however, dysregulated expression of HSPs can prevent cell death and apoptosis, ultimately promoting the development of diseases such as cancer. Oncoproteins in cancer cells are often misfolded and require augmented chaperone activity for correction, hence tumour cells are more chaperone-dependent than normal cells for proliferation and survival (Chatterjee and Burns, 2017). Therefore, tight control in the regulation of these proteins is required to ensure that there are no imbalances, which may contribute to cellular dysfunctions and consequent pathology.

## Small Heat Shock Proteins

Small heat shock proteins (HSPBs) are part of the superfamily of molecular chaperones and are present in all kingdoms of life; yet they are poorly conserved, and their functions are still largely unknown (Carra et al., 2019). In mammals, there are 10 genes encoding for HSPBs, named HSPB1-HSPB10 according to the new nomenclature. While some HSPBs are ubiquitously expressed, such as HSPB1 and HSPB5, others have restrictive expression, such as HSPB2 and HSPB3, which are predominantly expressed in the muscle system, or HSPB9 and HSPB10, which are only found in the testis (Table 1) (Janoswka et al., 2019).

| HSPB | Other names | Tissue distribution | Disease | Mutation |
|---|---|---|---|---|
| HSPB1 | Hsp27 | Ubiquitous | CMT2/ dHMN | P7S, P7R, G34R, P39L, E41K, G43D, L58fs*105, A61fs*100, G84R, L99M, R127W, R127L, Q128R, S135F, S135C, S135Y, R136W, R136L, R140G, K141Q, T151I, S158fs*200, T164A, Q175X, T180I, P182A, P182L, P182S, S187L, R188W |
| HSPB2 | MKBP | Cardiac and skeletal muscle | | NA |
| HSPB3 | HSPL27 | Cardiac and skeletal muscle, brain | CMT2/ dHMN<br>myopathy | R7S, Y118H<br>R116P, A33AfsX50 |
| HSPB4 | αA-crystallin | Eye lens | Cataract | W9X, R12C, R21Q, R21W, R49C, R54C, G98R, R116C, R116H |
| HSPB5 | αB-crystallin | Ubiquitous | CMD<br>MFM<br>Cataract | R157H, G154S<br>R120G, Q151X, S21A, D109H, 464delCT<br>P20S, 450delA, R56W, D140N |
| HSPB6 | Hsp20, p20 | Ubiquitous | | NA |
| HSPB7 | cvHsp | Cardiac and skeletal muscle | | NA |
| HSPB8 | Hsp22 | Ubiquitous | CMT2/ dHMN<br>myopathy | P90L, N138T, K141N, K141M, K141E, K141T<br>P173SFS*43, T194Sfs*23 |
| HSPB9 | CT51 | Testis | | NA |
| HSPB10 | ODF1 | Testis | | NA |

Table 1 Human HSPB tissue expression and motor neuropathy-associated mutations (Janoswka et al., 2019; Evgrafov et al., 2004; Irobi et al., 2004; Kolb et al., 2010; Morelli et al., 2017; Nam et al., 2018; Vicart et al., 1998; Shroff et al., 2000; Al-Tahan et al., 2019; Vendredy, Adriaenssens and Timmerman, 2020; Nicolaua et al., 2020). CMT2 – Charcot-Marie-Tooth type 2; dHMN – distal hereditary motor neuropathy; CMD – cardiomyopathy; MFM – myofibrillar myopathy.

## HSPB structure

From a structural point of view, HSPBs are characterized by their low molecular weight, ranging from 12-43 kDa, and by their ability to interact with themselves and other members of the HSPB family forming higher molecular weight assemblies (homo or hetero-oligomers) (Carra et al., 2019). All small HSPs are characterized by the presence of a highly-conserved alpha-crystallin domain (ACD) of 80-100 amino acids, flanked by less conserved N-terminal and C-terminal domains (Sudnitsyna et

al., 2012). The ACD is the only natively folded region, forming an IgG like β-sandwich structure (Rajagopal et al., 2015) and represents the signature of these proteins (Figure 1).


Figure 1 Representation of one member of the alpha-crystallin domain (PDB ID 2N0K) (Rajagopal et al., 2015). The six strands of the β-sandwich structure are labelled using previously defined nomenclature for ACD structures. The dimer is formed by antiparallel arrangement of the β6+7 strands at the interface.

The C-terminal is the less conserved domain in the HSPB structure; it is enriched in polar and charged residues and is highly disordered (Janowska et al., 2019). In many HSPBs, the C-terminal contains a three-residue motif known as "I/V-X-I/V" (i.e., isoleucine or valine, followed by any amino acid - usually a proline- followed by isoleucine or valine), which is involved in the interactions for oligomerization. An exception is represented by HSPB3, which contains the "I/V-X-I/V" motif in its N-terminal domain (Clark et al. 2018). The N-terminus is enriched in hydrophobic residues, is disordered, and often contains multiple phosphorylation sites (Kriehuber et al. 2010; Mymrikov et al., 2011). Although the N-terminal domain is poorly conserved, it contains a core motif (RLFDQxFG) conserved in all human HSPBs (Figure 2). Nevertheless, the function of this motif remains unclear (Shatov et al., 2018).

Even though HSPBs' primary structure is simple, their quaternary structure is highly complex due to the propensity of these proteins to form homo- and hetero-oligomers that range from dimers to 40-mers (van Montfort et al. 2001). This complexity is further enhanced by the fact that there is no rule in the ability of these HSPBs to form high molecular weight assemblies/oligomers. In fact, HSPB1, HSPB4 and HSPB5 primarily tend to form large oligomers, while other HSPBs such as e.g. HSPB6-8 predominantly form dimers. As both homo- and hetero-typic oligomers and dimers can be formed, a large variety of HSPB complexes exist.

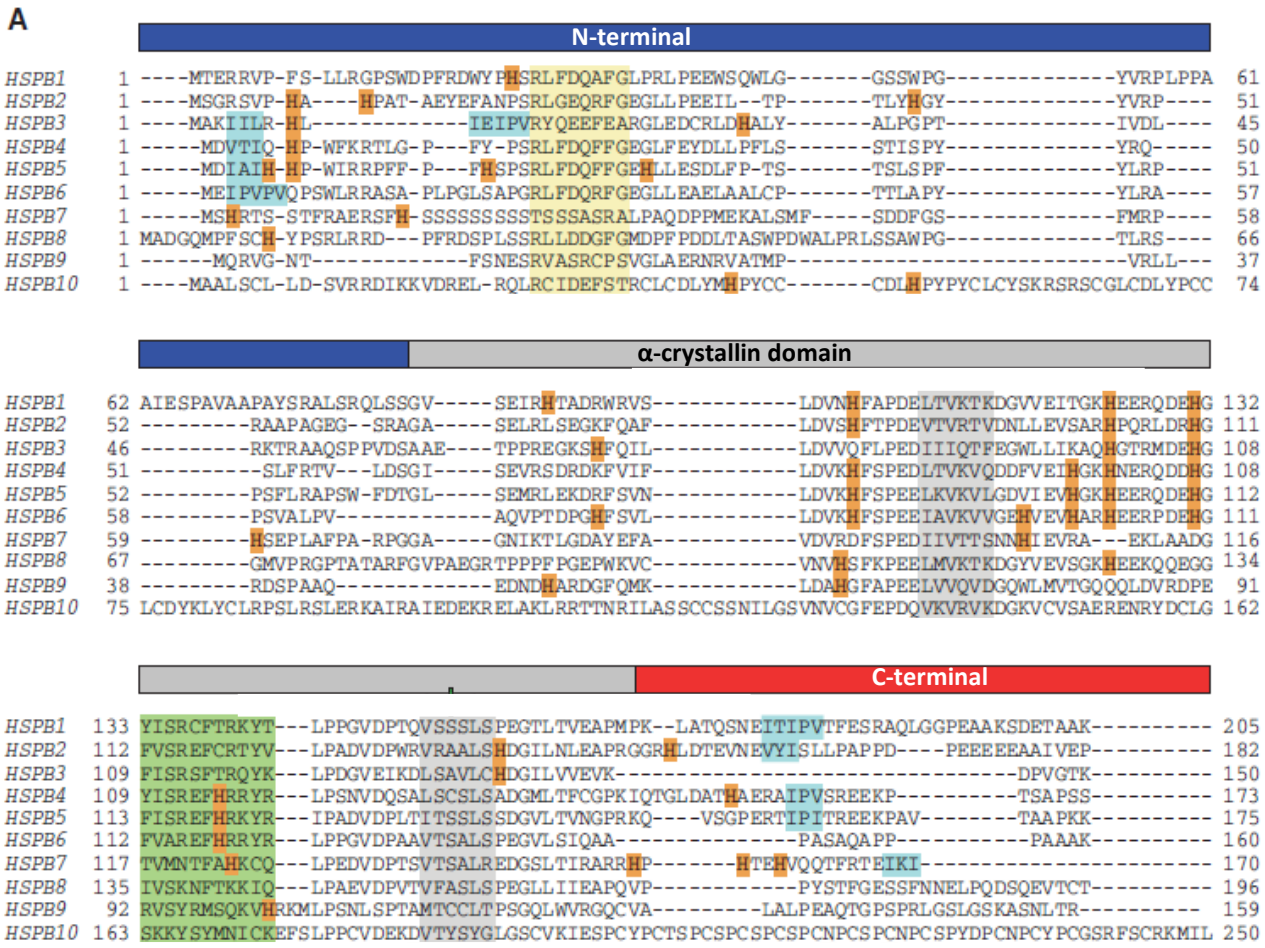


Figure 2 Sequence alignment of the 10 human HSPBs (adapted from Janowska et al., 2019). Important sequence elements are highlighted in different colours: the conserved N-terminal sequence (yellow), the β4 and β8 strands that compose the groove (grey), the β6 + 7 strand that make the dimer interface (green), and amino and carboxy-terminal I/V-X-I/V motifs (blue). Histidine residues are highlighted in orange.

Furthermore, HSPBs possess intrinsically disordered regions (IDR), which confer these proteins a lack of a defined three-dimensional structure in their native state (Sudnitsyna et al., 2012; Babu 2016). The lack of a defined structure allows HSPBs to adopt different conformational states when interfacing with different substrates, therefore permitting the interaction with a large variety of substrates. The presence of disordered domains and their dynamic oligomerization confer flexibility to HSPB structure; this flexibility is further influenced by HSPBs' post-translational modifications such as phosphorylation. Together these features enable HSPBs to bind to a large variety of substrates, thus playing, with yet unknown molecular mechanisms, a wide variety of functions (Carra and Landry, 2006). Based on these features, HSPBs are considered as reservoir of the cellular chaperone power that can very rapidly bind to different types of substrates upon acute stress, representing the first line of defence to avoid irreversible protein aggregation.

## HSPB client interaction

The mechanisms by which HSPBs recognize clients and mediate interactions are not completely understood. This is challenged by the fact that HSPB structure is highly dynamic and can differently adapt based on the substrates.

The heterodimers in HSPBs are usually formed by the docking of the "I/V-X-I/V" motif of one HSPB in the β4/β8 groove in the ACD of the other HSPB (Slingsby and Clark, 2016). HSPB subunits stay dynamic in HSPB/client complexes and fluctuate between bound and dissociated states. The association/dissociation cycle correlates to the dynamic assembly of HSPBs into oligomers of variable size. The oligomeric state of HSPBs/client complexes and the rate at which subunits exchange in and out of oligomers also influence chaperone activity, but there is no consensus on the role of these factors. The specific effect is likely dependent on the HSPBs/client pair studied and the conditions under which chaperone activity is assessed (Peschek et al.2013; Jovcevski et al. 2015). For example, HSPB5 interacts with clients primarily via weak, transient interactions. However, the pH-mimicking mutant H104K-HSPB5 shows enhanced chaperone activity toward destabilized α-lactalbumin, through its ability to disassemble into smaller species with a higher affinity to the client (Rajagogal et al., 2015). Furthermore, the presence of the "I/V-X-I/V"-like motifs in putative clients, such as α-synuclein, would suggest competition between HSPB subunits and clients for binding to the grooves (Liu et al.2018; Baughman et al.2018). Accordingly, HSPB5 ACD has enhanced chaperone activity relative to full-length HSPB5 toward the clients α-synuclein and tau, leading to the proposal that the C- or N-terminal domains may inhibit chaperone activity of the ACD (Liu et al. 2018). Yet, using solid state NMR, HSPB5 was shown to bind through its N-terminal to lysozyme, which forms amorphous aggregates. Deletion of this N-terminal domain abolished HSPB5 chaperone activity toward this client (Mainz et al., 2015).

Another aspect that is considered to be involved in the HSPB/client interaction is the phosphorylation status, where the N-terminal would play a critical role being the domain where phosphorylation occurs. For example, phosphorylation of HSPB6 within its intrinsically disordered N-terminal domain leads to direct contact with the universal signalling hub 14-3-3, ultimately triggering smooth muscle relaxation (Sluchanko et al. 2017). Conversely, phosphorylation of HSPB1 leads to a significant decrease of the oligomeric size, partially inhibiting its chaperone activity,

suppressing thermal denaturation and facilitating refolding of citrate synthase *in vitro* (Rogalla et al.,1999).

Together these findings indicate that both the N-Terminal domain and ACD are involved in client recognition and chaperone activity, with varying roles that depend on the client protein and on the HSPB. To date the C-terminal domain has not been shown to directly interact with any client protein, but its roles in oligomerization and subunit exchange likely contribute to HSPBs' chaperone activity (Janowska et al., 2019). Thus, the precise details of how a given HSPB might affect a client's activity is a complicated and interconnected process to which all these factors contribute: oligomerization and subunit exchange dynamics, binding site accessibility, affinity for client protein, HSPB post-translational modifications, and concerning the client itself, mechanism of aggregation and nature of the client species formed along the pathway.

## HSPB function

From the functional point of view, HSPBs have been implicated in a large variety of processes, ranging from the response and adaptation to cell stress, thermotolerance, cell movement, cell differentiation and development, as well as cell apoptosis (Lavoie et al, 1993; Perng et al, 1999; Wang and Spector 1996; Mounier and Arrigo, 2002; Arrigo et al. 2007; Bryantsev et al, 2007; Kamradt et al. 2001; Sui et al., 2009; Andrieu et al., 2010; Kanagasabai et al., 2010; Bruinsma et al., 2011; Almeida-Souza et al, 2011; Clemen et al, 2013). These different activities are all linked to the flexibility of HSPB structures, which as previously mentioned confer them different affinities for a wide range of proteins. The two best characterized functions of HSPBs are the chaperone-like activity to prevent irreversible aggregation, and the modulation of the structure and dynamics of the cytoskeleton (Carra and Landry, 2006). Other HSPB functions that have been investigated are the anti-apoptotic activity and the role in muscle development and maintenance (Janowska et al., 2019). Here, the key principles of these functions are briefly summarized.

### *Chaperone-like activity*

One of the core functions of HSPBs is their chaperone-like activity (Jakob et al., 1993). HSPBs were originally termed "holdases" due to their role in capturing unfolded or misfolded proteins preventing them from irreversible aggregation (Haslbeck et al., 1999; Ungelenk et al., 2016). HSPBs protect substrates from uncontrolled aggregation, but do not possess enzymatic function and are not able to refold clients; which is due to HSPBs lack of ATP hydrolysis (De Jong, 1993). For client refolding, HSPB rely on the collaboration with other ATP-driven chaperones, such as HSPAs (Mogk and Bukau, 2017). Similar to the refolding, also the release of non-native proteins from HSPBs/client complexes does not occur spontaneously. Experimental studies demonstrated that the release of the substrate from HSPBs occurs via the transfer of the client (that is hold by the HSPBs) to the HSPA machinery; this step is regulated by ATP-dependent chaperones and co-factors (Bryantsev et al, 2007). Thus, HSPB reversibly sequester unfolded/misfolded substrates into a state that is competent for further refolding or for targeting to degradation, in assistance with other chaperones and co-chaperones. It is thought that the reversible sequestration of misfolded substrates by HSPBs serves as a protective strategy to enhance cellular fitness during stress (De Los Rios and Goloubinoff 2016; Vos et al. 2008). The aggregates of non-native proteins formed in the presence of HSPBs differ in size, composition and architecture from those formed in their absence. The altered architecture avoids the exposure of hydrophobic surfaces to other cellular components and protects the substrates from proteases. By binding to a large variety of substrates and thereby facilitating the disaggregation and folding executed by ATP-dependent chaperones, HSPBs act as the first line of defence for the maintenance of the cellular proteostasis (Haslbeck and Vierling, 2015).

However, in recent years HSPBs have been found as part of protein inclusions themselves, where they seem to act to facilitate disaggregation (Muchowski and Wacker, 2005; Vleminckx et al., 2002; Seidel et al., 2012). Based on these data, it has been proposed that HSPBs do not act only as "holdases", but would also actively regulate the aggregation process, avoiding the formation of irreversible, potentially toxic aggregates (Carra et al., 2019). Indeed, *in vitro* studies of HSPBs such as HSPB1, HSPB6, HSPB8 and HSPB2/HSPB3 have been shown to inhibit protein aggregation of model substrate proteins such as citrate synthase, in the absence of HSPA (Carra et al., 2005; Binger et al., 2013). These data suggest that HSPBs may play an active role in aggregation prevention. The chaperone activity towards misfolded proteins has been further demonstrated over the last years,

where several HSPBs, namely HSPB1-HSPB6 and HSPB8, have been shown to modulate α-synuclein aggregation, involved in Parkinson's disease, and reduce its mediated-toxicity *in vitro*, in neuronal cell and in Drosophila models (Horwitz 1992; Rekas et al., 2004; Tue et al., 2012; Bruinsma et al., 2011; Cox et al., 2017). Yet, although their protective effect was mainly attributed to the ability of the HSPBs to transiently and weakly bind to α-synuclein, their exact mechanism of action is not yet fully understood.

### *Cytoskeleton stabilization*

Another well-characterized function of HSPBs is their ability to interact and modulate the structure and dynamics of the cytoskeleton (Mounier and Arrigo, 2002). The cytoskeleton is a dynamic structure composed of an interconnected network of three major filament systems: microfilaments (MFs), microtubules (MTs) and intermediate filaments (IFs) (Fuchs and Weber, 1994; Lazarides, 1980; Steinert , Steven and Roop, 1985). When exposed to stress, cells respond by drastically modifying their cytoskeletal network; for instance, the MTs are disassembled, MFs collapse and actin microfilaments lose their organization (Arrigo et al. 2007). Concomitantly, upon proteotoxic stress cells rapidly induce the expression of selective HSPBs, such as HSPB1, HSPB5 and HSPB6, which interact with intermediate filaments and actin microfilaments sustaining their stability and assembly/disassembly (Lavoie et al, 1993; Perng et al, 1999). In particular, HSPB1 acts as an inhibitor of actin polymerization by being able to cap the plus end of actin filaments, thus preventing the fixation of a new actin monomer, and consequently stabilizing the fibres and preventing their aggregation (Miron et al., 1991, Miron et al., 1988). Albeit to a lesser extent, HSPB5 appears to show similar properties. HSPB5 inhibits actin fibre depolymerization and prevents their aggregation induced by stress (Singh et al., 2007). Furthermore, during the formation of the microtubule network, HSPB1 binds to MT and enhances their stability and maturation; upon MTs stabilization, HSPB1 is released (Wang and Spector 1996). HSPB5 and HSPB1 were also shown to colocalize with the IF protein GFAP (glial fibrillary acidic protein), strengthening the hypothesis that HSPBs play a role during IF assembly, as well as in the control of cytoskeleton interactions (Perng et al., 1999).

The most relevant observations confirming the importance of HSPBs and cytoskeleton interactions, probably come from the phenotypic description of cells expressing HSPB mutants and which are characterized by altered cytoskeletal stability (Vicart et al., 1998; Almeida-Souza et al, 2011; Clemen

et al, 2013; Dimauro et al., 2017). Aggregation of cytoskeletal elements has been suggested to play an important role in neurodegenerative and muscular diseases. For example, mutations of desmin, a protein that regulates sarcomere architecture in muscle cells (Hein et al, 2000) have been linked to myofibrillar myopathy (Goebel, 1995). HSPB5 interacts with desmin and stabilizes it, decreasing its aggregation propensity. Interestingly, mutated R120G-HSPB5 is also associated with myofibrillar myopathy (Vicart et al., 1998). Conversely to the WT protein, the mutated form shows increased affinity for desmin, causing aberrant desmin aggregation; this, in turn, alters sarcomere structure and is thought to contribute to myofibrillar myopathy (Clemen et al, 2013). Thus, there are probably two mechanisms by which the R120G-HSPB5 mutation causes myofibrillar myopathy: 1) a loss of chaperone function of HSPB5 at the level of neurofilament network assembly (HSPB5 directly interacts with desmin); 2) a toxic gain of function of mutated R120G-HSPB5 (the accumulation of large amounts of aggregated HSPB5 in muscle cells contributes to the disease due to the inherent toxicity of the aggregate) (Dimauro et al., 2017). Furthermore, mutant forms of HSPB1 linked to Charcot-Marie-Tooth disease (for details see "Distal Hereditary Motor Neuropathies and myopathies" for detailed description) bind more strongly to MTs, promoting their hyper-stabilization; consequently, this leads to altered microtubule dynamism. In addition, HSPB1 mutants remain bound to mature MTs, rather than being released after their maturation, which is also thought to contribute to increase neuronal vulnerability and disease (Almeida-Souza et al, 2011).

As a consequence of their role as stabilizing agents of the cytoskeleton, HSPBs participate indirectly in the regulation of complex processes such as the response and adaptation to cell stress, thermotolerance, cell differentiation and development, cell movement and cell apoptosis, which are characterized by profound rearrangements and breakage of the cytoskeleton (Lavoie et al. 1993; Perng et al. 1999; Arrigo 2000; Kamradt et al. 2002; Clemen et al, 2013; Haslbeck et al. 2016; Litt et al. 1998; Nicholl and Quinlan 1994; Parcellier et al. 2006; Park et al. 2016; Qian et al. 2009; Quinlan and Van Den Ijssel 1999; Takayama et al. 2003; Tanguay and Hightower 2015; Webster 2003). Thus, at least in part due to dysfunction at the level of the stabilization of the cytoskeleton, malfunction of HSPBs, due to genetic mutations or improper expression, can have adverse effects in a number of diseases and are the cause of a wide range of pathologies including cardiomyopathy, myofibrillar myopathy, motor neuron diseases, and cataracts (Vicart et al. 1998; Perng et al. 1999; Evgrafov et al. 2004; Irobi et al. 2004; Kolb et al. 2010). Indeed, the histopathological aggregates that typify such diseases often contain both intermediate filaments and HSPBs (Toivola et al. 2010). Since HSPBs,

like intermediate filaments, are stress responsive, it has been proposed that they act as evolutionary capacitors that cooperate with the intermediate filament cytoskeleton to act as a transcellular network that not only partitions efficiently the intracellular space of individual cells, but also integrates the individual cell into the context of the tissue, with far more complex implications in (cardiac and muscle) tissue maintenance/function (Carra et al., 2017).

### *HSPB and their potential function in muscle differentiation, development, and function*

An emerging area of investigation is the role for HSPBs in muscle development and maintenance (for details see "Myogenesis – Section I"), which has been suggested to occur through the regulation of cytoskeleton stability, cell migration and cell cycle regulation (Golenhofen et al., 2002; During et al., 2007; Lee et al., 2007; Clemen et al, 2013). Muscles have a complex cytoskeletal system, which is fundamental for their contraction, and are subject to high oxidative stress conditions in their normal working modes; leading to destabilization and misfolding of important cytoskeletal proteins (Arndt et al., 2010). So, given their role in the stabilization of the cytoskeleton and as molecular chaperones that prevent irreversible protein aggregation and assist misfolded proteins clearance, it is perhaps not surprising that many HSPBs are expressed at high levels in different types of muscle tissues. Indeed, cardiac and skeletal muscle cells express the largest variety of HSPBs: HSPB1, HSPB2, HSPB3, HSPB5, HSPB6, HSPB7, and HSPB8 (Beall et al. 1997; Sugiyama et al. 2000; Kappé et al. 2001; Dubińska-Magiera et al., 2014). Recent evidence suggests that HSPBs contribute to the proteostasis of sarcomeres, the fundamental unit of myocyte contraction that consists of thick and thin filaments bordered by two Z-disks. The sarcomeric Z-disk components titin and the actin-binding protein filamin C (FLNC) undergo repeated cycles of folding-unfolding during muscle contraction and are particularly sensitive to protein misfolding and aggregation upon mechanical stress (Carlisle et al., 2017; Collier et al., 2019; Juo et al., 2016; Kotter et al., 2014). HSPB1, HSPB5 and HSPB7 directly bind to titin and FLNC, preventing their aggregation and providing skeletal and cardiac muscle protection (Kotter et al., 2014; Mercer et al., 2018). Conversely, loss of HSPB7 leads to FLNC aggregation and skeletal muscle degeneration (Juo et al., 2016). In addition, the HSPB8-BAG3-HSP70 (or CASA) complex facilitates the autophagy-mediated degradation of FLNC, thus maintaining Z-disk integrity (Arndt et al., 2010). Impairment of the CASA complex in flies and mice leads to muscle weakness accompanied by a rapid deterioration of cytoskeleton architecture under mechanical strain (Ardnt

et al., 2010). Together these data suggest that HSPB1, HSPB5, HSPB7 and HSPB8 are mechanoresponsive chaperones that play housekeeping and redundant roles aimed at maintaining a proper mechanical stress response, which is fundamental for muscle functionality and viability.

Alternatively, but not mutually exclusive, HSPBs may exert specific yet unidentified functions that are required for muscle cell development and maintenance. Expression levels of HSPB7, HSPB5, HSPB3 and HSPB2 increase upon myogenic differentiation; instead, HSPB6 levels slightly decrease while HSPB1 levels are maintained throughout the differentiation process (Sugyama et al., 2000; Mercer et al., 2018). Analysis of the promoters of several HSPBs have identified the presence of binding regions specific for myogenic transcription factors. For example, HSPB2 and HSPB3 are specifically induced during myogenesis via the muscle regulatory factor MyoD (Sugiyama et al., 2000) (see also this thesis). Similarly, the promoter region of HSPB5 contains potential binding sites for MyoD, as well as other muscle-specific factors such as myogenin, Myf-5, and MRF4 in the muscle-preferred enhancer region (Dubin et al., 1991). Whether specific HSPBs are required for proper muscle cell differentiation is unclear. However, the implication of specialized chaperone machineries in the muscle differentiation program was previously described in several organisms. (Sala et al., 2017). For example, in C. elegans, the myogenic transcription factor HLH-1 (MYOD) induces the expression of muscle-specific chaperones, including HSPC and the small heat shock protein hsp-12.2, which are required to maintain the folding and assembly of muscle-specific proteins; conversely, reducing the expression of these muscle-specific chaperones impairs myogenesis and muscle development, with important implications for muscle disease (Bar-Lavan et al., 2016). Upon differentiation, murine myoblasts switch the expression of the chaperone HSPC2 and the co-chaperone p23 with HSPC3 and Aarsd1L, respectively; the formation of this HSPC2/ Aarsd1L specialized chaperone machinery, in turn, promotes myotube formation (Echeverria et al., 2016). Recently, HSPB1 was shown to take part in regulation of craniofacial muscle development in zebrafish. HSPB1 depletion influenced the optimal growth of craniofacial myocytes rather than determination or proliferation of myogenic precursors (Middleton and Shelden, 2013). Thus, the reason why some of these proteins are specifically upregulated during myogenesis is still enigmatic. Yet, a recent transcriptomic analysis revealed HSPB3 as one of the top genes that might serve as differentiation marker (Ghosh and Som, 2020), highlighting the need to better study the functional significance of HSPB upregulation during cell differentiation, especially in neurons and muscle cells. Mechanistically, the chaperones may regulate the folding and stability of highly specialized

substrates that are required for the differentiation process; alternatively, HSPB function in the apoptotic cascade may have functional consequences for muscle cell differentiation. In fact, an interplay between HSPBs and apoptosis and between apoptosis and cell differentiation exists. In particular, the process of cell differentiation requires the activation of cell-death associated caspases, whose activation needs to be tightly controlled to avoid excessive apoptosis, which would lead to tissue degeneration and improper tissue development. HSPBs have been suggested to participate to differentiation of muscle cells at least in part, by acting at the level of the apoptotic process (for details see "Anti-apoptotic activity") (Bakthisaran et al., 2015; Kamradt et al., 2002). For example, HSPB5 induces resistance to differentiation-induced apoptosis in C2C12 myoblasts at the early stages of differentiation (Kamradt et al., 2002). This regulation of differentiation-induced apoptosis is due to the inhibition of the proteolytic activation of caspase-3. In addition, HSPB5 was shown to participate in the maintenance of the antioxidant glutathione (GSH) levels, and consequently modulate oxidative stress. Mice models carrying the R120G-HSPB5 mutation develop cardiomyopathy due to oxido-reductive stress and consequent protein aggregation (Rajasekaran et al., 2007). Furthermore, Escobedo et al. (2004) showed that HSPB1 protects skeletal muscle cells from reactive oxygen species (ROS)-induced damage by increasing the GSH level and suggested that HSPB1 protects skeletal myoblasts against oxidative stress and may play a key role in regulating the GSH system and resistance to ROS in skeletal muscle cells. As previously mentioned, HSPB1, HSPB5, HSPB7 and HSPB8 play an important role in Z disks maintenance by acting on proteostasis of sarcomeres (read "Distal Hereditary Motor Neuropathies and myopathies" for information on Z disks role in muscle) as part of the CASA complex, mediating the degradation of large cytoskeleton components damaged during contraction (Ulbricht et al., 2015). However, confining the ability of HSPBs to regulate differentiation via their anti-apoptotic activity may be too simplistic and most likely, the various HSPBs take part in this process with distinct mechanisms, acting on different cellular targets. This idea is suggested by the finding that HSPB8 promotes neuronal differentiation by enhancing phosphorylation of Akt. Intriguingly, a truncated form of HSPB8 comprising its ACD was sufficient to maintain the neuronal differentiation promotion, opening the possibility that this function might be shared by other HSPBs (Ramírez-Rodríguez et al., 2013).

Albeit the functions of HSPBs in the context of cell differentiation are still poorly understood (and have not been extensively studied so far), several experimental findings support the idea that HSPBs may contribute with different mechanisms to the correct functioning and maintenance of muscle

cells. First, mutations in HSPB1, HSPB3, HSPB5 and HSPB8 have been directly associated with myofibrillar myopathy or motor neuron disease (Table 1). Second, experimental evidence suggests the ability of various HSPBs to protect neuronal and muscle cells from stress and damage. For example, in double knockout experiments, loss of HSPB5 and HSPB2 functions leads to degeneration of skeletal muscle tissue in mice, supporting the notion that these chaperones are required for muscle health and maintenance (Brady et al., 2001). As previously mentioned, HSPB5 was shown to interact with intermediate filaments, in particular with the muscle-specific intermediate filament protein desmin that regulates sarcomere architecture (Hein et al, 2000). HSPB5 stabilizes not only intermediate filaments but also actin filaments, as well as the myofibrillar protein titin (Golenhofen et al., 2002). The protective effects of HSPB5 against muscle cell damage seems to also be linked to the maintenance of the cellular redox state. In the presence of an excessive amount of oxygen, cardiomyocytes are exposed to increased ROS production, which may lead to oxidative stress-inducible tissue damage and can induce apoptosis. HSPBs seem to be the first line of defence under these circumstances, as discussed previously.

All together these data are consistent with the hypothesis that HSPBs play an important role in myogenic and neuronal maintenance and aging.

### *Anti-apoptotic activity*

As previously mentioned, HSPBs also act as anti-apoptosis regulators (Kamradt et al. 2001; Sui et al., 2009; Kanagasabai et al., 2010). Two fundamentally different pathways are involved in apoptosis, although crosstalk between the two signal transducing cascades exists (Franco and Cidlowski, 2009) (Fig.3). Briefly, the extrinsic pathway, or death receptor pathway, is triggered through plasma membrane protein of the TNF receptor family, which lead to the activation of caspases such as caspase-8 through the death-inducing signalling complex (DISC). The intrinsic pathway, or mitochondrial pathway, involved intracellular signalling that elicit the production or activation of pro-apoptotic molecules, in particular cytochrome c (Garrido et al., 2003). Cytochrome c, along with Apaf-1 and pro-caspase-9 form the apoptosome, which is the complex responsible for caspase-3 (-6, or -7) activation (Li et al., 1997). Both pathways culminate in the execution pathway, which is initiated by the activation of caspase-3 (-6, or -7) and leads to DNA fragmentation, degradation of

cytoskeletal and nuclear proteins, cross-linking of proteins, and formation of apoptotic bodies (Elmore, 2007).

Several HSPBs display anti-apoptotic activity and they seem to exert this function with distinct mechanisms. Three main mechanisms have been proposed: 1) HSPBs, as well as other HSPs such as HSP70, can enhance the proteostasis capacity of the cells, thereby providing protection to the cells; 2) HSPBs, along with HSP70, can inhibit key effectors of the apoptosis; 3) HSPBs can regulate the proteasome-mediated degradation of proteins that regulate apoptosis (Garrido et al., 2003). For example, HSPB1 can directly bind to cytochrome-c, released from stress-damaged mitochondria, thus preventing apoptosome formation and consequent apoptosis (Bruey et al., 2000). Moreover, HSPB1 is implicated in increased phosphorylation and cytoplasmic localization of cyclin-dependent kinase inhibitor p21, promoting cell survival and cell cycle progression (Kanagasabai et al., 2010).

Similar to HSPB1, HSPB5 prevents cell death induced upon oxidative stress and upon cell treatment with pro-apoptotic drugs such as e.g. staurosporin and doxorubicin (Kamradt et al. 2001; Li et al. 2005). However, it does so with a different mechanism acting through the extrinsic pathway (Mehlen et al., 1996). The anti-apoptotic function of HSPB5 was shown to involve inhibition of the RAS-initiated RAF/MEK/ERK signalling pathway, as well as interaction with p53 leading to its retention in the cytoplasm (Li et al. 2005). Moreover, HSPB5 is able to inhibit the autocatalytic maturation of caspase-3, negatively regulating apoptosis during myogenesis (Kamradt et al. 2001; Kamradt et al., 2002).

Also, HSPB8 has been shown to possess anti-apoptotic activity (Rusmini et al., 2017; Modem et al., 2011; Shen, Li and Min, 2018). In breast cancer and glioblastoma cells, HSPB8 functions in cell cycle regulation to prevent apoptosis, potentially through activation of the growth-associated transcription factor E2f and the cyclin-dependent kinase CDK4 (for details on cell cycle regulation, see below) (Modem et al., 2011). Furthermore, the complex formed by HSPB8 along with its co-chaperone BAG3 (Bcl2-associated athanogene 3) modulate intracellular pathways involved in apoptosis or development altered in several tumours (Romano et al., 2003; Chiappetta et al., 2007; Rapino et al., 2014). HSPB8 was also shown to promote the proliferation and inhibit the apoptosis of gastric cancer cells by activating ERK-CREB signalling (Shen, Li and Min, 2018). The anti-apoptotic function of HSPBs may have implications beyond the regulation of cell death, such as for example, for cell differentiation and myogenesis. By contrast, HSPB8 was shown to lead to pro-apoptotic

activity in some cells. In Ewing's sarcoma and hematologic malignancies, restored HSPB8 expression induces cell death through caspase-3 activation and inhibits tumour growth in xenograft models (Gober et al., 2003; Gober et al., 2005; Li et al., 2007; Cui et al., 2012). The activation of apoptosis was described to be due to the activation of the TGF-beta-activated kinase 1(TAK1) /p38MAPK/caspase-3/caspase-7 pathway. Similarly, HSPB8 expression was demonstrated to induce the death of genetically diverse melanoma lines and inhibit tumour growth through the activation of TAK1-dependent death pathways (Smith et al., 2012).

Thus, selective inhibition of HSPBs, along with inhibition of other HSPs (such as HSP70 and HSP90) may represent a valuable strategy to treat cancer (for detailed information about HSP90 and cancer (Zuehlke et al., 2018; Schwartz et al., 2015).

### *New potential functions of HSPBs in the extracellular space and in cell-to-cell communication*

During the last decades, the study of HSPB functions has been focused on their intracellular roles. Yet, several HSPBs, such as HSPB1, HSPB5 and HSP6 have been found in the extracellular environment (Clayton et al., 2005; Sreekumar et al., 2010; Gangalum et al., 2011; Zhang et al., 2012; Bakthisaran et al., 2015; Batulan et al., 2016). Thus, several researchers shifted their focus on the potential functions of HSPBs at the extracellular level. The most widely accepted secretion pathway for HSPBs to exit from the cells is via exosomes (Clayton et al., 2005; Sreekumar et al., 2010; Gangalum et al., 2011). Exosomes are extracellular vesicles involved in the transfer of molecules from one cell to another via membrane vesicle trafficking. These vesicles are considered potential extracellular signalling machines due to their role in lateral transfer of molecular information, i.e. transfer of certain proteins into non-expressing cells (Gangalum et al., 2011).

HSPB1 was the first HSPB to have been shown to be secreted by a non-classical pathway involving exosomes (Rayner et al. 2009). Shortly after, also HSPB5 and HSPB6 were shown to be secreted via exosomes (Sreekumar et al., 2010; Gangalum et al., 2011; Zhang et al. 2012). An alternative, mutually existing mechanism is represented by direct interaction of HSPBs with membranes (Batulan et al., 2016). Indeed, several HSPBs, namely HSPB1, HSPB4, HSPB5, and HSPB8 directly bind to lipid vesicles *in vitro* (Cobb et al., 2002; Grami et al., 2005; Chowdary et al., 2007; Gangalum et al., 2011; Tjondro et al., 2016; De Maio et al., 2019).

Although HSPB extracellular functions are not yet clear, extracellular HSPBs have been implicated in cell-to-cell communication, signalling, inflammation, and immunity (Binder et al., 2004; Schmitt et al., 2007; Rayner et al., 2008; Reddy et al., 2018). Assuming that distinct pools of extracellular HSPBs exist, these may exert distinct functions. The HSPBs that are confined inside the exosomes could be targeted to other cell types and therefore act intracellularly in these target cell types. By contrast, HSPBs that are directly released via binding to membrane lipids, once in the extracellular space may either bind to extracellular components or to membrane receptors. In agreement, extracellular HSPB1 displays a neuroprotective effect by reducing α-synuclein cellular toxicity through inhibition of extracellular fibril formation (Cox et al., 2018). Extracellular HSPBs might also act as molecular chaperones, by forming associations with antigenic polypeptides and thus efficiently delivering exogenous antigens to the endogenous antigen-processing-pathway of dendritic cells (Binder et al., 2001; Manjili et al., 2002; Srivastava and Udono, 1994; Zeng et al., 2003). For example, HSPB8 has been found in the extracellular space, where it binds to the Toll like receptor 4 (TLR4) abundantly expressed in the synovial fluid of rheumatoid arthritis patients leading to activation of dendritic cells (Roelofs et al., 2006). Similarly, extracellular HSPB1 was reported to act as a signalling molecule to activate NF-κB in macrophages, providing a protective mechanism against atherosclerosis (Salari et al., 2013). Finally, HSPB5 autoantibodies have been detected in the serum of Alzheimer's and Parkinson's disease patients, providing additional evidence for the presence of extracellular HSPBs in neurodegenerative disease (Papuć et al., 2015; Papuć et al., 2016). Of course, one cannot exclude the possibility that a pool of HSPBs found extracellularly accumulates as a consequence of cellular injury, rather than of regulated secretion or release (Clayton et al., 2005).

## HSPB and human diseases

HSPBs have been directly or indirectly implicated in three major types of diseases: Distal Hereditary Motor Neuropathies (dHMNs), myopathies (desmin-related myopathy, rimmed vacuolar myopathy and cardiomyopathy), which affect the neuromuscular system, and age-related protein conformational diseases (or protein misfolding diseases). Genetic evidence shows that mutations in HSPB genes are causative for dHMNs and several types of myopathies (see Table 1) (Vendredy, Adriaenssens and Timmerman, 2020). By contrast, so far no genetic mutations in HSPBs have been linked to age-related protein conformational diseases; however, a large body of evidence demonstrates that HSPB dysfunction, as well as a general decline in the expression and function of

chaperones that occurs during aging (Hipp, Kasturi and Hartl, 2019), contributes to disease progression and, conversely, HSPB boosting may play protective roles (Boncoraglio, Minoia and Carra, 2012).

## List of mutations in HSPBs and their link to human disease

The updated list of the mutations found in HSPB genes and associated with human diseases (referred to as chaperonopathies) is shown in Table 1. In summary, mutations in HSPB1, HSPB3 and HSPB8 are primarily associated with dHMNs and Charcot Marie Tooth (CMT) disease (Evgrafov et al., 2004; Irobi et al., 2004; Kolb et al., 2010; Morelli et al., 2017; Nam et al., 2018; Vendredy, Adriaenssens and Timmerman, 2020), while mutations in HSPB5 are associated with cardiomyopathy (CMD), desmin-related and myofibrillar myopathy (DRM and MFM) and cataract (Vicart et al., 1998, Shroff et al., 2000). Recently a new mutation in the HSPB8 gene (c.515dupC; p.P173SFS*43) has been linked to autosomal dominant rimmed vacuolar myopathy (RVM) (Al-Tahan et al., 2019) (for details see "Distal Hereditary Motor Neuropathies and myopathies"). Besides, mutations in the HSPB4 gene, which is only expressed in the eye lens, are linked to cataract (Janoswka et al., 2019; Shroff et al., 2000; Vendredy, Adriaenssens and Timmerman, 2020; Nicolaua et al., 2020). Considering that the majority of the patients with mutations of HSPBs develop symptoms during adulthood and the disease progression is relatively slow, it is likely that HSPB function is important for the maintenance of motor neuron and muscle cell survival during aging, which also requires repair and regeneration of injured neuronal and muscular cells.

The disease-causing mutations have been reported to occur mainly at the level of the ACD, hitting a highly conserved "hot-spot" arginine (R)/lysine (K) residue (R140-HSPB1 is equivalent to R116-HSPB3, to R116-HSPB4, to R120-HSPB5 and to K141-HSPB8) (Houlden et al., 2008; Morelli et al., 2017; Litt et al., 1998; Richter et al., 2008; Vicart et al., 1998; Irobi et al., 2004). Besides this "hot-spot" residue, mutations in residues located both at the N terminus and within the ACD have been linked to disease. All these mutations are thought to be critical for the structure and chaperone activity of the HSPB proteins (Boncoraglio, Minoia and Carra, 2012). This is supported by the identification of protein aggregates in several chaperonopathies and by experimental evidence showing that most of the HSPB-mutated forms are aggregation prone and that most of these mutated forms lose their chaperone activity when tested using *in vitro* and/or cellular assays.

Mutations of HSPB4 and HSPB5 reduce lens transparency due to protein aggregation leading to cataract, the primary cause of blindness worldwide (Sun and MacRae, 2005). Furthermore, the "hot-spot" located R120G mutation in HSPB5 leads to disruption of its structure, chaperone activity and interaction with desmin resulting in protein aggregation of HSPB5 itself together with desmin in the so-called desmin-related myopathies (Vicart et al., 1998; Perng et al., 1999). Conversely, some HSPB mutations, in particular ACD mutants of HSPB1 (E127W, S135F, and R136W) are found predominantly in the monomeric state and display increased chaperone activity (Almeida-Souza et al., 2010). Besides the increased chaperone activity, these ACD mutants also shown an increased the affinity of HSPB1 for its clients, which might lead to pathogenesis (Vendredy, Adriaenssens and Timmerman, 2020). An example of this are S135F-HSPB1 and P182L-HSPB1 which decrease tubulin acetylation due to their increased affinity for tubulin leading to axonal transport deficits and CMT (d'Ydewalle et al., 2011).

Previous data demonstrated that HSPB8 K141E has reduced ability to inhibit the aggregation of polyglutamine-disease causing Htt43Q, SCA3(64)Q, and the neuropathy-causing mutant HSPB1 P182L in cells, suggesting a partial loss of chaperone activity (Carra et al., 2010). Thus, both a toxic gain of function, due to the increased aggregation propensity of mutated HSPBs (e.g. P182L-HSPB1, R116P-HSPB3, R120G-HSPB5 and K141E/N-HSPB8) and a loss of function, due to decreased chaperone activity of these mutated proteins compared to their wildtype counterpart, are thought to contribute to disease pathogenesis (Carra et al., 2019). Likewise, a number of mutations in HSPB1 (R127W, S135F, and P182L) have been linked to impairment of autophagy leading to accumulation of misfolded proteins and damaged organelles in the cytoplasm (Vendredy, Adriaenssens and Timmerman, 2020). In addition, the mutated form can exert a dominant negative effect on the wildtype protein, contributing to a loss of its function.

While the main physiological functions of some HSPBs and how their mutants alter them have been well-characterized, providing potential pathomechanisms that should be pharmacologically targeted (e.g. HSPB1 and HSPB5), very little is known about other HSPB members and how they may lead to disease, such as e.g. HSPB3.

## Distal Hereditary Motor Neuropathies and myopathies

Distal Hereditary Motor Neuropathies (dHMN) are a group of progressive disorders characterized by lower-motor-neuron weakness, and many forms include minor sensory abnormalities. dHMNs are genetically and clinically heterogenous, with the onset ranging from adolescence through mid-adulthood (Irobi, De Jonghe and Timmerman, 2004). Initial symptoms include progressive length-dependent motor weakness and atrophy and wasting of the extensor muscles of the toes and feet. Diagnosis is often done based on a slow progressive length-dependent condition, which is ultimately confirmed by muscle wasting and weakness with reduced or even absent reflexes, as well as reduced motor amplitude potentials suggesting chronic distal denervation (Rossor et al., 2011). It is not uncommon for "non cardinal" signs to be present, such as predominance in the hands, vocal cord paralysis, diaphragm paralysis and pyramidal tract signs, which might be due to the diversity of causative genes (Irobi, De Jonghe and Timmerman, 2004). Indeed, the gene mutations associated with dHMN include proteins implicated in diverse functions such as protein misfolding (HSPB1, HSPB8, BSCL2), RNA metabolism (IGHMBP2, SETX, GARS), axonal transport (HSPB1, DYNC1H1, DCTN1) and cation-channel dysfunction (ATP7A and TRPV4) in motor-nerve disease (Rossor et al., 2011).

There are numerous overlapping characteristics between dHMN and Charcot-Marie Tooth disease (CMT), particularly in the axonal forms. However, in CMT sensory involvement is a significant component of the disease. Nevertheless, complete distinction between the two pathologies is difficult, and often they are referred simultaneously (Irobi, De Jonghe and Timmerman, 2004).

Charcot-Marie-Tooth (CMT) is a group of inherited diseases affecting the peripheral nervous system (PNS) first described by three physicians: Jean-Martin Charcot, Pierre Marie, and Howard Henry Tooth. It is one of the most common inherited disorders with a frequency of 1 case in 2500 individuals. CMT can be divided into 2 main groups: demyelinating (CMT1) and axonal (CMT2) disease forms, which are distinguished according to the primarily affected cell types, the Schwann cells or the neurons, respectively (Patzko and Shy, 2011). Similarly, to dHMN, the onset of CMT ranges between adolescence and early adulthood. Symptoms initiate with muscle weakness in the lower leg muscles and feet, slowly progressive degeneration of peripheral nerves, reaching then the hands and arms and gradually developing into complete muscle atrophy. Foot deformities such as high arches and hammertoes are not unusual in CMT. In the later stages, the disease leads to

progressive inability to walk and manipulate small objects. Additionally, these symptoms are sometimes associated with hand tremor, diaphragm palsy, optical nerve atrophy, and renal failure (Reilly, 2007). Progression of symptoms is usually slow, and the severity varies greatly among individuals, possibly due to the several mechanisms that might lead to the pathology. Similar to dHMN, also CMT is genetically linked to mutations in different proteins, including HSPB1, HSPB3, HSPB8, RAB7, NEFL, GDAP1, among others (El-Abassi et al., 2014). Currently there are no treatments available for neither dHMN nor CMT, therefore pathology management relies on physiotherapy, occupational therapy, and walking aids at the later stages of the diseases.

Desmin-related myopathy (DRM), rimmed vacuolar myopathy (RVM), and dilated cardiomyopathy (CMD) belong to the family of myopathies, which affect either the skeletal or the cardiac muscular systems, or both. Briefly, these diseases are a group of genetic muscle disorders characterized clinically by hypotonia and weakness, and a static or slowly progressive clinical course. Both DRM and RVM are part of the subgroup of myofibrillar myopathies (MFMs), in which skeletal muscles are primarily affected. To date, all MFM mutations have been traced to Z-disk associated proteins, namely, desmin, HSPB5, myotilin, ZASP, filamin C, and Bag3 (Selcen, 2011). The Z-disk provides an important structural linkage in the transmission of tension and contractile forces along the muscle fibre and has a role in sensing of muscle activity and signal transduction. Therefore, deficiency in the proteins mentioned not only results in disturbance to the structure of the sarcomere (defined as repeating unit between two Z lines), but also results in striking changes to the cellular morphology, which may have direct implications for muscle function (Ardnt et al., 2010). In contrast, in CMD cardiac muscle is primarily affected, and is characterized by enlargement, rigidity, and stiffness of the cardiac tissue leading to a reduced ability to pump blood through the body and maintain a normal electrical rhythm (Vicart et al., 1998). Mutations in more than 30 genes have been found to cause familial dilated cardiomyopathy, but many are associated with the cytoskeleton of cardiomyocytes, such as actin, lamins, dystrophin, titin, HSPB5 and BAG3 (Hershberger, Hedges, and Morales, 2013). Sarcomeric proteostasis has been recently suggested to represent an important process that is regulated by several chaperones, including several HSPBs and whose dysregulation is involved in disease manifestation and progression.

## Protein conformational diseases: loss of proteostasis and the potential protective role of HSPBs

The conversion of normal and soluble polypeptides into amyloid-like deposits has been associated with more than 50 disorders, with disparate symptoms and referred to as protein conformational or protein misfolding diseases (Chiti and Dobson, 2006). Examples are: Alzheimer's disease (AD), Parkinson's disease (PD), frontotemporal dementia (FTD), amyotrophic lateral sclerosis (ALS), polyglutamine diseases and inclusion body myopathy (IBM) (Chiti and Dobson, 2006). Although protein misfolding diseases are disparate in term of origin and symptoms, they are all associated with the accumulation of proteins that are highly organized in fibrillar structures and are referred to as amyloid fibrils or proteinaceous inclusions, when they accumulate intracellularly, or amyloid plaques, when they accumulate extracellularly. Although heterogeneous in their composition and often containing a number of proteins that are not directly linked to disease, the amyloid fibrils are enriched for specific aggregation-prone proteins that are also genetically linked to the familial forms of these diseases, such as e.g. α-synuclein and tau. In particular, α-synuclein and tau are the main components of the inclusions found in patients affected by PD, AD and FTD (Ciryam et al, 2016; Ciryam et al., 2015; Kundra et al, 2017). Genetic mutations in the genes encoding for these proteins enhance their vulnerability to misfolding and cause familial forms of PD and FTD (Papanikolopoulou & Skoulakis, 2020; Wong & Krainc, 2017).

Protective effects against protein aggregation diseases have been observed *in vitro* and in cellular and animal models overexpressing different types of chaperones, including HSPA, DNAJ (Muchowski et al., 2000) and HSPBs (Carra et al., 2013; Mogk and Bukau ,2017; Haslbeck, Weinkauf and Buchner, 2019; Horwitz 1992; Bruinsma et al., 2011; Cox et al., 2017). Focusing on HSPBs, previous studies demonstrated that several proteins of this family, namely HSPB1-HSPB6 and HSPB8, modulate α-synuclein and amyloid-β aggregation and reduce their mediated-toxicity *in vitro*, in neuronal cell and in Drosophila models (Horwitz 1992; Tue et al., 2012; Bruinsma et al., 2011; Cox et al., 2017; Wilhelmus et al., 2006). So far, the inhibitory effect towards protein aggregation has been mainly attributed to the ability of the HSPBs to transiently and weakly bind to α-synuclein and amyloid-β (Bruinsma et al., 2011; Wilhelmus et al., 2006). When using cellular and animal models of protein aggregation diseases, HSPBs seem to provide protection with distinct and more complex mechanisms. For example, using a cellular model of polyglutamine/polyQ disease (namely Huntington's disease), it was shown that HSPB1 protected against polyQ-mediated toxicity, acting

at the level of the production of reactive oxygen species, but could not prevent polyQ aggregation (Wyttenbach et al., 2002); by contrast, HSPB8 prevented polyQ aggregation by facilitating its autophagy-mediated clearance and by concomitantly decreasing its translation (Carra et al., 2008; Carra et al., 2009).

Given the potential contribution of alterations in HSPB expression and function to human disease, a better understanding of their roles and how defects in their basic functions could result in disease might widen the opportunities for therapeutic avenues, as well disease prevention.

## Focus on HSPB3: a poorly characterized HSPB with implications for skeletal muscle and motor neuron maintenance.

HSPB3, HSPL27 by the old denomination system, is one of the smallest members of the HSPB family with a molecular mass of 17kDa (150aa) (Boelens et al. 1998). HSPB3 expression has been primarily detected in cardiac and skeletal muscle tissue, where the presence of this protein has been confirmed both at the mRNA and protein levels (Lam et al. 1996; Sugiyama et al., 2000) (Table 1). In addition, mRNA studies have revealed the presence of low levels of HSPB3 mRNA in the grey matter of the spinal cord in mice, including large cells in the ventral horn that are morphologically motor neurons (Allen Spinal Cord Atlas) (Lein et al. 2007). HSPB3 mRNA has also been found in several foetal tissues, suggesting that it might have a role in foetal development (La Padula et al, 2012). Nevertheless, the mRNA HSPB3 expression pattern in the brain is controversial, with reports stating the detection of expression in the whole brain, cortex and cerebellum in rats (Kirbach and Golenhofen, 2010), and others affirming that expression is restricted to hypothalamus, frontal cortex, hippocampus, striatum, and midbrain in mice (Kondaurova et al., 2010). To date there is a single report showing expression of both HSPB3 mRNA and protein in the peripheral nervous system, more specifically in axons of both motor and sensory neurons of chicken, mouse, and human samples (La Padula et al., 2012).

In muscle cells, HSPB3 has been described to form an oligomeric 150kDa complex with HSPB2, with a stoichiometry of 3:1 HSPB2:HSPB3 (Sugiyama et al., 2000; den Engelsman et al. 2009) (Figure 3). Both mRNA and protein levels of HSPB2 and HSPB3 are strongly upregulated during myogenesis

(Sugiyama et al., 2000; den Engelsman et al. 2009). Yet, the functions of this complex during muscle differentiation are unknown.

## Structure

HSPB3 is the most deviating protein among the human HSPBs. First, the ACD of HSPB3 shows only 40% sequence identity with the other human HSPB proteins (Figure 2). The C-terminus of HSPB3 contains only five residues. Consequently, HSPB3 is unable to form a bridge between adjacent ACD dimers, and primarily exists in low molecular weight oligomers (den Engelsman et al., 2009). In addition, the N-terminal domain of HSPB3 is considerably different to that of all the other HSPBs. In the case of HSPB3, the "I/V-X-I/V" motif is not located in the C-terminus (which is absent), but in the N-terminus; thus, the N-terminal region of HSPB3 docks in the β4/β8 pocket of the ACD of HSPB2, enabling the formation of the HSPB2:HSPB3 complex with the 3:1 ratio (Clark et al. 2018) (Figure 3).

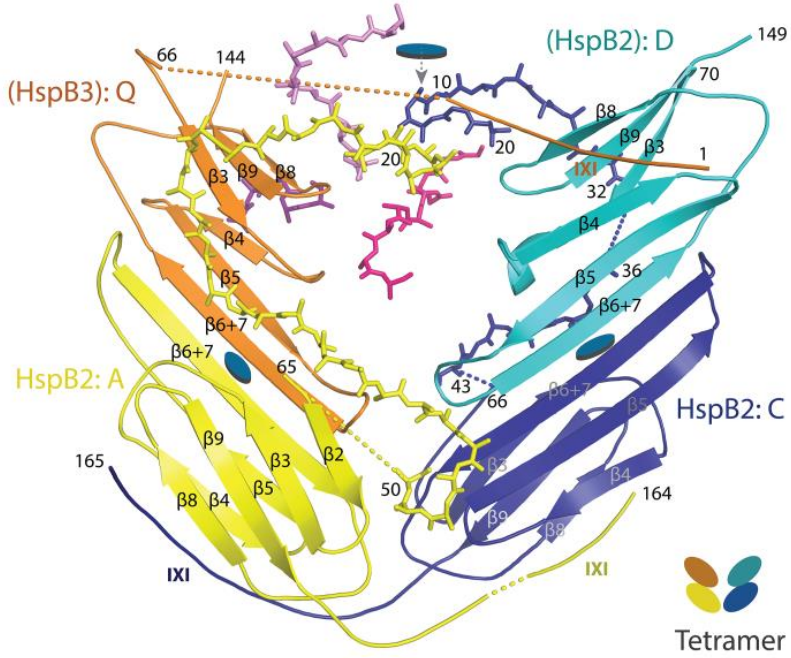


Figure 3 Tetramer structure of HSPB3/HSPB2 complex (Clark et al., 2018). The yellow (chain A), blue (chain C), and cyan (chain D) chains are parts of the HspB2 N-terminal regions. HspB3 is represented by the orange chain (chain Q), with the N-terminal region of this chain reaching across the pseudo-twofold to bind to the pocket of the cyan chain in the adjacent dimer, while chain 1 patches the pocket of chain Q.

Unlike all the other HSPBs, HSPB3 is not subjected to splicing since it is encoded by a single exon and its mRNA is intronless (Kappé, 2003). Importantly, functional analysis of intronless genes has

revealed over-representation of signal transduction genes and genes encoding regulatory proteins important for growth, proliferation, and development (Grzybowska, 2012). Whether HSPB3 falls within these categories is unclear.

## HSPB3 chaperone function

*In vitro* studies aimed at characterizing the chaperone activity of HSPB3 have demonstrated that HSPB3 alone can exhibit molecular chaperone-like activity and can prevent, for example, the heat-induced aggregation of alcohol dehydrogenase (ADH) (Ashtana et al., 2012). However, when compared to other HSPBs, HSPB3 is far less efficient as a chaperone (PMID: 27909051). The lack of chaperone activity has been attributed to the very short C-terminal tail of HSPB3. In agreement with this idea, Ashtana and colleagues demonstrated that a chimeric protein formed by the fusion of HSPB5's C-terminal to HSPB3 provided to HSPB3 enhanced chaperone activity towards DTT-induced aggregation of insulin.

Considering that in muscle cells HSPB3 forms a stoichiometric complex with HSPB2 (Sugiyama et al., 2000; den Engelsman et al. 2009), most of the studies that aimed at characterizing HSPB3 chaperone activity *in vitro* have so far been performed using a mixture of HSPB2 and HSPB3. The results obtained depend on the type of substrate used. For example, due to its reduced surface hydrophobicity, in complex with HSPB2, HSPB3 has poor chaperone activity towards DTT-induced aggregation of insulin (den Engelsman et al. 2009). By contrast, HSPB3 could inhibit α-synuclein aggregation *in vitro*, when in complex with HSPB2, due to direct weak binding to both WT and mutant α -synuclein (Bruinsma et al., 2011). As well as, exhibiting moderate chaperone-like activity towards heat-induced aggregation of citrate synthase (Sugiyama et al. 2000).

## HSPB3, muscle cells and motor neurons

In contrast to other types of HSPBs, such as for example HSPB1, HSPB3 is not upregulated upon heat-shock (Sugiyama et al. 2000) and it does not confer thermotolerance (den Engelsman et al. 2009). The best characterized stimulus that upregulates transcriptionally HSPB3 is muscle cell differentiation; mechanistically HSPB3 is induced upon differentiation under the control of MyoD

(Sugiyama et al., 2000). Yet, its putative function in differentiation has not been well characterized. Morelli et al. (2017) reported that in differentiating myoblasts HSPB3 might regulate the subcellular distribution and function of its binding partner HSPB2. In particular, HSPB3 avoids aberrant phase separation of HSPB2, which could lead to sequestration of nuclear lamin A, with consequences on lamin A function, as well as RNA transcription (Morelli et al., 2017). Whether HSPB3 exerts specific functions that are unrelated to binding to HSPB2 is currently unknown.

Four missense variants in HSPB3 have been linked to neuromuscular diseases (Table 1): R7S-HSPB3 (rs139382018) and Y118H-HSPB3 lead to dHMN2C (Kolb et al., 2010; Nam et al., 2018) (Kolb et al., 2010); R116P-HSPB3 (rs150931007) and A33AfsX50-HSPB3 were identified in two patients affected by congenital myopathy, with neuropathy signs (Morelli et al., 2017). However, very little information exists about how these mutations mechanistically contribute to the progressive degeneration of the neuromuscular system. A33AfsX50-HSPB3, which was identified in 70-year-old Italian man who presented shoulder-girdle muscle weakness and atrophy, is a truncated and unstable protein that is rapidly degraded upon synthesis (Morelli et al., 2017). R116P-HSPB3 was detected on a 25-year-old woman of Italian origin who had developed weakness of the upper and lower limbs, along with neurogenic changes in the lower limbs compatible with axonal neuropathy; R116P-HSPB3 cannot bind to HSPB2 and cannot prevent the aberrant phase separation of HSPB2 (Morelli et al., 2017). By contrast, R7S-HSPB3 which was described in 2 sisters with adult-onset HMN2C, maintained its binding affinity to HSPB2 unchanged compared to HSPB3 (Kolb et al., 2010; Morelli et al., 2017). Overexpression of R7S in chicken embryos resulted in reduction of motor neuron formation, supporting a possible gain of toxic function (or a loss of protective function of HSPB3-WT) (La Padula et al., 2016). No data are available yet concerning Y118H-HSPB3 identified in a family affected by autosomal dominant axonal CMT2 neuropathy. Together these results suggest that both loss and toxic gain of function mechanisms may contribute to HSPB3-linked diseases, similar to what has been so far observed for e.g. HSPB5 disease-causing HSPB mutants (Brady et al., 2001; Perng et al., 2004; Vicart et al., 1998).

Motor neuropathies and congenital myopathies associated with HSPB3 mutations develop with aging, when the peripheral nerve and muscle regeneration capacities decline (Carosio et al., 2011; Li et al., 2018; Wallace and McNally, 2009). Muscle regeneration recapitulates many aspects of myogenesis. In fact, muscle cell differentiation occurs not only during embryogenesis, to sustain muscle development, but also during adulthood, to enable the repair and regeneration of muscles

that have been damaged after injury or exercise (Biressi and Gopinath, 2015; Le Grand and Rudnicki, 2007). It is thus not surprising that a decline in the regenerative abilities of peripheral nerves and muscles contributes to the deterioration of the neuromuscular system during natural aging and to age-related neuromuscular diseases (Carosio et al., 2011; Li et al., 2018; Wallace and McNally, 2009). Considering that HSPB3 is absent in cycling cells and is specifically upregulated in muscle cells by the transcription factor MYOD, these data together lead to these important questions: Could HSPB3 promote muscle cell differentiation? And could altered muscle cell differentiation as a consequence of HSPB3 mutations participate to the degeneration of the neuromuscular system? Of note, mutations in genes that play a role in cell differentiation, including neuronal and muscle cell differentiation, as well as defects in the differentiation process have been linked to motor neuropathies. For example, IGHMBP2 (immunoglobulin mu DNA binding protein 2) is mutated in Charcot-Marie-Tooth (CMT) type 2S disease and leads to differentiation defects in primary motoneurons (Shi et al., 2015); MORC2 (microrchidia family CW-type zinc-finger 2) is a chromatin remodeling protein that regulates cell differentiation and is mutated in CMT disease (Albulym et al., 2016; Liu et al., 2019; Schottmann et al., 2016); NDRG1 (N-myc downstream regulated gene 1) promotes differentiation and is mutated in CMT type 4D disease (Echaniz-Laguna et al., 2007); Sbf1 (SET binding factor 1) and Sbf2 (SET binding factor 2) are members of the myotubularin family that play a role in the epigenetic regulation of cell growth and differentiation and are also mutated in CMT (Lassuthova et al., 2018; Nakhro et al., 2013; Senderek et al., 2003), as well as myotubularin-related protein 2 and 13 (MTMR2, MTMR13), that were suggested to play important roles during skeletal muscle, neuronal and Schwann cells differentiation and whose mutations are linked to CMT (Azzedine et al., 2003; Bolino et al., 2000).

## Myogenesis – Section I

Muscle fibres are composed of multinucleated myotubules that result from the fusion of hundreds or thousands of mononucleated myoblasts, a process referred to as myogenesis. Myogenesis is a highly coordinated and defined process that occurs during embryonic development, when the tissue that constitutes the muscular system is being formed, and also postnatally, when it is activated to heal and repair damaged muscle fibres (Braun and Gautel, 2011; Biressi and Gopinath, 2015; Le Grand and Rudnicki, 2007). In both embryonic and postanal stages, myogenesis is characterized by a sequential expression of myogenic factors known as Myogenic Regulatory Factors (MRFs: Myf5, MyoD, MRF4, and myogenin) (Figure 5), which in turn activate the expression of muscle-specific genes and the signalling cascades required for the various steps of muscle development(Rhodes et al., 1989; Braun et al., 1990; Miner et al., 1990).

Muscle development is continuously required for growth and wound repair after damage. The regeneration, maintenance, and growth of skeletal muscles postnatally rely mainly on a small population of muscle stem cells, termed satellite cells (SCs) (Chen et al., 2006; Biressi and Gopinath, 2015). SCs are located between the sarcolemma and the basal lamina where, in absence of stimuli, they are kept in a quiescent state (Jone and Wagers, 2008). Quiescent SCs do not express any of the four MRFs (Cornelison et al., 1997) and their myogenic potential is dependent on the sequential repression of Pax genes and expression MRFs (Figure 5). In response to stress, the SC population transitions from quiescent to proliferative state, yet the activators involved in this transition remain largely unknown (Chen, Datzkiw and Rudnicki, 2020). Following activation, SCs start to cycle and induce the expression of Pax7 and MyoD, giving origin to cycling myoblasts. These cycling myoblasts are able to undergo several rounds of division, until expression of myogenin, or MRF4, is induced and, concomitantly Pax7 is downregulated; the sequential expression of these genes commit SCs to terminal differentiation. Importantly, not all SCs differentiate and a small population of activated satellite cells reverse to quiescence to replenish the stem cell pool; this process is known as self-renewal and is fundamental to ensure tissue maintenance with aging and tissue repair upon damage (Yin et al., 2013). Therefore, myogenesis is delimited by a number of stages characterized by withdrawal from the cell cycle and fusion of mononucleated myocytes to form multinucleated myofibres. At the molecular level, the cellular events that determine skeletal myogenesis rely on

the expression and function of muscle-specific transcription factors that orchestrate myogenic gene expression, in collaboration with chromatin-remodelling complexes.

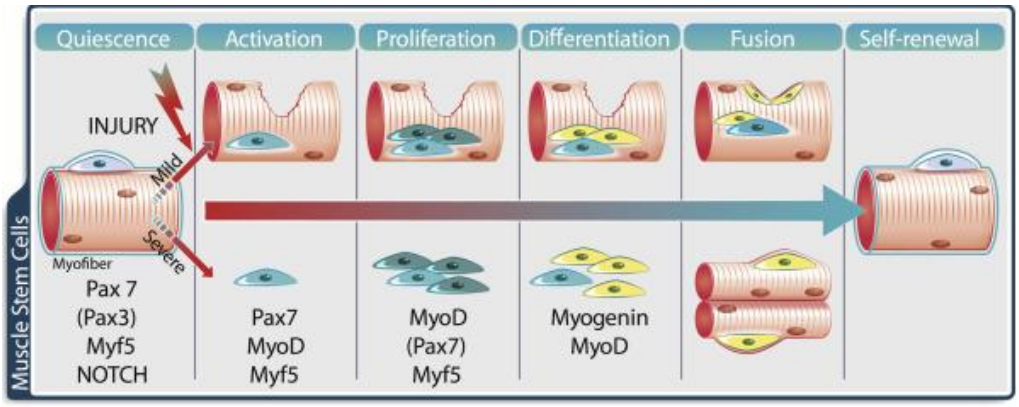


Figure 4 Synoptic view of the different steps involved in muscle differentiation and repair (adapted from Baghdadi and Tajbakhsh, 2018). During the quiescent state SCs express Pax7 (and Pax3 in some muscles) and Myf5, and Notch signalling is highly active. Upon damage, they rapidly upregulate Myod and Myf5, and Pax7 protein remains detectable. Following the amplification phase, myoblasts express the terminal differentiation gene Myogenin and exit the cell cycle. Differentiated myoblasts fuse to the pre-existing fibre (mild) or together to form new fibres (severe). During this process, some satellite cells self-renew to replenish the stem cell pool.

## Chromatin and nuclear envelope remodelling during myogenesis

Remodelling of chromatin is an important step in myogenic differentiation as it allows for the expression of muscle-specific genes. The nuclear lamina has been reported to play a pivotal role in maintenance and remodelling of chromatin during differentiation (Deniaud and Bickmore, 2009). There are two main types of lamins: A-type and B-type, which are intermediate filament proteins and constitute the nuclear lamina scaffold. Expression of A-type lamins, in contrast to the homologous B-type lamins, is largely restricted to differentiated tissues with high expression in skeletal muscle (Butin-Israeli et al., 2012).

During myogenic differentiation chromatin changes have been shown to be determined by the switch of the expression of the Lamin B Receptor (LBR) and lamin A/C (LMNA), the two major tethers for heterochromatin in eukaryotic cells (Figure 6) (Solovei et al., 2013). These mechanisms occur in a sequential manner upon differentiation commitment. LBR in an integral protein able to bind heterochromatin through HP1α, and Lamin B1 type proteins. Targeting of chromatin to the nuclear envelope (NE) silences its transcription in a histone-deacetylation-dependent manner. During

muscle cell differentiation, LBR expression levels decrease, as well as its anchoring to the NE; in addition, the LBR tether is partially replaced by the lamin A/C (LMNA) tether. This tether switch modifies discrete peripheral chromatin regions, inducing the expression of genes that are required for cell differentiation (Solovei et al., 2013). These include genes responsible for the remodelling of the generic cytoskeleton into the specialized contractile cytoskeleton and of the extracellular matrix (ECM), which sustains cell migration, cell-cell fusion, and assembly into myofibrils (Solovei et al., 2013) (for details see "Extracellular Matrix remodelling").

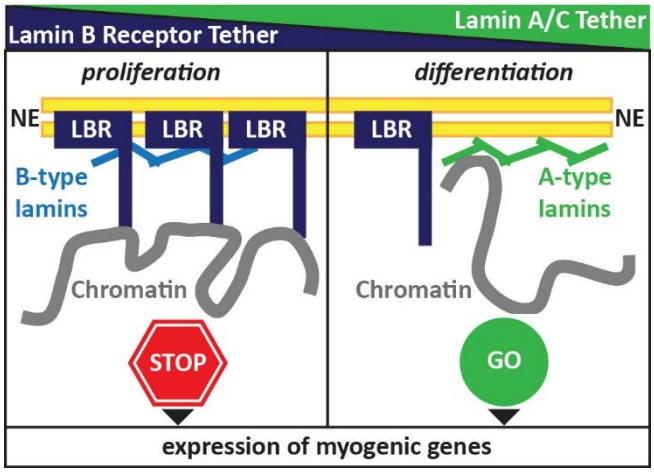


Figure 5 Schematic representation showing that the LBR chromatin tether is replaced by the LMNA chromatin tether during cell differentiation and the impact on myogenic gene expression (adapted from Solovei et al., 2013).

Furthermore, DNA dense regions denominated chromocenters have been shown to be altered upon myogenic differentiation. In cycling myoblasts, chromocenters are present in high numbers appearing with a low volume and predominantly present in the nuclear periphery; conversely, in differentiated myotubes, chromocenters fuse therefore reducing its numbers while increasing the volume, and also move into the nuclear centre (Brero et al., 2005). LBR downregulation has been reported to be essential for chromocenter fusion and movement from the nuclear periphery (Solovei et al., 2013), reinforcing its importance for the regulation of cell differrentiation. Yet how the expression of LBR is temporarily coordinated and how its localization at the NE is spatially modulated during muscle cell differentiation are largely unknown.

## Extracellular Matrix Remodelling

The ECM is a mesh-like structure present in the interstitial space between cells and tissues and is involved in mechanical support for cell anchorage and migration, maintenance of cell polarity, as well as scaffolding for tissue renewal (Bentzinger et al., 2013; Urciuolo et al., 2013; Csapo et al., 2020; Goody et al., 2015). Furthermore, it functions as a mechanical force transducer thereby allowing for the activation of several signalling pathways required for muscular function (Kjaer, 2004). The muscle ECM is comprised of basement membrane and endomysium, the layer that surrounds each individual myocyte; perimysium, groups the myofibrils into bundles; and epimysium, the dense layer that encloses the entire muscle tissue corresponding to the interstitial matrix (Kjaer, 2004). The basement membrane keeps in contact with the cells, providing structural support and dividing tissues into compartments, thereby regulating cell behaviour. Its major constituents are collagen IV, laminins, entactin/nidogen 2, and sulphated proteoglycans such as perlecan and agrin (Gullberg et al., 1999; Tunggal et al., 2000; Jimenez-Mallebrera et al., 2005). The interaction between the ECM and the intracellular environment is accomplished by the integrins, which connect the cytoskeleton to the ECM. The cytoskeleton is coupled to the nuclear lamina via LINC (Linker of Nucleoskeleton and Cytoskeleton) complex (Figure 6). The LINC complex is composed of SUN and Nesprin proteins and is connected to lamins A and B, lamin B receptor (LBR), LAP proteins, and emerin (Bouzid et al., 2019). The LINC complex functions as a structural support to the nucleus and plays a mechanosensory role to translate mechanical cues and alterations in the extracellular matrix into biochemical signals (Bouzid et al., 2019), thereby allowing the cell to adapt to its surrounding environment by modulation of cytoskeleton organization, gene expression, nuclear organization, and structure. Being a central complex in signal transduction, the LINC complex is involved in nuclear migration, maintenance of the proper nuclear morphology and positioning of the nucleus, maintenance of the centrosome–nucleus connection via direct or indirect interaction, DNA repair, and movement of chromosomes within the nucleus during meiosis (Hieda, 2019).

The ECM plays a crucial role during muscle development and differentiation. Myogenesis is accompanied by remodelling of ECM proteins as well as by changes in integrin receptor expression pattern. Specifically, the proteins fibronectin (Bentzinger et al., 2013) and collagen VI (Urciuolo et al., 2013), as well as the proteoglycans syndecan 3, syndecan 4, perlecan, and decorin (Cornelison

et al., 2001; Brack et al., 2008) have been identified as the niche constituents influencing the balance between differentiation and self-renewal and, thus, the maintenance of skeletal muscles' regenerative capacity.

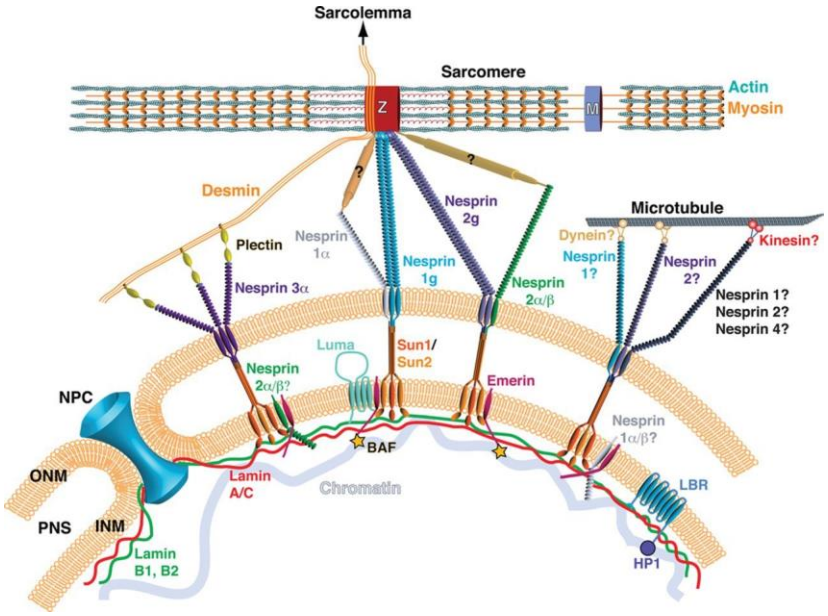


Figure 6 The LINC complex in the cardiomyocyte (Adapted from Stroud et al., 2014). The LINC complex couples the nuclear lamina to the cytoskeleton. SUN domain proteins, SUN1 and SUN2, located at the inner nuclear membrane (INM) interact with the nuclear lamins, Lamin A/C, B1, and B2, that line the nucleoplasmic face of the INM. SUN domain proteins interact with Nesprins in the perinuclear space (PNS). Nesprins protrude from the outer nuclear membrane (ONM) and interact with the cytoskeleton, often through an intermediate binding partner. Various proteins are associated with the LINC complex, such as Emerin and Luma. Chromatin directly interacts with Lamin A/C and indirectly with Emerin and Lamin B Receptor (LBR) via barrier to autointegration factor (BAF) and heterochromatin protein 1 (HP1), respectively. NPC indicates nuclear pore complex; and M, M-band.

The glycoproteins fibronectin and laminins display an opposite pattern of changes in time during myogenesis. Cycling myoblasts secrete a large amount of fibronectin, which allows for myoblast adhesion and proliferation, yet inhibits differentiation. Upon differentiation, fibronectin gets replaced by laminins in myotubes, leading to enhanced myoblast proliferation, migration, and alignment preceding the fusion (Bentzinger et al., 2013; Urciuolo et al., 2013). Proteoglycans are essential for signal transduction, as they act as co-receptors of growth factors. In particular, perlecan has been demonstrated to be downregulated during myogenesis, yet its expression is increased upon damage (Larrain et al., 1997). Conversely, decorin's expression is upregulated during myogenesis, leading to increased myoblast proliferation and myogenesis. In addition, decorin upregulation promotes muscle differentiation, as well as muscle regeneration in vivo (Li et al., 2007); and decorin interacts with the epidermal growth factor receptor or oncogenic ErbB receptors,

leading to activation of the mitogen-activated protein kinase (MAPK) signal transduction pathway, eventually inducing p21 and cell cycle arrest (Li et al., 2008) (for details see “Cell cycle arrest in myogenesis”).

Besides its important role during myogenesis, ECM is essential also for muscle growth and repair. Upon damage, extensive ECM remodelling supports satellite cell activation, migration, and myogenic differentiation, enabling muscle repair (Csapo et al., 2020; Goody et al., 2015). This is accomplished mainly by degradation of ECM surrounding satellite cells, thereby enabling their migration and subsequent relocation to the damaged site, where the SCs can become activated and restore muscle tissue by differentiating. Matrix metalloproteinases (MMPs) degrade extracellular matrix components such as collagens, elastin, fibronectin, laminin, and proteoglycans. Among the MMPs expressed in skeletal muscle, MMP-2 appears particularly critical as it is secreted by satellite cells and regenerating myofibers. Indeed, it acts as a mechanical barrier to prevent migration of satellite cells and their loss from normal muscle, repressing satellite cell mitosis and differentiation in the absence of muscle injury (Thomas et al., 2015). Further support for the notion that the ECM is actively involved in the maintenance of satellite cell quiescence comes from reports that satellite cells removed from their niche quickly enter the cell cycle and lose their capacity for myogenic differentiation (Gilbert et al., 2010).

### Cell cycle arrest in myogenesis

Myoblast commitment to differentiation initiates with irreversible withdrawal of cycling myoblasts from the cell cycle. This growth arrest is mediated and maintained by the retinoblastoma protein (Rb), together with p21 and other inhibitors of cell cycle progression (Figure 7) (De Falco, Comes and Simone, 2006). Indeed, myotubes express high levels of p21 and hypophosphorylated Rb, which maintain terminal differentiation and protect these multinucleated cells against apoptosis (Peschiaroli et al., 2002). The cell-cycle inhibitor p21 (encoded by CDKN1A) has been shown to be upregulated in a MyoD-dependent manner upon induction of myogenic differentiation (Halevy et al., 1995) and high expression of p21 has been correlated with the activation of the myogenin gene during embryogenesis (Parker et al., 1995).

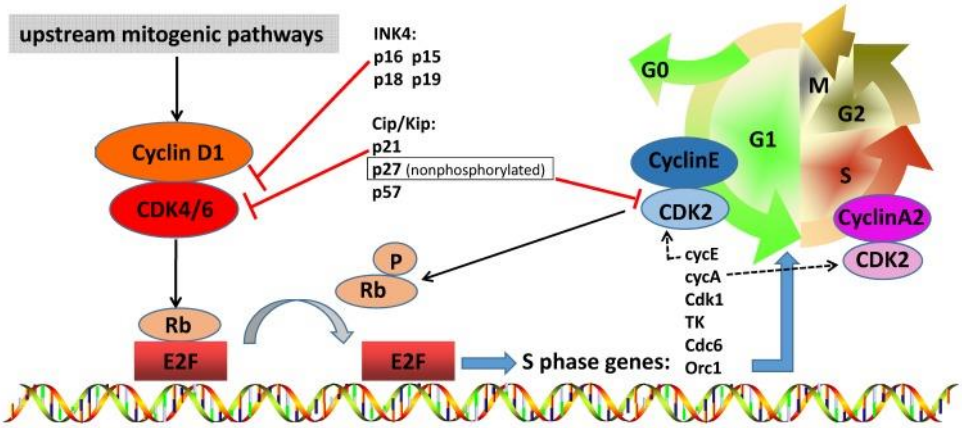


Figure 7 Schematic overview of the role of cyclin D-CDK4/6-INK4-Rb pathway in cell cycle arrest during myogenic differentiation (Niu, Xu and Sun, 2019)

Induction of p21 leads to the blockage of Cyclin Dependent Kinase (CDK) 2 and 4, whose activity is involved in the progression of G1 to S phase of the cell cycle (De Falco, Comes and Simone, 2006). Conversely, MyoD, which upregulates p21, is inhibited by the overexpression of cyclin D1, a G1-S cyclin and a CDK4 activator. The repression of cyclin D1 is required for terminal arrest of the cell cycle and initiation of differentiation, orchestrated by Rb. In dividing conditions, Rb is phosphorylated (pRb) by the activated CDK4 and bound to cyclin D1, which leads to the release of the transcription factor E2F. E2F family of transcription factors in turn, transcriptionally activates cycling A and E, thus allowing for normal cell cycle progression (Bracken et al., 2004). However, hypophoshorylation of Rb, due to CKD2/4 inhibition (by p21), releases it from cyclin D1 and increases its association with E2F1-3, culminating in repression of E2F target genes and leading to cell cycle arrest (Pantoja and Serrano, 1999) (Figure 7). Of note, Rb deficiency leads to skeletal muscle defects due to reduction of myofiber quantity and reduction of late muscle-specific genes in mice, further confirming the role of Rb in cell cycle arrest in myogenesis (Zacksenhaus et al., 1996). Furthermore, expression of MyoD leads to apoptosis in a p21-dependent manner in myoblasts lacking Rb function (Peschiaroli et al., 2002).

## α-synuclein aggregation – Section II

As previously mentioned, the misfolding and aggregation of the presynaptic protein α-synuclein is associated with development of PD, but not only (see "Protein conformational diseases: loss of proteostasis and the potential protective role of HSPB"). Indeed, α-synuclein is associated with a broad range of diseases known as synucleinopathies, which include PD, Lewy body dementia, Lewy body variant of Alzheimer's disease, Krabbe disease to neurodegeneration with brain iron accumulation (Burre et al, 2018).

The aggregation of soluble polypeptides into fibrillar amyloids is a multi-step process that includes a nucleation event, which consists in the random generation of nanofibrils, followed by fibril elongation, fibril amplification and culminating with the accumulation of an amyloid mass (Buell, 2017; Buell et al, 2014). This multi-step process is influenced by several environmental factors such as contact surfaces, temperature, and pH (Buell et al., 2014; Galvagnion et al, 2016). The initiation of aggregate formation is characterized by a slow formation of growth-competent nuclei from monomeric α-synuclein in solution, termed primary nucleation event. Using α-synuclein as a model protein, it has been recently demonstrated that the primary nucleation process is strongly enhanced by its contact with lipids, the major constituent of biological membranes (Fusco *et al*, 2017). Aggregation at physiological concentrations has been recently achieved by taking advantage of lipid contact surfaces to induce primary nucleation. In particular, small unilamellar vesicles (SUVs) prepared from model membrane lipid DMPS (1,2-dimyristoyl-sn-glycero-3-phospho-L-serin) have been shown to significantly increase α-synuclein aggregation rate in vitro (Galvagnion et al., 2015). α-synuclein binding to lipids is emerging as a double-edged sword: on the one hand, it is associated with α-synuclein physiological functions. In fact, α-synuclein binds to synaptic vesicles and regulates their docking at the presynaptic membrane, their clustering and recycling (Maroteaux et al., 1988); α-synuclein also binds to other types of membranes, including mitochondrial membranes and lipid droplets (Burre *et al.*, 2018). On the other hand, α-synuclein binding to lipids is associated with its pathological functions, since the interaction between α-synuclein and lipid vesicles triggers the initial primary nucleation process (Galvagnion *et al*, 2015).

Taking advantage of lipid contact surfaces to induce primary nucleation, a lipid-induced primary nucleation assay has been developed. The assay allows to study α-synuclein aggregation at physiological concentrations, which are estimated to be lower than 30 - 60 μM (Figure 8, Step 1) (Flagmeier *et al*, 2016; Galvagnion *et al.*, 2015; Perni *et al*, 2018). Primary nucleation is then followed

by secondary nucleation events that lead to proliferation of mature amyloid fibrils, such as elongation and surface-assisted nucleation (Buell et al., 2014). Upon formation of mature fibrils generated through primary nucleation, monomeric α-synuclein assembles into the growing extremity of an existing fibrils, thereby elongating the fibril. Thus, a second assay has been developed to monitor fibril elongation in the presence of preformed seed fibrils, where the kinetics are dominated by elongation of the added seeds (Figure 8, Step 2). Next, a third assay has been developed to study fibril amplification, which occurs via secondary pathways, such as formation of surface-catalysed aggregates, under conditions of mildly acidic pH (Figure 8, Step 3) (Flagmeier *et al.*, 2016). These mildly acidic environmental conditions mimic the low pH (5.5) that characterizes dopaminergic neurons, which express the highest levels of α-synuclein (Sinning & Hubner, 2013). Using this three-pronged approach it is now possible to separately evaluate each step of α-synuclein aggregation, identifying the contribution of specific environmental factors that are biologically relevant such as e.g. lipid composition and pH variation.

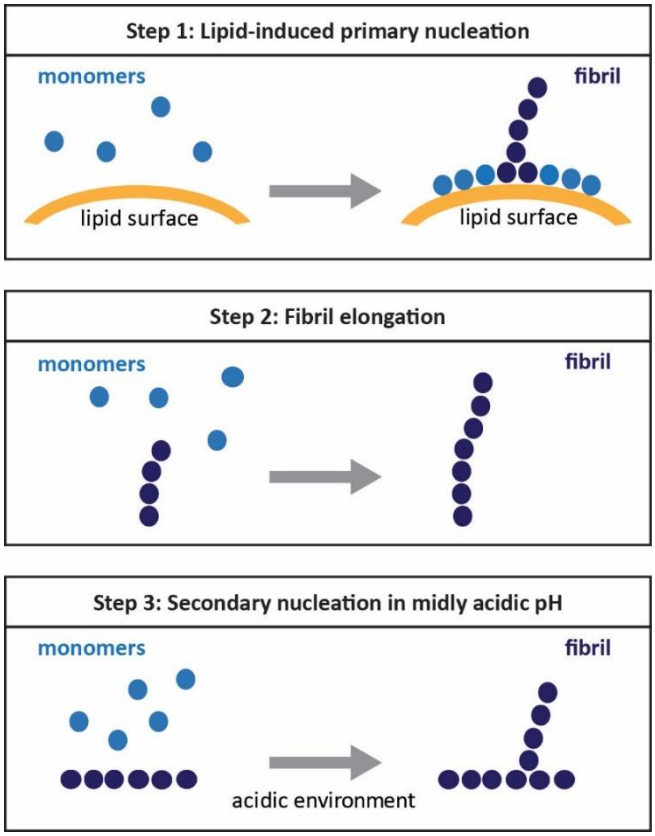


Figure 8 Three-pronged approach to characterise a-synuclein aggregation. (1) lipid-induced nucleation, where growth-competent nuclei form from monomeric species due to the interaction with lipid surfaces, (2) elongation, where existing preformed fibrils at high concentrations and in presence of monomeric a-synuclein lead to their assembly and formation of longer fibrils, and (3) secondary nucleation, where preformed fibrils at low concentrations along with monomeric a-synuclein under mildly acidic pH conditions, lead to the generation of secondary pathways such as surface-catalysed aggregates.

# Aim of the thesis

HSPB3 is a small heat shock protein belonging to the mammalian family of sHSP/HSPBs, being the most deviating member of the HSPB family. HSPB3 is absent in cycling cells and is predominantly expressed in differentiated muscle cells and in selected neuronal cell types, including motor neurons. In contrast to other HSPBs, HSPB3 is not upregulated upon heat-shock and it does not confer thermotolerance, yet the physiological functions of HSPB3 are poorly understood. Nevertheless, four mutations in the HSPB3 gene have been identified in patients affected by hereditary peripheral neuropathies and congenital myopathies. Together these data suggest that HSPB3 is important for motor neurons and muscle cell viability, underlining the importance of understanding HSPB3 functions for the neuromuscular system. This thesis aimed at characterizing HSPB3 properties and functions in different systems, focussing on two main aims:

1) determine whether and how HSPB3 participates in myogenic differentiation, and how the R116P-HSPB3 mutation affects HSPB3 properties and functions. In human myoblasts, HSPB3 is induced upon differentiation under the control of the myogenic regulatory factor MyoD. Yet whether HSPB3 plays a role in myogenic differentiation is unknown. Cell cycle exit and commitment to differentiation are regulated at the transcriptional level and require extensive chromatin remodelling. This process is modulated by the downregulation of Lamin B Receptor (LBR) and its detachment from chromatin and the nuclear envelope (NE). Immunofluorescence studies show that HSPB3 is enriched at the NE. Previous RNA analysis showed that HSPB3 expression levels correlated with the one of myogenin, one of the key muscle-specific transcription factors (Morelli et al., 2017). Based on these observations we asked whether HSPB3 could act at the nuclear level facilitating the chromatin remodelling during muscle differentiation.

2) investigate whether HSPB3, and other better characterized HSPBs (HSPB5, HSPB6, HSPB7 and HSPB8) affect α-synuclein interaction with lipids and aggregation. So far, no physiological role has been identified for HSPB3 in neuronal populations. One of the best characterized function of HSPBs is their chaperone activity and prevention of irreversible aggregation. In vitro studies aimed at characterizing the chaperone activity of HSPB3 have demonstrated its ability to inhibit α-synuclein aggregation. Importantly, recent evidence demonstrates that the interaction between α-synuclein and lipid surfaces triggers its conversion from a soluble state into the aggregated stated, which is associated to Parkinson's disease development. Of note, several HSPBs have been shown to interact

with lipids; however, whether lipid binding is required for or participates to regulate the chaperone activity and anti-aggregation functions of HSPBs is currently unknown. Here we aimed at addressing this specific question and understanding how at the molecular level HSPBs affect α-synuclein aggregation using an in vitro three-pronged approach developed in the laboratory of Prof. M. Vendruscolo (Flagmeier *et al*, 2016).

# Materials & Methods

## Reagents

| REAGENT or RESOURCE | SOURCE | IDENTIFIER |
|---|---|---|
| Experimental Models: Cell Lines | | |
| HeLa Kyoto cell line | (Poser et al., 2008) | N/A |
| HeLa cell line | (Morelli et al., 2017) | N/A |
| LHCNM2 cell line | (Zhu et al., 2007) | N/A |
| HeLa GFP-LMNB1 | (Poser et al., 2008) | N/A |
| NSC34 cell line | (Morelli et al., 2017) | N/A |
| Vectors | | |
| pcDNA5/FRT/TO GFP | (Hageman and Kampinga, 2009) | N/A |
| myc-HSPB1 | (Vos et al., 2010) | N/A |
| myc-HSPB3 | (Vos et al., 2010) | N/A |
| mCherry-HSPB3 | Generated for this article | Genewiz |
| GFP-HSPB3 | (Vos et al., 2010) | N/A |
| myc-R116P | Generated for this article | Genewiz |
| myc-R7S | Generated for this article | Genewiz |
| myc-Y118H | Generated for this article | Genewiz |
| His-HSPB2 | (Vos et al., 2010) | N/A |
| LBR-GFP | (Ellenberg et al., 1997) | N/A |
| myc-HSPB3 d37-43 | Generated for this article | Genewiz |
| myc-HSPB3 dN | Generated for this article | Genewiz |
| mCherry-H2B | AddGene | Hs01072232_m1 |
| α-synuclein | Flagmeier et al., 2016 | N/A |
| pET21a-HSPB3 | Asthana et al., 2012 | N/A |
| pET23b-HSPB7 | Mymrikov et al., 2016 | N/A |
| pUBS520-HSPB6 | Bukach et al., 2004 | N/A |

| | | |
|---|---|---|
| pET28b(+)-HSPB5 | Peschek et al., 2013 | N/A |
| pGEX-4T-GST-HSPB8 | Carra et al., 2005 | N/A |
| shRNA HSPB3 | Dharmacon | VGH5518-200215240 |
| Reagents | | |
| Lipofectamine 2000 | Life Technologies | 11668019 |
| Lipofectamine 3000 | Life Technologies | L3000015 |
| Complete-EDTA | Roche | 11873580001 |
| DAPI | Santa Cruz Biotechnology | SC3598 |
| poly-L-lysine | Sigma-Aldrich | P8920 |
| rh FGF-b/FGF-2 | ImmunoTool | 11343625 |
| Human Insulin Solution | Sigma-Aldrich | I9278 |
| Ham-F12 | Aurogene | L0135 |
| Fetal Bovine Serum (FBS) | Invitrogen | Gibco 10106-169 |
| DMEM | EuroClone | ECM0728L |
| Fetal Bovine Serum (FBS) | Sigma-Aldrich | F7524 |
| Trizol | Zymo Research | R2050 |
| Penicillin/streptomycin | EuroClone | ECB3001D |
| Urea | Sigma-Aldrich | U5378 |
| B-mercaptoethanol | Sigma-Aldrich | M3148 |
| Complete™, EDTA-free Protease Inhibitor Cocktail | Roche | 11873580001 |
| Cycloheximide (used at 50µg/mL) | Sigma-Aldrich | C7698 |
| Polybrene (Hexadimethrine bromide) | Sigma-Aldrich | H9268 |
| Puromycin | Sigma-Aldrich | P8833 |
| IPTG | Invitrogen | 15529-019 |
| Benzonase 250 U/mL | Sigma-Aldrich | E8263-5ku |
| Arabinose | Lucigen | 490234 |
| GsH | Sigma-Aldrich | G4251 |

| | | |
|---|---|---|
| Thioflavin T UltraPure Grade | Eurogentec | AS-88306 |
| NaH2PO4 , BioPerformance Certified > 99.0% | Sigma-Aldrich | S6191 |
| Na2HPO4, ReagentPlus, > 99.0% | Sigma-Aldrich | S0876 |
| NaN3, ReagentPlus, >99.5% | Sigma-Aldrich | S2002 |
| DMPS (1,2-Dimyristoyl-sn-glycero-3-phospho-L-serine) sodium salt | Avanti Polar Lipids | 840033 |
| POPS (1-palmitoyl-2-oleoyl-sn-glycero-3-phospho-L-serine) | Avanti Polar Lipids | 840034 |
| DOPS (1,2-dioleoyl-sn-glycero-3-phospho-L-serine) | Avanti Polar Lipids | 840035 |
| Diphenylhexatriene (DPH) | Sigma-Aldrich | SML0202 |
| Triton X-100 | Sigma-Aldrich | T8787 |
| Bovine serum albumin (BSA) | Sigma-Aldrich | A7906 |
| DABCO | Sigma-Aldrich | 290734 |
| Mowiol | Sigma-Aldrich | M5661 |
| HEPES | Sigma-Aldrich | H3375 |
| DTT | Sigma-Aldrich | D0632 |
| Nonidet 40 (IGEPAL) | Sigma-Aldrich | I8896 |
| NaCl | Sigma-Aldrich | S3014 |
| KCl | Sigma-Aldrich | P3911 |
| Sodium Phosphate dibasic | Sigma-Aldrich | S9763 |
| Potassium Phosphate monobasic | Sigma-Aldrich | P0662 |
| Tween-20 | Sigma-Aldrich | P1379 |
| Commercial kits and enzymes | | |
| Duolink™ In Situ Red Starter Kit Mouse/Rabbit | Sigma-Aldrich | DUO92101 |

| | | | |
|---|---|---|---|
| Lenti-Pac HIV Expression Packaging Kit | GeneCopoeia | HPK-LvTR-20 LT001 | |
| ReliaPrep RNA Cell Miniprep | Promega | Z6011 | |
| RNA Clean & Concentrator | Zymo Research | R1017 | |
| DNase I Set | Zymo Research | E1010 | |
| Maxima First Strand cDNA Synthesis Kit for RT-qPCR | ThermoFisher | K1671 | |
| TAQ SYBR Green qPCR SYBR | ThermoFisher | K0251 | |
| ECL kit Westar Eta C Ultra 2.0 | Cyanogen | XLS075 | |
| ECL kit Westar Supernova | Cyanogen | XLS3 | |
| MycoAlert™ Mycoplasma Detection Kit | Lonza | LT07-318 | |
| Escherichia coli strain BL21 | Thermo Fisher | C607003 | |
| High-Trap Q HP column | GE Healthcare | 17-1154-01 | |
| Sephacryl S300 High-Prep 16/60 column | GE Healthcare | | |
| Superdex 200-pg column | GE Healthcare | | |
| Protino GST/4B Column | Macherey-Nagel | 745515 | |
| Primary antibodies | | | Application |
| c-myc (mouse) | Santa Cruz Biotechnology | SC-40 | 1:500 IF |
| | | | 1:1000 WB |
| TUBA4A (mouse) | Sigma-Aldrich | T6074 | 1:1000 WB |
| LMNB1 (goat) | Santa Cruz | Sc-6217 | 1:100 IF |
| | | | 1:1000 WB |
| LMNB1 (8D1) (mouse) | Santa Cruz | Sc-56144 | 1:100 IF |
| | | | 1:1000 WB |
| LMNA/C (rabbit) | Santa Cruz | Sc-20681 | 1:100 IF |
| | | | 1:1000 WB |
| LBR (rabbit) | Atlas antibodies | HPA062236 | 1:200 IF |

| | | | |
|---|---|---|---|
| | | | 1:1000 WB |
| HSPB3 (rabbit) | Sigma-Aldrich | SAB1100972 | 1:100 IF |
| | | | 1:500 WB |
| HSPB2 (mouse) | Santa Cruz | SC-136339 | 1:100 IF |
| | | | 1:1000 WB |
| V5 (mouse) | LifeTechnologies | R960-25 | 1:100 IF |
| | | | 1:1000 WB |
| GFP Living Colors® (mouse) | Takara | JL-8 | 1:100 IF |
| | | | 1:1000 WB |
| Secondary antibodies | | | |
| Donkey anti-Mouse IgG (H+L), Alexa Fluor® 594 | Thermo Scientific | A-21203 | |
| Donkey anti-Mouse IgG (H+L), Alexa Fluor® 488 | Thermo Scientific | A-21202 | |
| Donkey anti-Mouse IgG (H+L), Alexa Fluor® 647 | Thermo Scientific | A-31571 | |
| Donkey anti-Rabbit IgG (H+L), Alexa Fluor® 488 | Thermo Scientific | A-21206 | |
| Donkey anti-Rabbit IgG (H+L), Alexa Fluor® 594 | Thermo Scientific | A-21207 | |
| Donkey anti-Goat IgG (H+L), Alexa Fluor® 647 | Thermo Scientific | A-21447 | |
| MOUSE IGG HRP LINKED WHOLE AB | GE Healthcare | NXA931 | |
| Rabbit IgG HRP-Linked Whole | GE Healthcare | NA934 | |
| Mouse IgG HRP-Linked Whole | GE Healthcare | NA931 | |
| Donkey anti-Goat IgG-HRP | Santa Cruz) | sc-2020 | |
| Oligomers | Forward | Reverse | |
| Myc-HSPB3 (EX-T1904-Lv107) | TCTAGAACCATGGAGCAGAAAC | ATGATTTTTGCCATGGTACCG | |

| | | |
|---|---|---|
| RPL0 | TTAAACCCTGCGTGGCAATCC | CCACATTCCCCCGGATATGA |
| MYOG | CACTCCCTCACCTCCATCGT | CATCTGGGAAGGCCACAGA |
| HSPB2 | CATGGTCCACAATGTATGGT | ATTTGGGTTTATTCAGCTCCAC |
| HSPB3 | GACTAAGTGACATCGTATCGG | ACAAACATTCTCGTAGTACCAG |
| LMNA | CTCCTACCTCCTGGGCAACT | AGGTCCCAGATTACATGATGCT |
| LMNB1 | GCTGCTCCTCAACTATGCTAAG | GAATTCAGTGCTGCTTCATATTCTC |
| LBR | ATTTGCCGATGGTGAAGTG | TGAGCCACCTTTCCTTTGC |
| LMNB2 | GCCATGAGGACTGTGAAGAAG | AAGGTGTGTGGATGAGGAGTG |
| NOTCH3 | GCCAAGCGGCTAAAGGTA | CACTGACGGCAATCCACA |
| ACTA1 | CTTCGTCGCACATTGTGTCT | GACAGCGCCAAGTGAAGC |
| DES | GGAGAGGAGAGCCGGATCA | GGGCTGGTTTCTCGGAAGTT |
| CADM1 | GAGTTAACATGTGAAGCCATCG | CGACTCTCACCCAAGTTACCA |
| LUM | CTTCAATCAGATAGCCAGACTGC | AGCCAGTTCGTTGTGAGATAAAC |
| NID2 | TAGGCGCTTACGAGGAGGTCAA | TATCAGACCCATCAGATGCCAAAAC |
| DCN | TGCAGGTCTAGCAGAGTTGTGT | AATGCCATCTTCGAGTGGTC |
| SVIL | CTGAAGTTGGACAGGCTGGAAAC | CACCTCCTTCACAGATTTGCCG |
| MFAP5 | GTGCAATATCAGCCAAA | ATTCCAGCCTCATTG |
| GADD45B | GTCGGCCAAGTTGATGAAT | CACGATGTTGATGTCGTTGT |
| Software and Algorithms | | |
| Daniel's XL Toolbox | open-source add-in for Microsoft® Excel® | https://www.xltoolbox.net/ |
| Fiji | NIH | https://fiji.sc/ |
| R Studio | RStudio | http://www.rstudio.com/ |
| ScanR Olympus analysis software | Olympus | https://www.olympus-lifescience.com |
| R2 | N/A | hgserver1.amc.nl/cgi-bin/r2/main.cgi |

| | | |
|---|---|---|
| MARS Data Analysis | BMG LABTECH | https://www.bmglabtech.com/mars-data-analysis-software/ |
| Reader Control | BMG LABTECH | https://www.bmglabtech.com/reader-control-software/ |
| AmyloFit | Meisl et al., 2016 | https://www.amylofit.ch.cam.ac.uk/login |

## Section I

### Cell lines and treatments

HeLa, HeLa Kyoto, HeLa GFP-LMNB1 and NSC-34 cells were maintained in DMEM supplemented with 100 U/mL penicillin/streptomycin and 10% Fetal Bovine Serum (FBS) in a humidified atmosphere at 37°C incubator with 5% CO2. LHCN-M2 cells were maintained in Ham-F12 supplemented with 100 U/mL penicillin/streptomycin, 20% Fetal Bovine Serum (FBS) (Gibco), and 25 ng/mL of rh FGF-b/FGF-2. For induction of myogenic differentiation, LHCN-M2 cells were cultured in DMEM supplemented with 100 U/mL penicillin/streptomycin, and 30ug/mL Human Insulin Solution. Cells were routinely tested for mycoplasma contamination using the MycoAlert kit.

### DNA transfection

Transfections of cDNAs were performed using Lipofectamine 2000 in HeLa, HeLa Kyoto and HeLa GFP-LMNB1 and Lipofectamine 3000 in LHCN-M2, and NSC-34 following manufacturer's instructions. Experiments were performed 48h after transfection of cDNAs for HeLa, HeLa Kyoto and HeLa GFP-LMNB1 and 24h after transfection for LHCN-M2 and NSC-34, unless specified otherwise.

### Viral vector production and viral transduction

Lentiviral particles for GFP, myc-HSPB3 and myc-R116P were packaged with Lentipak packaging system in HEK293T cells using Endofectin, following manufacturer's instructions. 32h post-transfection, the cell culture supernatants containing the viral particles were harvested, filtered with 0.45 µm filter (Minisart Syringe Filter 0.45 µm, cellulose acetate, 16555K, Sartorius) and stored at -80°C in aliquots. shRNA Control and shRNA HSPB3 lentiviral particles were packaged using 2nd generation vectors pPAX2 and pMD2.VSVG into HEK293T cells using the calcium-phosphate method. Filtered lentiviral particles were stored at -80°C in aliquots, as previously described (Morelli et al., 2017).

For viral transduction with lentiviral particles encoding for GFP, myc-HSPB3, myc-R116P, myc-R7S, and myc-Y118H, cycling LHCN-M2 cells were seeded at $5x10^5$ cells/6-well and after 24h culture media was replaced with 1mL of viral suspension supplemented with 8µg/mL of polybrene and incubated for 16h in a humidified atmosphere at 37°C incubator with 5% CO2. The cells were then harvested with trypsin and reseeded in a T25 flask to which cycling media was added and incubated for further 48h. Culture media was then replaced with fresh cycling media supplemented with 4 µg/mL puromycin for selection. Cells were harvested/fixed after 4 days of selection, unless stated otherwise.

For viral transduction with lentiviral particles for shControl and shHSPB3, cycling LHCN-M2 cells were seeded at $5x10^5$ cells/6-well and after 24h culture media was replaced with 1mL of viral suspension supplemented with 8µg/mL of polybrene and incubated for 16h in a humidified atmosphere at 37°C incubator with 5% CO2. Media volume was made up to 2mL by adding 1mL of cycling media, and the culture was further incubated 48h. Culture media was then replaced with fresh cycling media supplemented with 4 µg/mL puromycin for selection. At day 4 of selection, cells were washed twice with PBS and differentiation media (as described above) supplemented with 4 µg/mL puromycin was added. Cells were differentiated for 5 days before being harvested/fixed, with media being replaced every 2 days.

### Immunofluorescence Microscopy

HeLa, HeLa Kyoto, NSC-34 cells and cycling LHCN-M2 were grown on poly-L-lysine coated glass-coverslip, while LHCN-M2 to be differentiated were grown on SPL cell culture chambers (330068; Biosigma). Cells were fixed with 3.7% formaldehyde in PBS 1x for 9 minutes at room temperature, followed by permeabilization with ice-cold acetone 100% for 5 minutes at -20°C. Coverslips were blocked with blocking solution (PBS 1x containing 3% BSA and 0.1% Triton X-100) for 1hours at room temperature and then incubated overnight with primary antibodies at 4°C. Following PBS 1x wash, cells were incubated with fluorescent secondary antibodies for 1 hour at room temperature in the dark.

Primary and secondary antibodies were diluted in blocking solution. Primary and secondary antibodies used are listed below. Cells were then washed with PBS 1x and the coverslips were mounted on glass microscope slides with mounting solution (PBS pH 7,4, Mowiol 20%, 1.4-diazabiciclico-[2,2,2]-ottano DABCO as antifading agent). Slides were stored at 4°C.

The primary and secondary antibodies used in this study are detailed in the table above.

### *Immunofluorescence microscopy acquisition, processing, and image analysis*

Confocal microscopy of fixed samples was performed using a Leica TCS SP8 microscope (Leica Microsystems) equipped with a White Light Laser and a 63x oil-immersion lens. Images were acquired at 1024x1024 pixel resolution and 400Hz scanning speed.

### *Cellular distribution analysis*

Fields were randomly selected, and confocal images were analysed using ImageJ Fiji cell counter and manually assessed for nuclear and/or cytoplasmic enrichment.

### *LBR rim analysis*

LBR enrichment at the nuclear rim was performed using ScanR software (Olympus Corporation). Myoblast nuclei were segmented based on DAPI signal using intensity detection algorithm. The LMNB1 (8D1) signal detection at the nuclear rim was performed by applying a fixed distance in pixels from the segmented nucleus. Similar fixed distance was applied to measure fluorescence intensity inside the nucleus (nucleoplasm). The mean fluorescence intensity of LBR was measured at the rim and inside the nucleoplasm. The relative enrichment of LBR at the rim was calculated as a ratio of mean fluorescence intensity at the rim divided by mean intensity in nucleoplasm. From the values obtained ratios of above 1.2 were considered as “Nuclear envelope enriched” whereas ratio under 1.2 were considered as “diffuse in the nucleus”.

### *Proximity Ligation Assay (PLA)*

Proximity Ligation Assay (PLA) was performed on HeLa cells using Duolink In Situ Red (Sigma) with the antibodies anti-GFP and anti-HSPB3, as per manufacturer’s instructions. Z-stack images were acquired every 1 µm using Leica TCS SP8 at 1024x1024 pixel resolution, 400Hz scanning speed. Quantification of PLA foci was performed using ScanR. Cell bodies were segmented using the GFP signal and the intensity detection algorithm while PLA foci were segmented using the edge detection algorithm. Samples stained with anti-GFP only, anti-HSPB3 only or No Antibody were used as controls, and ratio of anti-GFP + anti-HSPB3 by anti-GFP only was calculated to normalize for background.

### *Chromocenter analysis*

Confocal microscopy images composed of 0.3µm Z-stacks spanning the whole nucleus, determined by DAPI staining were used for chromocenter analysis. Chromocenter analysis was performed using

the ImageJ Fiji NucleusJ plugin (Poulet et al, 2015). Briefly, images were first segmented using Nucleus Segmentation (batch mode) setting the Voxel Calibration at x = 0.075, y = 0.075, z = 0.029, units = pixel; volumes set as Min Volume = 7, Max Volume = 2000. Then analysis of segmentation was performed using Nucleus Segmentation and Analysis (batch mode) keeping the Voxel Calibration and volumes as before. The chromocenters were then identified using Chromocenter Segmentation (batch mode), consisting of 2 components: an automatic step using the voxel settings as before; followed by a manual step. For the manual step, the following setting were used for the Threshold: Stack Histogram, 99.5%, these setting were applied across all samples. Finally, Chromocenter Analysis (batch mode) was performed and NbCc (Number of Cc) and VCcMean (Mean volume of chromocenter/ nucleus) used for further analysis.

### Live-cell imaging and Fluorescence recovery after photobleaching (FRAP)

Live-cell imaging was done using the Leica SP8 system. FRAP measurements on HeLa cells transfected with LBR-GFP in presence of absence of mCherry-HSPB3 were performed using a confocal microscope Leica TCS SP8 (Leica Systems).

For FRAP analysis we used a 63× oil immersion objective. A region of approximately 2.2–2.5 × 2.2–2.5µm was bleached for 1 s using a laser intensity of 100% at 405 nm. For FRAP analysis of untreated cells or in cells during the stress recovery in drug-free medium, a laser intensity of 100% for 5 s was used. Recovery was recorded for 300 time points after bleaching (300 s). Analysis of the recovery curves were carried out with the FIJI/ImageJ. The flow of the protein was measured by quantifying the recovery of the bleached area at the cost of the unbleached region and using a custom written FIJI/ImageJ routine. The bleached region was corrected for general bleaching during image acquisition. We quantified the molecules that move from the unbleached region to the bleached region, leading to recovery of the bleached region.

Prior to FRAP analysis, we corrected the images for drift using the StackReg plug-in function of the FIJI software suite. The equation used for FRAP analysis is as follows ((Ibleach − Ibackground)/(Ibleach(t0) − Ibackground(to)))/((Itotal-Ibackground)/(Itotal(t0) − Ibackground(to))), where Itotal is the fluorescence intensity of the entire cellular structure, Ibleach represents the fluorescence intensity in the bleach area, and Ibackground the background of the camera offset. FRAP curves were averaged to obtain the mean and standard deviation. Fluorescent density analysis was performed using FIJI/ImageJ and selecting specific region of interest (ROI).

### Protein extract preparation and western blottling

For whole cell lysates, cells were harvested and lysed in Laemmli buffer (2%) with 4M urea (Sigmal-Aldrich, U5378) and homogenized by sonication for 5 seconds. Protein samples were reduced with β-mercaptoetanol (Sigma-Aldrich, M3148) (final 3-5%) and boiled for 3 minutes at 100 °C and were separated on SDS-PAGE gels at 10% or 12.5% (Laemmli et al. 1970) at 50mV for 30min then 100mV for 1h. After separation by electrophoresis, proteins were transferred into nitrocellulose membrane using Bio-rad Wet/Tank Blotting System at 70mV for 90min.

Nuclear and cytoplasmic fractions were isolated in lysis buffer (10mM HEPES pH7.9, 10mM KCl, 0.1 mM EDTA, 0.1 mM GDTA, 1mM DTT, 0.15% nonidet 40, 1% Phosphatase Inhibitor Cocktail 1X) and homogenized using a 26G needle followed by 5s sonication. Lysates were centrifuged at 12,000g for 30s, the nuclear fraction (pellet) was resuspended in Laemmli buffer (2%); to the cytoplasmic fraction was added Laemmli buffer (8%). Protein samples were reduced with β-mercaptoetanol (final 3-5%) and boiled for 3 minutes at 100 °C, run and blotted as above.

Membranes were blocked with PBS-T (137mM NaCl, 2.7mM KCl, 10mM Sodium Phosphate dibasic, 2mM Potassium Phosphate monobasic, 0.1% Tween-20, pH 7,4) and 5% dried non-fat milk for 1hour at room temperature. Primary antibodies diluted in PBS-T containing 3% BSA and 0.02% Na-azide were added and incubated overnight at 4°C. HRP-conjugated secondary antibodies (GE Healtcare) were prepared in PBS-T and 3% dried non-fat milk and incubated for at least 1hour at room temperature. Protein signals were visualized using ECL kit Westar. Chemiluminescence signals were acquired on a ChemiDoc imaging system. Images were analysed with ImageLab analysis tools, and signal intensities measured and normalized to the loading control.

The primary and secondary antibodies used in this study are detailed in the table below. Where quantifications are provided, samples were processed in parallel and run/blotted within the same gel to avoid run discrepancies, and quantification performed using ImageLab.

### RNA extraction and RT-qPCR

For gene expression analysis on HeLa cells, total RNA was isolated using ReliaPrep RNA Cell Miniprep system according to the manufacturer's instructions. For gene expression analysis on LHCN-M2 cells, total RNA was isolated using Trizol, as per manufacturer’s instructions. Followed by purification using RNA Clean & Concentrator, and DNase I Set, as per manufacturer’s instructions.

First-strand cDNA was generated using Maxima First Strand cDNA Synthesis Kit for RT-qPCR according to the manufacturer's instructions. For each reaction 1ug of total RNA was used. The samples were incubated at 25°C for 10 minutes followed by a step of 50°C for 15 minutes, and then 85°C for 5 minutes. The cDNA was stored at -20°C or used immediately for real-time PCR (Q-PCR).

cDNA was amplified using Relative in a CFX96 Touch Thermal cycler (Bio-Rad, Hercules, CA, USA) using TAQ SYBR Green qPCR SYBR. For each reaction 50ng of cDNA was used. The real-time PCR was performed as follow: one cycle of denaturation (95°C for 3 minutes) followed by 40 cycles of amplification (95°C for 10 seconds, 60°C for 30 seconds). Each reaction was monitored by the use of a negative control (no template). DNA amounts were quantified using the ΔΔCt method, and the nontreated (or lentiviral control i.e. LVGFP or shCtrl) condition was set to 1. A list of all primers used is in Supplementary Table 2.

### RNAseq

For RNAseq analysis, LHCNM2 total RNA was extracted as described above. Libraries were prepared using the TruSeq Stranded mRNA Library Prep Kit. Library preparation started with 1 µg total RNA. After selection (using poly-T oligo-attached magnetic beads), mRNA was purified and fragmented using divalent cations under elevated temperature. The RNA fragments underwent reverse transcription using random primers followed by second strand complementary DNA (cDNA) synthesis with DNA Polymerase I and RNase H. After end repair and A-tailing, indexing adapters were ligated. The products were then purified and amplified (20 µl template, 14 PCR cycles) to create the final cDNA libraries. After library validation and quantification (Agilent 2100 Bioanalyzer), equimolar amounts of library were pooled. The pool was quantified by using the Peqlab KAPA Library Quantification Kit and the Applied Biosystems 7900HT Sequence Detection System. The pool was sequenced on an Illumina HiSeq 3000 sequencer with a paired-end (2 × 75 bp) protocol.

RNA-seq data were analysed using a SnakePipes pipeline. Raw counts (output of SnakePipes RNA-seq module) were used as input for DESeq2. FPKMs, FC and P-values were calculated with DEseq2.

### Statistical analysis

One-way ANOVA followed by Bonferroni–Holm post-hoc test was used for comparisons between three or more groups using R. Student’s t-test was used for comparisons between two groups. *P<0.05; **P<0.01; ***P<0.001. Where specified Kruskall-Wallis test was used for comparison between non-normally distributed data using R. *P<0.05; **P<0.01; ***P<0.001. For RNA-seq data, FC and P-values were calculated with DEseq2 using R.

## Section II

### Protein production

#### *α-synuclein*

α-synuclein was expressed and purified as described previously (Nakajo et al., 1990; Shibayama-Imazu et al., 1999; Kim et al., 2014). To determine the concentrations in solution absorbance value of the protein measured at 275 nm and an extinction coefficient of 5,600 M−1 were used. The protein solutions were divided into aliquots, flash frozen in liquid N2 and stored at -80°C, until required for use.

#### *HSPB3 and HSPB7*

HSPB3 and HSPB7 were expressed and purified as described previously in Asthana et al. (2012). Briefly, pET21a containing the human HSPB3 coding sequence, or pET23b containing HSPB7 (kindly provided by Prof. Johannes Buchner, Technische Universität München) were transformed into Escherichia coli strain BL21. Protein expression was induced with 1mM IPTG at 37°C for 4h. E. coli pellet was lysed in Buffer A (20 mM phosphate buffer, pH 7.4150; 100 mM NaCl; 2 mM DTT) supplemented with 1 tablet of cOmplete Protease Inhibitor Cocktail and Benzonase 250 U/mL for 40min on ice, followed by sonication: 1x5 min 60% amp, 2sec ON/ 2sec OFF. Inclusion bodies containing protein were isolated by centrifugation (JA-20 @ 13,500rpm for 1h), and washed with Wash Buffer (20 mM phosphate buffer, pH 7.4; 100 mM NaCl; 0.05 % Triton X-100) using 4 to 6mL per g of wet cell weight. It was further washed twice with buffer A to remove Triton X-100 (4 to 6mL per g of wet cell weight). The inclusion bodies were then solubilized in buffer A containing 6 M urea (2 to 4mL per g of wet cell weight) and incubated at 30°C for 15min. After centrifugation at 100,000g for 1h (to remove aggregated protein), the solution was filtered through 0.22 µm filter. The protein was allowed to refold by diluting the solution twofold with buffer A (to 3 M urea) and then fivefold from the sample in 3 M urea (to 0.6 M urea), followed by dialysis (in phosphate buffer). The protein solutions were divided into aliquots, flash frozen in liquid N2 and stored at -80°C, until required for use.

#### *HSPB6*

HSPB6 was expressed and purified as described previously in Bukach et al. (2004). Briefly, pUBS520 containing the human HSPB6 coding sequence (kindly provided by Prof. Johannes Buchner, Technische Universität München) was transformed into Escherichia coli strain BL21. Protein expression was induced with 1mM IPTG at 30°C for 4h. E. coli pellet was lysed in Buffer A (50 mM

Tris/HCl, pH 8.0; 100 mM NaCl; 1 mM EDTA; 2 mM DTT) supplemented with 1 tablet of cOmplete Protease Inhibitor Cocktail and Benzonase 250 U/mL by sonication: 1x5 min 60% amp, 2sec ON/ 2sec OFF. The crude extract of HSPB6 was fractionated with $(NH_4)_2SO_4$ (50% saturation) and allowed precipitate to form for 30min at 4°C with stirring. Precipitate was resuspended to the original volume with Buffer A. Solution then subjected to ion-exchange chromatography on a High-Trap Q column equilibrated with Buffer B and developed by a linear (10 – 410 mM) gradient of NaCl. Fractions containing the protein were gel filtrated on a Sephacryl S300 High-Prep 16/60 column, followed by dialysis (in phosphate buffer). The protein solutions were divided into aliquots, flash frozen in liquid N2 and stored at -80°C, until required for use.

### *HSPB5*

HSPB5 was expressed and purified as described previously in Peschek et al. (2013). Briefly, pET28b+ containing the human HSPB5 coding sequence (kindly provided by Prof. Johannes Buchner, Technische Universität München) was transformed into Escherichia coli strain BL21. Protein expression was induced with 1mM IPTG at 30°C for 4h. E. coli pellet was lysed in Buffer A (50 mM Tris/HCl, pH 8.0; 100 mM NaCl; 1 mM EDTA; 2 mM DTT) supplemented with 1 tablet of cOmplete Protease Inhibitor Cocktail and Benzonase 250U/mL by sonication:1x5 min 60% amp, 2sec ON/ 2sec OFF. After cell disruption, the cleared lysate was applied on a Hi-Trap column equilibrated with TE buffer pH 9.0 B and developed by a linear (20mM–1M) gradient of NaCl. Fractions containing the target protein were pooled, concentrated, and loaded onto a Superdex 200-pg column run in TE, and eluted with linear (20mM–1M) NaCl gradient, followed by dialysis (in phosphate buffer). The protein solutions were divided into aliquots, flash frozen in liquid N2 and stored at -80°C, until required for use.

### *HSPB8*

HSPB8 was expressed and purified as described previously in Carra et al. (2005). Briefly, pGEX-4T containing the GST-tagged human HSPB8 coding sequence (Carra et al., 2005) was transformed into Escherichia coli strain BL21(C607003, Thermo Fisher). Protein expression was induced with 1mM IPTG and 10mL/L arabinose at 30°C for 4h. E. coli pellet was lysed in PBS buffer (supplemented with 1mM DTT, 1 tablet of cOmplete Protease Inhibitor Cocktail and Benzonase 250U/mL by sonication:1x5 min 60% amp, 2sec ON/ 2sec OFF. After cell disruption, the cleared lysate was applied on a Protino GST/4B Column, equilibrated PBS buffer and eluted with elution buffer containing GsH (PBS pH7.4 KOH, 1mM DTT, 1mM EDTA, 20mM GsH. Eluate is dialysed in PBS buffer (supplemented

with 1mM DTT, 1 table of cOmplete and Benzonase 250U/mL ON at 4°C with rotation. Solution is reapplied into Protino GST/4B Column and developed by a linear KCl gradient (20mM - 1M). Fractions are run through SDS-PAGE and the ones containing HSPB8 only are pooled and applied on a Hi-Trap column equilibrated with low salt buffer (40mM Hepes pH 7.4, 20mM KCl, 1mM DTT, 1mM EDTA) and and developed by a linear KCl gradient (20mM - 1M), followed by dialysis (in phosphate buffer). The protein solutions were divided into aliquots, flash frozen in liquid N2 and stored at -80°C, until required for use.

### Far-UV circular dichroism (CD) spectroscopy

CD samples were prepared by incubating 25 µM of HSPBs in 20 mM phosphate buffer, pH 6.5 or 5.5, or in absence or presence of 100 µM DMPS in 20 mM phosphate buffer, pH 6.5. Far-UV CD spectra were recorded on a JASCO J-810 spectrophotometer (JASCO UK, Ltd) equipped with a Peltier thermally controlled cuvette holder at 30°C. Quartz cuvettes with path lengths of 1 mm were used and CD spectra were obtained by averaging three individual spectra recorded between wavelengths of 250 and 200 nm, with a bandwidth of 1 nm, a data pitch of 0.2 nm, a scanning speed of 50 nm/min, and a response time of 1 s. For each protein sample, the CD signal of the buffer used to solubilize the protein, or the signal of DMPS alone, was recorded and subtracted from the CD signal of the protein. The CD data was normalized in molar ellipticity per residue as per below:

[q]res(deg cm2 dmol-1) = [q(mdeg) • mol weight > (g/mol)] / [(10 • number of res.• optical path(cm) • C (mg/cm3)]

### Lipid vesicle preparation

DMPS lipid powder was dissolved in 20 mM phosphate buffer (NaH2PO4/$Na_2HPO_4$), pH 6.5, 0.01% $NaN_3$ and stirred at 45°C for 4 h. The solutions were then frozen and thawed five times using dry ice and a water bath at 45°C. Lipid vesicles were prepared by sonication (Bandelin, Sonopuls HD 2070, 3 x 5 min, 50% cycle, 10% maximum power) and centrifuged at 15,000 rpm for 30 min at 25C.

POPS and DOPS lipid films were prepared by transferring the desired volume of lipid stock solution with a Hamilton syringe into a round bottom flask and the solvent was evaporated using a gentle flow of nitrogen gas. The flasks were then incubated overnight under vacuum to remove any residual traces of solvent. The lipid films or powders were dissolved in 20 mM phosphate buffer (Na2HPO4/NaH2PO4), pH 6.5, 0.01% $NaN_3$), and stirred at 45°C for 2 h. The solutions were then frozen and thawed five times using dry ice and a water bath at 45°C. Lipid dispersions were prepared

using sonication (3 × 5 min, 50 % cycles, 10 % maximum power) on ice, and centrifuged at 15,000 rpm for 30 min at 25C.

### Seed fibril preparation

Seed fibrils were produced as described previously (Kim et al., 2014). 500 µL samples of α-synuclein at concentrations from 500-800 µM were incubated in 20 mM phosphate buffer (pH 6.5) for 48-72 h at ca. 40◦C and stirred at 1,500 rpm with a Teflon bar on an RCT Basic Heat Plate (IKA, Staufen, Germany). Fibrils were diluted to a monomer equivalent concentration of 200 µM, divided into aliquots, flash frozen in liquid N2 and stored at -80◦C. For experiments at pH 6.5 the 200 µM fibril stock was sonicated for between 0.5 and 1 min using a probe sonicator (Bandelin, Sonopuls HD 2070, Berlin, Germany), using 10% maximum power and a 50% cycle. For experiments at low pH with nM fibril concentrations the 200 µM stock was diluted to 10 µM in water, sonicated 3 times for 5 s using 10% maximum power and 50% cycles using the probe sonicator.

### Measurements of aggregation kinetics (ThT assay)

WT α-synuclein were incubated at 20 µM, in the presence or absence of HSPBs at the concentrations indicated, and of 50 µM ThT and either preformed fibrils or DMPS vesicles at 37◦C or 30◦C, respectively (Flagmeier et al., 2016). The change in the ThT fluorescence signal was monitored using a Fluostar Optima or Polarstar Omega fluorescence plate reader (BMG Labtech, Aylesbury, UK) in bottom reading mode under quiescent conditions. Corning 96 well plates with half-area (3881, polystyrene, black with clear bottom) non-binding surfaces sealed with metal sealing tape were used for each experiment. At the end of each aggregation experiment the concentrations of monomeric and fibrillar states of the protein were determined as described previously (Flagmeier et al., 2016).

### Analysis of the aggregation kinetics

#### *Determination of the lipid-induced aggregation rate*

By fitting a linear slope to the early time points of the aggregation reaction, we can obtain the value of 2k+P(0)m(0). For the comparison of the effective rate constants when different HSPBs are introduced, we then calculated the ratio of the extracted k+ value for each chaperone to that of the control experiment with α-synuclein alone.

The change in mass concentration of fibrils with time M(t) was fitted using the model described previously (Galvagnion 2015; Flagmeier et al., 2016) and the following equation:

$$\boldsymbol{M(t) = \frac{K_M k + m(0)^{n+1} k_n b t^2}{2\left(K_M + m(0)\right)}}$$

where $k_+$ is the elongation rate constant of fibrils from lipid vesicles, $k_n$ is the heterogeneous primary nucleation rate constant, n is the reaction order of the heterogeneous primary nucleation reaction relative to the free monomer, m, b is the total mass concentration of the protein bound to the lipid at 100% coverage ($\boldsymbol{b = \frac{[DMPS]}{L}}$, with L the stoichiometry) and $K_M$ is the Michaelis constant (fixed at 125 µM, as determined previously (Galvagnion et al., 2015). This global analysis yields $k_n k_+$ and n, for each variant. We then estimated the rate of aggregation of each variant on lipid vesicles, using AmyloFit (Meisl et al., 2016) to fit the kinetics to the model described above.

### *Derivation of the approach used to analyse highly seeded aggregation data*

The change in mass concentration of fibrils for aggregation experiments at high seed concentrations (µM) was fitted using the model described previously (Flagmeier et al., 2016). For aggregation experiments at high seed concentrations (µM), under which primary nucleation of α-synuclein can be neglected, and under quiescent conditions, where fragmentation is negligible, the aggregation kinetics for the consumption of monomers can be described by

$$\boldsymbol{\frac{dm(t)}{dt} = -\frac{dM(t)}{dt} = -2k_+ P(t) m(t)}$$

where $k_+$ is the fibril elongation rate constant, $m(t)$ the monomer concentration, M(t) is the mass concentration of fibrils and $P(t)$ the number concentration of fibrils. At early times in the aggregation reaction, the monomer concentration and the fibril number concentration can be assumed to be constant, hence $m(t) = m(0)$ and $P(t) = P(0)$, and:

$$\boldsymbol{\frac{dM(t)}{dt}|_{t=0} = 2k_+ P(0) m(0)}$$

By fitting a linear slope to the early time points of the aggregation reaction, we can obtain the value of 2k+P(0)m(0). For the comparison of the effective rate constants when different HSPBs are introduced, we then calculated the ratio of the extracted k+ value for each chaperone to that of the control experiment with α-synuclein alone.

# Results

## Section I – Role of HSPB3 in myogenesis

### HSPB3 is enriched at the nuclear envelope

HSPB3 was first identified in a complex with HSPB2 in skeletal muscle cells (den Engelsman et al., 2009). HSPB3 expression is absent in cycling cells, being specifically upregulated by MYOD during muscle cell differentiation (Sugiyama et al., 2000). LHCN-M2 cells, which are human myoblasts immortalized with human telomerase (hTERT) that were previously characterized (Zhu et al., 2007) were used to address the question whether HSPB3 participates in myogenic differentiation. In particular, upon serum starvation LHCN-M2 cells exit the cell cycle and commit to differentiation, forming myotubes. Key steps in the differentiation process are the increase in the expression of myogenic transcription factors such as MYOD and myogenin (MYOG). In agreement with the literature (Morelli et al., 2017; Sugiyama et al., 2000), HSPB3 and its partner HSPB2 were confirmed to be absent in cycling human LHCN-M2 cells (herein referred to as myoblasts), but were upregulated in differentiating myoblasts, along with the muscle-specific transcription factor MYOG (Figure 9A).

Immunofluorescence (IF) experiments followed by confocal microscopy were performed with the aim of characterizing HSPB3 expression and localization on myoblasts and HeLa cells. Confocal microscopy studies confirmed HSPB3 induction during differentiation and highlighted a heterogeneous subcellular distribution of HSPB3 in this cell type, similar to what was previously found for HSPB2 (Morelli et al., 2017). Specifically, some differentiating myoblasts cells showed a diffuse HSPB3 staining both in the cytoplasm and nucleoplasm, while others showed an enrichment of HSPB3 at the nuclear envelope (NE) (Figure 9B). Staining of the NE with lamin B1 (LMNB1) further confirmed the recruitment of HSPB3 at the NE in differentiating myoblasts (Figure 9C). To avoid possible misinterpretation due to antibody artifact, myc-tagged HSPB3 was transduced in cycling myoblasts that do not express the endogenous protein and its subcellular distribution and colocalization with LMNB1 was assessed. Overexpressed myc-HSPB3 showed a distribution resembling the one of the endogenous protein, with enrichment at the NE and colocalization with LMNB1 at the NE and at lamin filaments/folds (Figure 9D).

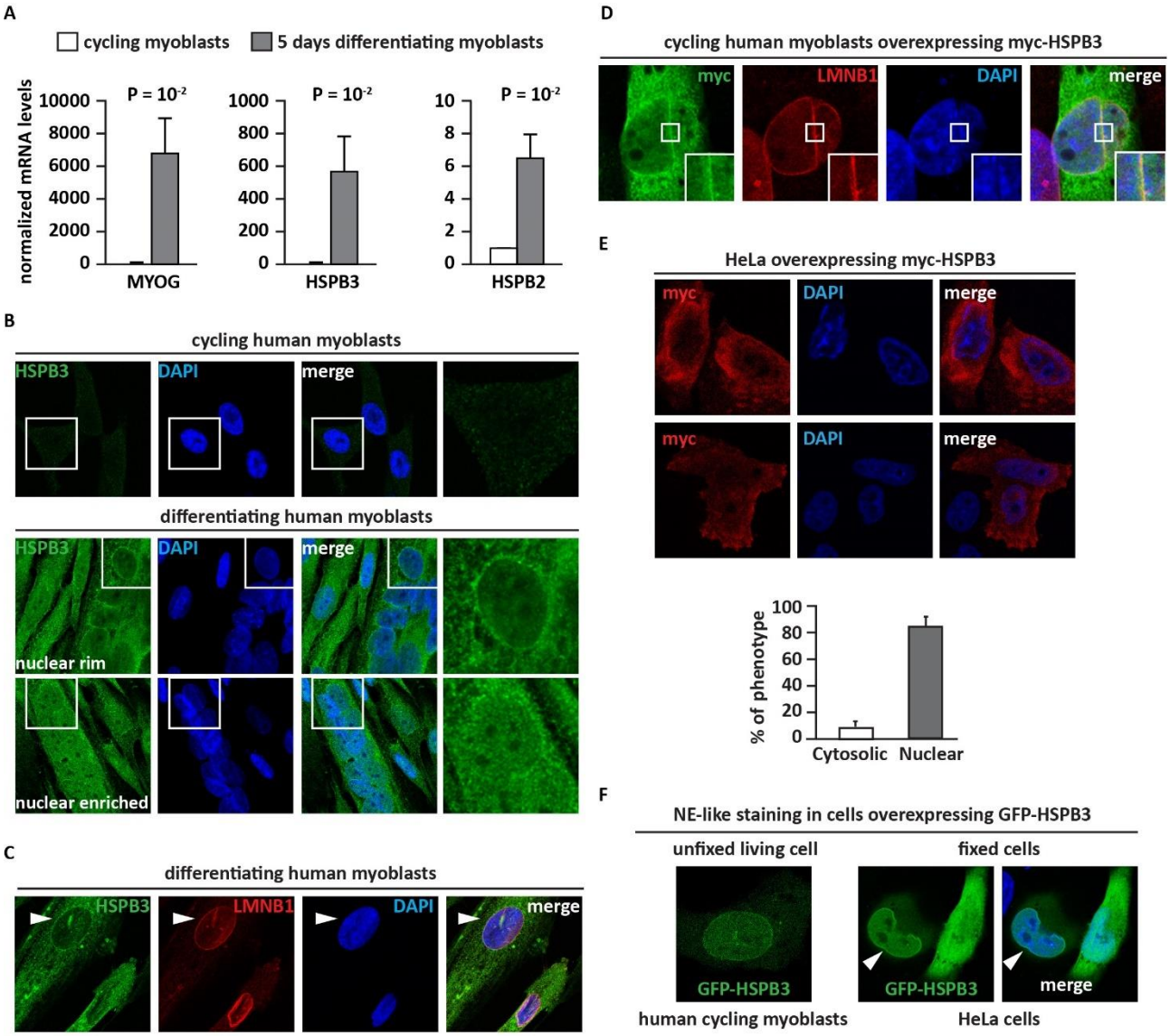


Figure 9 HSPB3 is upregulated in differentiating myoblasts and is enriched at the nuclear envelope. (A) HSPB2, HSPB3 and myogenin (MYOG) mRNA levels were measured by qPCR in cycling and 5-days differentiating human myoblasts. n= 3, ± sem; p =$10^{-2}$ (HSPB3, HSPB2 and MYOG). (B) Immunofluorescence pictures showing absence of endogenous HSPB3 (green) in cycling human myoblasts (top panel) and its subcellular distribution in 7-day differentiating human myoblasts (lower panel). DAPI staining is shown. (C) 7-day differentiating human myoblasts expressing endogenous HSPB3 and stained for HSPB3 and lamin B1 (LMNB1). (D) Cycling human myoblasts infected with lentiviral particles expressing myc-HSPB3 immunostained with antibodies against myc and LMNB1. (C, D) Endogenous HSPB3 and myc-HSPB3 colocalize with LMNB1. DAPI staining is shown. (E) Immunofluorescence pictures showing the subcellular localization of myc-HSPB3 after 48h of transfection in HeLa cells. Quantitative percentage of myc-HSPB3 phenotypes observed in HeLa - 3 experiments; n = 331. Data indicate mean ± SEM. (F) Overexpressed GFP-HSPB3 (co-expressed at a 1:8 ratio with myc-HSPB3 for 24 hrs) shows a NE-like staining in living human myoblasts (left panel) and in fixed HeLa cells (right panel). DAPI staining is shown.

To understand whether the enrichment of HSPB3 at the NE was cell-type specific, HSPB3 subcellular distribution was further analysed in HeLa cells. Since HeLa cells do not express detectable levels of endogenous HSPB3, according to The Human Protein Atlas, myc-tagged HSPB3 was transiently transfected in these cells. Overexpression of myc-HSPB3 led to a predominantly nuclear-enriched

expression with approximately 80% of the protein being present in the nucleus as compared to the cytoplasm (Figure 9E). Finally, NE-like staining was also observed on GFP-tagged HSPB3 in living myoblasts and in HeLa cells (Figure 9F). Together these data indicate that a pool of HSPB3 is enriched at the NE and this occurs independent on the cell type.

It was also noted that HSPB3 was not homogeneously distributed inside the nucleus, but instead was enriched in structure resembling amorphous or liquid-like condensates (Figure 10A, B) (Banani et al., 2017). Morelli et al. (2017) previously reported that HSPB2 formed intranuclear liquid-like condensates via liquid-liquid phase separation and in a concentration dependent manner. Therefore, this raised the question whether HSPB3 behaved in a similar manner to HSPB2. Firstly, HeLa cells co-expressing GFP-tagged and myc-tagged HSPB3 in cycling myoblasts and were analysed for protein dynamics by live-cell imaging. In both cell lines, overexpressed HSPB3 formed dynamic nuclear condensates that touched one another and coalesced (Figure 10A). These condensates dissolved with time in cycling myoblasts, while they persisted in HeLa cells (Figure 2B). As the N-terminus of HSPB3 is intrinsically disordered (Sudnitsyna et al., 2012), series of experiments were set up to determine if the N-terminus was required for HSPB3 condensate formation.

Deletion mutants that lack the entire N-terminus (myc-HSPB3 dN) or a short fragment of 7-residues that is predicted to be unfolded (myc-HSPB3 d37-43) (Figure 10C) were analysed for their subcellular distribution and tendency to form condensates. Confocal microscopy studies clarified that deletion of the N-terminus ($p < 10^{-3}$), but not of the short fragment of 7 residues, reduced the nuclear localization of HSPB3, as well as its ability to form condensates, which mainly occurred inside the nucleus (Figure 10D). This observation was confirmed through the analysis of nuclear and cytosolic fractions by western blotting (Figure 10E). A similar phenotype was observed in cycling myoblasts, where deletion of the N-terminal also led to a reduction in nuclear localization ($p < 10^{-3}$) (Figure 10F). This observation was confirmed by analysis of nuclear and cytosolic protein fractions by western blot: while full-length HSPB3 was enriched in the nuclear fraction, the N-terminal mutant was present at an equivalent level in the cytoplasmic and nuclear fractions (Figure 10G). Thus, the nuclear accumulation of HSPB3 and its self-assembly into dynamic condensates are driven by the N-terminus of HSPB3. The lack of effect of the 7-residue deletion mutant (myc-HSPB3 d37-43) supports the interpretation that other residues within the N-terminus of HSPB3 contribute to the intrinsicly disordered domain (Sudnitsyna et al., 2012).

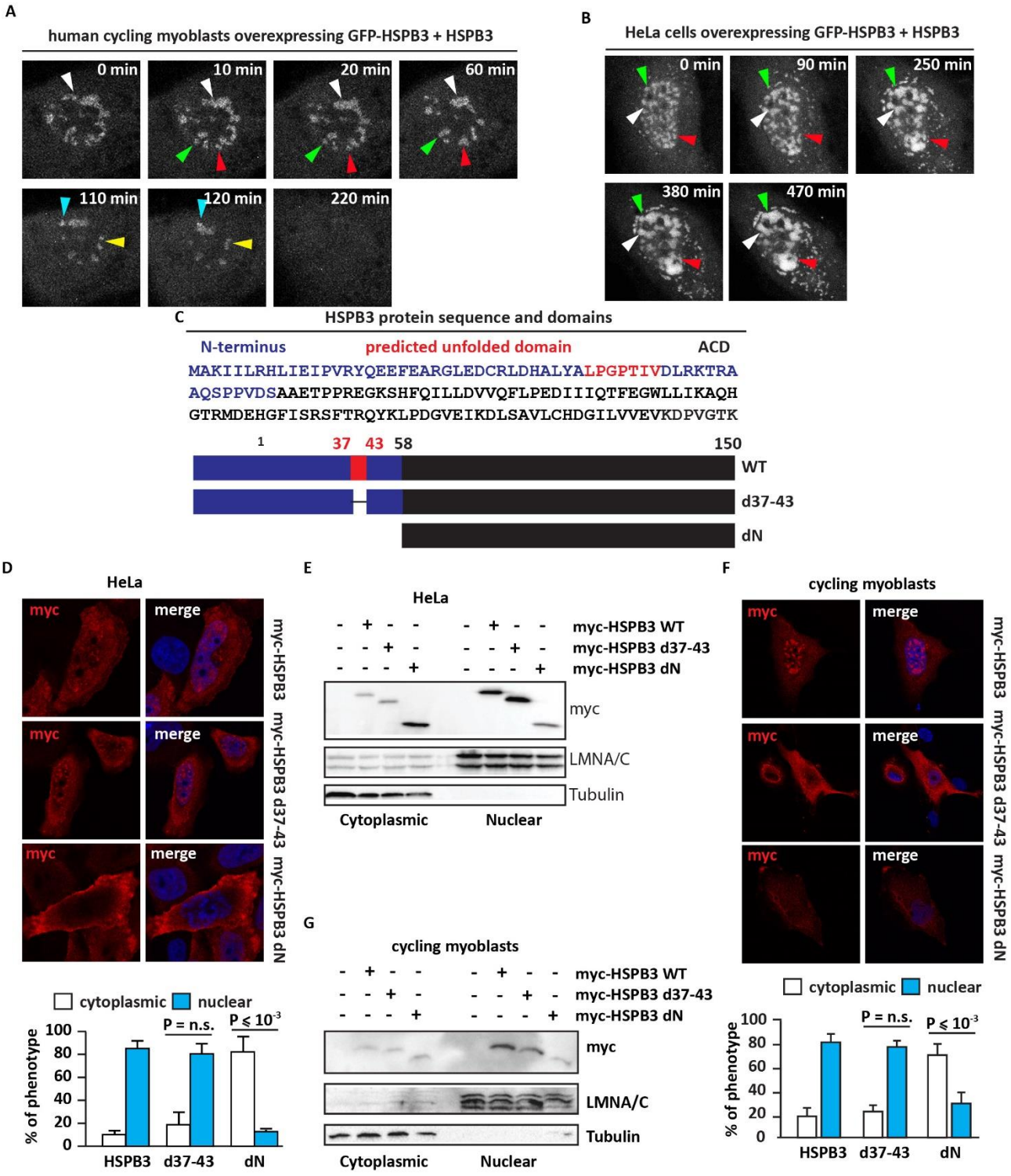


Figure 10 HSPB3 nuclear localization is dependent on its N-terminus. (A) Live-cell confocal imaging of human cycling human myoblasts overexpressing GFP-HSPB3 + myc-HSPB3 (at a 1:8 ratio) for 24 hrs. Pictures were taken every 10 min. Representative pictures are shown. Arrowheads show dynamic nuclear condensates that touch one another, fuse, and then dissolve. (B) Live-cell confocal imaging in HeLa cells overexpressing GFP-HSPB3 + myc-HSPB3 (at a 1:8 ratio) for 48 hrs. Pictures were taken every 10 min. Representative pictures are shown. Arrowheads show dynamic nuclear condensates that touch one another and fuse, growing in size. (C) Sequence and schematic representation of the HSPB3 protein and the deletion mutants lacking the N-terminus (dN) and the predicted IDR domain (d37-43), respectively. Blue indicates the N terminus; black indicates the alpha-crystallin domain (ACD); red indicates the predicted IDR. (D) Immunofluorescence of HeLa cells overexpressing myc-HSPB3 WT, dN or d37-43 for 48h. Quantitative percentage of

myc-HSPB3 distribution is reported; n = 4 independent experiments, ± sem. $P < 10^{-3}$ between cells expressing HSPB3 WT or dN. Total number of cells analysed: 440 (WT), 458 (dN), and 384 (d37-43). (E) Immunoblotting of nuclear/cytoplasmic fractions of HeLa cells overexpressing myc-HSPB3 WT, dN or d37-43 for 48h. Tubulin and LMNAC were used as loading controls for cytoplasmic and nuclear fractions, respectively. (F) Immunofluorescence of cycling human myoblasts overexpressing myc-HSPB3 WT, dN or d37-43 for 24 hrs. Quantitation of HSPB3 distribution is reported. n = 3 independent experiments, ± sem. $P < 10^{-3}$ between cells expressing HSPB3 WT or dN. Total number of cells analysed: 93 (WT), 61 (dN), and 132 (d37-43). (G) Immunoblotting of nuclear/cytoplasmic fractions of cycling human myoblasts overexpressing myc-HSPB3 WT, dN or d37-43 for 24h. TUBA4A and LMNAC were used as loading controls for the cytoplasmic and nuclear fractions, respectively.

## HSPB3 affects myogenin expression

HSPB3 was first identified as a complex with HSPB2 in skeletal muscle cells (den Engelsman et al., 2009). However, expression of HSPB3 has also been reported in the hypothalamus, frontal cortex, hippocampus, striatum, and midbrain in mice, while HSPB2 has only been detected in the hippocampus and cortex (Kondaurova et al., 2010). In differentiating myoblasts, HSPB2 and HSPB3 displayed different subcellular localizations during the early steps of differentiation. HSPB2 has been described to form intranuclear foci previously characterized as phase-separated compartments in differentiating LHCN-M2 (Morelli et al., 2017); instead, in the same cells HSPB3 was enriched at the NE and in nuclear filaments, which are reminiscent of the nuclear lamin meshwork (Figure 11A). This observation, together with previous reports of different expression patterns, led to the question whether HSPB3 might also exist in a pool separate from HSPB2. To assess this, the colocalization of endogenous HSPB2 and HSPB3 differentiating myoblasts was analysed through the use of Pearson Correlation Coefficient (PCC), in which a value of +1 represents total positive linear correlation, 0 no linear correlation, and −1 total negative linear correlation. This analysis resulted in a PCCs of 0.13, confirming the distinct subcellular pattern of HSPB2 and HSPB3 ($p < 10^{-16}$) (Figure 11B). As a control, PCCs of the myc and HSPB3 staining in myoblasts overexpressing myc-tagged HSPB3 was significantly higher (PCC = 0.7); this significance was lost by rotating of 90 degrees the red channel (PCC = 0.03), as expected. These results suggest that, during the early steps of myoblast differentiation, HSPB2 and HSPB3 exist in separate pools that may exert distinct functions.

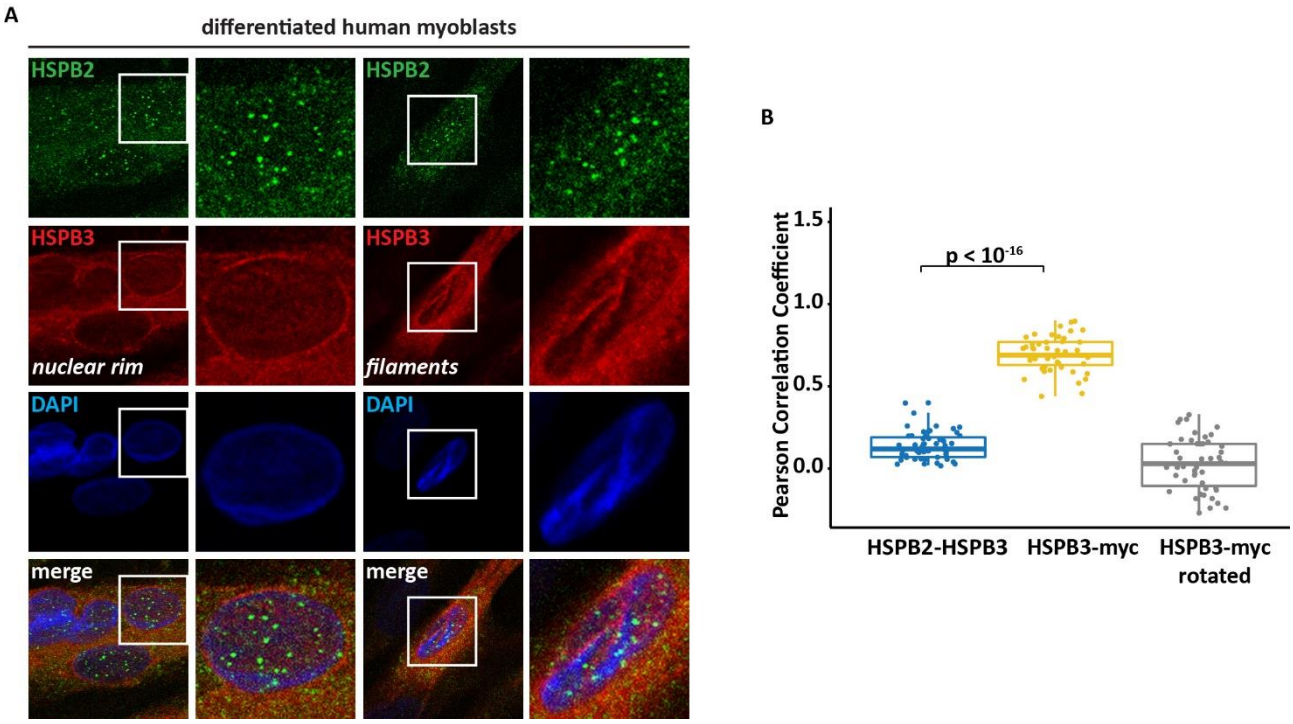


Figure 11 HSPB3 and HSPB2 show distinct distribution in differentiating myoblasts. (A) Immunofluorescence pictures showing that HSPB3 (red) does not colocalize with nuclear HSPB2 (green) foci in in differentiating human myoblasts. DAPI staining is shown. (B) Quantification of HSPB2 and HSPB3 colocalization in differentiating human myoblasts. Pearson's correlation coefficients (PCCs) of images of Alexa Fluor 488-HSPB2 and Alexa Fluor 594-HSPB3 in 7-day differentiating myoblasts cells expressing endogenous HSPB2 and HSPB3 (n = 55 multinucleated myotubes). PCCs of images of Alexa Fluor 488-myc and Alexa Fluor 594-HSPB3 in cycling human myoblasts cells overexpressing myc-HSPB3 for 24 hrs, before and after rotating Alexa Fluor 594-HSPB3 image by 90 degrees (n = 47 myoblasts). $P < 10^{-10}$, +/- sem. (C)

## HSPB3 influences nuclear envelope remodelling during myogenic differentiation by affecting LBR levels

### *HSPB3 and LBR expression level are inversely correlated*

Besides its main function as a protective coat for the segregation of the genome within the nucleus of eukaryotic cells, the NE also acts as a malleable compartment barrier that responds to mechanical challenges such as cell migration and nuclei fusion, two typical events that occur during the early steps of myogenesis (Ungricht and Kutay, 2017). Importantly, changes in the composition and morphology of the NE occur during cell differentiation and regulate the spatial segregation of euchromatic and heterochromatic regions, influencing gene expression. In particular, during myogenic differentiation these chromatin changes are determined by the switch of the Lamin B

Receptor (LBR) and lamin A/C (LMNA), the two major tethers for heterochromatin in eukaryotic cells (Figure 5) (Solovei et al., 2013).

It was previously published that downregulation of HSPB3 during the early steps of myogenesis inhibited the upregulation of MYOG, a muscle-specific transcription factor that is required for the differentiation of precursor myoblasts (Morelli et al., 2017). Compared to overexpression of GFP, used as a control, overexpression of myc-tagged HSPB3 (myc-HSPB3) in cycling myoblasts enhanced MYOG mRNA levels ($p = 10^{-5}$), mimicking the activation of myogenesis (Figure 12A). Together these data point to an active role of HSPB3 during myogenic differentiation. Considering that the results presented point to an enrichment of HSPB3 at the NE during differentiation, it led to the question whether HSPB3 participates in the NE remodelling responsible for the sequential tethering of LBR and Lamin A/C to peripheral heterochromatin. Thus, firstly it was monitored whether HSPB3 genetic manipulation, via downregulation or overexpression could affect the expression levels of LBR. As a control, LBR mRNA levels decreased (approximately 50%, $p < 10^{3}$) in myoblats upon differentiation (Figure 12B), in line with the observations previously reported by Solovei et al (2013). Interestingly, LBR levels were reduced by approximately 50% ($p < 10^{4}$) in cycling myoblast stably overexpressing HSPB3 due to lentiviral transduction (Figure 12C), mimicking differentiation conditions. Furthermore, downregulation of HSPB3 in differentiating myoblasts led to a 2-fold increase in LBR expression levels ($p = 0.007$) compared to control cells expressing a non-targeting shRNA sequence (Figure 12D). Thus, the expression levels of HSPB3 influence the ones of during differentiation.

LMNA substitutes LBR in the tethering of chromatin upon differentiation (Solovei et al., 2013). In agreement with the literature, in differentiating myoblasts the mRNA levels of LMNB1 and LMNB2 were also significantly downregulated compared to cycling myoblasts; instead, LMNA mRNA levels did not significantly change (Figure 12E). It was then tested whether HSPB3 affected specifically LBR levels, or it could also affect the ones of LMNB1, LMNB2 and LMNA. In cycling myoblasts overexpression of myc-HSPB3 also significantly downregulated LMNB1 and LMNB2 mRNA levels compared to GFP overexpression; by contrast, LMNA expression was not significantly affected (Figure 12F). Moreover, depletion of endogenous HSPB3 in differentiating myoblasts significantly enhanced the expression of LMNB1, but not of LMNA or LMNB2, compared to control cells infected with a non-targeting shRNA control (Figure 12G). Thus, modulation of HSPB3 levels influences the expression of LBR and LMNB1, leaving LMNA unchanged and mimics the changes that sequentially occurs during cellular differentiation.

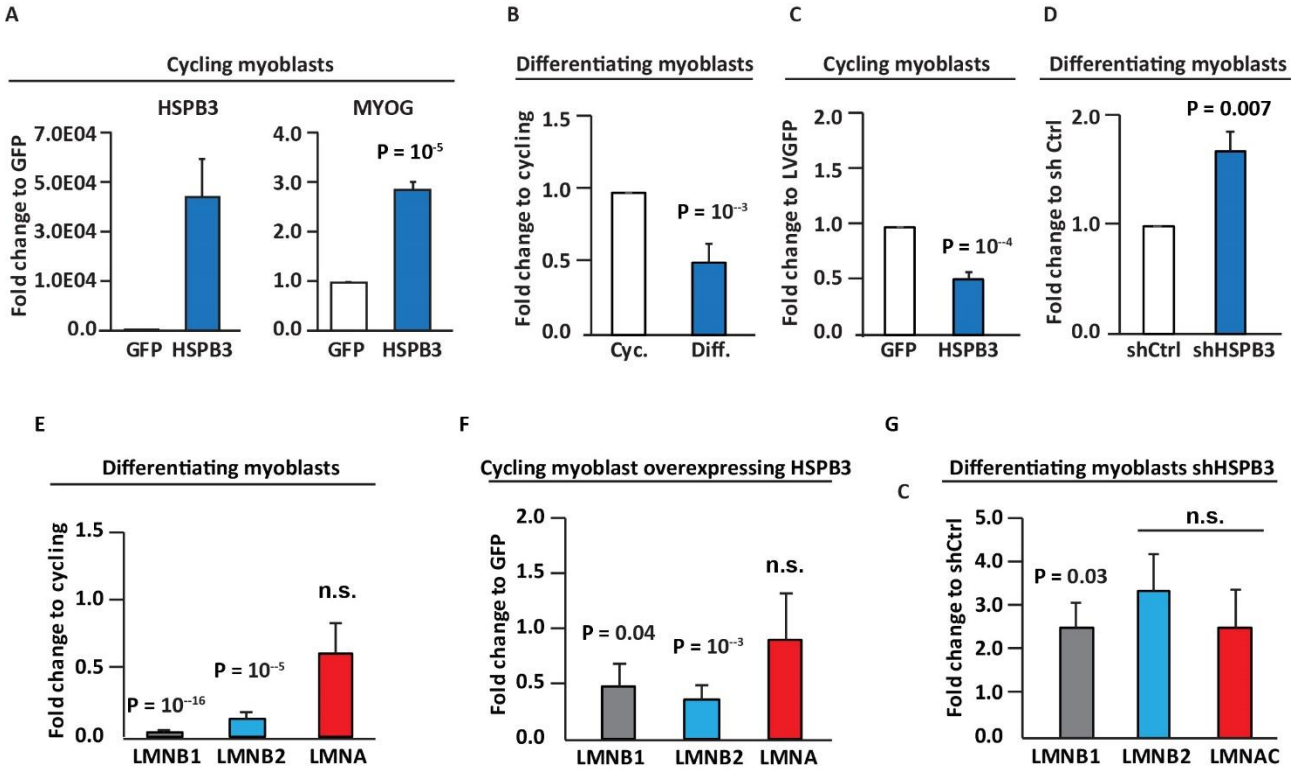


Figure 12 LBR mRNA levels are altered by HSPB3 expression in human myoblasts. (A) RT-qPCR analysis of HSPB3 and MYOG mRNA levels in cycling human myoblasts infected with lentiviral particles expressing GFP (used as control) or myc-HSPB3 for 7 days. RPLO was used as housekeeping control gene. n = 3, ± sem; p = $10^{-5}$. (B) RT-qPCR analysis of LBR expression in 7 days differentiating human myoblasts compared to cycling myoblasts. RPLO was used as housekeeping control gene. n = 3, ± sem; p = 10-3. (C) RT-qPCR analysis of LBR expression in cycling human myoblasts overexpressing myc-HSPB3 for 7 days compared to GFP (used as control). RPLO was used as housekeeping control gene. n = 3, ± sem; p = $10^{-4}$. (D) RT-qPCR analysis of LBR expression in differentiated human myoblasts (5 days) infected with lentiviral particles expressing an shRNA against HSPB3 (shHSPB3) compared to a non-targeting shRNA control sequence (shRNA control). RPLO was used as housekeeping control gene. n = 3, ± sem; p = 0.007. (E) RT-qPCR analysis of LMNB1, LMNB2 and LMNA expression in 7 days differentiating human myoblasts compared to cycling myoblasts. RPLO was used as housekeeping control gene. n = 3, ± sem; p = non-significant (n.s.). (F) RT-qPCR analysis of LMNB1, LMNB2 and LMNA expression in cycling human myoblasts overexpressing myc-HSPB3 for 7 days compared to GFP (used as control). RPLO was used as housekeeping control gene. n = 3, ± sem; p = non-significant (n.s.). (G) RT-qPCR analysis of LMNB1, LMNB2 and LMNA expression in differentiated myoblasts (5 days) infected with lentiviral particles expressing an shRNA against HSPB3 (shHSPB3) compared to a non-targeting shRNA control sequence (shRNA control). RPLO was used as housekeeping control gene. n = 3, ± sem; p = non-significant (n.s.).

## *LBR relocalizes to the nucleoplasm in the presence of HSPB3*

During cell differentiation the downregulation of LBR levels is accompanied by a decreased insertion of LBR in the NE. Moreover, LBR relocalization to the nucleoplasm has been associated with its inability to anchor to the nuclear membrane and bind to chromatin (Giannios et al., 2017). Based on these data, it is possible that HSPB3 also affects the subcellular distribution of LBR, and consequently has an effect on the LBR tethering to the NE. First, the enrichment of LBR at the NE in HSPB3 proficient and deficient differentiating myoblasts was investigated by confocal microscopy. For this analysis, the NE was marked by LMNB1 and the intensity of LBR staining measured in this region was fractioned by the intensity present in the total nuclear area (Figure 13A). In agreement with the literature (Solovei et al., 2013), upon differentiation in myoblasts LBR detached from the NE and redistributed to the nucleoplasm, with less than 5% of the cells showing enrichment at the NE (Figure 13A, B). By contrast, upon HSPB3 depletion, more than 30% of the differentiating myoblasts maintained LBR at the NE (Figure 13B, C). This opens the possibility that HSPB3 is not only correlated with the reduction in LBR levels, but also to its detachment from the NE upon differentiation.

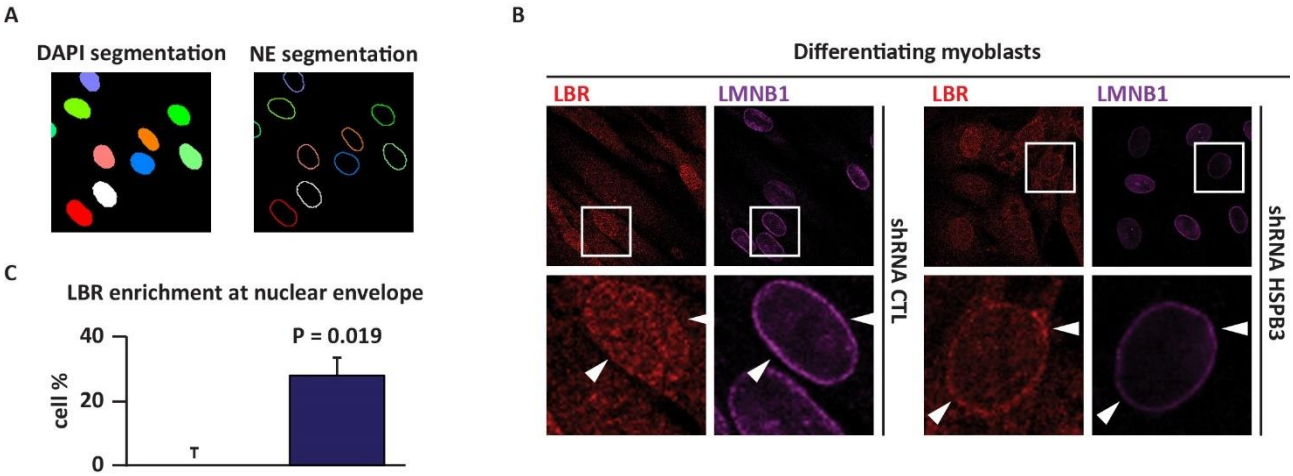


Figure 13 HSPB3 is required for LBR relocalization during myogenesis. (A) Schematic representation of segmentation of the NE for automated quantification of LBR enrichment at the NE with ScanR. Segmentation of the nucleus (using DAPI staining) and NE are shown. (B) Immunofluorescence pictures showing the subcellular distribution of LBR (red) and mature LMNB1 (8D1 antibody), used as NE marker. LBR (red) is mainly found in the nucleoplasm in differentiating human myoblasts expressing a non-targeting shRNA control sequence (shRNA control), while it is enriched at the NE, where it colocalizes with mature LMNB1 upon downregulation of HSPB3 for 5 days. (C) Quantification of LBR NE:nucleoplasm signal ratio at the NE in differentiating human myoblasts (5 days) control (shRNA control) or HSPB3-depleted (shHSPB3) is shown (ratio > 1.2). n = 3, ± sem; p = 0.019. Total number of cells analysed: 864 (shRNA control); 710 (shHSPB3).

LBR is a very stable protein characterized by a long half-life. Indeed, its half-life is longer than 16 hours both in HeLa and cycling myoblasts, as evidenced by the lack of protein level variation upon protein synthesis blockage with cycloheximide (Figure 14A). Furthermore, LBR is a highly insoluble protein and therefore challenging to characterize through cellular and molecular based assays. Hence, a shorter fragment of the protein, consisting of the LBR N-terminal and the first transmembrane domain is widely used to study its localization and turnover (Ellenberg et al., 1997). The N-terminal region contains all the binding sites for LMNB1 and HP1 (Heterochromatin Protein 1) while the transmembrane domain guarantees its anchorage to the NE; thus, the LBR fragment maintains all the functionality of the endogenous protein (Ye and Worman, 1994). The GFP-tagged shorter LBR fragment was used to further characterize the effects of HSPB3 overexpression on LBR localization.

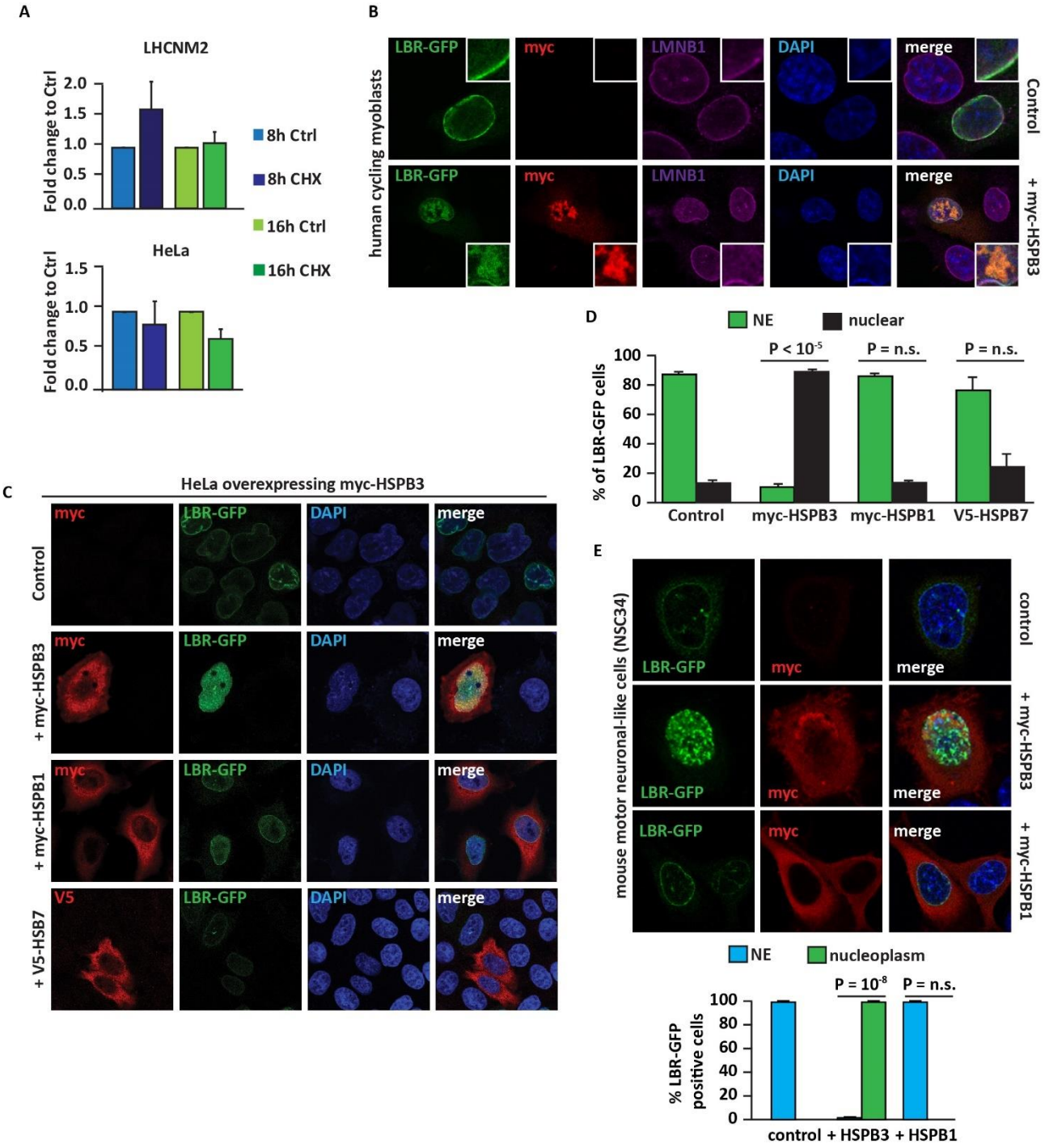


Figure 14 HSPB3 leads to the delocalization of LBR from the NE to the nucleoplasm. (A) Quantitative fold change of LBR protein levels assessed by western blotting after cycloheximide (CHX) treatment versus the respective control in human cycling myoblasts (top panel) and HeLa cells (lower panel). Data indicate mean of three independent experiments ± SEM. (B) Immunofluorescence of human cycling myoblasts transfected with vectors coding for LBR-GFP and either an empty vector or myc-HSPB3 for 48 hrs. DAPI staining is shown. (C) Immunofluorescence pictures showing the distribution of LBR-GFP in HeLa cells overexpressing LBR-GFP alone or with myc-HSPB3, myc-HSPB1 or V5- for 48 hrs. DAPI staining is shown. (D) Quantification of transfected cells from C showing LBR-GFP at the NE or delocalized to the nucleoplasm. n = 3 independent experiments, ± sem. $P < 10^{-5}$ between control and myc-HSPB3; p = n.s. between control and myc-HSPB1 or V5-HSPB7. Total number of cells analysed: LBR-GFP (273); + myc-HSPB3 (149); + myc-HSPB1 (226); + V5-HSPB7 (129). (E) Immunofluorescence pictures of motoneuronal-like NSC34 cells overexpressing LBR-GFP alone, or in presence of myc-HSPB3 or myc-HSPB1 for 48h. Quantitation of LBR-GFP distribution is reported. n = 3 independent experiments, ± sem. $P < 10^{-8}$ between cells expressing LBR-GFP alone or with myc-HSPB3; P = n.s. between cells

expressing LBR-GFP alone or with myc-HSPB1. Total number of cells analysed: control (175); + myc-HSPB3 (125); + myc-HSPB1 (178).

To further test whether HSPB3 directly influences the subcellular distribution of LBR, GFP-tagged LBR (LBR-GFP) was overexpressed in mammalian cells alone or together with myc-HSPB3 and LBR-GFP localization was observed by confocal microscopy. In cycling myoblasts, LBR-GFP was diffusely distributed in the nucleus and enriched at the NE, as expected (Figure 14B, upper panel). Instead, co-overexpression with myc-HSPB3 led to its redistribution into the nucleoplasm as demonstrated by IF (Figure 14B, lower panel). In addition, we found that upon transient transfection, HSPB3 could form nuclear condensates depending on the overexpression levels; LBR-GFP accumulated into the nucleoplasm and colocalized with the myc-HSPB3 nuclear condensates (Figure 6B, lower panel). A similar subcellular distribution and relocalization of LBR-GFP was observed upon co-expression with myc-HSPB3 in HeLa cells and the mouse motor neuron-like cells NSC-34 (Figure 14C, E). More specifically, myc-HSPB3 led to the redistribution of LBR-GFP into the nucleoplasm in more than 80 % of the cells ($p < 10^{-5}$) (Figure 14D). It was then verified whether HSPB3 specifically affects LBR distribution or rather this may represent a general function shared by several HSPB members. Thus, the subcellular localization of LBR-GFP was examined in cells co-expressing HSPB1 or HSPB7, two other members of the HSPB family that similarly to HSPB3 are highly expressed in muscle cells (Sugiyama et al., 2000; Mercer et al., 2018). Neither of these HSPBs led to the nucleoplasmic redistribution of LBR-GFP observed upon co-expression with myc-HSPB3 (Figure 14C, lower 2 panels). Together these results suggest that HSPB3 specifically affects LBR localization in the nucleus; in particular, overexpression of HSPB3 decreased the presence of LBR at the NE, similar to pro-differentiating stimuli.

As HSPB3 showed a predominantly nuclear distribution, it opened the question if this subcellular localization was required for the LBR-GFP relocalization into the nucleoplasm. In cells expressing myc-HSPB3 dN, there was a marked decrease in the delocalization of LBR-GFP compared to cells expressing myc-HSPB3, from 80% of the cells when in presence of myc-HSPB3 to 60% with cells in myc-HSPB3 dN cells (Figure 15A, B) ($p = 0.003$). Importantly, approximately 14% of the cells overexpressing myc-HSPB3 dN displayed nuclear localization (Figure 10D). Analysis of the cells characterized by completely cytoplastic myc-HSPB3 dN showed that only 38% of these cells presented LBR-GFP in the nucleoplasm ($p = 0.004$) (Figure 15C). Conversely, LBR-GFP was mainly found in the nucleoplasm in the cells characterized by nuclear myc-HSPB3 dN enrichment. Hence,

these results suggest that the delocalization of LBR-GFP is dependent on the nuclear localization of HSPB3.

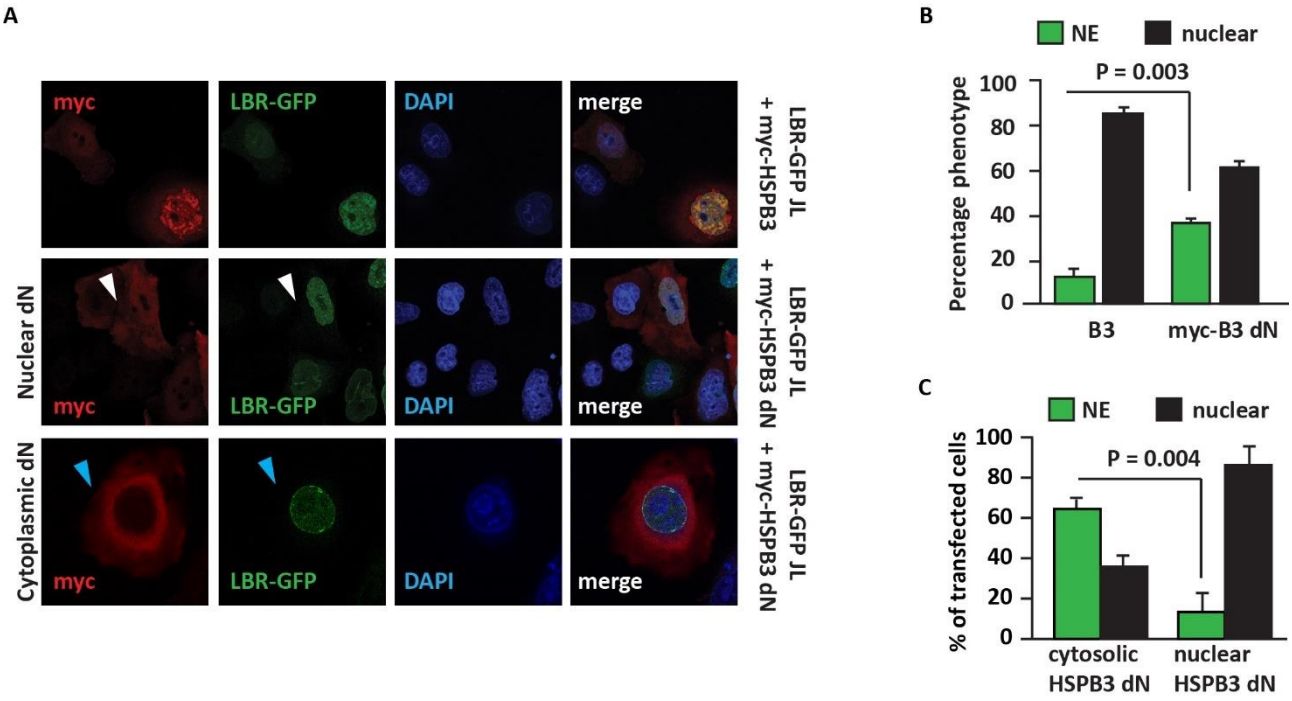


Figure 15 Nuclear localization of myc-HSPB3 required for LBR-GFP nucleoplasmic delocalization in HeLa. (A) Immunofluorescence of HeLa cells transfected for 48 hrs with vectors coding for LBR-GFP alone or with HSPB3-WT or a deletion mutant of HSPB3 that has a decreased propensity to accumulate inside the nucleus (HSPB3-dN). The white arrowhead points to a cell with nuclear HSPB3-dN that displaces LBR-GFP; the blue arrowhead points to a cell with cytoplasmic HSPB3-dN that does not displace LBR-GFP from the NE. (B) Quantification of HeLa cells displaying the phenotypes described in A. n = 3 independent experiments, ± sem; p = 0.004. Total number of cells analysed: HSPB3-WT (105); HSPB3-dN (158). (C) Quantitation of distribution of LBR-GFP in HeLa cells transfected for 48 hrs with vectors coding for LBR-GFP alone or with a deletion mutant of HSPB3 that accumulates in the cytoplasm (HSPB3-dN). n = 3 independent experiments, ± sem; p = 0.004. Total number of cells analysed: cytosolic (74); nuclear (84).

LBR anchoring to the NE has been linked to its ability to bind chromatin, and while bound to the NE LBR is characterized by a low mobility rate typical of transmembrane proteins (Giannios et al., 2017). Conversely, LBR fragments that do not contain transmembrane domains and are unable to anchor the NE and display high mobility rates (Giannios et al., 2017). Since HSPB3 led to the relocalization of LBR-GFP into the nucleoplasm, which has been linked to its inability to anchor to the NE, it opened the possibility that HSPB3 affected LBR mobility. Thus, the mobility of the pool of LBR-GFP at the NE was investigated in control cells, as well in cells co-expressing mCherry (used as a control) or mCherry-HSPB3, using Fluorescence Recovery After Photobleaching (FRAP) on HeLa cells (Figure 16A). As previously reported, the pool of LBR-GFP inserted at the NE displayed low mobility rate

under all conditions tested: this was evidenced by the low recovery of fluorescence intensity, which only recovered up to 50% over the 310s of imaging (Figure 16B, black and grey lines). This was consistent with its anchored state (Figure 8A, two upper panels). Instead, in cells co-expressing mCherry-HSPB3, the nucleoplasmic pool of LBR-GFP was highly dynamic (Figure 16A, third panel). Indeed, nucleoplasmic LBR-GFP due to the presence of mCherry-HSPB3 recovered most of the fluorescence intensity only 40s after FRAP (Figure 16B, green line); by contrast, myc-HSPB3 did not affect the mobility of the pool of LBR-GFP that remained bound to the NE (Figure 16A, lower panel and Figure 16B, blue line). This suggests that HSPB3 disrupts LBR-GFP anchorage to the NE, leading to an increase in its mobility rate. Furthermore, Proximity Ligation Assay (PLA) studies revealed direct interaction of LBR with HSPB3 (Figure 16C), confirming that the relocalization of LBR observed is due to the direct association of HSPB3 with LBR.

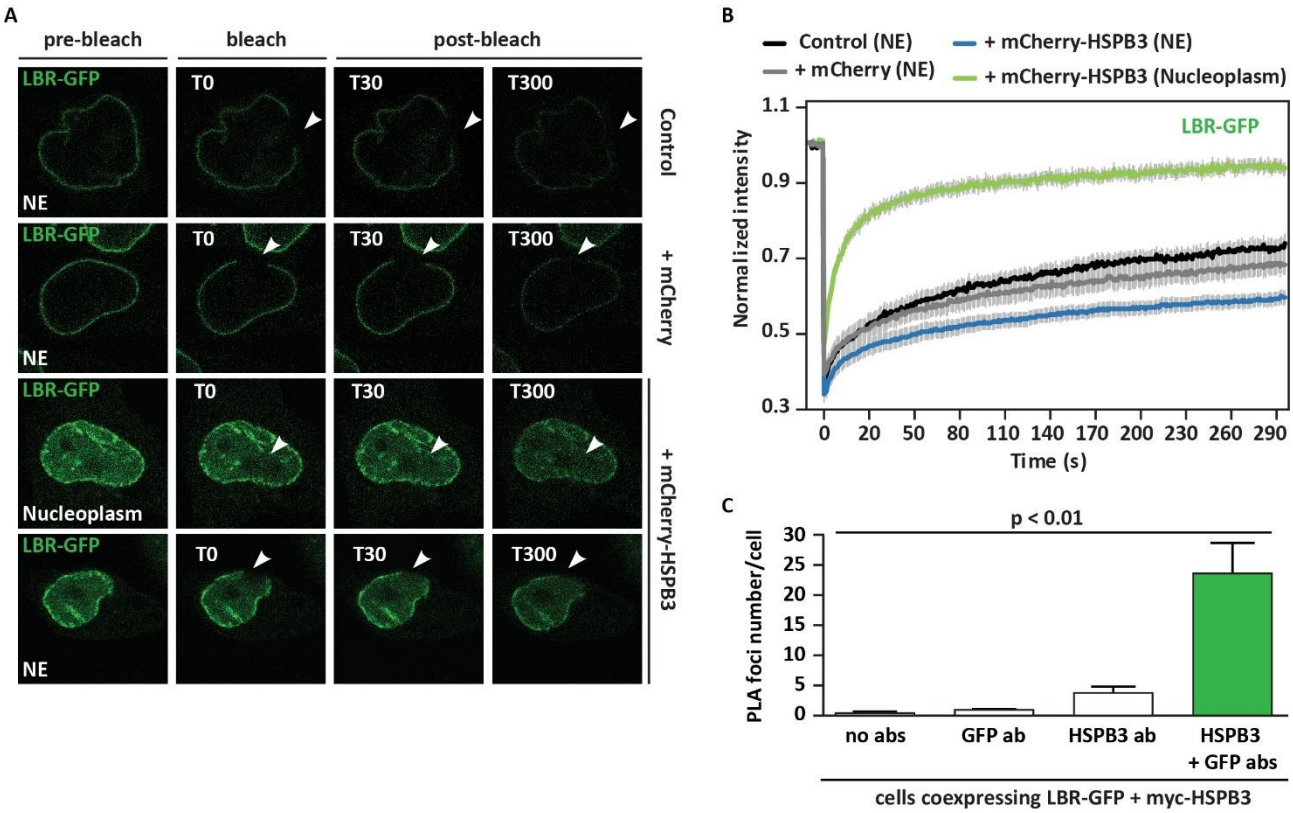


Figure 16 HSPB3 relocalizes LBR-GFP into the nucleoplasm and increases its mobility. (A) HeLa cells overexpressing LBR-GFP alone, with mCherry or with mCherry-HSPB3 + myc-HSPB3 (at a 1:8 ratio) were subjected to fluorescence recovery after photobleaching (FRAP). Pre-bleach, bleach, and post-bleach images of LBR-GFP inserted at the NE and diffusely distributed in the nucleoplasm are shown. (B) Quantitation of the fluorescence intensity recovery after bleach of cells treated as described in D. The mean of 12-14 FRAP curves and the fitting curves are shown. sem is shown in grey. (C) HeLa cells co-expressing LBR-GFP and myc-HSPB3 were subjected to proximity ligation assay (PLA) using antibodies specific for GFP and HSPB3. GFP-positive cells were segmented, and PLA foci/cell were automatically quantified using ScanR. The average number of PLA foci in cells incubated with GFP or HSPB3 antibody (used as controls) or with both antibodies is shown. The PLA foci number was normalized for cells incubated with the GFP antibody alone. n = 4 independent experiments, ± sem; total number cells analysed/sample: 78-90, $p < 0.01$.

To test whether HSPB3 effect on LBR distribution is specific, the impact of HSPB3 on LMNB1 and chromatin was monitored, as these are known to interact with LBR (Nikolakaki et al., 2017; Solovei et al., 2013). First, by live-cell imaging in HeLa cells stably expressing GFP-tagged LMNB1 (Poser et al., 2008) there was no observation of colocalization of GFP-LMNB1 with HSPB3, nor relocalization into the nucleoplasm, as reported for LBR-GFP (Video S1). Second, no colocalization was noted between the chromatin marker protein H2B-mCherry when co-expressed with GFP-HSPB3 in both HeLa cells and cycling myoblasts (Video S2 and S3). Together these data support the idea that LBR is a novel substrate of HSPB3, whose intracellular localization is influenced by interaction with HSPB3.

### Chromocenter distribution is affected by HSPB3

Chromocenters are highly condensed, repetitive stretches of DNA which are mostly transcriptionally silent (Brero et al., 2005). During differentiation, chromocenters undergo morphological changes due to fusion and relocation. In quiescent cells, chromocenters are mostly small in size and high in number, being mainly found in the nuclear periphery. Upon differentiation, chromocenters fuse becoming larger in size and lower in number and relocate into the central regions of the nucleus (Jost et al., 2015) (Figure 17 A). Alteration of chromocenter morphology and distribution were previously reported upon C2C12 (murine myoblast cell line) myogenic differentiation (Brero et al., 2005). Furthermore, LBR downregulation was reported to be fundamental for chromocenter fusion and relocation (Solovei et al., 2013).

This opens the question whether HSPB3 expression could have an impact on chromocenter alterations. Firstly, the chromocenter distribution was characterised in myoblasts upon differentiation. Confocal microscopy analysis of chromocenter morphology and distribution showed that these cells behave similarly to C2C12: in differentiating myoblasts chromocenter number was reduced upon differentiation ($p = 1.7E^{-6}$), with concomitant increase of the mean volume due to fusion ($p = 0.00075$) (Figure 17 B, C). Next, chromocenter distribution was analysed in cycling myoblasts overexpressing HSPB3 by transduction with lentiviral particles. Interestingly, we found that overexpression of HSPB3 led to a reduction of the chromocenter number ($p = 0.00016$), mimicking what happens during differentiation (Figure 17 D). HSPB3 overexpression also led to a slight increase in chromocenter mean volume, (Figure 17 E).

Next, chromocenter number and area were verified in HSPB3 proficient (control) or deficient differentiating myoblast. HSPB3 increased the number of chromocenters ($p = 0.032$) when compared to silencing control (Figure 17 F, G). There were no significant differences when analysing the mean volume; this might be due to the minor differences in volume between conditions, with high internal variability as shown in Figure 17 C, right panel.

Together, these data support the hypothesis that HSPB3 might play a role in modulating myogenic differentiation by affecting chromatin tethering and consequent gene expression (Figure 17 H). How mechanistically HSPB3 can affect myoblast differentiation is unknown, but our results suggest that LBR may be a novel and specific HSPB3 substrate involved in this specific function.

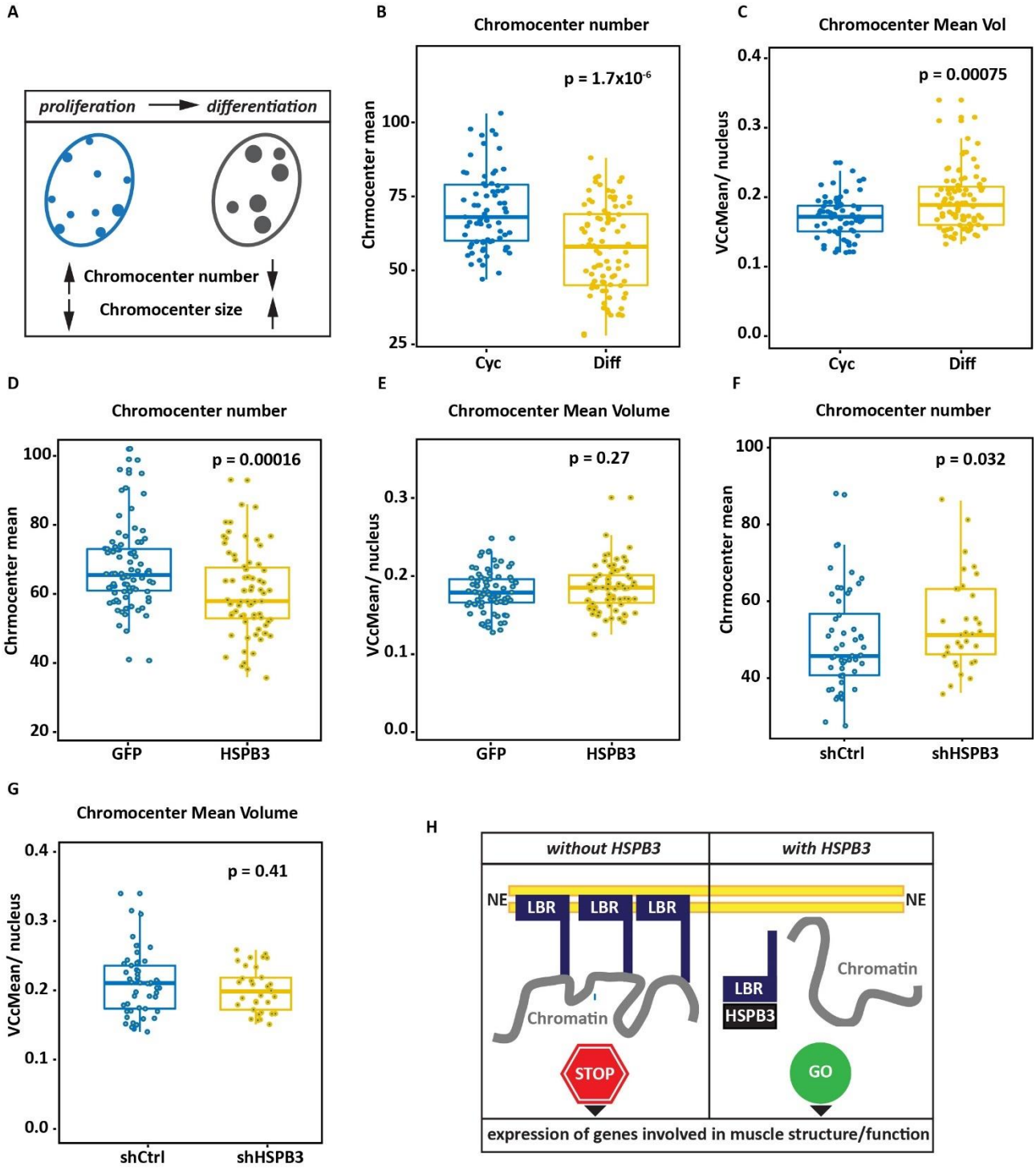


Figure 17 HSPB3 affects chromocenter number in human myoblasts. (A) Schematic representation of the changes in chromocenter number and size that occur during cell differentiation (Brero et al., 2005; Jost et al., 2015). (B, C) Quantification of chromocenter number (B) and mean volume (Vol) (C) in cycling and 7 days differentiating human myoblasts, using ImageJ plug-in NucleusJ from Z-stack images. n = 73 cells (from 4 independent experiments, B) and n = 87 cells (from 5 independent experiments, C). Wilcoxon, p = 1.7x10-6 (B), p = 0.00075 (C). (D, E) Quantification of chromocenter number (D) and mean volume (Vol) (E) in cycling human myoblasts infected with lentiviral particles expressing GFP (control) or myc-HSPB3, using ImageJ plug-in NucleusJ from Z-stack images. n = 82 cells (from 4 independent experiments, D) and n = 74 cells (from 4 independent experiments, E). Wilcoxon, p = 0.0001. (F, G) Quantification of chromocenter number (F) and mean volume (G) in differentiating human myoblasts control (shRNA control) or HSPB3-depleted (shHSPB3), using ImageJ plug-in NucleusJ from Z-stack images. n = 66 cells (shRNA control; from 3 independent experiments) and n = 57 cells (shRNA control; from 4 independent experiments). Wilcoxon, p =

0.014. (H) Schematic representation of the putative effect of HSPB3 on the LBR-tether, with potential implications on myogenic gene expression.

## HSPB3 deficiency leads to downregulation of muscle-specific genes

As LBR and LMNA inversely regulate the transcription of myogenic genes upon differentiation (Solovei et al., 2013), the impact of downregulation and upregulation of HSPB3 on the global muscle cell transcriptome of myoblasts was tested by RNAseq. First, HSPB3 was depleted by shRNA in differentiating myoblasts, and we verified whether this negatively influenced the expression of genes that positively regulate myogenesis, compared to cells expressing a non-targeting shRNA control (GSE160027). HSPB3 downregulation significantly altered the expression of 112 genes (Figure 18 A; $p < 0.01$), 80 of which were downregulated, while 32 were upregulated (Table 1). Since the Log2 fold change was not high in most significant genes, only the genes that were very highly differentially regulated ($p < 10^{-5}$) were considered for further analysis. From the 80 downregulated genes, 48 belong to this category (Figure 18 B upper left quadrant). Within these highly significant genes we found MYOG, hence confirming its downregulation due to HSPB3 silencing. Other genes belonging to the highly significant downregulated genes were the muscle specific genes coding for actin alpha 1 (ACTA1) and desmin (DES) (Figure 18 B, upper left quadrant), which we further validated by qPCR (Figure 18 C). To further analyse the impact of HSPB3 downregulation on myogenesis, gene annotation analysis was performed using Metascape to identify the pathways and biological functions affected. The analysis revealed the ten biological processes that were affected the most by HSPB3 downregulation; these include skeletal muscle differentiation, structure development and function, as well as muscle contraction (Figure 18 D), further indicating an important role of HSPB3 in myogenesis.

Conversely, only 7 genes were highly significantly ($p < 10^{-5}$) upregulated, namely CCL5, MMP3, MIR30A, TFPI2, IFI6, SLC39A8, CTSS (Figure 18 B upper right quadrant, Table 1). Hence, no Metascape analysis was performed on upregulated genes. Interestingly, both Chemokine (C-C motif) ligand 5 (CCL5) and Cathepsin S (CTSS) upregulation in muscle tissues has been linked to chronic inflammation (Ishiuchi et al., 2018; Tjondrokoesoemo et al., 2016). Therefore, the upregulation of these genes in absence of HSPB3 might indicate a protective role by HSPB3.

A

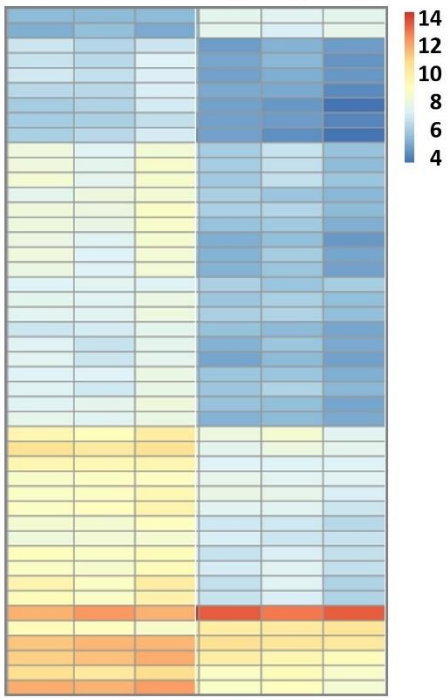


B

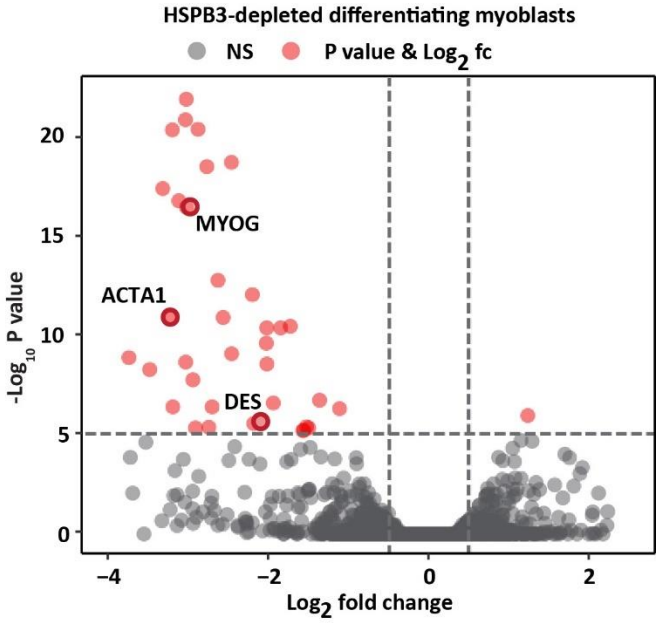


C

| GENE | P (RNAseq) | qPCR validation fold change | |
|---|---|---|---|
| ACTA1 | 1.16E-11 | 0.2 | DOWN |
| DES | 5.10E-05 | 0.4 | DOWN |

D

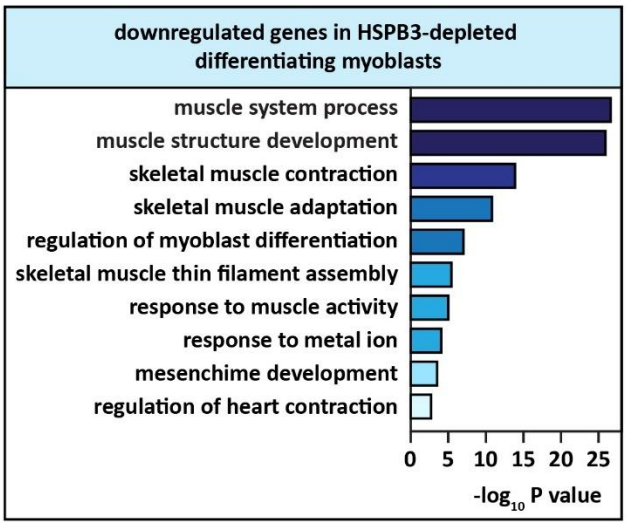


Figure 18 Downregulation of HSPB3 leads to downregulation of myogenesis-specific genes in differentiating myoblasts. (A) Heatmap showing the genes that are differentially expressed in 3 independent biological replicates of differentiated control myoblasts (shRNA Control) versus HSPB3-depleted myoblasts (shRNA HSPB3). Genes that displayed greater than $p < 0.01$ are shown. (B) Volcano plot highlighting that in differentiating myoblasts HSPB3 depletion downregulates the muscle specific genes coding for myogenin (MYOG), actin alpha 1 (ACTA1) and desmin (DES), compared to control myoblasts. Horizontal dotted line represents $p < 10^{-5}$, vertical dotted lines highlight log2 fold-changes of -0.5 and 0.5. Highly significant genes ($p < 10^{-10}$) with log2 fold-change higher than 0.5 (or lower than -0.5) are marked in red; low significance genes ($p > 10^{-5}$) with log2 fold-change higher than 0.5 (or lower than -0.5) and non-significant genes are marked in grey. (C) Validation by RT-qPCR of actin alpha 1 (ACTA1) and desmin (DES) downregulation in differentiated HSPB3-depleted myoblasts compared to control differentiated myoblasts. (D) Gene-set enrichment analysis: downregulated genes upon HSPB3 depletion in differentiating myoblasts. Analysis performed using Metascape Express Analysis on genes highly significant ($p < 10^{-10}$) (Zhou et al., 2019). The top 10 hits are shown.

## HSPB3 upregulation leads to ECM & cell cycle regulation

Next, myc-HSPB3 was overexpressed in cycling human satellite cells, in presence of high serum concentrations to maintain cycling conditions, and their transcriptome was compared to the one of GFP overexpressing cells (GSE160027). Overexpression of myc-HSPB3 in cycling myoblasts significantly affected the expression of 381 genes (Figure 19 A, Table 2, $p < 0.01$), of which 188 were upregulated and 193 were downregulated. Again, since the Log2 fold change was not high in most significant genes, only the genes that were very highly differentially regulated ($p < 10^{-5}$) were considered for further analysis. From the 188 upregulated genes, 52 belong to this category (Figure 19 B, upper right quadrant). Amongst the genes that were upregulated following myc-HSPB3 overexpression in cycling myoblasts were the genes coding for lumican (LUM), nidogen 2 (NID2) and several types of collagens, which are key components of the skeletal muscle extracellular matrix (ECM), as well as the cell adhesion molecule 1 (CADM1), which regulates cell-cell and ECM adhesion (Hynes and Naba, 2012). It was confirmed by qPCR that overexpression of HSPB3 in cycling myoblasts led to the upregulation of the matrisome genes LUM, CADM1, NID2 and DCN, as well as the SVIL and NOTCH3 genes (Figure 19 C). DCN upregulation promotes muscle differentiation, as well as muscle regeneration in vivo (Li et al., 2007). SVIL encodes for supervillin, which links the actin cytoskeleton to the membrane, regulating the early assembly of the myogenic membrane during the early steps of myogenesis (Oh et al., 2003). NOTCH3 encodes for the Notch3 receptor, a transmembrane protein that together with the other 3 family members Notch 1, 2 and 4 are responsible for the Notch signalling. Notch signalling is a well-known regulator of myogenesis and skeletal muscle repair. Notch3 induction plays a dual role during myogenesis: it promotes differentiation during the early steps, when myoblasts are activated by the myogenic transcription factor MyoD and it inhibits the terminal differentiation of myoblasts into myotubes which is regulated by the myogenic transcription factor Mef2c (Berkes and Tapscott, 2005; Gagan et al., 2012). Of note, RNA-seq data showed that HSPB3 downregulation significantly reduced the expression of Notch3 in early differentiating myoblasts, further linking HSPB3 expression levels to myogenesis (Table 1). Gene annotation analysis revealed the top ten biological processes that were positively regulated by HSPB3 overexpression in cycling myoblasts; these include extracellular structure organization, ErbB pathway, connective tissue development, tissue morphogenesis and NABA matrisome associated proteins (Figure 19 D). The ErbB pathway plays an important role in both muscle development and regeneration. In particular, neuregulins (NRG) stimulate muscle

differentiation by increasing myosin heavy chain levels thereby supporting myotube formation (Kim et al., 1999). Moreover, amphiregulin (AREG), a ligand of the ErbB family tyrosine kinase EGFR, has been shown to enhance muscle regeneration upon injury (Burzyn et al., 2013). Interestingly, both NRG1 and AREG are two of the ErbB pathway genes that are upregulated upon HSPB3 overexpression (Table 2, $p < 10^{-5}$). NABA matrisome refers to the ensemble of genes encoding for ECM associated proteins, such as ECM proteins, ECM regulators and secreted factors (Naba et al., 2016). Of note, interactions between myoblasts and their ECM are required for muscle development, growth, and functioning, including lateral transfer of the contractile force (Kjaer, 2004; Bentzinger et al., 2013; Urciolo et al., 2013). In addition, skeletal muscles are a post-mitotic tissue and depend on muscle resident stem cells, named satellite cells, to regenerate throughout their life. Upon damage, extensive ECM remodelling supports satellite cell activation, migration, and myogenic differentiation, enabling muscle repair (Csapo et al., 2020; Goody et al., 2015). It is thus not surprising that dysregulation of ECM remodelling has been linked to muscle aging and disease (Goody et al., 2015). Importantly, the disintegrin and metalloprotease ADAM-12 has been shown to have a restricted spatial-temporal expression pattern that correlated well with early skeletal muscle development (Yagami-Hiromasa et al., 1995; Kurasaki et al., 1998). Interestingly, ADAM-12 is one of NABA matrisome genes upregulated by HSPB3 overexpression in myoblasts (Table 2, $p < 0.01$). Likewise, matrix metalloproteinases MMP14 and MMP16, which hydrolyse and activate MMP-2 known to be secreted by regenerating myofibers (Ioth, 2015; Thomas et al., 2015) are also upregulated upon HSPB3 overexpression (Table 2, $p < 0.01$).

From the 193 downregulated genes due to overexpression of HSPB3, 72 were highly significant ($p < 10^{-5}$) (Table 2). Amongst these were genes encoding for the cell cycle arrest associated Growth Arrest And DNA Damage Inducible Beta (GADD45B), the Microfibrillar-associated protein 5 (MFAP5), and the Cyclin-dependent kinase 4 (CDK) (Figure 19 B, upper left quadrant). As validation of the RNAseq data, analysis of mRNA levels by qPCR further confirmed that overexpression of HSPB3 in cycling myoblasts leads to the downregulation of GADD45B and MFAP5 (Figure 19 C). Interestingly, overexpression of MFAP5 has been described in mouse models of Duchenne muscular dystrophy which leads to transdifferentiation of myoblasts into myofibroblasts and consequent muscle fibrogenesis (Wang et al., 2012). Hence, it is possible that HSPB3 does not only promote expression of ECM proteins, but also modulates protein expression of key proteins thereby acting as a muscle protector. Upon induction of myogenic differentiation, the cell-cycle inhibitor p21 is upregulated in

a MyoD-dependent manner (Halevy et al., 1995). CDK4 is subsequently inhibited by p21 leading to the blockage of the cell cycle. Interestingly, p57 (CDKN1C), another cell-cycle inhibitor with analogous function to p21, is upregulated upon HSPB3 overexpression (Table 2, $p < 10^{-5}$). Another gene involved in the regulation of the cell cycle and upregulated by HSPB3 is the gene coding for E2F7 (Table 2, $p < 0.01$). E2F7 is an atypical E2F family member that acts as a transcriptional repressor of E2F target genes by cooperating with retinoblastoma (Rb), thereby contributing to cell cycle arrest (Aksoy et al., 2012).

Gene annotation analysis revealed that the top biological processes downregulated by HSPB3 overexpression included ribosomal assembly and FoxO signalling (Figure 19 E). Interestingly, FoxO1 has been shown to act as an inhibitor of muscle differentiation by directly binding and increasing the activity of myogenesis repressor myostatin (Accili and Arden, 2004; Allen and Unterman, 2007). Ribosomal protein large 3-like (RPL3) which has been described to impair myotube growth (Chaillou, Zhang and McCarthy, 2016), is one of the ribosomal genes that is highly downregulated by HSPB3 (Table 2, $p < 10^{-5}$). Therefore, downregulation of ribosomal assembly by HSPB3 might be linked to regulation of muscle-specific ribosomal functions. Altogether the transcriptomic data together with the expression and distribution analysis of LBR support the idea that HSPB3 is a specialized nuclear chaperone that engages in the muscle differentiation program.

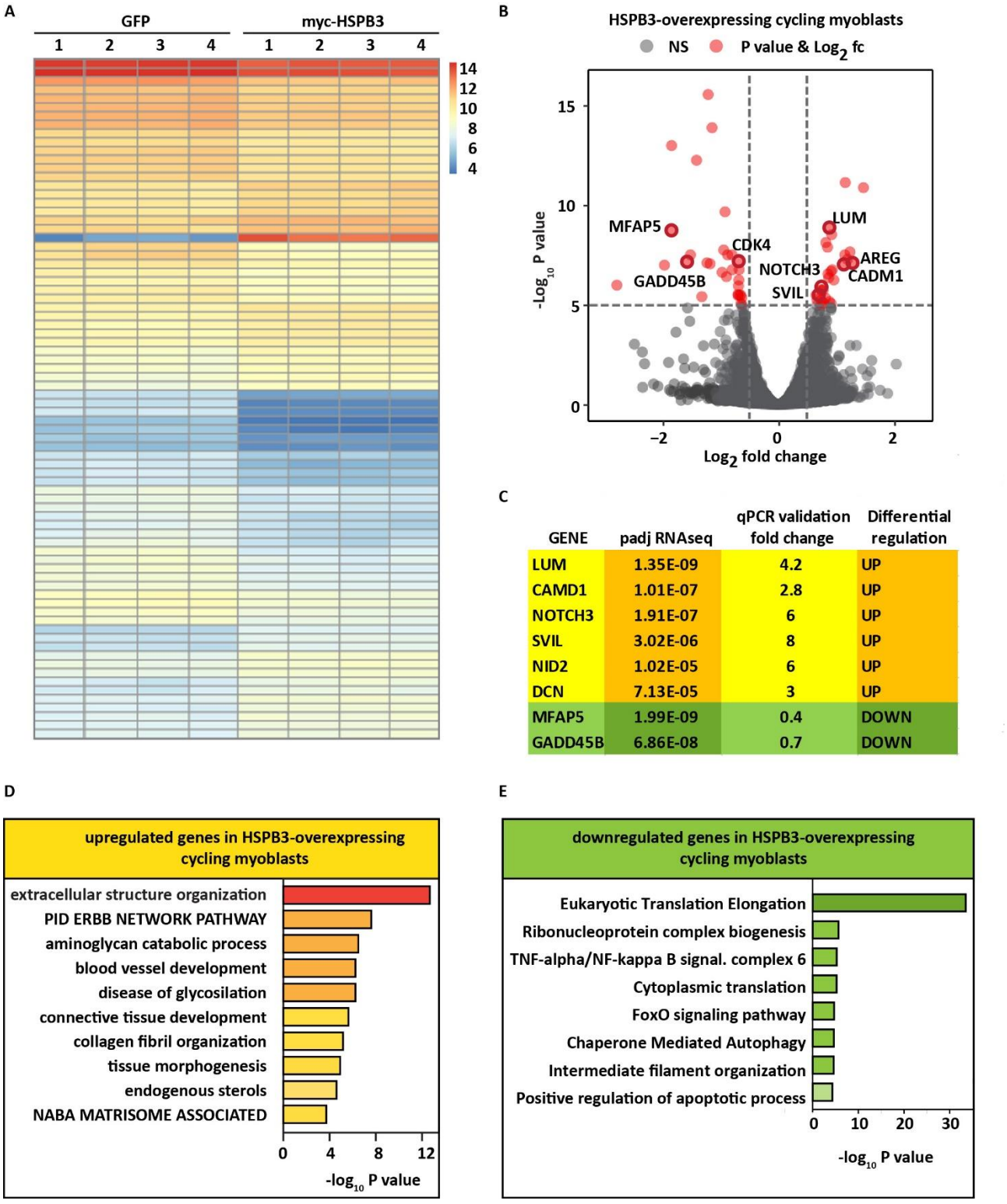


Figure 19 Overexpression of HSPB3 incudes transcriptional changes that mimic myogenesis. (A) Heatmap showing the genes that are differentially expressed in 4 independent biological replicates of cycling myoblasts that overexpress GFP versus myc-HSPB3. Genes that displayed greater than $p < 0.01$ are shown. (B) Volcano plot highlighting that HSPB3 overexpression upregulates the matrisome genes lumican (LUM), Cell adhesion molecule 1 (CADM1), nidogen 2 (NID2) and decorin (DCN), as well as amphiregulin (AREG), supervillin (SVIL) and NOTCH3 genes, while downregulating microfibril associated protein 5 (MFAP5), growth arrest and DNA-damage-inducible (GADD45B), and Cydlin-dependent kinase 4 (CDK4), compared to GFP overexpression, used as a control. Horizontal dotted line represents $p < 10^{-5}$, vertical dotted lines highlight log2 fold-changes of -0.5 and 0.5. Highly significant genes ($p < 10^{-10}$) with log2 fold-change higher

than 0.5 (or lower than -0.5) are marked in red; low significance genes ($p > 10^{-5}$) with log2 fold-change higher than 0.5 (or lower than -0.5) and non-significant genes are marked in grey. (C) Validation by RT-qPCR of LUM, CADM1, NOTCH3, SVIL, NID2 and DCN upregulation, and MFAP5 and GADD45B downregulation in cycling myoblasts overexpressing HSPB3 compared to control myoblasts overexpressing GFP. (D) Gene-set enrichment analysis: upregulated genes upon HSPB3 overexpression in cycling myoblasts. Analysis performed using Metascape Express Analysis on genes highly significant ($p < 10^{-10}$). The top 10 hits are shown. (E) Gene-set enrichment analysis: downregulated genes upon HSPB3 overexpression in cycling myoblasts. Analysis performed using Metascape Express Analysis on genes highly significant ($p < 10^{-10}$). The top 10 hits are shown.

## Disease mutants display different subcellular localisation to WT

As HSPB3 nuclear localization plays a role in its ability to affect the LBR tether to the NE, and consequently chromatin, HSPB3 localization might be disturbed by disease-associated mutations.

First, protein levels and subcellular distribution of WT-HSPB3, R7S-HSPB3, R116P-HSPB3, Y118H-HSPB3 and A33AfsX50-HSPB3 overexpressed in HeLa cells were assessed by fractionation of cytoplasmic and nuclear proteins. As previously reported (Morelli et al., 2017), A33AfsX50 which encodes a truncated fragment of HSPB3 is rapidly degraded after synthesis and therefore no expression was detected in neither the cytoplasm nor the nucleus. WT-HSPB3 was predominantly expressed in the nuclear fraction, while R7S-HSPB3 was mainly distributed in the cytoplasmic fraction, although being present also in the nuclear fraction (Figure 20 A). By contrast, R116P-HSPB3 and Y118H-HSPB3 accumulated inside the nucleus, with Y118H-HSPB3 being absent in the cytoplasmic fraction (Figure 20 A, B).

Second, using confocal microscopy the subcellular distribution of HSP3 disease mutants was further analysed. R7S-HSPB3 was confirmed to have a higher cytoplasmatic expression than WT-HSPB3 in HeLa cells (Figure 20 C, D). This was further confirmed by quantifying the ratio between the cytoplasmic and nuclear proteins (Figure 10 E). Microscopy analysis also confirmed that R116P-HSPB3 and Y118H-HSPB3 accumulated inside the nucleus, where they formed nuclear assemblies (Figure 20 C, D).

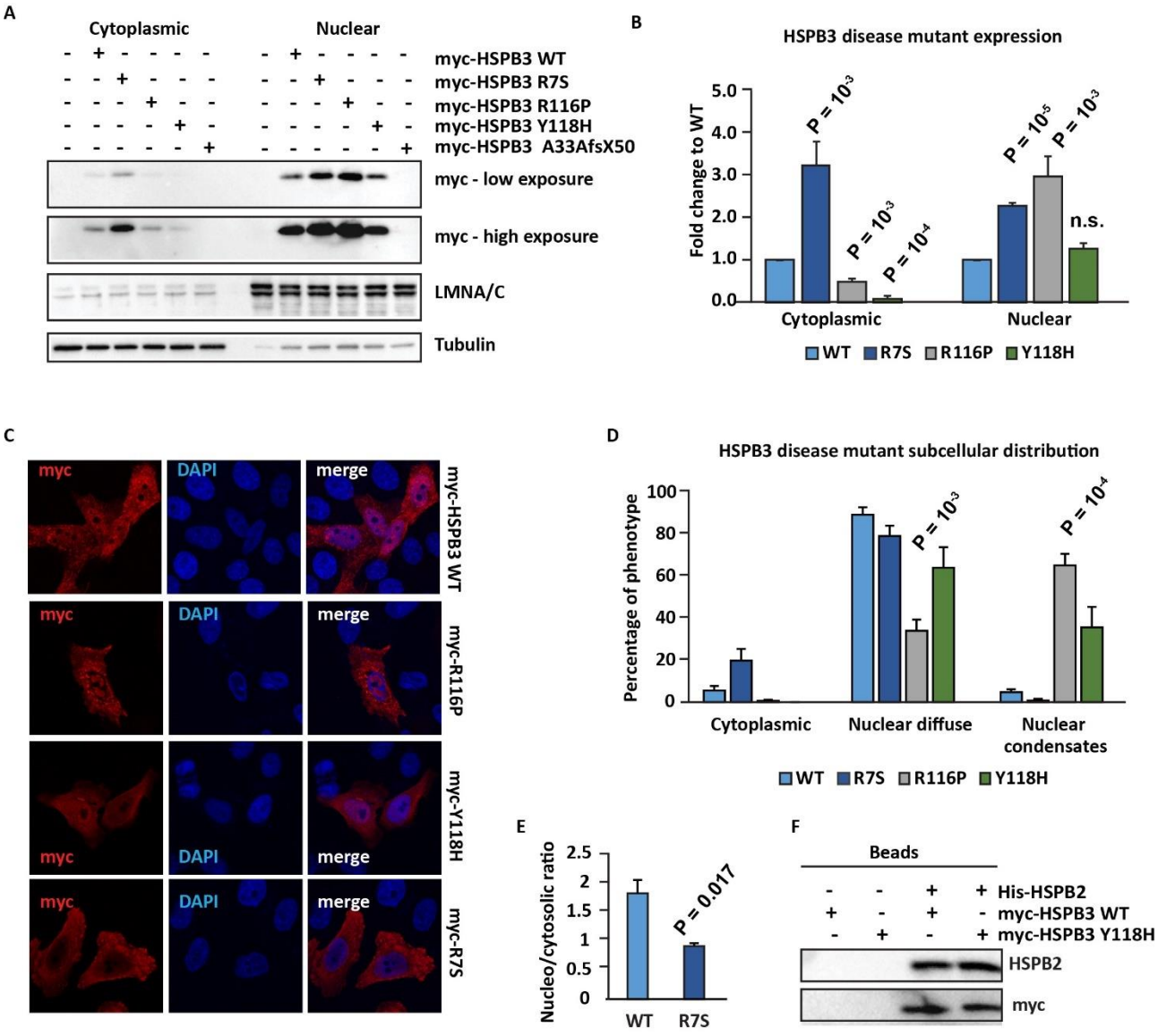


Figure 20 HSPB3 disease mutants show a distinct subcellular localization and expression levels compared to WT-HSPB3. (A) HeLa cells overexpressing WT-HSPB3, R7S-HSPB3, R116P-HSPB3, Y118H-HSPB3 or A33AfsX50-HSPB3 for 48 hrs were subjected to fractionation of cytoplasmic and nuclear proteins and HSPB3 expression levels were analysed by immunoblotting. TUBA4A and LMNAC were used as loading controls for the cytoplasmic and nuclear fraction, respectively. (B) Quantitation of the wester blotting shown in A. n = 3 independent experiments, ± sem. p = non-significant (n.s.). (C) Confocal microscopy on HeLa cells overexpressing myc-tagged WT-HSPB3, R7S-HSPB3, R116P-HSPB3 or Y118H-HSPB3, using a myc-specific antibody. DAPI staining is shown. (D) Quantitation of myc distribution in HeLa cells transfected for 48 hrs with vectors coding myc-tagged WT-HSPB3, R7S-HSPB3, R116P-HSPB3 or Y118H-HSPB3. n = 3 independent experiments, ± sem; Total number of cells analysed: WT-HSPB3 (98); R7S-HSPB3 (141); R116P-HSPB3 (152); Y118H-HSPB3 (103). (E) Automated quantification using ScanR of nucleo/cytosolic ratio of myc signal in HeLa cells overexpressing HSPB3-WT or HSPB3-R7S for 48h. (F) Western blotting analysis of co-immunoprecipitation using Ninta beads with affinity for His of HeLa cells transfected with His-HSPB2 and myc-HSPB3 WT or myc-HSPB3 Y118H for 48h.

### *The recently described HSPB3-Y118H can still efficiently bind to HSPB2*

HSPB3 mutants linked to disease were assessed by their ability to complex with HSPB2, where R116P-HSPB3 was reported to lose the ability to complex with HSPB2, while R7S-HSPB3 was still able to form a stable complex (Morelli et al., 2018). In 2018, a new HSPB3 mutation at the residue 118 (c.352T>C, p.Tyr118His) was described in a CMT2 patient in Japan by Nam et al. Here, the newly discovered Y118H-HSPB3 mutation was assessed by Ni-NTA pull-down on its ability to interact with HSPB2. Y118H-HSPB3 precipitated along with HSPB2, similarly to WT-HSPB3. Thus, the Y118H-HSPB3 mutation does not affect the HSPB2-HSPB3 complex formation (Figure 20 F).

## Myopathy-associated HSPB3-R116P forms aggregates that sequester LBR-GFP

In light of the emerging role of HSPB3 in promoting muscle cell differentiation and considering that R116P-HSPB3 was identified in a myopathy patient with altered chromatin distribution and muscle fibre disorganization (Morelli et al., 2017), this thesis focused on R116P-HSPB3. Due to its very short half-file, A33AfsX50-HSPB3 was excluded from further analysis, which was also identified in a patient affected by congenital myopathy (Morelli et al., 2017).

R116P-HSPB3 assemblies did not colocalize, but rather displaced the chromatin, as evidenced by confocal microscopy in cells co-expressing chromatin marker mCherry-H2B (Figure 21 A). Accumulation of R116P-HSPB3 in nuclear assemblies occurred also in differentiating myoblasts or motoneuronal-like NSC34 cells (Figure 21 B, C). Since upon overexpression WT-HSPB3 forms dynamic nuclear condensates in HeLa and muscle cells (Figure 10 A, B), the mobility of R116P-HSPB3 was then verified by FRAP. In contrast to WT-HSPB3, which showed partial mobility within the nuclear condensates, R116P-HSPB3 was completely immobile, demonstrating that R116P-HSPB3 forms nuclear aggregates in HeLa cells (Figure 21 D, middle panel).

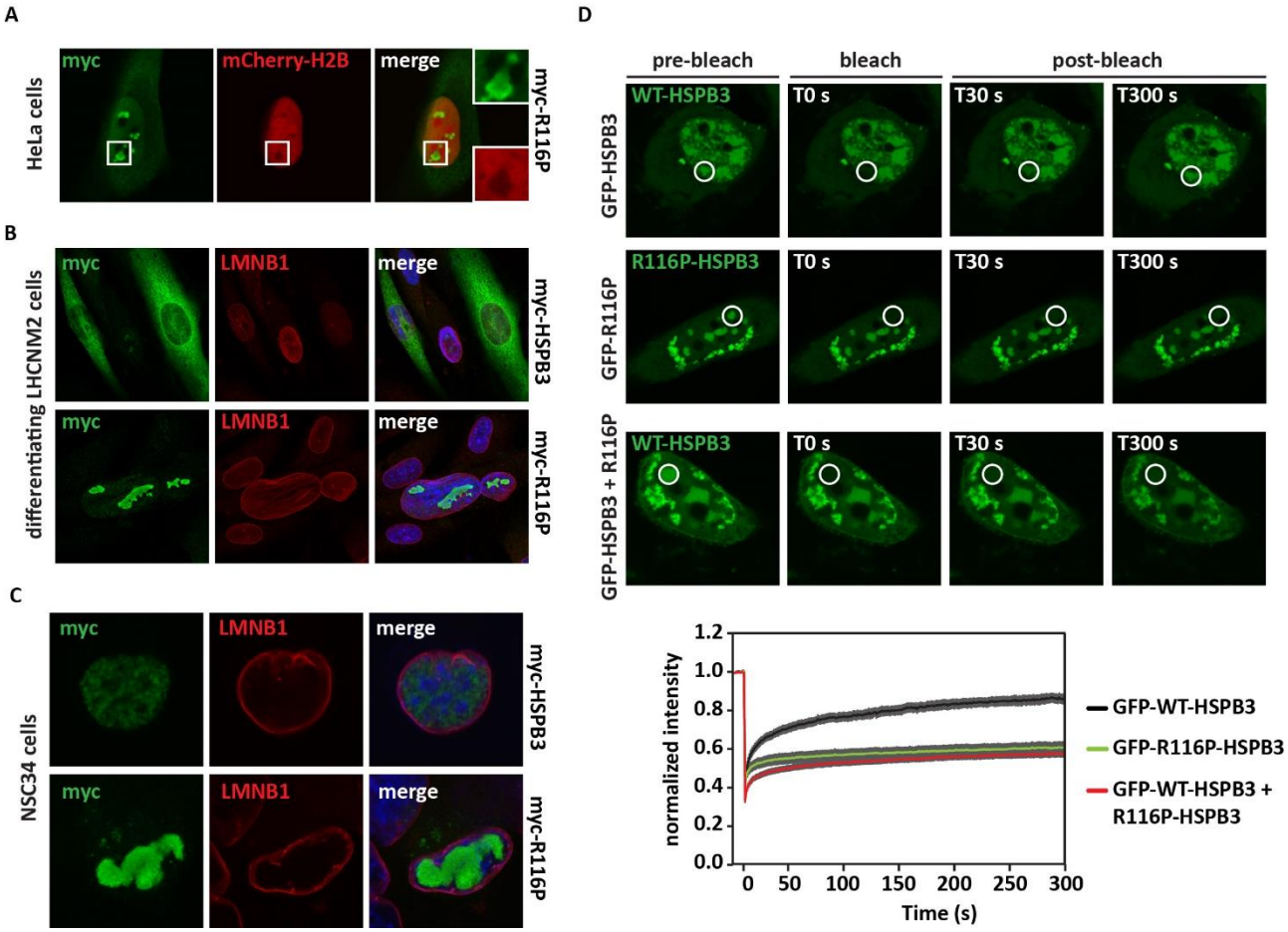


Figure 21 R116P-HSPB3 forms nuclear aggregates. (A) Confocal microscopy on HeLa cells expressing myc-tagged R116P-HSPB3 and mCherry-H2B, using a myc-specific antibody. (B) Confocal microscopy on differentiating LHCNM2 cells expressing myc-tagged WT-HSPB3 or R116P-HSPB3, using myc and LMNB1 antibodies. Nucleic acid was stained with DAPI. (C) Confocal microscopy on motoneuronal-like NSC34 cells expressing myc-tagged WT-HSPB3 or R116P-HSPB3, using myc and LMNB1 antibodies. Nucleic acid was stained with DAPI. (D) HeLa cells were transfected as follows: GFP-WT-HSPB3 (at a 1:8 ratio with myc-WT-HSPB3, upper panel), GFP-R116P-HSPB3 (at a 1:8 ratio with myc-R116P-HSPB3, middle panel) or GFP-WT-HSPB3+R116P (at a 1:8 ratio with myc-R116P-HSPB3, lower panel); 24 hrs post-transfection, cells were subjected to fluorescence recovery after photobleaching (FRAP). Pre-bleach, bleach and post-bleach images of GFP-WT-HSPB3 (upper and lower panels) and GFP-R116P-HSPB3 (middle panel) nucleoplasmic foci are shown. Quantitation of the fluorescence intensity recovery after bleach is reported. The mean of 10 FRAP curves for WT-HSPB3, 13 FRAP curves for R116P-HSPB3 and 13 FRAP curves for WT-HSPB3+R116P-HSPB3 and the fitting curves are shown. sem is shown in grey.

Next, it was tested whether R116P-HSPB3 nuclear aggregates affect the distribution and mobility of LBR-GFP, as well as of WT-HSPB3. Confocal microscopy revealed that R116P-HSPB3 nuclear aggregates sequester LBR-GFP in both HeLa cells and myoblasts (Figure 22 A, B). Subsequently, FRAP experiments showed immobilization of LBR-GFP inside the R116P-HSPB3 nuclear aggregates (Figure 22 C). This effect is in sharp contrast with the increased nucleoplasmic mobility of LBR-GFP observed in cells co-expressing WT-HSPB3 (Figure 16 A, B).

These results suggest that R116P-HSPB3 may acquire a toxic gain of function; therefore, it opened the possibility that it could act in a dominant negative manner by also immobilizing WT-HSPB3. FRAP analysis of HeLa overexpressing GFP-tagged HSPB3 and myc-HSPB3-R116P demonstrated that in presence of R116P-HSPB3, the WT counterpart is sequestered inside nuclear aggregates, where it is becomes immobile (Figure 21 D, lower panel). These results confirm that myc-HSPB3-R116P acts as a dominant negative that impairs the functionality of the WT protein.

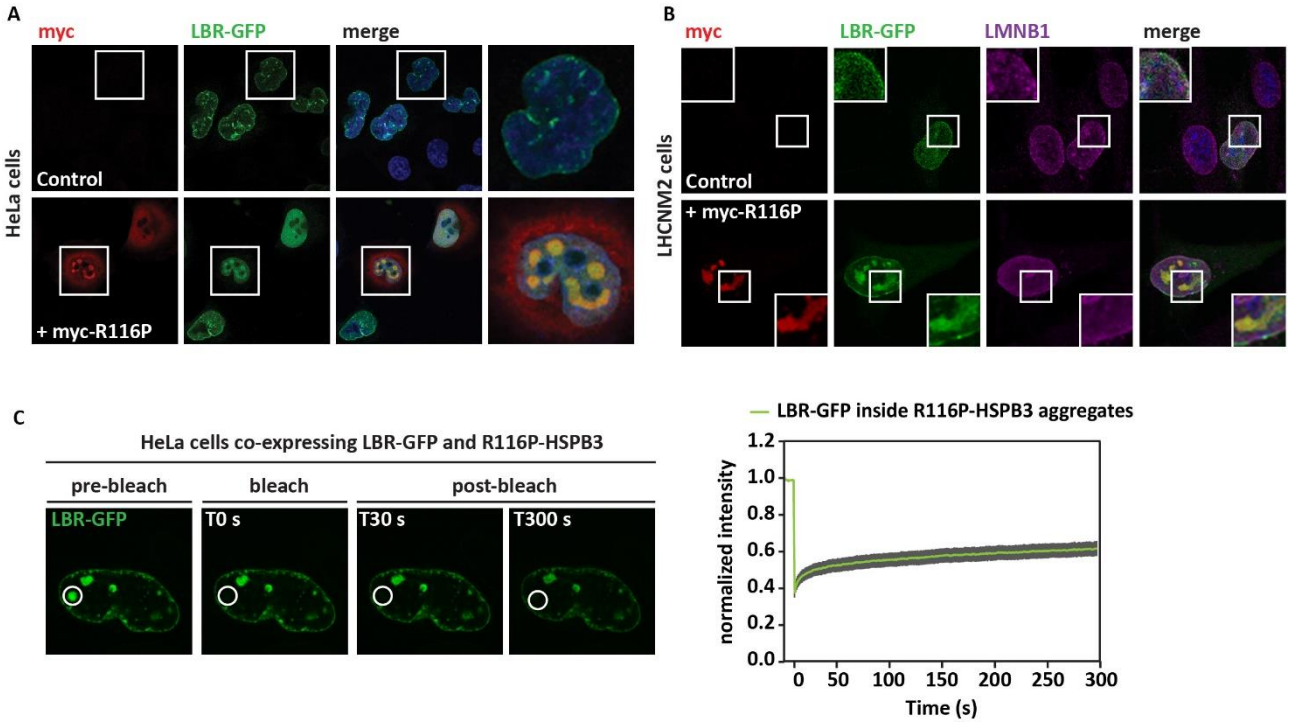


Figure 22 R116P-HSPB3 nuclear aggregates sequester LBR-GFP. (A) Confocal microscopy on HeLa cells expressing LBR-GFP alone or with myc-tagged R116P-HSPB3, using a myc-specific antibody. Nucleic acid was stained with DAPI. (B) Confocal microscopy on LHCNM2 cells expressing LBR-GFP alone or with myc-tagged R116P-HSPB3, using myc and LMNB1 antibodies. Nucleic acid was stained with DAPI. (C) HeLa cells overexpressing LBR-GFP with R116P-HSPB3 were subjected to fluorescence recovery after photobleaching (FRAP). Pre-bleach, bleach, and post-bleach images of LBR-GFP nucleoplasmic foci are shown. Quantitation of the fluorescence intensity recovery after bleach is reported. The mean of 20 FRAP curves and the fitting curves are shown. sem is shown in grey.

## R116P fails to promote myogenic differentiation and induces the unfolded protein response

As previously mentioned, the LBR-tether plays an important role in the regulation of the chromatin remodelling during cell differentiation (Solovei et al., 2013). Thus, it was verified whether R116P-HSPB3 differentially affects the transcriptional program of cycling myoblasts compared to WT-HSPB3. First, compared to the muscle transcriptome of cycling myoblasts overexpressing GFP, used

as a control, R116P-HSPB3 affected the expression of 695 genes (295 genes were upregulated and 400 genes were downregulated) (Figure 23 A, Table 3), while WT-HSPB3 changed the expression of 381 genes (Figure 19 A, Table 2). Importantly, when comparing both WT-HSPB3 and R116P-HSPB3 to GFP, we found that the impact of R116P-HSPB3 on the muscle cell transcriptome was often reversed to the one of WT-HSPB3 (Figure 23 B). For example, LUM and DCN were upregulated by WT-HSPB3, while they were strongly downregulated by R116P-HSPB3 ($p \leq 10^{-10}$) (Figure 23 C, upper left quadrant). Direct comparative analysis was then performed between the transcriptome of myoblasts overexpressing R116P-HSPB3 or WT-HSPB3, which allowed to further appreciate the reverse effects of R116P-HSPB3 (Figure 23 D, E, Table 4). Many of the gene pathways that were upregulated by overexpressing WT-HSPB3 and play a fundamental role in myoblast differentiation, such as ECM remodelling and organization, collagen fibril organization, cell migration, were downregulated by R116P (Figure 23 D).

In addition, compared to WT-HSPB3, overexpression of R116P-HSPB3 in cycling myoblasts induced the expression of genes involved in the unfolded protein response, general stress and ER stress response, as well as in protein degradation (via autophagy and proteasome) (Figure 23 E). Amongst the most highly significantly upregulated genes were those encoding for the Sequestosome-1 (SQSTM1), which is required for autophagic degradation of protein aggregates, the Hsp70 co-chaperone proteins BAG3 and the chaperone HSP90AA1 (Figure 23 C, upper right quadrant). Interestingly, HSP90AA1 (HSP90α) has been described to dissipate upon myogenic differentiation (Echeverría, Briand and Picard, 2016), hence its upregulation by R116P-HSPB3 might further indicate a decrease in the differentiation capacity of the myoblasts. These results suggest that R116P-HSPB3 loses the ability to regulate the expression of genes involved in ECM remodelling, while acquiring aggregation-prone properties that can evoke ER stress and the unfolded protein response, similar to what previously reported for other aggregation-prone proteins that accumulate in the nucleus (Hetz and Saxena, 2017; Kouroku et al., 2002). Both mechanisms may contribute to the muscle degeneration that was previously described in the patient carrying the R116P-HSPB3 mutation (Morelli et al., 2017).

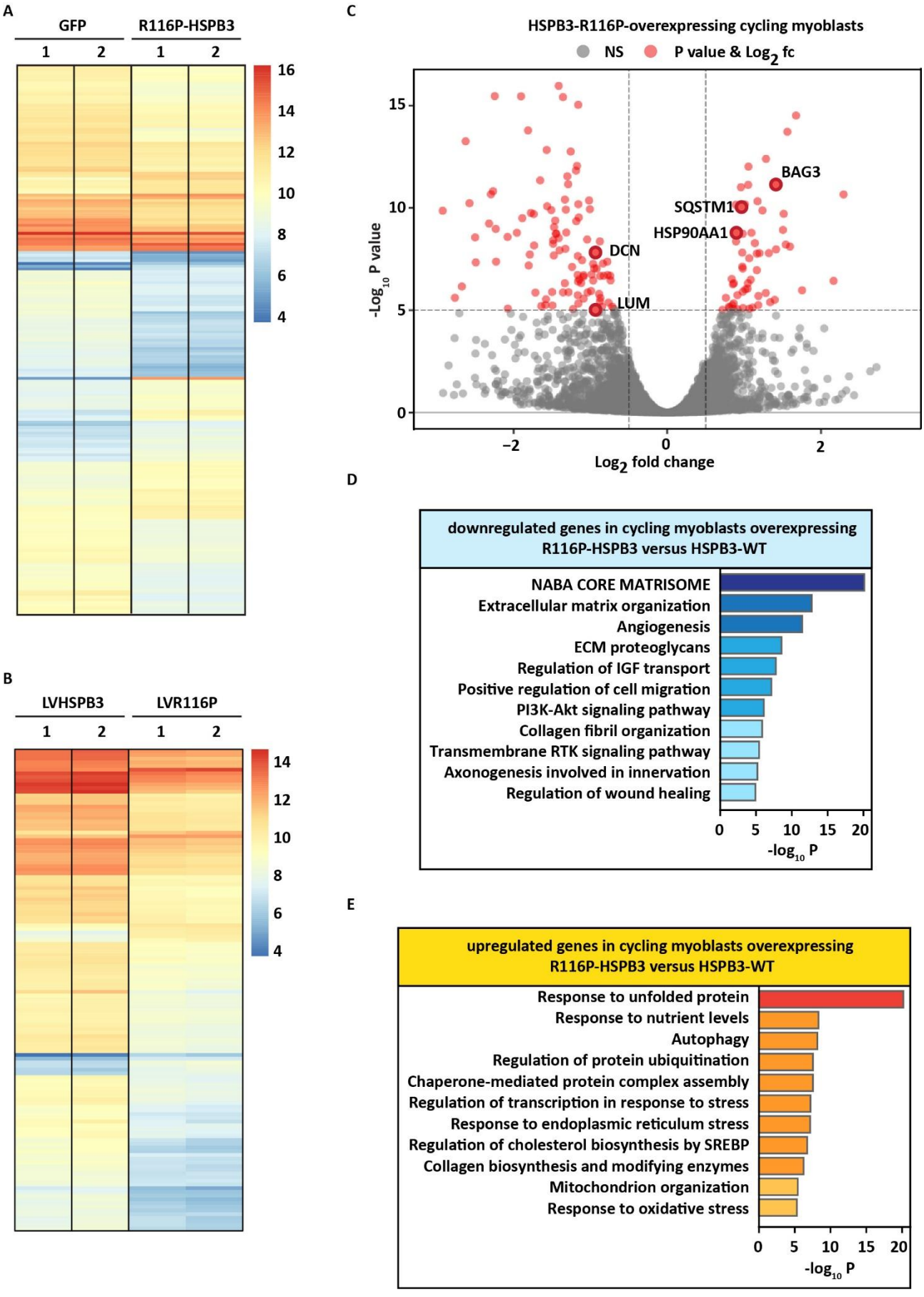
A
GFP
R116P-HSPB3
1
2
1
2
16
14
12
10
8
6
4
B
LVHSPB3
LVR116P
1
2
1
2
14
12
10
8
6
4
C
HSPB3-R116P-overexpressing cycling myoblasts
NS
P value & Log2 fc
15
10
5
0
-Log10 P value
BAG3
SQSTM1
HSP90AA1
DCN
LUM
−2
0
2
Log2 fold change
D
downregulated genes in cycling myoblasts overexpressing
R116P-HSPB3 versus HSPB3-WT
NABA CORE MATRISOME
Extracellular matrix organization
Angiogenesis
ECM proteoglycans
Regulation of IGF transport
Positive regulation of cell migration
PI3K-Akt signaling pathway
Collagen fibril organization
Transmembrane RTK signaling pathway
Axonogenesis involved in innervation
Regulation of wound healing
0
5
10
15
20
-log10 P
E
upregulated genes in cycling myoblasts overexpressing
R116P-HSPB3 versus HSPB3-WT
Response to unfolded protein
Response to nutrient levels
Autophagy
Regulation of protein ubiquitination
Chaperone-mediated protein complex assembly
Regulation of transcription in response to stress
Response to endoplasmic reticulum stress
Regulation of cholesterol biosynthesis by SREBP
Collagen biosynthesis and modifying enzymes
Mitochondrion organization
Response to oxidative stress
0
5
10
15
20
-log10 P

Figure 23 R116P-HSPB3 loses the capacity to promote myogenesis and instead induce a stress response. (A) Heatmap showing the genes that are differentially expressed in 2 independent biological replicates of cycling myoblasts overexpressing myc-R116P-HSPB3 versus GFP, used as control. Genes that displayed greater than $p < 0.01$ are shown. (B) Heatmap showing the genes that are differentially expressed in 2 independent biological replicates of cycling myoblasts overexpressing myc-R116P-HSPB3 versus myc-WT-HSPB3, used as control. Genes that displayed greater than $p < 0.01$ are shown. (C) Volcano plot highlighting that R116P-HSPB3 overexpression upregulates the UPR genes sequestosome 1 (SQSTM1), Heat shock protein 90α (HSP90AA1), and BAG3, while downregulating matrisome genes lumican (LUM) and decorin (DCN), compared to GFP overexpression, used as a control. Horizontal dotted line represents $p < 10\text{-}5$, vertical dotted lines highlight log2 fold-changes of -0.5 and 0.5. Highly significant genes ($p < 10\text{-}10$) with log2 fold-change higher than 0.5 (or lower than -0.5) are marked in red; low significance genes ($p > 10\text{-}5$) with log2 fold-change higher than 0.5 (or lower than -0.5) and non-significant genes are marked in grey. (D, E) Gene-set enrichment analysis: downregulated (D) and upregulated (E) genes upon R116P-HSPB3 overexpression in cycling myoblasts (compared to WT-HSPB3). Analysis performed using Metascape Express Analysis on genes highly significant ($p < 10^{-10}$). The top 10 hits are shown.

## Section II – HSPBs inhibit α-synuclein in vitro

Amongst the molecular chaperones investigated for their potential anti-aggregation function against α-Synuclein are the small heat shock proteins (HSPBs). HSPBs are ATP-independent molecular chaperones and in mammals there are 10 genes encoding for HSPBs (HSPB1-HSPB10). While some HSPBs are ubiquitously expressed, such as HSPB1 and HSPB5, others have restrictive expression and function, such as HSPB3, HSPB9 and HSPB10 (Boncoraglio et al., 2012). HSPBs are characterized by their low molecular weight (12-43kDa) and the presence of a highly-conserved alpha-crystallin domain (ACD) of 80-100 amino acids, flanked by less conserved N-terminal and C-terminal domains. All these regions are involved in regulating the interaction of HSPB monomers, building up oligomers of variable size (Sudnitsyna et al., 2012). The N-terminus and, in some instances the C-terminus of HSPBs possess intrinsically disordered regions (IDR), which confer these proteins a lack of a defined three-dimensional structure in their native state (Sudnitsyna et al., 2012; Babu 2016). The undefined three-dimensional structure allows the interaction of HSPBs with a large variety of substrates. This is also influenced by the ability of HSPBs to reversibly oligomerise. Together the flexibility of HSPB oligomerization, which is also influenced by HSPB post-translational modifications, and the presence of disordered domains enable HSPB to play a wide variety of functions, ranging from prevention of irreversible aggregation to modulation of the structure and dynamics of the cytoskeleton (Carra and Landry, 2006). As molecular chaperones, one of HSPBs main functions correlates with neutralization of non-native and aggregate-prone intermediates, preventing irreversible aggregation (Carra et al., 2013; Mogk and Bukau 2017; Haslbeck, Weinkauf and Buchner, 2019).

This work sought to investigate whether/how HSPBs affect α-synuclein aggregation. More specifically, HSPBs could bind α-synuclein in its monomeric, oligomeric and fibrillar forms, the corresponding forms associated with lipid membranes, as well as to the lipid membranes themselves (Figure 24). Thus, HSPBs could modulate α-synuclein aggregation in a multitude of ways, by interacting with all these states of α-synuclein. To obtain insights into how different HSBPs affect α-synuclein aggregation, we applied a three-pronged approach (Figure 8). The effects of five HSPBs were studied, namely HSPB3 (Hsp17), HSPB5 (αB-crystallin), HSPB6 (Hsp20), HSPB7 (cardiovascular Hsp), and HSPB8 (Hsp22) on α-synuclein lipid-induced aggregation, elongation, and secondary nucleation.

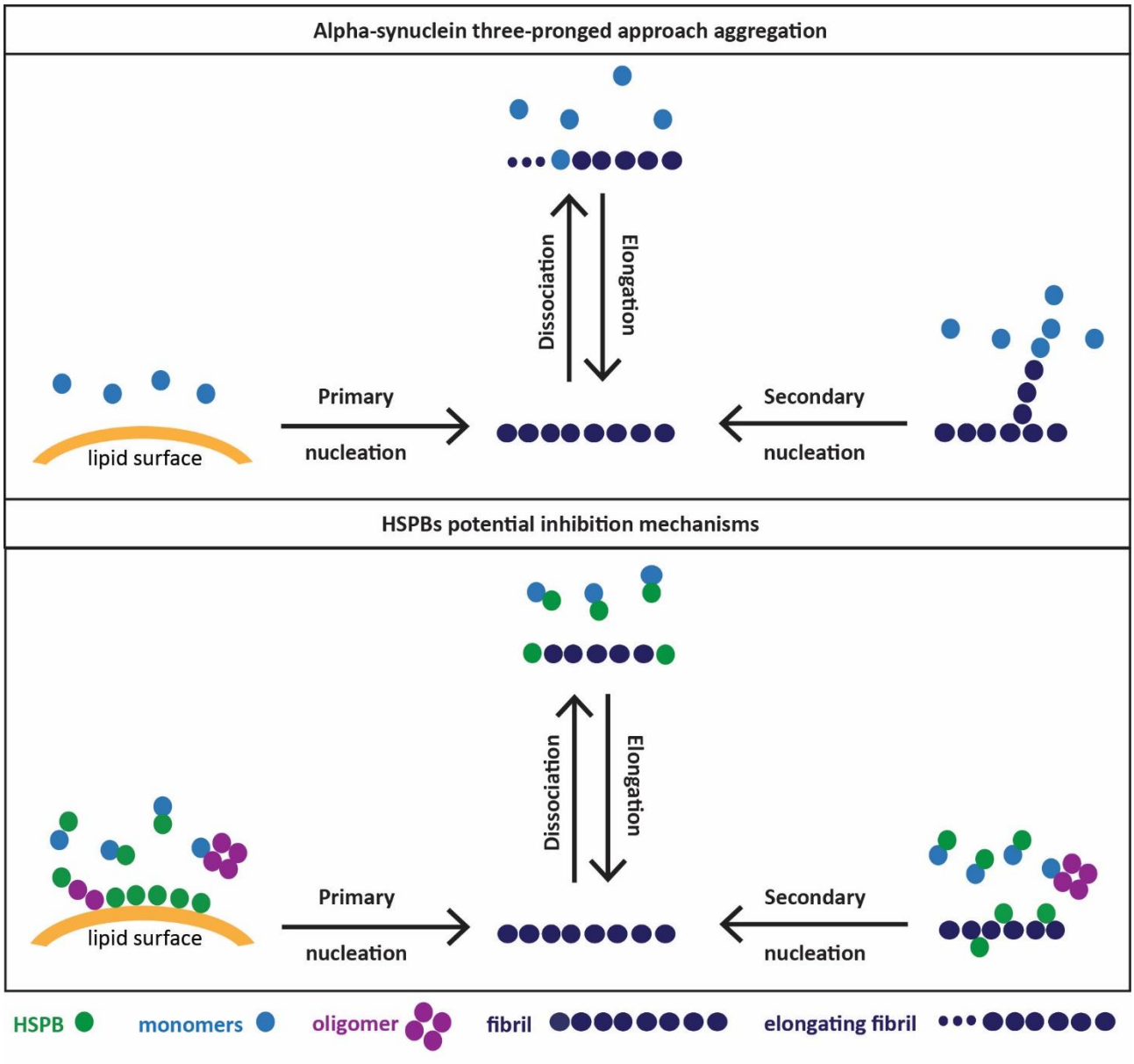


Figure 24 Identification of putative steps of the aggregation process that can be affected by HSPBs. HSPBs could bind α-synuclein in its monomeric, oligomeric and fibrillar forms. HSPBs could also bind to lipid-associated forms of α-synuclein. Alternatively, but not mutually exclusive, HSPBs might compete with α-synuclein for binding to lipids and displace α-synuclein (see bended arrow).

## HSPBs inhibit α-synuclein lipid-induced nucleation with different strengths

The binding of α-synuclein to lipid membranes facilitates its aggregation process (Fusco et al., 2017; Galvagnion et al., 2016; Galvagnion et al., 2015). It has been shown in particular that α-synuclein aggregation can be triggered by the binding of monomeric proteins with small unilamellar vesicles (SUVs) prepared from model membrane lipid DMPS (1,2-dimyristoyl-sn-glycero-3-phospho-L-serin) (Figure 8, step 1).

As amyloid fibril formation can be measured over time by ThT fluorescence, the question whether or not HSPBs affect the lipid-induced aggregation of α-synuclein was raised. This study focussed on five members of the HSPB family: HSPB3, HSPB5, HSPB6, HSPB7, and HSPB8. All these HSPBs could delay lipid-induced aggregation at low stoichiometries, but with different degrees of efficacy (Figure 25 A, B). In particular, HSPB6 showed the strongest effect as it completely inhibited α-synuclein lipid-induced aggregation on the timescale that we monitored, while HSPB3 had the lowest inhibitory effect (Figure 25 A, B). The other HSPBs tested had intermediate effects (Figure 25b). HSPB5, HSPB6, HSPB7 and HSPB8 all seemed to delay the onset of aggregation: the aggregation of α-synuclein alone was detectable already after 5 hours of incubation, while it was delayed to 30 – 40 hours in the presence of HSPB5-8 (Figure 25 A). However, once the aggregation was initiated, it proceeded with similar kinetics regardless of the presence of HSPB5-8 (Figure 25 A).

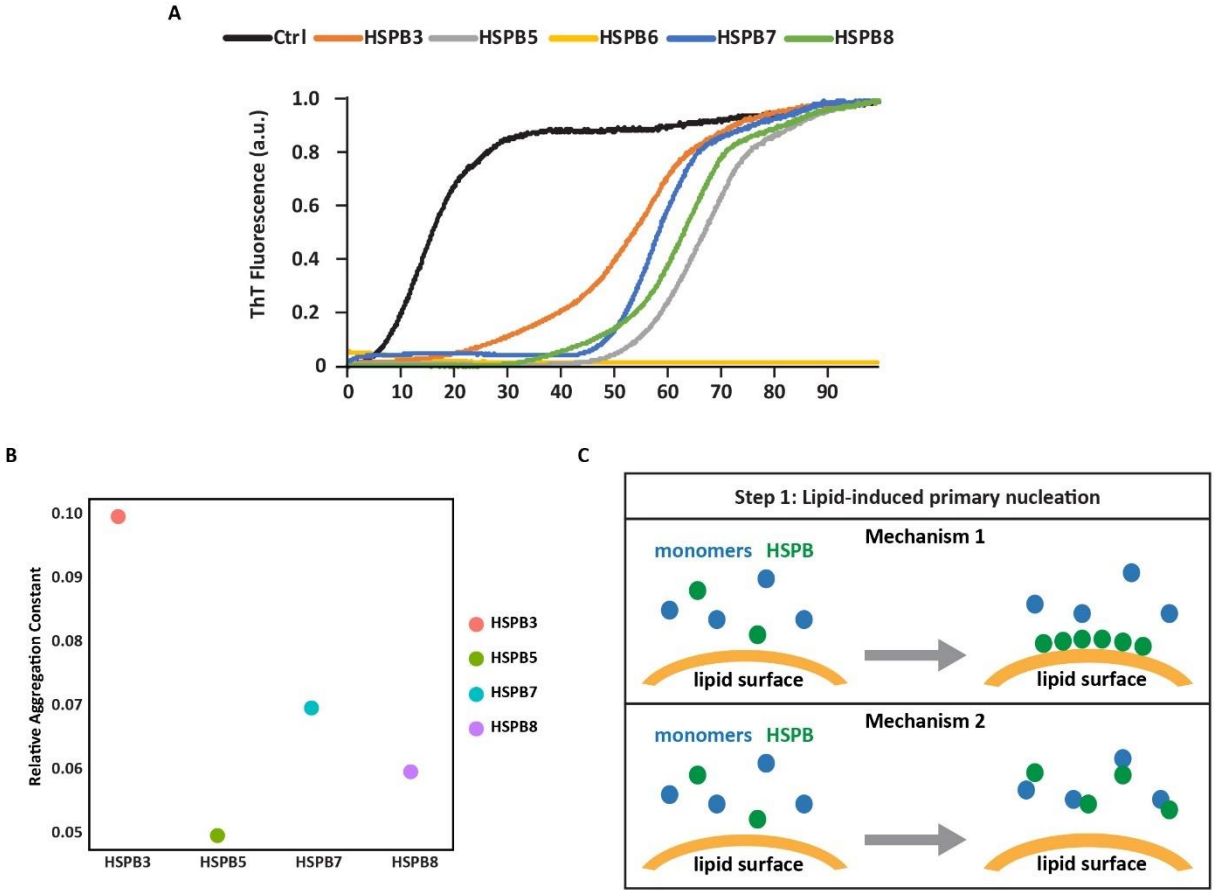


Figure 25 HSPBs inhibit lipid-induced alpha-synuclein primary nucleation. (A) Changes in ThT fluorescence intensity when monomeric alpha-synuclein (20µM) is incubated with 100µM DMPS at pH 6.5 and 30°C and in the absence (black) or presence of HSPBs (0.2µM): HSPB3 (orange), HSPB5 (grey), HSPB6 (yellow), HSPB7 (blue), HSPB8 (green). Data as absolute ThT fluorescence. a.u. arbitrary units. (B) Relative rate of lipid-induced alpha-synuclein aggregation constant, determined by AmyloFit (Meisl et al., 2016), in the presence of HSPB3 (pink), HSPB5 (green), HSPB7 (blue), HSPB8 (purple), as per conditions in detailed in A. n = 3; SEM = 3.4E-3 (HSPB3); 4.64E-3 (HSPB5); 7.27E-3 (HSPB7); 4.47E-3 (HSPB8). (C) Schematic representation of possible HSPBs effect on lipid-induced aggregation.

In light of these observations, the aggregation kinetics was then analysed in detail using a one-step nucleation model previously developed (Galvagnion *et al.*, 2015). In this model, the nucleation reaction is assumed to occur at the surface of the vesicles and is then followed by the growth of fibrils from the lipid-bound α-synuclein (Figure 25 B). To enable direct comparison of the various HSPBs, the elongation rates were normalized to that of α-synuclein alone. Due to the complete inhibition of primary-nucleation, HSPB6 was excluded from this analysis. Using this model, HSPB3 was confirmed to have the lowest efficacy, nevertheless it displayed a strong delaying capacity with a relative aggregation rate ratio to α-synuclein alone (Ctrl) of 0.10 (Figure 25 B); by contrast, HSPB5, HSPB7 and HSPB8 reduced the lipid-induced aggregation with a relative aggregation rate ratio between 0.05 and 0.07 (Figure 25 B).

These results are compatible with at least two possible, not mutually exclusive, mechanisms (Figure 25 C). In mechanism 1, HSPBs compete with α-synuclein for binding to lipid membranes, thus reducing α-synuclein lipid-induced aggregation. In mechanism 2, HSPBs bind to α-synuclein monomers, thus preventing their binding to the lipid surface.

### HSPB6 competes with α-synuclein for binding to lipids and inhibits its lipid-induced nucleation

To differentiate between the two possible mechanisms by which HSPBs may inhibit lipid-induced α-synuclein primary nucleation, a series of experiments were carried out with the aim of testing whether HSPBs can interact with lipid membranes. HSPB1, HSPB4, HSPB5 and HSPB8 were previously reported to interact with lipid membranes (Chowdary et al., 2007; Cobb & Petrash, 2002; De Maio et al., 2019; De Maio & Hightower, 2020; Gangalum et al., 2011). In these experiments it was exploited the observation that when proteins interact with lipid membranes, they can affect their fluidity and melting temperature. More specifically, the binding of monomeric α-synuclein to lipid vesicles containing DMPS decreases its melting temperature from 45 °C to 35 °C (Galvagnion et al., 2015). Thus, it was measured how the fluidity of these membranes changes in absence or presence of HSPBs by monitoring changes in fluorescence polarisation (FP) of diphenylhexatriene (DPH) with increasing temperatures (Figure 26). The impact of the various HSPBs on lipid membrane fluidity was compared to that in the presence of α-synuclein, employed as a positive control. HSPB3, HSPB6 and HSPB7, but not HSPB5 and HSPB8 reduced the melting temperature of DMPS, indicating

these HSPBs directly interact with the lipid vesicles (Figure 26 A). Of note, each HSPB examined displayed a different temperature at which it had a stronger impact: 35 °C for HSPB3, 37 °C for HSPB6 and 40 °C for HSPB7. In addition, the impact of HSPBs on the melting temperature of DMPS was lower compared to the one of α-synuclein (Figure 26 A). To further characterize the interaction of HSPBs with lipid membranes, SUVs prepared from POPS (1-palmitoyl-2-oleoyl-sn-glycero-3-phospho-L-serine) and DOPS (1,2-dioleoyl-sn-glycero-3-phospho-L-serine) were used, which have the same head group but different hydrocarbon chains to DMPS. POPS and DOPS are also considered to be more physiologically relevant lipid vesicles, given the fact that phosphatidylserine (PS) is highly abundant in synaptic vesicles (Galvagnion et al., 2015). However, compared to DMPS, POPS and DOPS have a lower protein-free melting temperature than DMPS, corresponding to 17 °C and <10 °C, respectively (Petrache et al, 2004). Therefore, the analysis of fusion temperature would not be possible using the same temperature ranges as DMPS. Incorporation of α-synuclein into POPS and DOPS lipid vesicles led to a decrease in DPH fluorescence polarisation, supporting its association (Figure 26 A). Using these vesicles, the impact on membrane fluidity of HSPB3, HSPB6 and HSPB7 was similar or even stronger than the one of α-synuclein (Figure 26 A). Instead, HSPB5 and HSPB8 had a lower impact on POPS and DOPS, similar to what observed using DMPS (Figure 26 A).

Once established that HSPB3, HSPB6 and HSPB7 affect the fluidity of lipid membranes, next it was measured their impact on the incorporation of α-synuclein into the lipid vesicles, including also HSPB5 and HSPB8 in the study. The embedding of α-synuclein within the lipid vesicle changed their fluidity in a concentration-dependent manner, as we found that the higher the amount of α-synuclein embedded, the higher the fluidity change (Galvagnion et al., 2015). When co-incubating α-synuclein with a given HSPB and DMPS, different results were obtained depending on the type of HSPB used. In line with previous findings, α-synuclein changed the fluidity of DMPS, POPS and DOPS vesicles (Figure 26 B). Compared to α-synuclein alone, all HSPBs tested, except for HSPB8, led to a reduction of lipid vesicles fluidity (Figure 26 B). Based on these data it was possible to conclude that HSPB3, HSPB5 and HSPB7 reduced α-synuclein embedding inside the lipid vesicles, with HSPB7 showing a stronger effect. By contrast, co-incubation of α-synuclein with HSPB6 increased even

further the fluidity curve, compared to α-synuclein alone, suggesting that both proteins are embedded in the lipid vesicles.

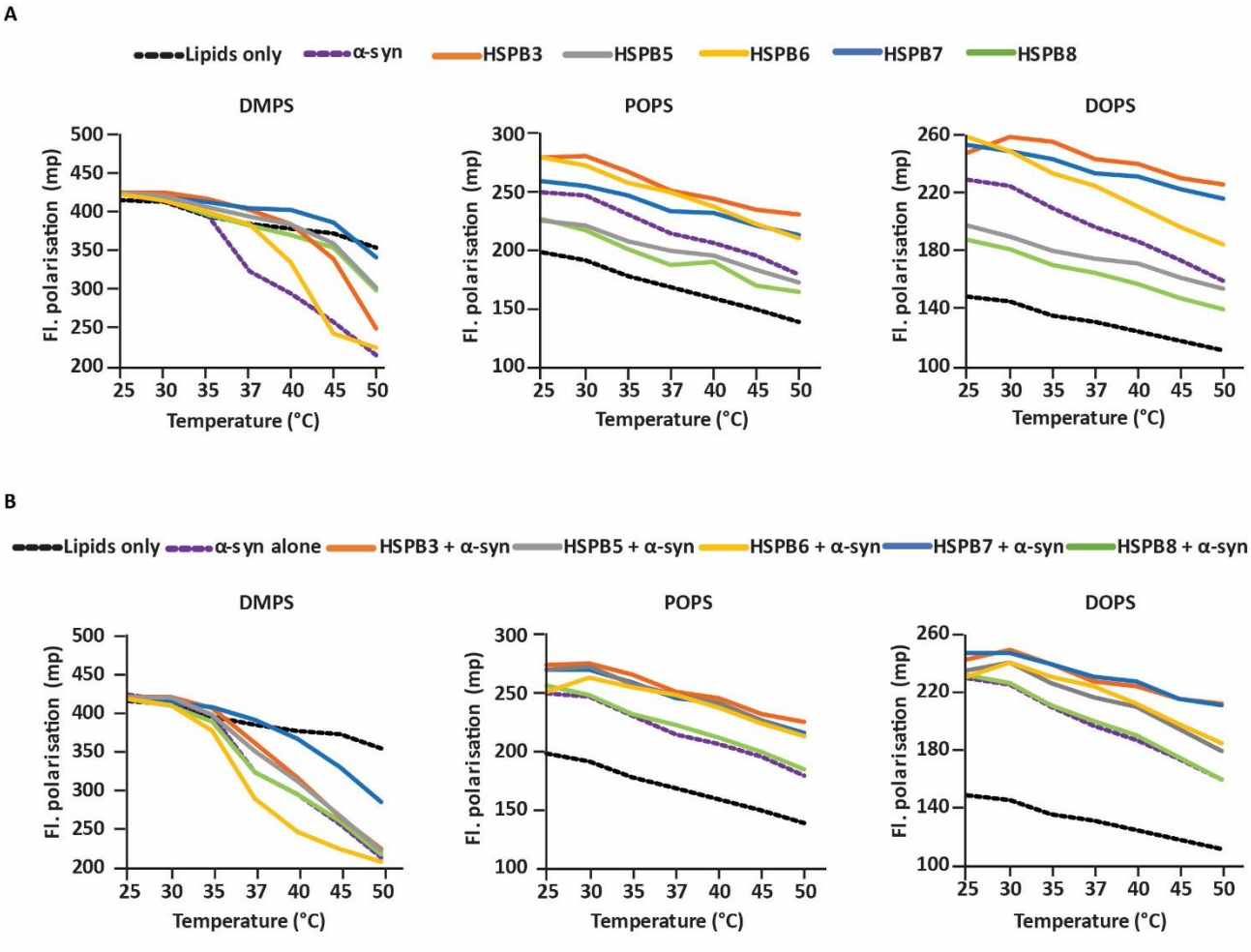


Figure 26 HSPBs interact with lipid vesicles. (A) Changes in lipid vesicle (100µM) membrane fluidity due to presence of alpha-synuclein or HSPBs (20µM) detected through fluorescence polarisation of DPH at increasing temperatures (25°C to 50°C). (B) Changes in lipid vesicle (100µM) membrane fluidity due to presence of alpha-synuclein and HSPBs (20µM) detected through fluorescence polarisation of DPH at increasing temperatures (25°C to 50°C).

In order to further elucidate how the interactions of HSPBs might have an impact on lipid-induced α-synuclein aggregation, the effect of HSPBs was observed over time in the conditions of the lipid-induced aggregation (DMPS at 30 °C). The fluidity of DMPS did not alter over time, but changes in fluidity were detected from the beginning of the measurement (Figure 27 A-E). As previously reported (Galvagnion et al., 2015), co-incubation of α-synuclein with DMPS lipid vesicle greatly increased the fluidity of the lipid vesicles, as evidenced by the decrease in fluorescence polarization of DPH. HSPB7 and HSPB8 did not affect the fluidity per se (Figures 27 D, E). However, in presence of α-synuclein, the fluidity was rescued (Figures 27 D, E).

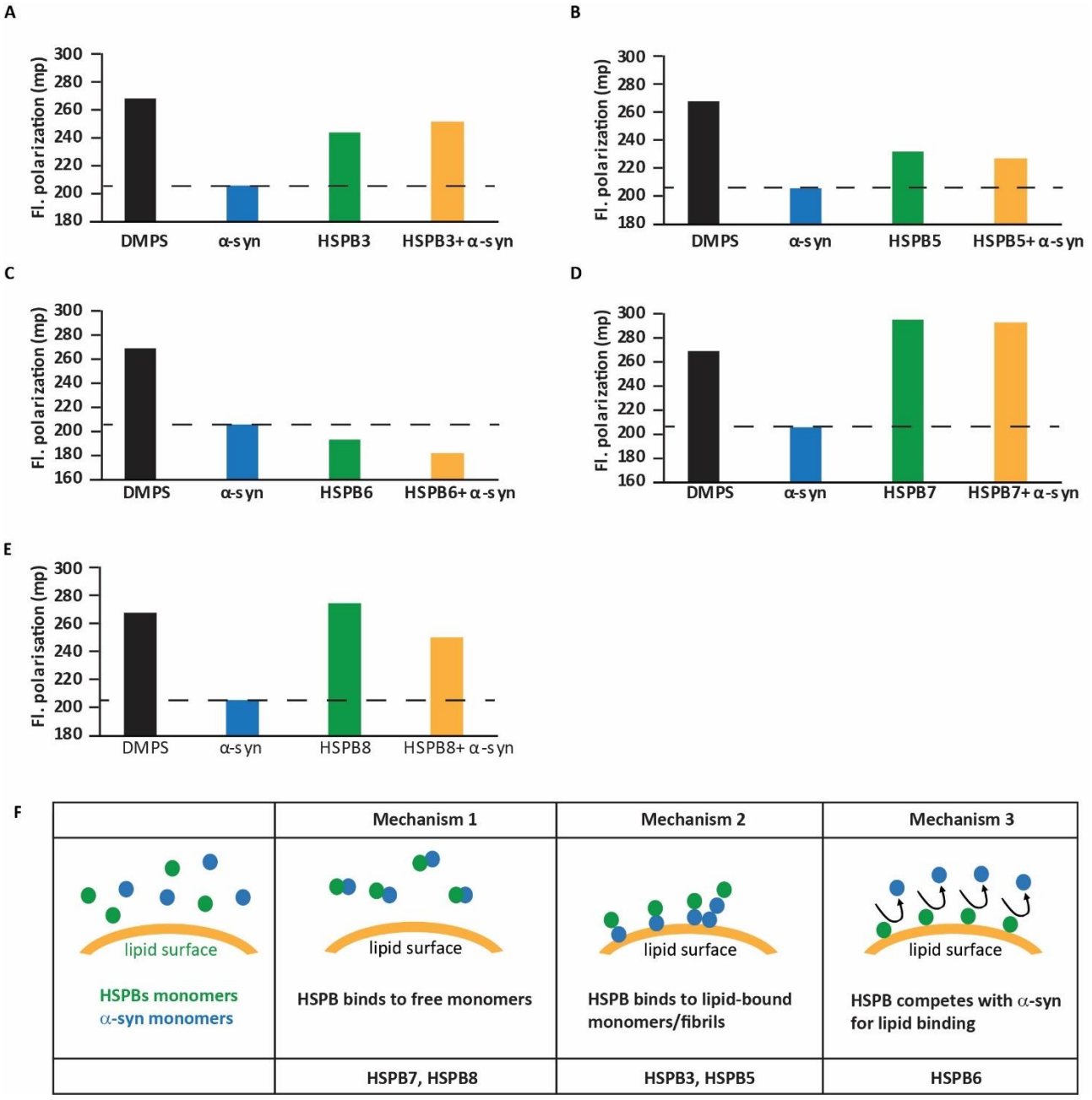


Figure 27 Impact of HSPBs on the fluidity of DMPS lipid vesicles and on α-synuclein lipid-induced aggregation. (A-E) Changes in DMPS (100µM) membrane fluidity due to presence of alpha-synuclein or HSPBs (20µM) detected through fluorescence polarisation of DPH at 30°C for 4h: HSPB3 (A), HSPB5 (B), HSPB6 (C), HSPB7 (D), HSPB8 (E). (F) Schematic representation of effect of HSPBs in alpha-synuclein/lipid interaction.

It is thus possible to propose that these HSPBs may bind to free α-synuclein monomers, thereby preventing α-synuclein association with lipids, thus maintaining the fluidity (Figure 27 F, mechanism 1). HSPB3 and HSPB5 both altered SUV fluidity when incubated alone, and slightly rescued the loss of membrane fluidity due to α-synuclein (Figures 27 A, B). These data may suggest that these HSPBs bind to monomers of α-synuclein embedded in the lipid membranes, thereby preventing α-synuclein aggregation, which would further affect membrane fluidity (Figure 27 F, mechanism 2).

Concerning HSPB6, when incubated alone with the SUVs, it reduced their fluidity more than α-synuclein alone; when HSPB6 and α-synuclein were co-incubated with the SUVs, the fluidity was not restored but further reduced (Figure 27 C). Together these results suggest that HSPB6 competes with α-synuclein for binding to lipids, partly displacing α-synuclein monomers and consequently abrogating its lipid-induced aggregation (Figure 27 F, mechanism 3).

### HSPBs delay α-synuclein fibril elongation with different kinetics

As the initial formation of α-synuclein fibrils is followed by their growth by elongation (Flagmeier et al., 2016), it was investigated whether HSPBs inhibit α-synuclein fibril elongation using a method previously described (Flagmeier et al., 2016; Galvagnion et al., 2016; Galvagnion et al., 2015). In this assay, fibril growth is induced by the addition of monomeric α-synuclein to the ends of mature fibrils at neutral pH (Figure 8, step 2). All HSPBs tested delayed the elongation of the preformed fibrils, although with different kinetics (Figure 28 A). To enable direct comparison of the HSPBs, the measured elongation rates were normalised relative to the one of α-synuclein alone (Figure 28 B). HSPB3, HSPB5, and HSPB7 inhibited elongation with a relative fibril elongation ratio of approximately 0.1, independently of HSPB concentration. HSPB8 delayed fibril elongation with a relative fibril elongation ratio of 0.2 to 0.35; HSPB8 showed slightly reduced activity when used at lower concentrations (Figure 28 A, B). HSPB6 delayed fibrils elongation only at high concentration. When the concentration of HSPB6 was equal to that of monomeric α-synuclein, the relative fibril elongation ratio was of 0.2, and when HSPB6 concentration was 4-times lower that the one of monomeric α-synuclein, HSPB6 had almost no effect (Figure 28 A, B).

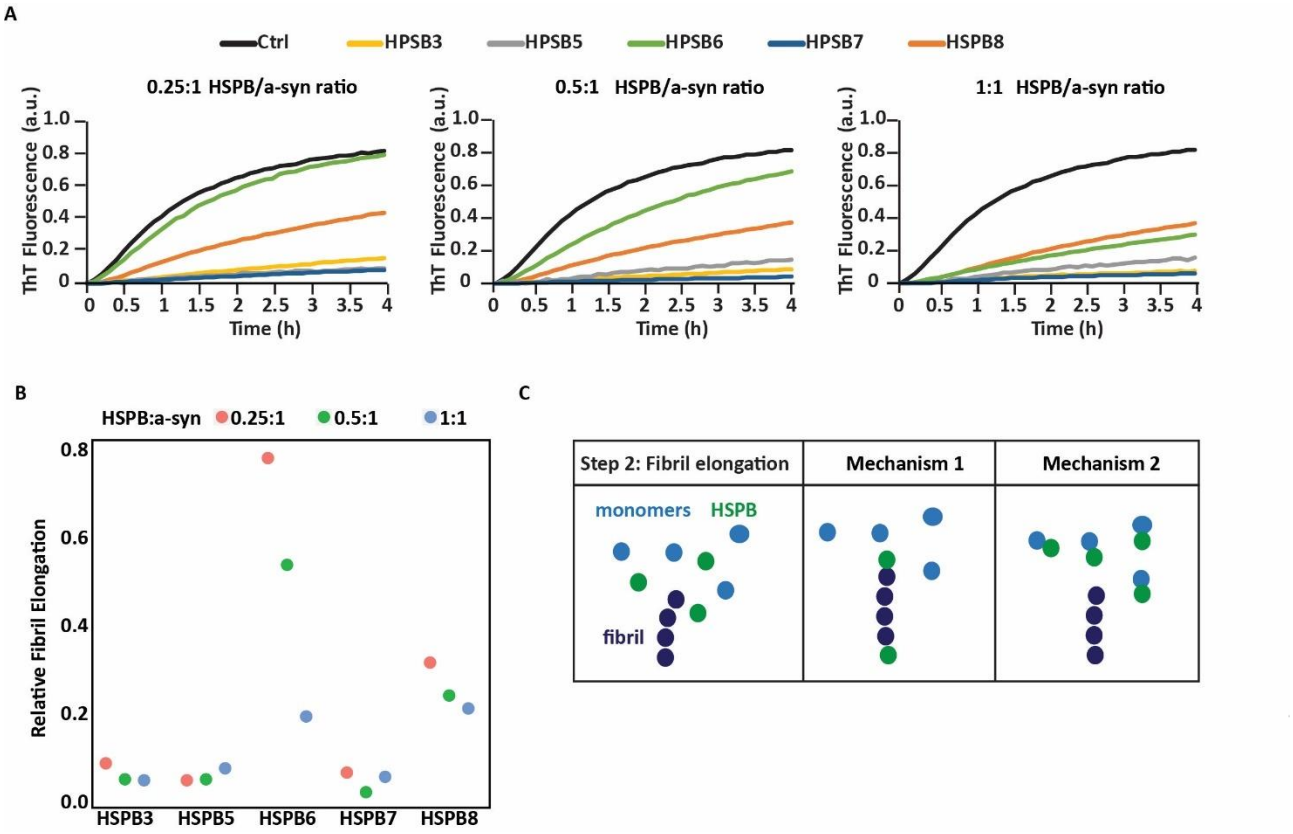


Figure 28 HSPBs delay alpha-synuclein fibril elongation. (A) Changes in ThT fluorescence intensity when monomeric alpha-synuclein (20uM) is incubated with 1uM preformed fibrils at pH 6.5 and 37°C and in the absence (black) or presence of HSPBs: HSPB3 (yellow), HSPB5 (light blue), HSPB6 (green), HSPB7 (blue), HSPB8 (orange), HSPBs at 5uM, 10uM or 20uM. Data as absolute ThT fluorescence. a.u. arbitrary units. (B) Relative rate of alpha-synuclein fibril elongation, determined as per Flagmeier et al., 2016. n = 3; SEM = 6.08E-4 (HSPB3 5 µM); 9.20E-3 (HSPB 5 µM); 7.99E-3 (HSPB6 5 µM); 7.17E-4 (HSPB7 5 µM); 2.73E-3 (HSPB8 5 µM); 2.12E-3 (HSPB3 10 µM); 7.53E-3 (HSPB 10 µM); 1.04E-4 (HSPB6 10 µM); 2-09E-4 (HSPB7 10 µM); 1.08E-2 (HSPB8 10 µM); 5.18E-3 (HSPB3 20 µM); 2.13E-3 (HSPB 20 µM); 1.24E-1 (HSPB6 20 µM); 2.62E-2 (HSPB7 20 µM); 7.97E-3 (HSPB8 20 µM). (C) Schematic representation of the putative effect of HSPBs on fibril elongation.

The poor efficacy of HSPB6 on fibril elongation, together with its high binding affinity for lipids reinforces the idea that HSPB6 interacts weakly with monomeric α-synuclein, hence the need for high concentrations of HSPB6 to have an effect on fibril elongation. Thus, the protective effect of HSPB6 would mainly consists in competing with α-synuclein for the interaction with lipid membranes, therefore inhibiting the lipid-induced primary nucleation. Concerning the other HSPBs tested, two distinct mechanisms of action could explain the results obtained. In the first mechanism, HSPBs bind the extremities of α-synuclein fibrils, thus preventing the incorporation of the added seeds into the pre-existing fibril. In the second mechanism, HSPBs bind to α-synuclein monomers and prevent their binding to the fibrils. It is entirely possible that both mechanisms might simultaneously occur (Figure 28 C). Importantly, on this assay the concentration of α-synuclein seeded fibrils (1 µM) is considerably lower than the monomer concentration (20 µM). Therefore,

the kinetics observed might be better explained by an affinity of HSPBs to intermediary forms of α-synuclein, leading to an arrest at the earlier stages of aggregation. Since the ability of HSPB8 to inhibit elongation is concentration dependent, the presented data suggest that HSPB8 would bind with higher affinity to α-synuclein monomers rather than to the fibril extremities. Thus, its ability to neutralize α-synuclein monomers is dependent on the HSPB8:α-synuclein monomers ratio. By contrast, the ability of HSPB3, HSPB5 and HSPB7 to prevent fibril elongation was not affected by their concentration, suggesting that they might bind with higher affinity to the pre-formed fibrils, rather than to free α-synuclein monomers (Figure 28 C).

### HSPBs delay α-synuclein secondary nucleation with different kinetics

To further understand how HSPBs affect α-synuclein aggregation, next it was studied their impact on α-synuclein fibril amplification, which occurs via secondary nucleation pathways including the formation of surface-catalysed aggregates, under conditions of mildly acidic pH ( Buell et al, 2014; Flagmeier *et al.*, 2016) (Figure 8 step 3). First, since the secondary nucleation assay is performed at low pH, by circular dichroism (CD) it was measured whether lowering the pH affects the folding and stability of the various HSPBs, which would influence their chaperone activity. Lowering the pH from 6.5 to 5.5 affected only the CD spectra of HSPB5, which was thus excluded from further analysis using the secondary nucleation assay to avoid data misinterpretation (Figure 29).

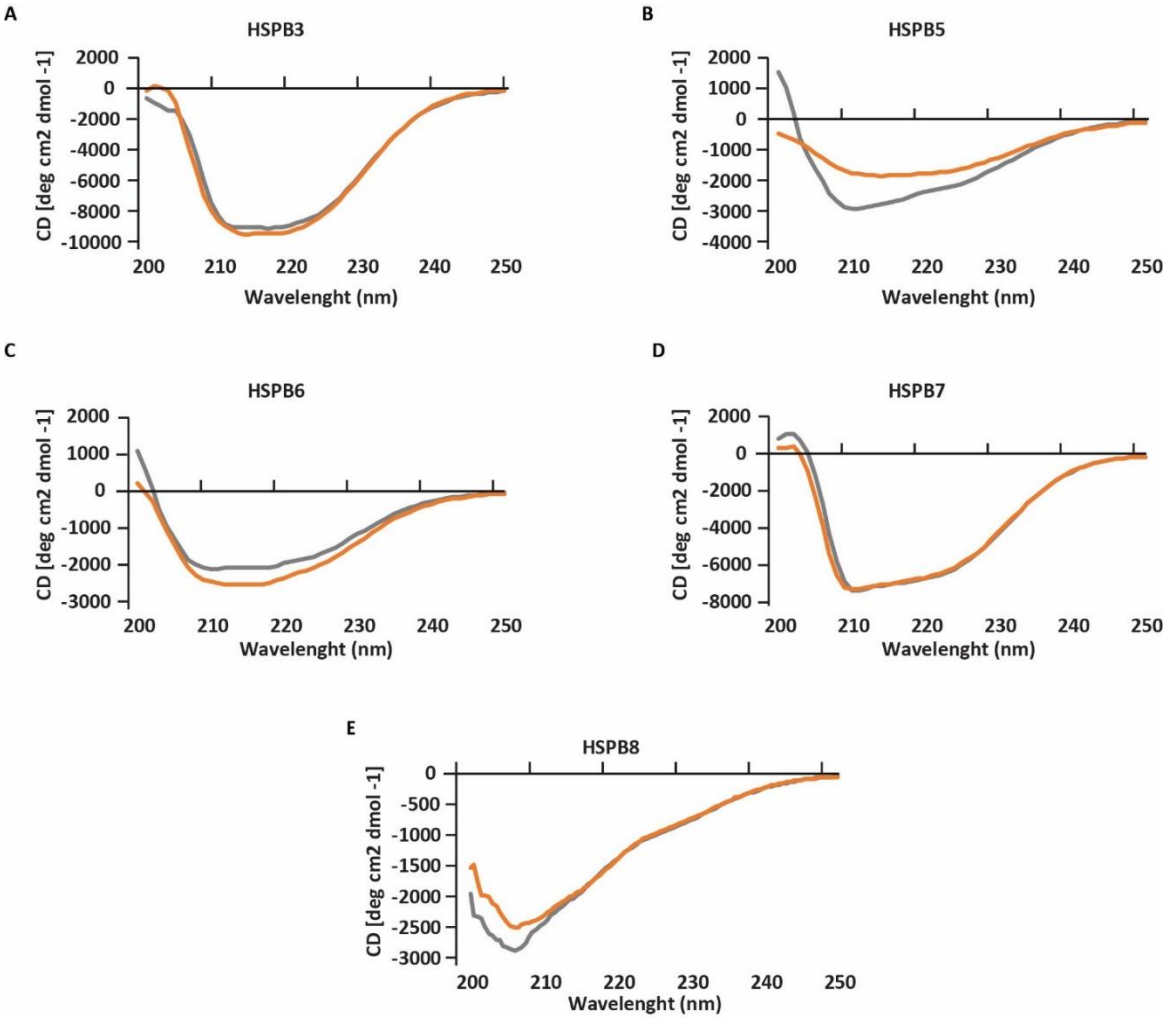


Figure 29 HSPBs CD spectra at different pH. (A-E) Change in the CD signal of HSPBs (25µM) when in sodium phosphate buffer at pH 6.5 (gray) or pH 5.5 (orange): HSPB3 (A), HSPB5 (B), HSPB6 (C), HSPB7 (D), HSPB8 (E).

The other HSPB studied, HSPB3, HSPB6-8 could all delay α-synuclein secondary nucleation, although with different strengths (Figure 30 A). HSPB7 and HSPB3 strongly delayed α-synuclein secondary nucleation, while HSPB8 had a moderate effect and HSPB6 performed poorly compared to α-synuclein alone, although still displaying some chaperone activity (Figure 30 A). As for primary nucleation and for elongation, two different, but not mutually exclusive, mechanisms of action could explain the results obtained. In the first mechanism, HSPBs bind to α-synuclein fibril surfaces and prevent the binding of monomers to the pre-formed fibril. In the second mechanism, HSPBs bind to α-synuclein monomers and prevent them from binding to and amplifying the pre-existing fibrils (Figure 30 B). Taken together the results obtained using the three-pronged approach support the

idea that HSPB8 inhibits α-synuclein aggregation by binding to and neutralizing its monomeric forms, while HSPB3 and HSPB7 preferentially bind to α-synuclein oligomer and/or fibrils.

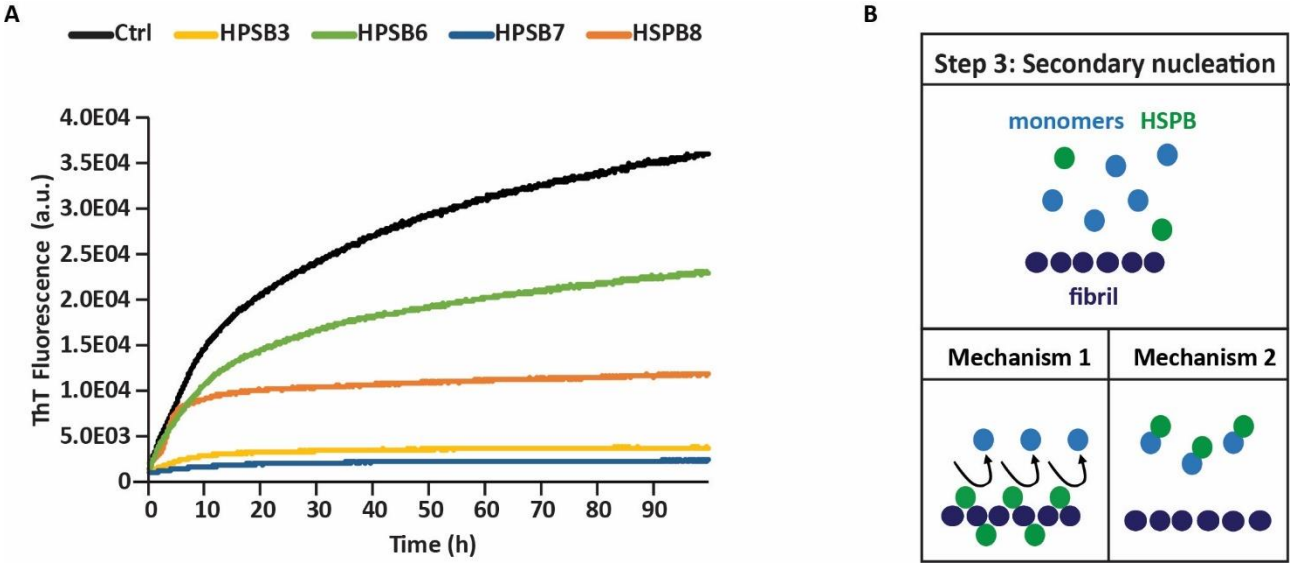


Figure 30 HSPBs delay alpha-synuclein secondary nucleation. (A) Changes in ThT fluorescence intensity when monomeric alpha-synuclein (20uM) is incubated with 50nM preformed fibrils at pH 5.5 and 37°C and in the absence (black) or presence of HSPBs (5uM): HSPB3 (yellow), HSPB5 (light blue), HSPB6 (green), HSPB7 (blue), HSPB8 (orange). Data are shown as absolute ThT fluorescence. a.u. arbitrary units. (C) Schematic representation of possible HSPBs effect on secondary nucleation.

## The disease-related mutant K141E-HSPB8 weakly inhibits fibril elongation compared to WT-HSPB8

Mutations in several HSPB genes have been linked to human neuromuscular diseases ranging from myofibrillar myopathy (e.g. HSPB5) to distal hereditary neuropathies (e.g. HSPB1, HSPB3 and HSPB8) (Evgrafov *et al*, 2004; Irobi *et al*, 2004; Kolb *et al*, 2010; Morelli *et al*, 2017; Nam *et al*, 2018; Vicart *et al*, 1998). Amongst the best characterized mutations in the HSPB genes is the K141E-HSPB8, which was the first disease-causing mutation discovered in the HSPB8 gene (Irobi *et al.*, 2004). Studies performed in mammalian cells and aimed at comparing the anti-aggregation properties of K141E and wild-type (WT) HSPB8 showed that K141E is characterized by a reduced ability to inhibit the aggregation of various misfolded proteins such as expanded huntingtin (Htt43Q), ataxin 3 (SCA3(64)Q), which lead to polyglutamine-diseases (Carra *et al*, 2010; Carra *et al*, 2005). Studies in vivo, using a *drosophila melanogaster* model of SCA3 further confirmed a partial loss of chaperone activity of K141E-HSPB8 compared to WT-HSPB8. In vitro studies using alcohol dehydrogenase and rhodanese as model proteins further confirmed the lower chaperone activity of K141E-HSPB8 compared to WT-HSPB8 and evidenced an increased susceptibility of K141E-HSPB8 to trypsinolysis (Kim *et al*, 2006). Based on these data here it was further investigated using the three-pronged

approach whether/how the K141E mutation affects the HSPB8 chaperone activity towards α-synuclein.

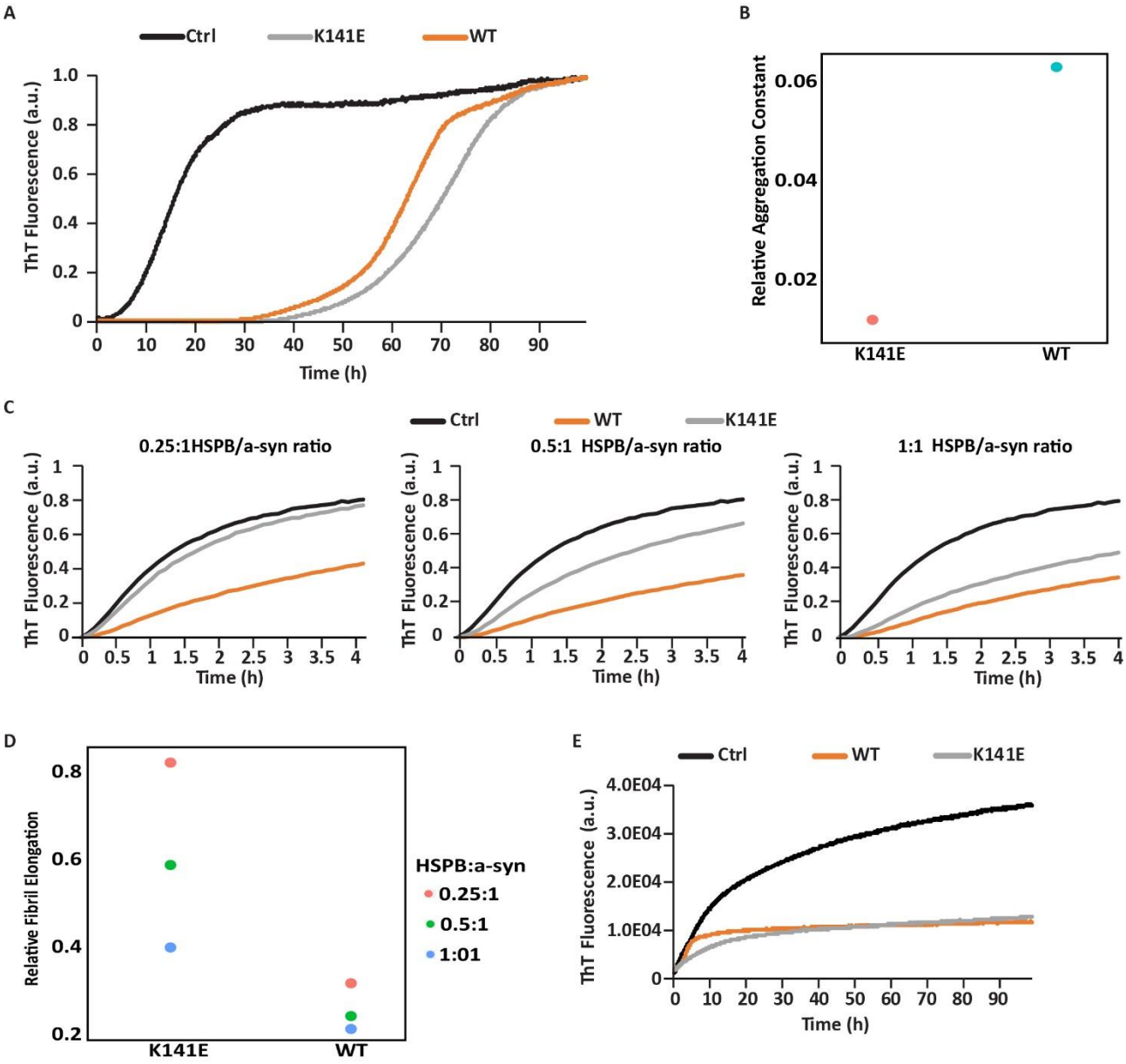


Figure 31 K141E-HSPB8 fails to inhibit fibril elongation. (A) Changes in ThT fluorescence intensity upon incubation of monomeric α-synuclein (20μM) with 100uM DMPS at pH 6.5 and 30°C and in the absence (black) or presence of HSPBs (0.2μM): HSPB8 WT (orange) or HSPB8 K141E (grey). Data as absolute ThT fluorescence. a.u. arbitrary units. (B) Relative rate of lipid-induced alpha-synuclein aggregation constant, determined by AmyloFit (Meisl et al., 2016), in the presence of HSPB8 WT (blue) or HSPB8 K141E (orange), as per conditions in detailed in A. n = 3; SEM = 4.47E-3 (HSPB8 WT); . 4.44E-3 (HSPB8 K141E) (C) Changes in ThT fluorescence intensity when monomeric alpha-synuclein (20μM) is incubated with 1μM preformed fibrils at pH 6.5 and 37°C and in the absence (black) or presence of HSPBs: HSPB8 WT (orange) or HSPB8 K141E (grey), at 5μM, 10μM or 20μM. Data as absolute ThT fluorescence. (D) Relative rate of alpha-synuclein fibril elongation, determined as per Flagmeier et al., 2016. n = 3. SEM = 2.73E-3 (HSPB8 WT 5 μM); 3.95E-3 (HSPB8 K141E 5 μM); 5.22E-3 (HSPB8 WT 10 μM); 1.08E-2 (HSPB8 K141E 10 μM); 7.97E-3 (HSPB8 WT 20 μM); 1.21E-2 (HSPB8 K141E 20 μM). (E) Changes in ThT fluorescence intensity when monomeric alpha-synuclein (20μM) is incubated with 50nM preformed fibrils at pH 5.5 and 37°C and in the absence (black) or presence of HSPBs (5uM): HSPB8 WT (orange) or HSPB8 Ks141E (grey). Data are shown as absolute ThT fluorescence. a.u. arbitrary units.

K141E-HSPB8 was very efficient in inhibiting the lipid-induced α-synuclein aggregation and actually displayed a slightly higher activity compared to WT-HSPB8 (lowering the relative aggregation rate ratio from 0.06 to 0.01; Figure 31 A, B). Similar to WT-HSPB8, K141E-HSPB8 did not reduce the melting temperature of DMPS, neither did it affect fluidity, indicating no direct interaction with lipid vesicles (Figure 32).

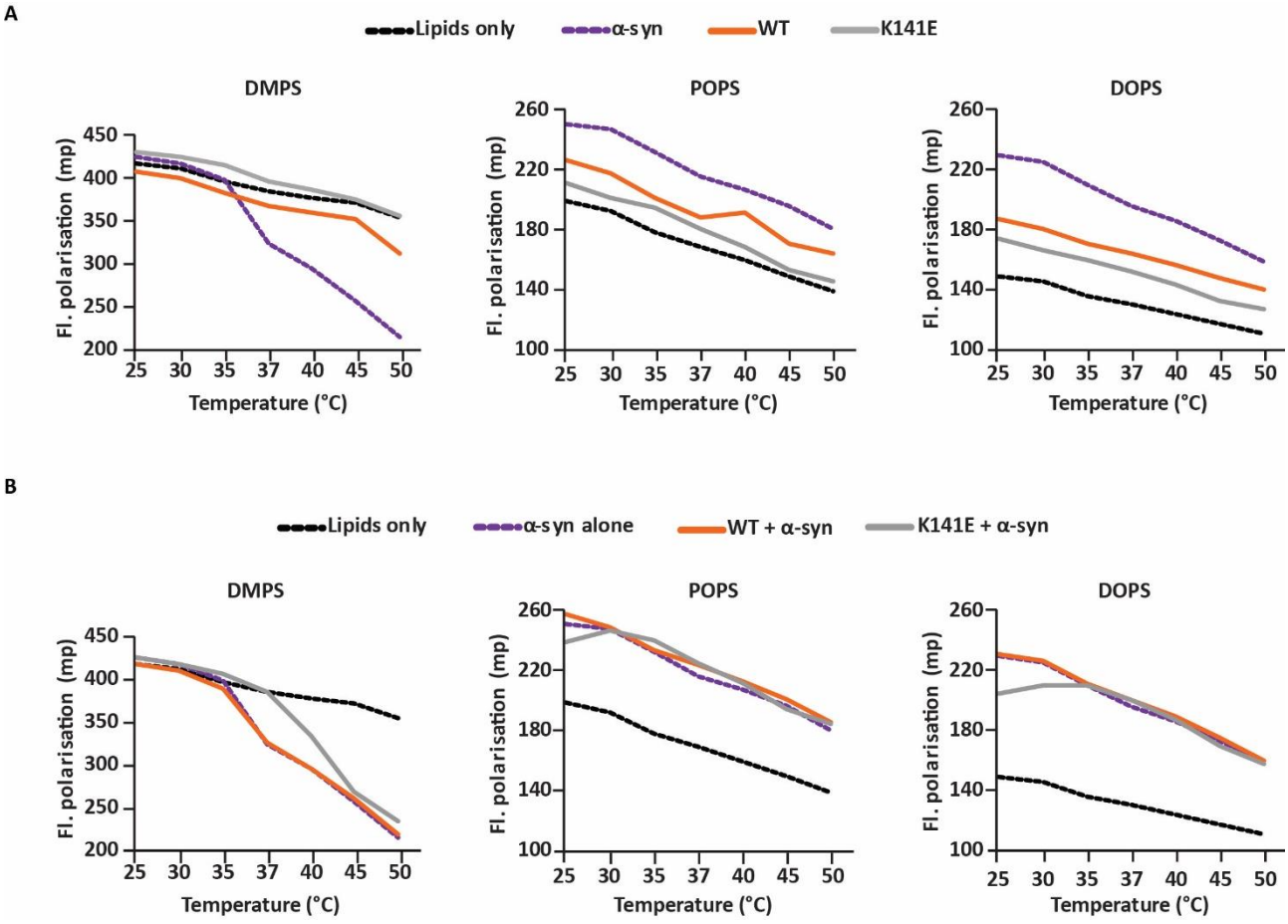


Figure 32 K141E-HSPB8 interact with lipid vesicles. (A) Changes in lipid vesicle (100µM) membrane fluidity due to presence of alpha-synuclein or HSPBs (20µM) detected through fluorescence polarisation of DPH at increasing temperatures (25°C to 50°C). (B) Changes in lipid vesicle (100µM) membrane fluidity due to presence of alpha-synuclein and HSPBs (20µM) detected through fluorescence polarisation of DPH at increasing temperatures (25°C to 50°C).

However, when K141E-HSPB8 was co-incubated with lipid vesicles and α-synuclein, K141E-HSPB8 rescued the vesicle fluidity; this result suggests that K141E-HSPB8 binds to free α-synuclein monomers, thereby preventing their association with lipids (Figure 33). By contrast, K141E-HSPB8 could delay fibril elongation less efficiently than WT-HSPB8, and this loss of function was particularly evident when K141E-HSPB8 was used at lower concentrations (Figure 31 C, D). Concerning fibril amplification, K141E-HSPB8 was as efficient as WT-HSPB8 in delaying secondary nucleation (Figure

31 E). Together these data suggest that K141E-HSPB8 is unable to inhibit fast rated aggregation, which is typical of α-synuclein fibril elongation.

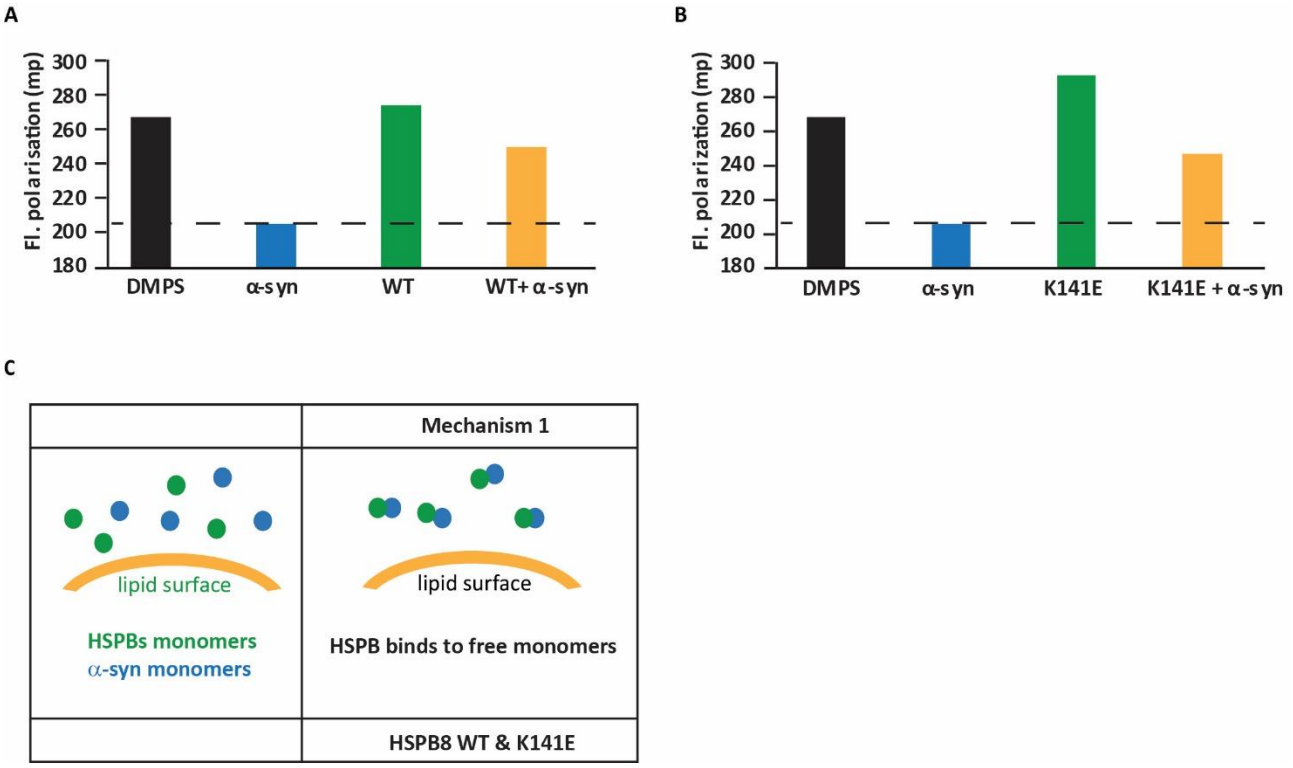


Figure 33 Impact of K141E-HSPB8 on the fluidity of DMPS lipid vesicles and on α-synuclein lipid-induced aggregation. (A and B) Changes in DMPS (100µM) membrane fluidity due to presence of alpha-synuclein or HSPBs (20µM) detected through fluorescence polarisation of DPH at 30°C for 4h: WT (A), K141E (B). (C) Proposed working model for WT and K141E-HSPB8.

# Discussion

## Section I

The mammalian HSPB family consists of ten members, some of which are ubiquitously expressed, such as HSPB1 and HSPB5, while others have restrictive expression, such as HSPB2 and HSPB3, which are predominantly expressed in muscle cells and restricted neuronal populations, including peripheral motor neurons (Janoswka et al., 2019). HSPB3 is the most deviating member of the HSPB family, which is mainly found in muscle and specific neuronal populations but whose physiological functions are largely unknown. Muscle cells orchestrate their differentiation by transcribing a set of specialized factors, ranging from muscle-specific structural proteins to a subset of specialized chaperones, which are expressed under the control of the muscle transcription factor MYOD (Sala et al., 2017). These chaperones include Hsp90 and the small HSP hsp-12.2 in *C. elegans* (Bar-Lavan et al., 2016), and HSPB2 and HSPB3 in mammalian cells (Sugiyama et al., 2000). This work provides compelling evidence supporting the idea that HSPB3 is a specialized chaperone that engages in the muscle differentiation program.

But what is the experimental evidence that supports an active role for HSPB3 in muscle differentiation? And how can a small HSP regulate the muscle transcriptional program? The finding that HSPB3 stands out as one of the top genes that are strongly downregulated in pluripotent cells and act as differentiation marker (Ghosh and Som, 2020) suggests that HSPB3 may actively participate in the differentiation process. In agreement with this hypothesis, HSPB3 was shown to facilitate the differentiation process in human myoblasts (LHCN-M2 cells) by promoting the ECM remodelling and the build-up of the specialized muscular cytoskeletal apparatus required for myogenesis (Bentzinger et al., 2013; Li et al., 2007; Cornelison et al., 2001; Brack et al., 2008; Csapo et al., 2020). In particular, HSPB3 upregulates the proteoglycan decorin, which has been shown to promote muscle differentiation, as well as muscle regeneration in vivo (Li et al., 2007). Conversely, HSPB3 depletion impairs the activation of the transcriptional program that is required for skeletal muscle differentiation, structure development and function, as well as muscle contraction. Importantly, HSPB3 depletion leads to the downregulation of the myogenic factor MYOG, which is required for the expression of muscle-specific genes and the activation of signalling cascades required for the various steps of muscle development (Rhodes et al., 1989; Braun et al., 1990; Miner

et al., 1990). A careful analysis of the genes affected by HSPB3 downregulation or overexpression highlighted many genes that have a recognized function in muscle differentiation and build-up. Myoblast commitment to differentiation initiates with irreversible withdrawal of cycling myoblasts from the cell cycle. In particular, upon induction of myogenic differentiation, the cell-cycle inhibitor p21 is upregulated in a MYOD-dependent manner (Halevy et al., 1995) leading to the blockage of CDK4 and cell cycle arrest (De Falco, Comes and Simone, 2006). Of note, CDK4 is downregulated by HSPB3 while p57, a cell-cycle inhibitor analogous to p21, is upregulated upon HSPB3 overexpression. Moreover, decorin interacts with ErbB receptors, leading to activation of the MAPK signal transduction pathway, eventually inducing p21 and cell cycle arrest (Li et al., 2008). Besides decorin also MAP2K2 is upregulated by HSPB3 overexpression in cycling myoblasts, as well as the ErbB pathway. These results point to a specific function of HPB3 at the early stages of differentiation, where it promotes the commitment to differentiation and induces the expression of proteins required for muscle development.

Skeletal muscle atrophy is associated with elevated apoptosis while muscle differentiation results in apoptosis resistance, indicating that apoptosis requires tight regulation in muscle cells to ensure homeostasis. Indeed, myotubes express high levels of p21 and hypophosphorylated Rb, which maintain terminal differentiation and protect these multinucleated cells against apoptosis (Peschiaroli et al., 2002). Moreover, the process of cell differentiation requires the activation of cell-death associated caspases, whose activation needs to be tightly controlled to avoid excessive apoptosis, which would lead to tissue degeneration and improper tissue development (Bakthisaran et al., 2015; Kamradt et al., 2002). Interestingly, one of biological processes downregulated by the expression of HSPB3 is the positive regulation of the apoptotic process. Of note, the positive mediator of apoptosis GADD45B (Cho et al., 2010) is highly downregulated by HSPB3. This is in line with previous data showing that HSPBs act as anti-apoptosis regulators (Kamradt et al. 2001; Sui et al., 2009; Kanagasabai et al., 2010). For example, HSPB1 can directly bind to cytochrome-c, preventing apoptosome formation and consequent apoptosis (Bruey et al., 2000). HSPB1 is a ubiquitously expressed HSPBs, therefore it is not surprising that the tight regulation of apoptosis during myogenesis would require a targeted chaperone. Hence, it is possible that while promoting differentiation, HSPB3 is also playing a role in the modulation of apoptosis thus protecting the myoblasts from cell death.

Finding that manipulation of the expression of HSPB3 changes the expression of many different gene pathways was unexpected. How changes in the expression levels of one single member of the HSPB family can have such a profound impact on a complex and highly regulated process such as muscle cell differentiation? HSPB3 would act on an upstream player that can indeed regulate the transcriptional program required for cell cycle exit and commitment to differentiation.

The transcriptional changes require extensive chromatin remodelling. One of the early events that regulates the chromatin remodelling is the switch between the LBR-tether and the LMNA-tether (Solovei et al., 2013). The finding that in differentiating muscle cells HSPB3 is localized in the nucleus and can be enriched at the NE suggested the idea that HSPB3 could indirectly participate to the NE and chromatin remodelling. Expression analysis and study of the subcellular localization of LBR in cycling myoblasts overexpressing HSPB3 or differentiating myoblasts downregulating HSPB3 demonstrated that an interplay exists between HSPB3 and LBR. The idea that LBR could be a novel molecular target of HSPB3 was substantiated by the findings that HSPB3 directly interacts with LBR and promotes its delocalization from the NE into the nucleoplasm. LBR binds to LMNB1 and tethers heterochromatin to the inner nuclear membrane in undifferentiated and embryonic cells (Solovei et al., 2013). Of note, the effects of HSPB3 on LBR were highly specific: HSPB3 selectively affected the nuclear distribution of LBR, leaving unchanged the one of LMNB1 and H2B. In addition, overexpression of HSPB7, another member of the HSPB family that, similar to HSPB3, shows a restricted expression profile or of the ubiquitous HSPB1 did not affect the distribution of LBR. Thus, the present data identifies LBR as one of the molecular targets of HSPB3 that regulates the transcriptional program of muscle cells. However, since the chromatin associates with the NE via multiple components, including not only lamins, but also LEM domain proteins and DNA binding factors, we cannot exclude the possibility that, besides LBR, HSPB3 might also interact with and regulate the subcellular localization of other NE-associated proteins. Future research will need to further address how HSPB3 influences NE and chromatin remodelling, ultimately promoting the expression of pro-differentiating genes. Independently on what are the exact molecular targets of HSPB3, our study clearly supports a role for HSPB3 as a facilitator of skeletal muscle cell differentiation, with clear implications for disease.

Concerning HSPB3-linked diseases, this work characterized the sub-cellular localization and expression of the 4 known mutations (R7S-HSPB3, R116P-HSPB3, Y118H-HSPB3 and A33AfsX50-HSPB3). WT-HSPB3 was predominantly expressed in the nuclear fraction, while R7S-HSPB3 was

mainly distributed in the cytoplasmic fraction. Interestingly, the HSPB3-dN mutant which had the N-terminal truncated, presents itself predominantly in the cytoplasm. Therefore, these results indicate that HSPB3 might have a nuclear localization signal on its N-terminal. Interestingly, HSPB1 and HSPB5 localize to the cytoplasm of myoblasts under normal conditions but translocate to the nucleus under conditions of stress (Adhikari et al., 2004). Hence, alteration of the subcellular localization by R7S-HSPB3 might lead to loss-of-function upon specific conditions where HSPB3 is required in the nucleus. Further research will need to be conducted to address how HSPB3 localization might play an important role in its function. By contrast, R116P-HSPB3 and Y118H-HSPB3 accumulated inside the nucleus, with Y118H-HSPB3 being almost absent in the cytoplasmic fraction. The mutation R116P-HSPB3, is located at the groove between HSPB2 and HSPB3 and resides in the highly conserved "hot-spot" arginine (R)/lysine (K) residue where many HSPB disease-causing mutations have been reported (Vendredy, Adriaenssens and Timmerman, 2020). The R116P-HSPB3 mutation disrupts the binding of HSPB3 to HSPB2 (Morelli et al 2017). By contrast, the mutation Y118H-HSPB3, which also lies at the border of the same grove does not impair HSPB3's ability to bind to HSPB2. This thesis focused on the R116P-HSPB3 mutation, previously identified in a myopathy patient displaying muscle fibre disorganization and chromatin alterations (Morelli et al., 2017). This work reveals that R116P-HSPB3 aggregates in the nucleus and immobilizes both WT-HSPB3 and LBR-GFP, with profound consequences on the transcriptome of skeletal muscle cells. Indeed, R116P-HSPB3 loses the ability of inducting ECM proteins required for myogenic differentiation, among which decorin. Not only decorin, but also the majority of the genes that promote cell differentiation and are upregulated by WT-HSPB3 were unaffected by R116P-HSPB3, pointing to a loss of this specific function. Of note, satellite cell activation and differentiation, as well as ECM remodelling are important to regenerate the muscle and neuromuscular junction that can be damaged because of aging or disease (Charge and Rudnicki, 2004; de Luca et al., 2014; Le Grand and Rudnicki, 2007; Yin et al., 2013). In addition, HSPB3-linked neuromuscular diseases develop with aging, when the peripheral nerve and muscle regeneration capacities decline (Carosio et al., 2011; Li et al., 2018; Wallace and McNally, 2009). These results open the possibility that, by exerting a dominant-negative effect, R116P-HSPB3 may decrease the differentiation capacity and regenerative potential of muscles during aging and in response to muscle damage. In addition, mutations in genes that decrease the differentiation capacity of muscle cells, such as dysferlin, have been linked to myopathies (Cohen et al., 2012; Klinge et al., 2007). On the other hand, not only does R116P-HSPB3 fails to promote myogenic differentiation but it also leads to the stimulation of the unfolded protein

response. Another “hot spot” mutation R120G-HSPB5 impaired the ability of HSPB5 to negatively regulates apoptosis during myogenesis (Kamradt et al. 2001; Kamradt et al., 2002). Intriguingly, R116P-HSPB3 does not downregulate apoptosis mediator GADD45B which might further indicate a loss of myogenic regulation. HSPB3 mutations are also genetically linked to motor neuropathies, opening the possibility that HSPB3 may display a pro-differentiation function also in motor neurons, and deregulation thereof may contribute to neuromuscular disease. Of note, the switch between the LBR and LMNA tethers is not specific to muscle cells, but occurs during the differentiation of different cell types, including neuronal cells (Solovei et al., 2013). Moreover, mutations in genes that play a role in cell differentiation, including neuronal and muscle cell differentiation, as well as defects in the differentiation process have been linked to motor neuropathies.

In summary, the findings presented in this thesis provide an additional example to how cells can regulate complex processes such as muscle cell differentiation by switching on the expression of highly specialized chaperones in a cell-type and temporal regulated manner. They also pave the way for a better understanding of HSPB3 implication in the physiology and pathology of the neuromuscular system, with implications that may extend to myopathy. Future work will need to address the role of HSPB3 in motor neuron differentiation and regeneration upon damage.

## Section II

Aggregation of α-synuclein has been recognized as one of the main factors for the development of Parkinson’s disease and dementia with Lewy Bodies (Spillantini et al., 1998; Polymeropoulos et al., 1997; Krüger et al., 1998; Zarranz et al., 2004; Appel-Cresswel et al., 2013; Lesage et al., 2013). Yet, our knowledge regarding both the pathophysiology and possible therapeutic strategies that could halt disease progression are still limited (Herrero and Morelli, 2017; Chakraborty et al., 2020; Pujols et al., 2020). Thus, approaches that aim at decreasing protein aggregation, by boosting for example the expression and function of molecular chaperones may offer a promising therapeutic avenue to treat these neurodegenerative diseases. This work compared the ability of five human HSPBs to inhibit α-synuclein aggregation using a previously developed three-pronged approach that enables to separately study three key steps in the α-synuclein aggregation process: lipid-induced primary

nucleation, fibril elongation and fibril amplification (Flagmeier *et al.*, 2016; Galvagnion *et al.*, 2015). All the HSPBs studied inhibit or delay α-synuclein aggregation, although with different efficacies and mechanisms that include HSPB binding to monomeric α-synuclein or to α-synuclein fibrils, as well as competition with α-synuclein for binding to lipids. These observations pave the way for further research which might prove useful in making use of molecular chaperones as a promising therapeutic avenue to treat these neurodegenerative diseases.

HSPB1 and HSPB5 were previously shown to bind to monomeric and fibrillar α-synuclein and to prevent fibril elongation (Bendifallah *et al.*, 2020; Cox *et al.*, 2018; Waudby *et al*, 2010). This work extends this property to HSPB3, HSPB6, HSPB7 and HSPB8. Together these data suggest that HSPB binding to α-synuclein fibrils represents a general mechanism by which HSPBs shield fibrils, limiting their growth. The affinity of HSPBs for pre-existing fibrils and their ability to prevent their elongation may explain why HSPBs can confer protection against α-synuclein-mediated toxicity in cells and why they colocalize with α-synuclein deposits, as well as with other types of inclusions that share the fibrillar structure such as amyloids (Cox & Ecroyd, 2017; Outeiro *et al*, 2006; Waudby *et al.*, 2010; Wilhelmus *et al*, 2006). In parallel, a decrease in HSPBs' ability to inhibit fibril elongation may have pathological implications that extend from misfolding diseases such as PD and AD to the neuromuscular and muscular diseases that are genetically linked to the HSPB themselves (Vendredy *et al*, 2020). This idea is suggested by our finding that, amongst all the properties analysed here, inhibition of fibril elongation is specifically affected by the K141E-HSPB8 mutation that is responsible for distal myopathy and motor neuropathies (Ghaoui *et al*, 2016). These data not only corroborate previous results showing that K141E-HSPB8 has a decreased chaperone activity against misfolded proteins in cells and flies (Carra *et al.*, 2010; Carra *et al.*, 2005); importantly, they identify a reduction in the inhibition of fibril elongation as the K141E-HSPB8 "Achilles heel". Future studies will need to address whether impaired binding to pre-formed fibrils and decreased ability to inhibit fibril elongation are a common characteristic shared by several HSPB disease-causing mutants. This may be relevant given the fact that the majority of the HSPB-linked mutations cause disease in the late adulthood (Vendredy *et al.*, 2020), when the general chaperone capacity declines and protein aggregation becomes widespread (Hipp *et al.*, 2019).

A specific aspect that was studied here is whether HSPB's ability to interact with lipids is functionally related to their activity as molecular chaperones or rather it represents an unrelated property, whose biological functions are yet unknown. Experimental evidence supports the interaction of

HSPBs with lipids. For example, HSPB8 is localized to the plasma membrane of neuronal cells and interacts *in vitro* with brain lipid extracts and lipid SUVs (Chowdary *et al.*, 2007). HSPB1 and HSPB5 associate with different types of liposomes, including POPS, POPC (palmitoyl oleoyl phosphatidylcholine) and POPG (palmitoyl oleoyl phosphatidylglycerol) (De Maio *et al.*, 2019). All the HSPBs tested were able to interact with lipid vesicle made of different lipid groups, namely DMPS, POPS or DOPS, although with different affinities. HSPB3, HSPB6 and HSPB7 showed higher binding affinities to the lipid vesicles compared to HSPB5 and HSPB8. Considering that α-synuclein embedding into the lipids triggers its aggregation, it was investigated whether HSPBs can specifically interfere with this primary nucleation step and how this could happen. The results presented here were quite surprising and open new avenues for a better understanding of HSPB function in both protein and lipid homeostasis. Only one HSPB, amongst the five studied, showed outstanding activity: HSPB6. Already at very low concentrations, HSPB6 was embedded into the lipid vesicles, even further than α-synuclein alone and completely inhibited α-synuclein lipid-induced aggregation. In addition, upon co-incubation with HSPB6 and α-synuclein, the fluidity of DMPS SUVs was not restored, but further reduced, indicating increased protein insertion within the lipid vesicle. Together these data support the interpretation that HSPB6 displaces α-synuclein preventing its binding to lipids, which, in turn, decreases its lipid-induced aggregation. When studying fibril elongation and secondary nucleation, assays that are performed in absence of lipid vesicles, HSPB6 performed poorly compared to the other HSPBs tested. Of note, secondary nucleation consists in the incorporation of monomers on the fibril surface, a process that generates new aggregates; these, in turn, quickly elongate by addition of α-synuclein monomers and serve as a platform that amplifies protein aggregation (Gaspar *et al*, 2017). When using monomeric α-synuclein at a low concentration (20 μM), a mild protective effect of HSPB6 was observed; by contrast, when monomeric α-synuclein was used at high concentration, HSPB6 could not prevent its aggregation into fibrils (Bruinsma *et al.*, 2011). Although HSPB6 was previously reported to weakly and transiently bind to monomeric α-synuclein (Bruinsma *et al.*, 2011), together these data suggest that HSPB6 binds with higher affinity to lipids, outcompeting α-synuclein. Is thus HSPB6 a highly specialized chaperone that combat protein aggregation induced by lipid surfaces? And what could be the physiological relevance of HSPB6 binding to lipids? Similar to what we observed with α-synuclein, HSPB6 could interfere with the tethering of specific molecules at the plasma membrane. Alternatively, it could modulate the activity of molecules that are recruited at the membrane, such as the phosphoinositide 3-kinase (PI3K). In particular, HSPB6 was shown to interact with the catalytic

and regulatory subunits of PI3K, a lipid kinase that converts phosphatidylinositol 4,5-bisphosphate (PIP2) to phosphatidylinositol 3,4,5-triphosphate (PIP3) (Matsushima-Nishiwaki *et al*, 2013). PI3K regulates a broad range of cellular processes including cell proliferation, migration, differentiation, as well as cell metabolism and autophagy, via the Akt/mTOR signalling pathway (Fruman *et al*, 2017). Binding of HSPB6 to PI3K correlated with its decreased activity in human cells (Matsushima-Nishiwaki *et al.*, 2013). Whether this is functionally related to its chaperone activity is currently unknown. However, using *C. elegans* it was recently shown that proteins that specifically bind to PIP3, the product generated by PI3K, promote age-dependent protein aggregation and decrease lifespan; conversely, mutant worms that lack class-I PI3K are more resistant to oxidative stress and amyloid-β mediated toxicity and live longer than their wild-type counterpart (Ayyadevara *et al*, 2016).

The functional consequences of decreased α-synuclein binding to lipids by HSPB6 may be multiple, besides reducing the lipid-induced aggregation. Intracellular accumulation of α-synuclein leads to increased extracellular release of the protein through exosomes (Danzer et al., 2012; Fussi et al., 2018). Extracellular α-synuclein has been shown to lead to plaque formation resulting in increased cytotoxicity. Hence, prevention of α-synuclein exosomal release has been proposed as a compelling approach to halt spreading in Parkinson's disease (Danzeret al., 2012). By hindering α-synuclein binding to lipid vesicles, HSPB6 may reduce α-synuclein exosomal release, a hypothesis that will require further investigations. Thus, in the future, it will be important to address in detail whether HSPB6 influences protein embedding into physiological membranes and whether this is directly or indirectly linked to its chaperone function or instead represents a novel mechanism that has indirect consequences on protein aggregation, acting on lipids.

Besides HSPB6, also the other HSPBs tested could effectively delay α-synuclein lipid-induced primary nucleation. However, it seems that they do so with distinct mechanisms. Based on the data present, it is proposed that HSPB5, which only mildly rescued the changes induced at the level of membrane fluidity by α-synuclein would preferentially bind to α-synuclein embedded in the lipids; instead, HSPB3, HSPB7 and HSPB8, which rescued more efficiently membrane fluidity in presence of α-synuclein, would preferentially bind to and neutralize its monomers or oligomers, preventing their embedding inside the liposomes. Nevertheless, it is important to note that HSPB5 binding to monomeric (Cox et al., 2016) and fibrillar (Binger et al., 2013; Cox et al., 2018) α-synuclein has been so far shown to be weak and transient, This suggests that these HSPBs are able to bind several

oligomeric forms of α-synuclein, explaining their capacity of delay several steps of the aggregation kinetics. Similar to HSPB5, also HSPB3 and HSPB7 seem to bind to α-synuclein fibrils or intermediate aggregates, hindering addition of monomeric forms into mature fibrils; in fact, they all inhibited fibril elongation, independently of their concentration in our assays. This interpretation is supported by previous findings reporting that HSPB5 acts through two different mechanisms: the first, it directly interacts with α-synuclein monomers to prevent aggregate formation; second, it interacts with exposed hydrophobicity of the intermediate aggregates hindering fibril formation (Rekas et al., 2004; Kulig and Ecroyd, 2012). Additionally, HSPB5 directly bound mature amyloid fibrils with stronger affinity than monomeric species, in apolipoprotein C-II (apoC-II) model of amyloid fibril formation (Binger et al., 2013). Yet, the affinity between HSPB and the different oligomeric forms of α-synuclein are most likely not equal throughout the HSPB family. In a recent study HSPB8 was described as the HSPB with the highest binding affinity to monomeric α-synuclein, while HSPB5 showed the lowest (Bruinsma et al., 2011). HSPB8 displayed an intermediate efficacy in all kinetics, when compared to other HSPBs, which might be explained due to direct binding to free α-synuclein monomers, thereby preventing their aggregation in all kinetic states. Also HSPB3 was shown to interact with monomeric α-synuclein with higher affinities compared to HSPB5 (Bruinsma et al., 2011). Thus, slight binding affinities to the various α-synuclein species and partial redundancy in their mechanism of action may guarantee that different HSPB cooperate to achieve proper anti-aggregation of α-synuclein.

The binding of HSPB5 to α-synuclein has been studied in detail: several peptide fragments on the ACD domain of HSPB5 bind to the α-synuclein N-terminal (Ghosh et al. 2008; Liu et al., 2018). The N-terminal of α-synuclein is responsible for membrane binding. Our data does not point to a role in displacing α-synuclein from lipid vesicles, as observed for HSPB6; yet, HSPB5 may regulate the binding of α-synuclein to membranes by controlling the amount of embedded monomers. This is consistent with previous reports showing that HSPB5 is inserted into lipid membranes, including POPS vesicles (Cobb and Petrash et al., 2002; De Maio et al., 2019). The HSPB5 regions reported to be inserted into POPS lipid vesicles were detected within the conserved ACD; hence it is possible that lipid interaction is an intrinsic property of HSPBs. Indeed, in the same study also HSPB1 was found to bind POPS, mainly through its ACD (De Maio et al., 2019), and here it was found that all the HSPBs tested, except for HSPB8, bound to lipids per se. Nevertheless, HSPB5 was previously described to have a higher tendency to bind disordered lipids, such as DMPC or DOPC, than ordered

lipid, such as DSPC (Cobb and Petrash et al., 2002). Therefore, it is possible that HSPBs are able to bind to a variety of lipids, but with slight differences in the levels of affinity. This would also influence their efficacy in preventing lipid-induced protein aggregation, which could vary also based on the membrane lipid composition; given that the lipid composition slightly differs between plasma membrane, ER membrane and exosome membranes, it is tempting to speculate that lipid composition would also influence the ability of HSPBs to influence lipid-induced protein aggregation.

In summary the results presented here demonstrate that HSPBs can regulate α-synuclein protein aggregation with multiple mechanisms, acting either directly on α-synuclein or at the intersection between α-synuclein and its embedding into lipid, which triggers α-synuclein aggregation. These findings contribute to the understanding of how HSPBs can prevent the formation of α-synuclein fibrils and lend further support to the notion that boosting HSPB function represents a promising therapeutic avenue to combat or delay the progression of neurodegenerative diseases.

## Conclusion

This thesis shows that HSPB3 is actively involved in the differentiation process of muscle cells, by influencing their transcriptional program. This novel function of HSPB3 is, at least in part, ascribed to its direct interaction with LBR and to chromatin remodelling. This novel pro-differentiation function of HSPB3 might be maintained in neuronal populations, which can also express HSPB3; further research will need to address this important question, given the implication of HSPB3 in neuromuscular diseases that affect both peripheral motor neurons and muscle cells.

LBR is a transmembrane protein; in this thesis, we also show that HSPB3 is able to interact directly with lipids and possibly prevent insertion into lipid vesicles of proteins such as α-synuclein. It is tempting to speculate that HSPB3 may act as a membrane chaperone influencing the membrane

embedding of specific substrates, such as LBR. This idea is supported by cellular data showing that HSPB3 relocates LBR from the nuclear envelope to the nucleoplasm and that depletion of HSPB3 stabilizes the LBR tether, in which LBR embedded in the nuclear envelope binds to peripheral chromatin. Although there is still a need to understand how mechanistically HSPB3 can influence LBR embedding into the nuclear envelope, to what extent this would influence the chromatin remodelling, ultimately regulating the transcriptional program of differentiating muscle cells, this work provides new clues for a better understanding of HSPB3 implications in the physiology and pathology of the neuromuscular system.

Moreover, here It was revealed that HSPB3 has a great impact on α-synuclein aggregation leading to a significant delay on fibril formation at diverse steps of aggregation. These results point to a possible important role as a neuronal protector. Several HSPBs have been linked to various neurodegenerative disorders; however, the data is not always straightforward to interpret. Hence, here it is presented a side-by-side comparison to aid further in assessing the potency of each of the chaperones individually. Using this approach, it was possible to assess the chaperone activity of HSPB3 in comparison to other 4 HSPBs to better described molecular chaperones and noted that for example HSPB6 seems to prevent α-synuclein aggregation solely through direct competition with lipid binding. Nevertheless, in vivo experiments are required which not only allow to assess whether a HSPB can reduce the protein aggregation but also whether this leads to phenotypic amelioration. In summary, this thesis paves the way for a better understanding of HSPB3 implication in the physiology and pathology of the neuromuscular system, with future implications in therapeutic approaches.

# References


Accili D and Arden KC, 2004. FoxOs at the crossroads of cellular metabolism, differentiation, and transformation. *Cell*, 117: 421-426.

Adhikari AS, Sridhar Rao K, Rangaraj N, Parnaik VK, Mohan Rao Ch, 2004. Heat stress-induced localization of small heat shock proteins in mouse myoblasts: intranuclear lamin A/C speckles as target for alphaB-crystallin and Hsp25. *Exp Cell Res*, 299(2):393-403

Aksoy O, Chicas A, Zeng T, Zhao Z, McCurrach M, Wang X, Lowe SW, 2012. The atypical E2F family member E2F7 couples the p53 and RB pathways during cellular senescence. *Genes & Development,* 26(14):1546-57

Albulym OM, Kennerson ML, Harms MB, Drew AP, Siddell AH, Auer-Grumbach M, Pestronk A, Connolly A, Baloh RH, Zuchner S, 2016. MORC2 mutations cause axonal Charcot-Marie-Tooth disease with pyramidal signs. *Ann Neurol* 79, 419-427.

Allen DL and Unterman TG, 2007. Regulation of myostatin expression and myoblast differentiation by FoxO and SMAD transcription factors. *The American Journal of Physiology*: *Cell Physiology* , 292: C188-C199.

Almeida-Souza L, Goethals S, de Winter V, Dierick I, Gallardo R, Van Durme J, Irobi J, Gettemans J, Rousseau F, Schymkowitz J, Timmerman V, Janssens S, 2010. Increased monomerization of mutant HSPB1 leads to protein hyperactivity in Charcot-Marie-Tooth neuropathy. *J Biol Chem* 285:12778–12786

Al-Tahan S, Weiss L, Yu H, Tang S, Saporta M, Vihola A, Mozaffar T, Udd B, Kimonis V, 2019. New family with HSPB8-associated autosomal dominant rimmed vacuolar myopathy. *Neurol Genet*, 10;5(4):e349

Andrieu C, Taieb D, Baylot V, Ettinger S, Soubeyran P, De-Thonel A, Nelson C, Garrido C, So A, Fazli L, Bladou F, Gleave M, Iovanna JL, Rocchi P, Nelson C, Garrido C, So A, Fazli L, Bladou F, Gleave M, Iovanna JL and Rocchi P, 2010. Heat shock protein 27 confers resistance to androgen ablation and chemotherapy in prostate cancer cells through eIF4E. *Oncogene*, 29: 1883–1896.

Appel-Cresswell S, Vilarino-Guell C, Encarnacion M, Sherman H, Yu I, Shah B, Weir D, Thompson C, Szu-Tu C, Trinh J, Aasly JO, Rajput A, Rajput AH, Jon Stoessl A, Farrer MJ, 2013. Alpha-synuclein p.H50Q, a novel pathogenic mutation for Parkinson's disease. *Mov Disord*, 28(6):811-3

Arndt V, Dick N, Tawo R, Dreiseidler M, Wenzel D, Hesse M, Fürst DO, Saftig P, Saint R, Fleischmann BK, Hoch M, Höhfeld J, 2010. Chaperone-assisted selective autophagy is essential for muscle maintenance. *Curr Biol*, 20(2):143-8

Arrigo AP, Simon S, Gibert B, Kretz-Remy C, Nivon M, Czekalla A, Guillet D, Moulin M, Diaz-Latoud C, Vicart P, 2007. Hsp27 (HspB1) and alphaB-crystallin (HspB5) as therapeutic targets. *FEBS Lett*, 581(19):3665-74

Asthana A, Raman B, Ramakrishna T, Rao ChM, 2012. Structural aspects and chaperone activity of human HspB3: role of the "C-terminal extension". *Cell Biochem Biophys*, 64(1):61-72

Ayyadevara S, Balasubramaniam M, Suri P, Mackintosh SG, Tackett AJ, Sullivan DH, Shmookler Reis RJ, Dennis RA, 2016. Proteins that accumulate with age in human skeletal-muscle aggregates contribute to declines in muscle mass and function in Caenorhabditis elegans. *Aging*, 8(12):3486-3497

Azzedine H, Bolino A, Taieb T, Birouk N, Di Duca M, Bouhouche A, Benamou S, Mrabet A, Hammadouche T, Chkili T, et al, 2003. Mutations in MTMR13, a new pseudophosphatase homologue of MTMR2 and Sbf1, in two families with an autosomal recessive demyelinating form of Charcot-Marie-Tooth disease associated with early-onset glaucoma. *American journal of human genetics* 72: 1141-1153.

Babu MM, 2016. The contribution of intrinsically disordered regions to protein function, cellular complexity, and human disease. *Biochemical Society Transactions*, 44:1185–1200

Baghdadi MB and Tajbakhsh S, 2018. Regulation and phylogeny of skeletal muscle regeneration. *Developmental Biology*,433(2): 200-209

Bailey CK, Andriola IF, Kampinga HH, Merry DE, 2002. Molecular chaperones enhance the degradation of expanded polyglutamine repeat androgen receptor in a cellular model of spinal and bulbar muscular atrophy. *Hum Mol Genet*,11(5):515-23

Bakthisaran R, Tangirala R, Rao ChM, 2015. Small heat shock proteins: Role in cellular functions and pathology. *Biochim Biophys Acta*, 1854(4):291-319

Balch WE, Morimoto RI, Dillin A, Kelly JW, 2008. Adapting proteostasis for disease intervention. *Science*, 319(5865):916-9

Banani SF, Lee HO, Hyman AA, Rosen MK, 2017. Biomolecular condensates: organizers of cellular biochemistry. *Nat Rev Mol Cell Biol*, 18(5):285-298

Bar-Lavan Y, Shemesh N, Dror S, Ofir R, Yeger-Lotem E, Ben-Zvi A, 2016. A Differentiation Transcription Factor Establishes Muscle-Specific Proteostasis in Caenorhabditis elegans. *PLoS Genet*, 12(12):e1006531

Batulan Z, VenuVKP, Li Y, Koumbadinga G, Alvarez-Olmedo DG, Shi G, and O'Brien ER, 2016. Extracellular Release and Signaling by Heat Shock Protein 27: Role in Modifying Vascular Inflammation. *Frontiers in Immunology*, 7: 285

Baughman HER, Clouser AF, Klevit RE, Nath A, 2018. HspB1 and Hsc70 chaperones engage distinct tau species and have different inhibitory effects on amyloid formation. *Journal of Biological Chemistry*, 293:2687–2700

Beall AC, Kato K, Goldenring JR, Rasmussen H, Brophy CM, 1997. Cyclic nucleotide-dependent vasorelaxation is associated with the phosphorylation of a small heat shock-related protein. *J Biol Chem*, 272(17):11283-7

Bendifallah M, Redeker V, Monsellier E, Bousset L, Bellande T, Melki R, 2020. Interaction of the chaperones alpha B-crystallin and CHIP with fibrillar alpha-synuclein: Effects on internalization by cells and identification of interacting interfaces. *Biochem Biophys Res Commun*, 527(3):760-769

Bentzinger CF, Wang YX, Dumont NA, Rudnicki MA, 2013. Cellular dynamics in the muscle satellite cell niche. *EMBO Rep*, 14(12):1062-72

Berkes, C.A., and Tapscott, S.J. (2005). MyoD and the transcriptional control of myogenesis. *Semin Cell Dev Biol,* 16:585-595.

Binder DK, Papadopoulos MC, Haggie PM, Verkman AS, 2004. In vivo measurement of brain extracellular space diffusion by cortical surface photobleaching. *J Neurosci*, 24(37):8049-56

Binder RJ, Vatner R, Srivastava P, 2004. The heat-shock protein receptors: some answers and more questions. *Tissue Antigens*, 64(4):442-51

Binger KS, Ecroyd H, Yang S, Carver JA, Howlett GJ, Griffin MDW, 2013. Avoiding the oligomeric state: αB-crystallin inhibits fragmentation and induces dissociation of apolipoprotein C-II amyloid fibrils. *FASEB J*. 27: 1214 –1222

Biressi S, and Gopinath SD, 2015. The quasi-parallel lives of satellite cells and atrophying muscle. *Front Aging Neurosci 7*: 140.

Boelens W, Van Boekel MAM, De Jong WW, 1998. HspB3, the most deviating of the six known human small heat shock proteins. *Biochimica et Biophysica Acta (BBA) - Protein Structure and Molecular Enzymology*, 1388 (2): 513-516

Bolino A, Muglia M, Conforti FL, LeGuern E, Salih MA, Georgiou DM, Christodoulou K, Hausmanowa-Petrusewicz I, Mandich P, Schenone A, et al, 2000. Charcot-Marie-Tooth type 4B is caused by mutations in the gene encoding myotubularin-related protein-2. *Nature genetics*, 25:17-19.

Boncoraglio A, Minoia M, Carra S, 2012. The family of mammalian small heat shock proteins (HSPBs): implications in protein deposit diseases and motor neuropathies. *Int J Biochem Cell Biol*, 44(10):1657-69.

Bouzid T, Kim E, Riehl BD, Esfahani AM, Rosenbohm J, Yang R, Duan B, and Lim JY, 2019. The LINC complex, mechanotransduction, and mesenchymal stem cell function and fate. *Journal of Biological Engineering*, 13 (68)

Brack AS, Conboy IM, Conboy MJ, Shen J, Rando TA, 2008. A temporal switch from notch to Wnt signaling in muscle stem cells is necessary for normal adult myogenesis. *Cell Stem Cell*, 2(1):50-9

Bracken AP, Ciro M, Cocito A, Helin K, 2004. E2F target genes: unraveling the biology. *Trends Biochem Sci,* 29(8):409-17

Brady JP, Garland DL, Green DE, Tamm ER, Giblin FJ, Wawrousek EF, 2001. AlphaB-crystallin in lens development and muscle integrity: a gene knockout approach. *Invest. Ophthalmol. Vis. Sci*., 42:2924-2934

Braun T, Bober E, Winter B, Rosenthal N, Arnold HH, 1990. Myf-6, a new member of the human gene family of myogenic determination factors: evidence for a gene cluster on chromosome 12. *Embo Journal*, 9: 821–831.

Braun T, Gautel M, 2011. Transcriptional mechanisms regulating skeletal muscle differentiation, growth and homeostasis. *Nature Reviews Molecular Cell Biology*, 12:349–361

Brero A, Easwaran HP, Nowak D, Grunewald I, CremerT, Leonhardt H, and Cardoso MC, 2005. Methyl CpG–binding proteins induce large-scale chromatin reorganization during terminal differentiation. *Journal of Cell Biology*, 169(5): 733–743.

Bruey JM, Ducasse C, Bonniaud P, Ravagnan L, Susin SA, Diaz-Latoud C, Gurbuxani S, Arrigo AP, Kroemer G, Solary E, Garrido C, 2000. Hsp27 negatively regulates cell death by interacting with cytochrome c. *Nat Cell Biol*, 2(9):645-52

Bruinsma, I. B., Bruggink, K. A., Kinast, K., Versleijen, A. A. M., Segers-Nolten, I. M. J., Subramaniam, V., Verbeek, M. M., 2011. Inhibition of α-synuclein aggregation by small heat shock proteins. *Proteins: Structure, Function, and Bioinformatics*, 79(10), 2956–2967

Bryantsev AL, Kurchashova SY, Golyshev SA, Polyakov VY, Wunderink HF, Kanon B, Budagova KR, Kabakov AE, Kampinga HH, 2007. Regulation of stress-induced intracellular sorting and chaperone function of Hsp27 (HspB1) in mammalian cells. *Biochem J*, 407(3):407-17

Buell AK, 2017. The Nucleation of Protein Aggregates - From Crystals to Amyloid Fibrils. *Int Rev Cell Mol Biol*, 329:187-226.

Buell AK, Galvagnion C, Gaspar R, Sparr E, Vendruscolo M, Knowles TP, Linse S, Dobson CM, 2014. Solution conditions determine the relative importance of nucleation and growth processes in α-synuclein aggregation. *Proc Natl Acad Sci U S A*, 111(21):7671-6.

Bukach O.V, Seit-Nebi A.S., Marston S.B., Gusev N.B, 2003. Some properties of human small heat shock protein Hsp20 (HspB6). *European Journal of Biochemistry*, 271(2): 291-302

Burré J, Sharma M, Südhof TC, 2018. Cell Biology and Pathophysiology of α-Synuclein. *Cold Spring Harb Perspect Med*, 8(3):a024091

Burzyn D, Kuswanto W, Kolodin D, Shadrach JL, Cerletti M, Jang Y, Sefik E, Tan TG, Wagers AJ, Benoist C, Mathis D, 2013. A Special Population of Regulatory T Cells Potentiates Muscle Repair. *Cell*, 155(6): 1282–1295

Butin-Israeli V, Adam SA, Goldman AE, and Goldman RD, 2012. Nuclear lamin functions and disease. *Trends in Genetics*. 28: 464–471

Carlisle C, Prill K, Pilgrim D, 2017. Chaperones and the Proteasome System: Regulating the Construction and Demolition of Striated Muscle. *Int J Mol Sci*, 19(1):32

Carosio S, Berardinelli MG, Aucello M, and Musaro A, 2011. Impact of ageing on muscle cell regeneration. *Ageing Res Rev,* 10:35-42

Carra S and Landry J, 2006. Small heat shock proteins in neurodegenerative diseases. In Heat Shock Proteins in Biology and Medicine, J. Radons, and G. Multhoff, eds, Research Signpost, Kerala, 331–351.

Carra S, Alberti S, Arrigo PA, Benesch JL, Benjamin IJ, Boelens W, Bartelt-Kirbach B, Brundel BJJM, Buchner J, Bukau B, Carver JA, Ecroyd H, Emanuelsson C, Finet S, Golenhofen N, Goloubinoff P, Gusev N, Haslbeck M, Hightower LE, Kampinga HH, Klevit RE, Liberek K, Mchaourab HS, McMenimen KA, Poletti A, Quinlan R, Strelkov SV, Toth ME, Vierling E, Tanguay RM, 2017. The growing world of small heat shock proteins: from structure to functions. *Cell Stress Chaperones*, 22(4):601-611

Carra S, Alberti S, Benesch JLP, Boelens W, Buchner J, Carver JA, Cecconi C, Ecroyd H, Gusev N, Hightower LE, Klevit RE, Lee HO, Liberek K, Lockwood B, Poletti A, Timmerman V, Toth ME, Vierling E, Wu T, Tanguay RM, 2019. Small heat shock proteins: multifaceted proteins with important implications for life. *Cell Stress Chaperones*, 24(2):295-308

Carra S, Boncoraglio A, Kanon B, Brunsting JF, Minoia M, Rana A, Vos MJ, Seidel K, Sibon OC, Kampinga HH, 2010. Identification of the Drosophila ortholog of HSPB8: implication of HSPB8 loss of function in protein folding diseases. *J Biol Chem*, 285(48):37811-22

Carra S, Rusmini P, Crippa V, Giorgetti E, Boncoraglio A, Cristofani R, Naujock M, Meister M, Minoia M, Kampinga HH, Poletti A, 2013. Different anti-aggregation and pro-degradative functions of the members of the mammalian sHSP family in neurological disorders. *Philos Trans R Soc Lond B Biol Sci*, 368(1617):20110409

Carra S, and Landry J, 2008. Role of HspB1 and HspB8 in Hereditary Peripheral Neuropathies: Beyond the Chaperone Function. In: Asea A.A., Brown I.R. (eds) Heat Shock Proteins and the Brain: Implications for Neurodegenerative Diseases and Neuroprotection. Heat Shock Proteins, vol 3. Springer, Dordrecht

Carra S, Sivilotti M, Chávez Zobel AT, Lambert H, Landry J, 2005. HspB8, a small heat shock protein mutated in human neuromuscular disorders, has in vivo chaperone activity in cultured cells. *Human Molecular Genetics,* 14(12): 1659-69

Chaillou T, Zhang X, McCarthy JJ, 2016. Expression of muscle-specific ribosomal protein L3-like impairs myotube growth. *Journal of Cellular Physiology*,231(9): 1894–1902.

Chakraborty A, Brauer S, Diwan A, 2020. Possible therapies of Parkinson's disease: A review. *J Clin Neurosci*, 75:1-4

Chargé SB, Rudnicki MA, 2004. Cellular and molecular regulation of muscle regeneration. *Physiol Rev*, 84(1):209-38

Chatterjee S and Burns TF, 2017. Targeting Heat Shock Proteins in Cancer: A Promising Therapeutic Approach. *Int J Mol Sci,* 18(9):1978

Chávez Zobel AT, Loranger A, Marceau N, Thériault JR, Lambert H, Landry J, 2003. Distinct chaperone mechanisms can delay the formation of aggresomes by the myopathy-causing R120G alphaB-crystallin mutant. *Hum Mol Genet*, 12(13):1609-20

Chen W, Datzkiw D, Rudnicki MA, 2020. Satellite cells in ageing: use it or lose it. *Open Biology*,10(5):200048.

Chen Y, Lin G, Slack JM, 2006. Control of muscle regeneration in the Xenopus tadpole tail by Pax7. *Development*, 133(12):2303-13

Chiappetta G, Ammirante M, Basile A, Rosati A, Festa M, Monaco M, Vuttariello E, Pasquinelli R, Arra C, Zerilli M, Todaro M, Stassi G, Pezzullo L, Gentilella A, Tosco A, Pascale M, Marzullo L, Belisario MA, Turco MC, Leone A, 2007. The antiapoptotic protein BAG3 is expressed in thyroid carcinomas and modulates apoptosis mediated by tumor necrosis factor-related apoptosis-inducing ligand. *J Clin Endocrinol Meta*., 92(3):1159-63

Chiti F, Dobson CM, 2006. Protein misfolding, functional amyloid, and human disease. *Annu Rev Biochem*, 75:333-66.

Chowdary TK, Raman B, Ramakrishna T, Rao ChM, 2007. Interaction of mammalian Hsp22 with lipid membranes. *Biochem J*, 401(2):437-45

Ciryam P, Kundra R, Freer R, Morimoto RI, Dobson CM, Vendruscolo M, 2016. A transcriptional signature of Alzheimer's disease is associated with a metastable subproteome at risk for aggregation. *Proc Natl Acad Sci U S A,* 113(17):4753-8

Ciryam P, Kundra R, Morimoto RI, Dobson CM, Vendruscolo M, 2015. Supersaturation is a major driving force for protein aggregation in neurodegenerative diseases. *Trends Pharmacol Sci*, 36(2):72-7

Clark AR, Egberts WV, Kondrat FDL, Hilton GR, Ray NJ, Cole AR, Carver JA, Benesch JLP, Keep NH, Boelens WC, Slingsby C, 2018. Terminal Regions Confer Plasticity to the Tetrameric Assembly of Human HspB2 and HspB3. *Journal of Molecular Biology*, 430(18Part B): 3297–3310.

Clayton A, Turkes A, Navabi H, Mason MD, and Tabi Z, 2005. Induction of heat shock proteins in B-cell exosomes. *Journal of Cell Science*,118: 3631-3638

Clemen CS, Herrmann H, Strelkov SV, Schroder R, 2013. Desminopathies: pathology and mechanisms. *Acta Neuropathol*, 125(1):47–75

Cobb BA, Petrash JM, 2002. alpha-Crystallin chaperone-like activity and membrane binding in age-related cataracts. *Biochemistry*, 41(2):483-90.

Cobb CM, 2002. Clinical significance of non-surgical periodontal therapy: an evidence-based perspective of scaling and root planing. *J Clin Periodontol*, 29 Suppl 2:6-16

Cohen TV, Cohen JE, Partridge TA, 2012. Myogenesis in dysferlin-deficient myoblasts is inhibited by an intrinsic inflammatory response. *Neuromuscul Disord*, 22(7):648-58

Collier MP, Alderson TR, de Villiers CP, Nicholls D, Gastall HY, Allison TM, Degiacomi MT, Jiang H, Mlynek G, Fürst DO, van der Ven PFM, Djinovic-Carugo K, Baldwin AJ, Watkins H, Gehmlich K, Benesch JLP, 2019. HspB1 phosphorylation regulates its intramolecular dynamics and mechanosensitive molecular chaperone interaction with filamin C. *Sci Adv*, 5(5):eaav8421

Cornelison DD and Wold BJ, 1997. Single-cell analysis of regulatory gene expression in quiescent and activated mouse skeletal muscle satellite cells. *Developmental Biology*, 191: 270–283.

Cornelison DD, Filla MS, Stanley HM, Rapraeger AC, Olwin BB, 2001. Syndecan-3 and syndecan-4 specifically mark skeletal muscle satellite cells and are implicated in satellite cell maintenance and muscle regeneration. *Dev Biol*, 239(1):79-94

Cox D, Selig E, Griffin MD, Carver JA, Ecroyd H, 2016. Small Heat-shock Proteins Prevent α-Synuclein Aggregation via Transient Interactions and Their Efficacy Is Affected by the Rate of Aggregation. *J Biol Chem*, 291(43):22618-22629

Cox D, Ecroyd H, 2017. The small heat shock proteins αB-crystallin (HSPB5) and Hsp27 (HSPB1) inhibit the intracellular aggregation of α-synuclein. *Cell Stress Chaperones*, 22(4):589-600

Cox D, Whiten DR, Brown JWP, Horrocks MH, San Gil R, Dobson CM, Klenerman D, van Oijen AM, Ecroyd H, 2018. The small heat shock protein Hsp27 binds α-synuclein fibrils, preventing elongation and cytotoxicity. *J Biol Chem,* 293(12):4486-4497

Csapo R, Gumpenberger M, and Wessner B, 2020. Skeletal Muscle Extracellular Matrix - What Do We Know About Its Composition, Regulation, and Physiological Roles? A Narrative Review. *Front Physiol,* 11:253

Cui XY, Wang N, Yang BX, Gao WF, Lin YM, Yao XR, Ma XT, 2012. HSPB8 is methylated in hematopoietic malignancies and overexpression of HSPB8 exhibits antileukemia effect. *Exp Hematol*, 40(1):14-21

Cummings CJ and Zoghbi HY, 2000. Fourteen and counting: unraveling trinucleotide repeat diseases. *Hum Mol Genet*, 9(6):909-16

Cummings CJ, Sun Y, Opal P, Antalffy B, Mestril R, Orr HT, Dillmann WH, Zoghbi HY, 2001. Over-expression of inducible HSP70 chaperone suppresses neuropathology and improves motor function in SCA1 mice. *Hum Mol Genet*, 10: 1511–1518

Danzer KM, Kranich LR, Ruf WP, Cagsal-Getkin O, Winslow AR, Zhu L, Vanderburg CR, McLean PJ, 2012. Exosomal cell-to-cell transmission of alpha synuclein oligomers. *Mol Neurodegener*, 7:42

De Luca AC, Lacour SP, Raffoul W, di Summa PG, 2014. Extracellular matrix components in peripheral nerve repair: how to affect neural cellular response and nerve regeneration? *Neural Regen Res*, 9(22):1943-8

De Falco G, Comes F, Simone C, 2006. pRb: master of differentiation. Coupling irreversible cell cycle withdrawal with induction of muscle-specific transcription. *Oncogene*, 25: 5244–524

De Jong WW, Leunissen JA, and Voorter CE, 1993. Evolution of the alphacrystallin/small heat-shock protein family. *Mol. Biol. Evol*. 10, 103-126

De Los Rios P, Goloubinoff P, 2016. Hsp70 chaperones use ATP to remodel native protein oligomers and stable aggregates by entropic pulling. *Nat Struct Mol Biol*, 23(9):766-9

De Maio A, Cauvi DM, Capone R, Bello I, Egberts WV, Arispe N, Boelens W, 2019. The small heat shock proteins, HSPB1 and HSPB5, interact differently with lipid membranes. *Cell Stress Chaperones*, 24(5):947-956

De Maio A, Hightower LE, 2020. Heat shock proteins and the biogenesis of cellular membranes. *Cell Stress Chaperones*. Online ahead of print

DeGeer J, Kaplan A, Mattar P, Morabito M, Stochaj U, Kennedy T E, et al. ,2015. Hsc70 chaperone activity underlies Trio GEF function in axon growth and guidance induced by netrin-1. *J. Cell Biol*, 210: 817–832

den Engelsman J, Boros S, Dankers PYW, Kamps B, Egberts WTV, Böde CS, Lane LA, Aquilina JA, Benesch JLP, Robinson CV, Jong W, and Boelens W, 2009. The Small Heat-Shock Proteins HSPB2 and HSPB3 Form Well-defined Heterooligomers in a Unique 3 to 1 Subunit Ratio. *Journal of Molecular Biology*, 393(5): 1022-1032

Deniaud E, Bickmore WA, 2009. Transcription and the nuclear periphery: edge of darkness? *Curr Opin Genet Dev*, 19(2):187-91

Dimauro I, Antonioni A, Mercatelli N, Caporossi D, 2018. The role of αB-crystallin in skeletal and cardiac muscle tissues. *Cell Stress Chaperones,* 23(4):491-505

Dubin RA, Gopal-Srivastava R, Wawrousek EF, Piatigorsky J, 1991. Expression of the murine alpha B-crystallin gene in lens and skeletal muscle: identification of a muscle-preferred enhancer. *Mol Cell Biol*, 11(9):4340-9

Dubińska-Magiera M, Jabłońska J, Saczko J, Kulbacka J, Jagla T, Daczewska M, 2014. Contribution of small heat shock proteins to muscle development and function. *FEBS Lett*, 588(4):517-30

During RL, Gibson BG, Li W, Bishai EA, Sidhu GS and Landry J, 2007. Anthrax lethal toxin paralyzes actin-based motility by blocking Hsp27 phosphorylation. *EMBO Journal*, 26: 2240–2250

d'Ydewalle C, Krishnan J, Chiheb DM, Van Damme P, Irobi J, Kozikowski AP, Vanden Berghe P, Timmerman V, Robberecht W, Van Den Bosch L, 2011. HDAC6 inhibitors reverse axonal loss in a mouse model of mutant HSPB1-induced Charcot-Marie-Tooth disease. *Nat Med*, 17(8):968-74

Echaniz-Laguna A, Nicot AS, Carré S, Franques J, Tranchant C, Dondaine N, Biancalana V, Mandel JL, Laporte J, 2007. Subtle central and peripheral nervous system abnormalities in a family with centronuclear myopathy and a novel dynamin 2 gene mutation. *Neuromuscul Disord*, 17(11-12):955-9

Echeverría PC, Briand PA, Picard D, 2016. A Remodeled Hsp90 Molecular Chaperone Ensemble with the Novel Cochaperone Aarsd1 Is Required for Muscle Differentiation. *Molecular and Cellular Biology*, 36(8):1310-21

El-Abassi R, England JD, and Carter GT, 2014. Charcot-Marie-Tooth Disease: An Overview of Genotypes, Phenotypes, and Clinical Management Strategies. *PM&R*, 6(4): 342–355

Ellenberg, J., Siggia, E.D., Moreira, J.E., Smith, C.L., Presley, J.F., Worman, H.J., and Lippincott-Schwartz, J., 1997. Nuclear membrane dynamics and reassembly in living cells: targeting of an inner nuclear membrane protein in interphase and mitosis. *The Journal of cell biology*, 138: 1193-1206.

Elmore S, 2007. Apoptosis: a review of programmed cell death. *Toxicol Pathol*, 35(4):495-516

Escobedo J, Pucci AM, Koh TJ, 2004. HSP25 protects skeletal muscle cells against oxidative stress. *Free Radic. Biol. Med*., 37: 1455-1462

Evgrafov OV, Mersiyanova I, Irobi J, Van Den Bosch L, Dierick I, Leung CL, Schagina O, Verpoorten N, Van Impe K, Fedotov V, Dadali E, Auer-Grumbach M, Windpassinger C, Wagner K, Mitrovic Z, Hilton-Jones D, Talbot K, Martin JJ, Vasserman N, Tverskaya S, Polyakov A, Liem RK, Gettemans J, Robberecht W, De Jonghe P, Timmerman V, 2004. Mutant small heat-shock protein 27 causes axonal Charcot-Marie-Tooth disease and distal hereditary motor neuropathy. *Nat Genet*, 36(6):602-6

Flagmeier P, Meisl G, Vendruscolo M, Knowles TPJ, Dobson CM, Buell AK, and Galvagnion C, 2016. Mutations associated with familial Parkinson's disease alter the initiation and amplification steps of α-synuclein aggregation. *PNAS*, 113(37): 10328–10333

Franco R, Cidlowski J, 2009. Apoptosis and glutathione: beyond an antioxidant. *Cell Death Differ,* 16:1303–1314

Fruman DA, Chiu H, Hopkins BD, Bagrodia S, Cantley LC, Abraham RT, 2017. The PI3K Pathway in Human Disease. *Cell,* 170(4):605-635

Fuchs E, Weber K, 1994. Intermediate filaments: structure, dynamics, function, and disease. *Annu Rev Biochem,* 63:345-82

Fusco G, Chen SW, Williamson PTF, Cascella R, Perni M, Jarvis JA, Cecchi C, Vendruscolo M, Chiti F, Cremades N, Ying L, Dobson CM, De Simone A, 2017. Structural basis of membrane disruption and cellular toxicity by α-synuclein oligomers. *Science*, 358(6369):1440-1443

Fussi N, Höllerhage M, Chakroun T, Nykänen NP, Rösler TW, Koeglsperger T, Wurst W, Behrends C, Höglinger GU, 2018. Exosomal secretion of α-synuclein as protective mechanism after upstream blockage of macroautophagy. *Cell Death Dis*, 9(7):757

Gagan, J., Dey, B.K., Layer, R., Yan, Z., and Dutta, A. (2012). Notch3 and Mef2c proteins are mutually antagonistic via Mkp1 protein and miR-1/206 microRNAs in differentiating myoblasts. *The Journal of biological chemistry,* 287: 40360-40370.

Galvagnion C, Brown JW, Ouberai MM, Flagmeier P, Vendruscolo M, Buell AK, Sparr E, Dobson CM, 2016. Chemical properties of lipids strongly affect the kinetics of the membrane-induced aggregation of α-synuclein. *Proc Natl Acad Sci U S A*, 113(26):7065-70

Galvagnion C, Buell AK, Meisl G, Michaels TCT, Vendruscolo M, Knowles TPJ, and Dobson CM, 2015. Lipid vesicles trigger α-synuclein aggregation by stimulating primary nucleation. *Nature Chemical Biology*, 11(3): 229–234.

Gangalum RK, Atanasov IC, Zhou ZH, and Bha SP, 2011. αB-Crystallin Is Found in Detergent-resistant Membrane Microdomains and Is Secreted via Exosomes from Human Retinal Pigment Epithelial Cells. *Journal of Biology and Chemistry*. 286(5): 3261–3269.

Garrido C, Schmitt E, Candé C, Vahsen N, Parcellier A, Kroemer G, 2003. HSP27 and HSP70: potentially oncogenic apoptosis inhibitors. *Cell Cycle*, 2(6):579-84

Gaspar R, Meisl G, Buell AK, Young L, Kaminski CF, Knowles TPJ, Sparr E, Linse S, 2017. Acceleration of α-synuclein aggregation. *Amyloid*, 24(sup1):20-21

Ghaoui R, Palmio J, Brewer J, Lek M, Needham M, Evilä A, Hackman P, Jonson PH, Penttilä S, Vihola A, Huovinen S, Lindfors M, Davis RL, Waddell L, Kaur S, Yiannikas C, North K, Clarke N, MacArthur DG, Sue CM, Udd B, 2016. Mutations in HSPB8 causing a new phenotype of distal myopathy and motor neuropathy. *Neurology*, 86(4):391-8

Ghosh JG, Houck SA, Clark JI, 2008. Interactive sequences in the molecular chaperone, human alphaB crystallin modulate the fibrillation of amyloidogenic proteins. *Int J Biochem Cell Biol,* 40(5):954-67

Ghosh A, and Som A, 2020. RNA-Seq analysis reveals pluripotency-associated genes and their interaction networks in human embryonic stem cells. *Comput Biol Chem,* 85: 107239.

Ghosh S, Sarkar P, Basak P, Mahalanobish S, Sil PC, 2018. Role of Heat Shock Proteins in Oxidative Stress and Stress Tolerance. *Heat Shock Proteins*, 15

Giannios, I., Chatzantonaki, E., and Georgatos, S. (2017). Dynamics and Structure-Function Relationships of the Lamin B Receptor (LBR). *PloS one,* 12: e0169626.

Gilbert PM, Havenstrite KL, Magnusson KE, Sacco A, Leonardi NA, Kraft P, Nguyen NK, Thrun S, Lutolf MP, Blau HM, 2010. Substrate elasticity regulates skeletal muscle stem cell self-renewal in culture. *Science*, 329(5995):1078-81

Gober MD, Smith CC, Ueda K, Toretsky JA, Aurelian L, 2003. Forced expression of the H11 heat shock protein can be regulated by DNA methylation and trigger apoptosis in human cells. *J Biol Chem*, 278(39):37600-9

Gober MD, Wales SQ, Aurelian L, 2005. Herpes simplex virus type 2 encodes a heat shock protein homologue with apoptosis regulatory functions. *Front Biosci*, 10:2788-803

Golenhofen N, Ness W, Wawrousek EF, Drenckhahn D, 2002. Expression and induction of the stress protein alpha-B-crystallin in vascular endothelial cells. *Histochem Cell Biol*, 117(3):203-9

Goody MF, Sher RB, and Henry CA, 2015. Hanging on for the ride: adhesion to the extracellular matrix mediates cellular responses in skeletal muscle morphogenesis and disease. *Dev Biol,* 401:75-91.

Grami V, Marrero Y, Huang L, Tang D, Yappert MC, Borchman D, 2005. alpha-Crystallin binding in vitro to lipids from clear human lenses. *Exp Eye Res*, 81(2):138-46

Grzybowska EA, 2012. Human intronless genes: Functional groups, associated diseases, evolution, and mRNA processing in absence of splicing. *Biochemical and Biophysical Research Communications*, 424 (1): 1-6

Gullberg D, Tiger CF, Velling T, 1999. Laminins during muscle development and in muscular dystrophies. *Cell Mol Life Sci*, 56(5-6):442-60

Halevy O, Novitch BG, Spicer DB, Skapek SX, Rhee J, Hannon GJ, Beac D, Lassa AB, 1995.Correlation of terminal cell cycle arrest of skeletal muscle with induction of p21 by MyoD. *Science*, 267: 1018–1021.

Hartl FU and Hayer-Hartl M, 2002. Molecular chaperones in the cytosol: From nascent chain to folded protein. *Science*, 295:1852-1858.

Hartl FU, Bracher A, Hayer-Hartl M, 2011. Molecular chaperones in protein folding and proteostasis. *Nature*, 475(7356):324-32

Haslbeck M, Peschek J, Buchner J, Weinkauf S, 2016. Structure and function of alpha-crystallins: traversing from in vitro to in vivo. *Biochim Biophys Acta*, 1860:149–166

Haslbeck M, Vierling E, 2015. A first line of stress defense: small heat shock proteins and their function in protein homeostasis. *J Mol Biol*, 427(7):1537-48

Haslbeck M, Walke S, Stromer T, Ehrnsperger M, White HE, Chen SX, Saibil HR, and Buchner J, 1999. Hsp26: a temperature-regulated chaperone. *EMBO J*., 18: 6744-6751

Haslbeck M, Weinkauf S, and Buchner J, 2019. Small heat shock proteins: Simplicity meets complexity. *The Journal of biological chemistry*, 294: 2121-2132

Hein S, Kostin S, Heling A, Maeno Y, Schaper J, 2000. The role of the cytoskeleton in heart failure. C*ardiovasc Res,* 45(2):273-8

Herrero MT, Morelli M, 2017. Multiple mechanisms of neurodegeneration and progression. *Prog Neurobiol,* 155:1

Hershberger R, Hedges D, and Morales A, 2013. Dilated cardiomyopathy: the complexity of a diverse genetic architecture. *Nat Rev Cardiol,* 10: 531–547

Hessling M1, Richter K, Buchner J, 2009. Dissection of the ATP-induced conformational cycle of the molecular chaperone Hsp90. *Nat Struct Mol Biol*, 16(3):287-93

Hetz C, and Saxena S, 2017. ER stress and the unfolded protein response in neurodegeneration. *Nat Rev Neurol*, 13: 477-491.

Hieda M, 2019. Signal Transduction across the Nuclear Envelope: Role of the LINC Complex in Bidirectional Signaling. *Cells*, 8(2):124

Hipp MS, Kasturi P, Hartl FU, 2019. The proteostasis network and its decline in ageing. *Nat Rev Mol Cell Biol*, 20(7):421-435

Horwitz J, 1992. Alpha-crystallin can function as a molecular chaperone. *Proc Natl Acad Sci U S A,* 89(21):10449-53

Houlden H, Laura M, Wavrant-De Vrieze F, Blake J, Wood N, Reilly MM, 2008. Mutations in the HSP27 (HSPB1) gene cause dominant, recessive, and sporadic distal HMN/CMT type 2. *Neurology,* 71: 1660-1668

Hynes, R.O., and Naba, A. (2012). Overview of the matrisome--an inventory of extracellular matrix constituents and functions. *Cold Spring Harb Perspect Biol,* 4:a004903

Irobi J, De Jonghe P, Timmerman V, 2004. Molecular genetics of distal hereditary motor neuropathies. *Hum Mol Genet*, 13 Spec No 2:R195-202

Irobi J, Van Impe K, Seeman P, Jordanova A, Dierick I, Verpoorten N, Michalik A, De Vriendt E, Jacobs A, Van Gerwen V, Vennekens K, Mazanec R, Tournev I, Hilton-Jones D, Talbot K, Kremensky I, Van Den Bosch L, Robberecht W, Van Vandekerckhove J, Van Broeckhoven C, Gettemans J, De Jonghe P, Timmerman V, 2004. Hot-spot residue in small heat-shock protein 22 causes distal motor neuropathy. *Nat Genet*, 36(6):597-601

Ishiuchi Y, Sato H, Komatsu N, Kawaguchi H, Matsuwaki T, Yamanouchi K, Nishihara M, Nedachi T, 2018.Identification of CCL5/RANTES as a novel contraction-reducible myokine in mouse skeletal muscle. *Cytokine*, 108;17-23

Jakob U, Gaestel M, Engel K, Buchner J, 1993. Small heat shock proteins are molecular chaperones. *J Biol Chem*, 268(3):1517-20

Jana NR, Tanaka M, Wang Gh, Nukina N, 2000. Polyglutamine length-dependent interaction of Hsp40 and Hsp70 family chaperones with truncated N-terminal huntingtin: their role in suppression of aggregation and cellular toxicity. *Hum Mol Genet*, 9(13):2009-18.

Janowska MK, Baughman HER, Woods CN, Klevit RE, 2019. Mechanisms of Small Heat Shock Proteins. *Cold Spring Harbour Perspective Biology*, 11(10): a034025

Jimenez-Mallebrera C, Brown SC, Sewry CA, Muntoni F, 2005. Congenital muscular dystrophy: molecular and cellular aspects. *Cell Mol Life Sci*, 62(7-8):809-23

Jones DL, Wagers AJ, 2008. No place like home: anatomy and function of the stem cell niche. *Nat Rev Mol Cell Biol*, 9(1):11-21

Jost, K.L., Bertulat, B., Rapp, A., Brero, A., Hardt, T., Domaing, P., Gosele, C., Schulz, H., Hubner, N., and Cardoso, M.C. (2015). Gene repositioning within the cell nucleus is not random and is determined by its genomic neighborhood. *Epigenetics Chromatin:* 8: 36.

Jovcevski B, Kelly MA, Rote AP, Berg T, Gastall HY, Benesch JL, Aquilina JA, Ecroyd H, 2015. Phosphomimics destabilize Hsp27 oligomeric assemblies and enhance chaperone activity. *Chem Biol* 22:186–95

Juo LY, Liao WC, Shih YL, Yang BY, Liu AB, Yan YT, 2016. HSPB7 interacts with dimerized FLNC and its absence results in progressive myopathy in skeletal muscles. *J Cell Sci*, 129(8):1661-70

Kampinga HH, Hageman J, Vos MJ, Kubota H, Tanguay RM, Bruford EA, Cheetham ME, Chen B, Hightower LE, 2009. Guidelines for the nomenclature of the human heat shock proteins. *Cell Stress Chaperones*, 14(1):105-11

Kamradt MC, Chen F, Cryns VL, 2001. The small heat shock protein alpha B-crystallin negatively regulates cytochrome c- and caspase-8-dependent activation of caspase-3 by inhibiting its autoproteolytic maturation. *J Biol Chem*, 276(19):16059-63

Kamradt MC, Chen F, Sam S, Cryns VL, 2002. The small heat shock protein alpha B-crystallin negatively regulates apoptosis during myogenic differentiation by inhibiting caspase-3 activation. *J Biol Chem* 277:38731–38736

Kanagasabai R, Karthikeyan K, Vedam K, Qien W, Zhu Q and Ilangovan G, 2010. Hsp27 protects adenocarcinoma cells from UV-induced apoptosis by Akt and p21-dependent pathways of survival. *Molecular Cancer Research*, 8: 1399–1412.

Kappé G, Franck E, Verschuure P, Boelens WC, Leunissen JA, de Jong WW, 2003. The human genome encodes 10 alpha-crystallin-related small heat shock proteins: HspB1-10. *Cell Stress Chaperones*, 8(1): 53–61

Kappé G, Verschuure P, Philipsen RL, Staalduinen AA, Van de Boogaart P, Boelens WC, De Jong WW, 2001. Characterization of two novel human small heat shock proteins: protein kinase-related HspB8 and testis-specific HspB9. *Biochim Biophys Acta*, 1520(1):1-6

Kim D, Chi S, Lee KH, Rhee S, Kwon YK, Chung CH, Kwon H, and Kang MS, 1999. Neuregulin stimulates myogenic differentiation in an autocrine manner. *Journal of Biological Chemistry*, 274: 15395-15400

Kim MV, Kasakov AS, Seit-Nebi AS, Marston SB, Gusev NB, 2006. Structure and properties of K141E mutant of small heat shock protein HSP22 (HspB8, H11) that is expressed in human neuromuscular disorders. *Arch Biochem Biophys*, 454(1):32-41

Kim W.S., Kågedal K., Halliday G.M., 2014. α-Synuclein biology in Lewy body diseases. *Alzheimer's Research & Therapy*, 6(5):73.

Kirbach BB, & Golenhofen N, 2010. Differential expression and induction of small heat shock proteins in rat brain and cultured hippocampal neurons. *Journal of Neuroscience Research*, 89(2), 162–175

Kjaer M, 2004. Role of extracellular matrix in adaptation of tendon and skeletal muscle to mechanical loading. *Physiol Rev*, 84(2):649-98

Klaips CL, Jayaraj GG, Hartl F U, 2017 Pathways of cellular proteostasis in aging and disease. *J. Cell Biol*., 217: 51–63

Klinge L, Laval S, Keers S, Haldane F, Straub V, Barresi R, Bushby K, 2007. From T-tubule to sarcolemma: damage-induced dysferlin translocation in early myogenesis. *FASEB J*, 21(8):1768-76

Kolb SJ, Snyder PJ, Poi EJ, Renard EA, Bartlett A, Gu S, Sutton S, Arnold WD, Freimer ML, Lawson VH, Kissel JT, Prior TW, 2010. Mutant small heat shock protein B3 causes motor neuropathy: utility of a candidate gene approach. *Neurology*, 74:502–506

Kondaurova EM, Naumenko VS, Sinyakova NA, Kulikov AV. Map3k1, Il6st, Gzmk, and Hspb3 gene coexpression network in the mechanism of freezing reaction in mice, 2011. *J Neurosci Res*, 89(2):267-73

Kötter S, Unger A, Hamdani N, Lang P, Vorgerd M, Nagel-Steger L, Linke WA. Human myocytes are protected from titin aggregation-induced stiffening by small heat shock proteins, 2014. *J Cell Biol*, 204(2):187-202

Kouroku Y, Fujita E, Jimbo A, Kikuchi T, Yamagata T, Momoi MY, Kominami E, Kuida K, Sakamaki K, Yonehara S*, et al.*, 2002. Polyglutamine aggregates stimulate ER stress signals and caspase-12 activation. *Human molecular genetics,* 11:1505-1515.

Kriehuber T, Rattei T, Weinmaier T, Bepperling A, Haslbeck M, Buchner J, 2010. Independent evolution of the core domain and its flanking sequences in small heat shock proteins. *FASEB J*, 24(10):3633-42

Krüger R, Kuhn W, Müller T, Woitalla D, Graeber M, Kösel S, Przuntek H, Epplen JT, Schöls L, Riess O, 1998. Ala30Pro mutation in the gene encoding alpha-synuclein in Parkinson's disease. *Nat Genet*, 18(2):106-8

Kulig M, Ecroyd H, 2012. The small heat-shock protein αB-crystallin uses different mechanisms of chaperone action to prevent the amorphous versus fibrillar aggregation of α-lactalbumin. *Biochem J*, 448(3):343-52

Kundra R, Ciryam P, Morimoto RI, Dobson CM, Vendruscolo M, 2017. Protein homeostasis of a metastable subproteome associated with Alzheimer's disease. *Proc Natl Acad Sci U S A*, 114(28):E5703-E5711

La Padula V, Staszewski O, Nestel S, Busch H, Boerries M, Roussa E, Prinz M, and Krieglstein K, 2016. HSPB3 protein is expressed in motoneurons and induces their survival after lesion-induced degeneration. *Exp Neurol,* 286:40-49.

Lam WY, Wing Tsui SK, Law PT, Luk SC, Fung KP, Lee CY, Waye MM, 1996. Isolation and characterization of a human heart cDNA encoding a new member of the small heat shock protein family--HSPL27. *Biochim Biophys Acta*, 1314(1-2):120-4

Larraín J, Alvarez J, Hassell JR, Brandan E, 1997. Expression of perlecan, a proteoglycan that binds myogenic inhibitory basic fibroblast growth factor, is down regulated during skeletal muscle differentiation. *Exp Cell Res*, 234(2):405-12

Lassuthova P, Rebelo AP, Ravenscroft G, Lamont PJ, Davis MR, Manganelli F, Feely SM, Bacon C, Brožková DŠ, Haberlova J, Mazanec R, Tao F, Saghira C, Abreu L, Courel S, Powell E, Buglo E, Bis DM, Baxter MF, Ong RW, Marns L, Lee YC, Bai Y, Isom DG, Barro-Soria R, Chung KW, Scherer SS, Larsson HP, Laing NG, Choi BO, Seeman P, Shy ME, Santoro L, Zuchner S, 2018. Mutations in ATP1A1 Cause Dominant Charcot-Marie-Tooth Type 2. *Am J Hum Genet*, 102(3):505-514

Lavoie JN, Gingras-Breton G, Tanguay RM, Landry J, 1993. Induction of Chinese hamster HSP27 gene expression in mouse cells confers resistance to heat shock. HSP27 stabilization of the microfilament organization. *J Biol Chem*, 268(5):3420-9

Lazarides E, 1980. Intermediate filaments as mechanical integrators of cellular space. *Nature*, 17;283(5744):249-256

Le Grand F, and Rudnicki MA, 2007. Skeletal muscle satellite cells and adult myogenesis. *Current opinion in cell biology,* 19:628-633.

Lee HM, Lee CK, Lee SH, Roh HY, Bae YM, Lee KY, Lim J, Park PJ, Park TK, Lee YL, Won KJ and Kim B, 2007. P38 mitogen-activated protein kinase contributes to angiotensin II-stimulated migration of rat aortic smooth muscle cells. *Journal of Pharmacological Sciences*, 105: 74–81.

Lein ES, Hawrylycz MJ, Ao N, Ayres M, Bensinger A, Bernard A, Boe AF, Boguski MS, Brockway KS, Byrnes EJ, Chen L, Chen L, Chen TM, Chin MC, Chong J, Crook BE, Czaplinska A, Dang CN, Datta S, Dee NR, Desaki AL, Desta T, Diep E, Dolbeare TA, Donelan MJ, Dong HW, Dougherty JG, Duncan BJ, Ebbert AJ, Eichele G, Estin LK, Faber C, Facer BA, Fields R, Fischer SR, Fliss TP, Frensley C, Gates SN, Glattfelder KJ, Halverson KR, Hart MR, Hohmann JG, Howell MP, Jeung DP, Johnson RA, Karr PT, et al., 2007. Genome-wide atlas of gene expression in the adult mouse brain. *Nature*, 445(7124):168-76

Lesage S, Anheim M, Letournel F, Bousset L, Honoré A, Rozas N, Pieri L, Madiona K, Dürr A, Melki R, Verny C, Brice A; French Parkinson's Disease Genetics Study Group, 2013. G51D α-synuclein mutation causes a novel parkinsonian-pyramidal syndrome. *Ann Neurol*, 73(4):459-71

Li B, Smith CC, Laing JM, Gober MD, Liu L, Aurelian L, 2007. Overload of the heat-shock protein H11/HspB8 triggers melanoma cell apoptosis through activation of transforming growth factor-beta-activated kinase 1. *Oncogene*, 26(24):3521-31

Li DW, Liu JP, Mao YW, Xiang H, Wang J, Ma WY, Dong Z, Pike HM, Brown RE, Reed JC, 2005. Calcium-activated RAF/MEK/ERK signaling pathway mediates p53-dependent apoptosis and is abrogated by alpha B-crystallin through inhibition of RAS activation. *Mol Biol Cell*, 16(9):4437-53

Li P, Nijhawan D, Budihardjo I, Srinivasula SM, Ahmad M, Alnemri ES, Wang X, 1997. Cytochrome c and dATP-dependent formation of Apaf-1/caspase-9 complex initiates an apoptotic protease cascade. *Cell*, 91(4):479-89

Li X, Colvin T, Rauch JN, Acosta-Alvear D, Kampmann M, Dunyak B, et al., 2015. Validation of the Hsp70-Bag3 protein-protein interaction as a potential therapeutic target in cancer. *Mol. Cancer Ther*., 14: 642–648

Li L, Xiong WC, Mei L, 2018. Neuromuscular Junction Formation, Aging, and Disorders. *Annu Rev Physiol*, 80:159-188

Litt M, Kramer P, LaMorticella DM, Murphey W, Lovrien EW, Weleber RG, 1998. Autosomal dominant congenital cataract associated with a missense mutation in the human alpha crystallin gene CRYAA. *Hum. Molec. Genet*., 7: 471-474

Liu L, Michowski W, Kolodziejczyk A, Sicinski P, 2019. The cell cycle in stem cell proliferation, pluripotency and differentiation. *Nat Cell Biol*, 21(9):1060-1067

Liu Z, Wang C, Li Y, Zhao C, Li T, Li D, Zhang S, Liu C, 2018. Mechanistic insights into the switch of αB-crystallin chaperone activity and self-multimerization. *Journal of Biological Chemistry*, 293:14880–14890

Lopez V, Cauvi DM, Arispe N, De Maio A, 2016. Bacterial Hsp70 (DnaK) and mammalian Hsp70 interact differently with lipid membranes. *Cell Stress Chaperones*, 21(4):609-16

Luo S, Mao C, Lee B, and Lee, A. S, 2006. GRP78/BiP is required for cell proliferation and protecting the inner cell mass from apoptosis during early mouse embryonic development. *Mol. Cell. Biol*, 26:5688–5697

M, Flagmeier P, Limbocker R, Cascella R, Aprile FA, Galvagnion C, Heller GT, Meisl G, Chen SW, Kumita JR, Challa PK, Kirkegaard JB, Cohen SIA, Mannini B, Barbut D, Nollen EAA, Cecchi C, Cremades N, Knowles TPJ, Chiti F, Zasloff M, Vendruscolo M, Dobson CM, 2018. Multistep Inhibition of α-Synuclein Aggregation and Toxicity in Vitro and in Vivo by Trodusquemine. *ACS Chem Biol*, 13(8):2308-2319.

Mainz A, Peschek J, Stavropoulou M, Back KC, Bardiaux B, Asami S, Prade E, Peters C, Weinkauf S, Buchner J, Reif B, 2015. The chaperone αB-crystallin uses different interfaces to capture an amorphous and an amyloid client. *Nature Structural & Molecular Biology*, ;22:898–905

Manjili MH, Henderson R, Wang XY, Chen X, Li Y, Repasky E, Kazim L, Subjeck JR, 2002. Development of a recombinant HSP110-HER-2/neu vaccine using the chaperoning properties of HSP110. *Cancer Res*, 62(6):1737-42

Maroteaux L, Campanelli JT, Scheller RH, 1988. Synuclein: a neuron-specific protein localized to the nucleus and presynaptic nerve terminal. *J Neurosci*, 8(8):2804-15

Matsushima-Nishiwaki R, Kumada T, Nagasawa T, Suzuki M, Yasuda E, Okuda S, Maeda A, Kaneoka Y, Toyoda H, Kozawa O, 2013. Direct association of heat shock protein 20 (HSPB6) with phosphoinositide 3-kinase (PI3K) in human hepatocellular carcinoma: regulation of the PI3K activity. *PLoS One*, 8(11):e78440

Meisl, G., Kirkegaard, J., Arosio, P. et al. Molecular mechanisms of protein aggregation from global fitting of kinetic models, 2016. *Nature Protocols,* 11:252–272

Mercer EJ, Lin YF, Cohen-Gould L, Evans T, 2018. Hspb7 is a cardioprotective chaperone facilitating sarcomeric proteostasis. *Dev Biol,* 435(1):41-55

Middleton RC and Shelden EA, 2013. Small heat shock protein HSPB1 regulates growth of embryonic zebrafish craniofacial muscles. *Exp. Cell Res*., 19: 860-874

Miner JH, Wold B, 1990. Herculin, a fourth member of the MyoD family of myogenic regulatory genes. *Proc Natl Acad Sci USA*, 87: 1089–1093.

Miron T, Vancompernolle K, Vandekerckhove J, Wilchek M, Geiger B, 1991. A 25-kD inhibitor of actin polymerization is a low molecular mass heat shock protein. *J Cell Biol*, 114(2):255-61

Miron T, Wilchek M, Geiger B, 1988. Characterization of an inhibitor of actin polymerization in vinculin-rich fraction of turkey gizzard smooth muscle. *Eur J Biochem*, 178(2):543-53

Modem S, Chinnakannu K, Bai U, Prem-Veer Reddy G and Reddy TR, 2011. Hsp22 (HspB8/H11) knockdown induces Sam68 expression and stimulates proliferation of glioblastoma cells. *Journal of Cellular Physiology*, 226: 2747–2751

Mogk A and Bukau B, 2017. Role of sHsps in organizing cytosolic protein aggregation and disaggregation. *Cell Stress and Chaperones*, 22: 493–502

Morelli, F.F., Verbeek, D.S., Bertacchini, J., Vinet, J., Mediani, L., Marmiroli, S., Cenacchi, G., Nasi, M., De Biasi, S., Brunsting, J.F., et al., 2017. Aberrant Compartment Formation by HSPB2 Mislocalizes Lamin A and Compromises Nuclear Integrity and Function. *Cell reports* 20, 2100-2115.

Morelli, F.F., Verbeek, D.S., Bertacchini, J., Vinet, J., Mediani, L., Marmiroli, S., Cenacchi, G., Nasi, M., De Biasi, S., Brunsting, J.F*., et al,* 2017. Aberrant Compartment Formation by HSPB2 Mislocalizes Lamin A and Compromises Nuclear Integrity and Function. *Cell reports*, 20:2100-2115.

Morimoto RI, 1993. Cells in stress: transcriptional activation of heat shock genes. *Science*, 259 (5100): 1409-1410

Morrow G and Tanguay RM, 2015. Drosophila melanogaster Hsp22: a mitochondrial small heat shock protein influencing the aging process. *Front Genet*, 6: 1026.

Mounier N, Arrigo AP, 2002. Actin cytoskeleton and small heat shock proteins: how do they interact? *Cell Stress Chaperone*s, 7(2):167-76

Muchowski PJ, Schaffar G, Sittler A, Wanker EE, Hayer-Hartl MK, Hartl FU, 2000. Hsp70 and hsp40 chaperones can inhibit self-assembly of polyglutamine proteins into amyloid-like fibrils. *Proc Natl Acad Sci U S A*, 97(14):7841-6

Muchowski PJ, Wacker JL, 2005. Modulation of neurodegeneration by molecular chaperones. *Nat Rev Neurosci,* 6(1):11-22

Mymrikov EV, Seit-Nebi AS, Gusev NB, 2011. Large potentials of small heat shock proteins. *Physiol Rev*, 91(4):1123-59

Naba A, Clauser KR, Ding H, Whittaker CA, Carr SA, and Hynes RO, 2016. The extracellular matrix: Tools and insights for the "omics" era. *Matrix Biol*, 49:10-24

Nakajo S., Omata K., Aiuchi T., Shibayama T., Okahashi I, Ochiai H, Nakai Y., Nakaya K., Nakamura Y., 1990. Purification and Characterization of a Novel Brain-Specific 14-kDa Protein. *Journal of Neurochemistry*, 55 (6): 2031-2038

Nakhro K, Park JM, Hong YB, Park JH, Nam SH, Yoon BR, Yoo JH, Koo H, Jung SC, Kim HL, Kim JY, Choi KG, Choi BO, Chung KW, 2013. SET binding factor 1 (SBF1) mutation causes Charcot-Marie-Tooth disease type 4B3. *Neurology*, 81(2):165-73

Nam DE, Nam SH, Lee AJ, Hong YB, Choi B and Chung KW, 2018. Small heat shock protein B3 (HSPB3) mutation in an axonal Charcot-Marie-Tooth disease family. *Journal of the Peripheral Nervous System*, 23(1): 60–66.

Nicholl ID, Quinlan RA, 1994. Chaperone activity of alpha-crystallins modulates intermediate filament assembly. *EMBO J*, 13(4):945-53

Nicolau S, Liewluck T, Elliott JL, Engel AG, Milone M, 2020. A novel heterozygous mutation in the C-terminal region of HSPB8 leads to limb-girdle rimmed vacuolar myopathy. *Neuromuscul Disord*, 30(3):236-240.

Nikolakaki E, Mylonis I, Giannakouros T, 2017. Lamin B Receptor: Interplay between Structure, Function and Localization. *Cells*, 6(3):28

Niu J, Sun Y, Chen B, Zheng B, Jarugumilli GK, Walker SR, Hata AN, Mino-Kenudson M, Frank DA, Wu X, 2019. Fatty acids and cancer-amplified ZDHHC19 promote STAT3 activation through S-palmitoylation. *Nature*, 573(7772):139-143

Oh, S.W., Pope, R.K., Smith, K.P., Crowley, J.L., Nebl, T., Lawrence, J.B., and Luna, E.J. (2003). Archvillin, a muscle-specific isoform of supervillin, is an early expressed component of the costameric membrane skeleton. *Journal of cell science,* 116:2261-2275

Outeiro TF, Klucken J, Strathearn KE, Liu F, Nguyen P, Rochet JC, Hyman BT, McLean PJ, 2006. Small heat shock proteins protect against alpha-synuclein-induced toxicity and aggregation. *Biochem Biophys Res Commun*, 351(3):631-8

Pantoja C, Serrano M, 1999. Murine fibroblasts lacking p21 undergo senescence and are resistant to transformation by oncogenic Ras. *Oncogene*, 18(35):4974-82

Papanikolopoulou K, Skoulakis EMC, 2020. Altered Proteostasis in Neurodegenerative Tauopathies. *Adv Exp Med Biol*, 1233:177-194

Papuć E, Krupski W, Kurys-Denis E, Rejdak K, 2016. Antibodies against small heat-shock proteins in Alzheimer's disease as a part of natural human immune repertoire or activation of humoral response? *J Neural Transm*, 123(4):455-61

Papuć E, Kurys-Denis E, Krupski W, Tatara M, Rejdak K, 2015. Can Antibodies Against Glial Derived Antigens be Early Biomarkers of Hippocampal Demyelination and Memory Loss in Alzheimer's Disease? *J Alzheimers Dis*, 48(1):115-21

Parcellier A, Brunet M, Schmitt E, Col E, Didelot C, Hammann A, Nakayama K, Nakayama KI, Khochbin S, Solary E, Garrido C, 2006. HSP27 favors ubiquitination and proteasomal degradation of p27Kip1 and helps S-phase re-entry in stressed cells. *FASEB J*, 20(8):1179-81

Park AM, Kanai K, Itoh T, Sato T, Tsukui T, Inagaki Y, Selman M, Matsushima K, Yoshie O, 2016. Heat Shock Protein 27 Plays a Pivotal Role in Myofibroblast Differentiation and in the Development of Bleomycin-Induced Pulmonary Fibrosis. *PLoS One*, 11(2):e0148998

Parker SB, Eichele G, Zhang P, Rawls J, Sands AT, Bradley A, Olson EN, Harper JW, Elledge SJ, 1995. p53-independent expression of p21Cip1 in muscle and other terminally differentiating cells. *Science*, 267: 1024–1027

Patzkó A, Shy ME, 2011. Update on Charcot-Marie-Tooth disease. *Curr Neurol Neurosci Rep*, 11(1):78-88

Perng MD, Cairns L, van den IJssel P, Prescott A, Hutcheson AM, Quinlan RA, 1999. Intermediate filament interactions can be altered by HSP27 and alphaB-crystallin. *J Cell Sci*, 112 ( Pt 13):2099-112

Peschek J, Braun N, Rohrberg J, Back KC, Kriehuber T, Kastenmuller A, Weinkauf S, Buchner J, 2013. Regulated structural transitions unleash the chaperone activity of alphaB-crystallin. *Proc Natl Acad Sci U S A*, 110:E3780–E3789

Peschiaroli A, Figliola R, Coltella L, Strom A, Valentini A, D'Agnano I, Maione R, 2002. MyoD induces apoptosis in the absence of RB function through a p21(WAF1)-dependent re-localization of cyclin/cdk complexes to the nucleus. *Oncogene*, 21(53):8114-27.

Polymeropoulos MH, Lavedan C, Leroy E, Ide SE, Dehejia A, Dutra A, Pike B, Root H, Rubenstein J, Boyer R, Stenroos ES, Chandrasekharappa S, Athanassiadou A, Papapetropoulos T, Johnson WG, Lazzarini AM, Duvoisin RC, Di Iorio G, Golbe LI, Nussbaum RL, 1997. Mutation in the alpha-synuclein gene identified in families with Parkinson's disease. *Science,* 276(5321):2045-7

Poser, I., Sarov, M., Hutchins, J.R., Heriche, J.K., Toyoda, Y., Pozniakovsky, A., Weigl, D., Nitzsche, A., Hegemann, B., Bird, A.W., et al., 2008. BAC TransgeneOmics: a high-throughput method for exploration of protein function in mammals. *Nature methods,* 5:409-415

Pujols J, Peña-Díaz S, Pallarès I, Ventura S, 2020. Chemical Chaperones as Novel Drugs for Parkinson's Disease. *Trends Mol Med*, 26(4):408-421

Qian J, Ren X, Wang X, Zhang P, Jones WK, Molkentin JD, Fan GC, Kranias EG, 2009. Blockade of Hsp20 phosphorylation exacerbates cardiac ischemia/reperfusion injury by suppressed autophagy and increased cell death. *Circ Res*, 105(12):1223-31

Quinlan R, Van Den Ijssel P, 1999. Fatal attraction: when chaperone turns harlot. *Nat Med*, 5(1):25-6

Rajagopal P, Liu Y, Shi L, Clouser AF, Klevit RE, 2015. Structure of the α-crystallin domain from the redox-sensitive chaperone, HSPB1. *J Biomol NMR,* 63(2):223-8

Rajasekaran NS, Connell P, Christians ES, Yan LJ, Taylor RP, Orosz A, Zhang XQ, Stevenson TJ, Peshock RM, Leopold JA, Barry WH, Loscalzo J, Odelberg SJ, Benjamin IJ, 2007. Human alpha B-crystallin mutation causes oxido-reductive stress and protein aggregation cardiomyopathy in mice. *Cell*, 130(3):427-39

Ramírez-Rodríguez G, Babu H, Klempin F, Krylyshkina O, Baekelandt V, Gijsbers R, Debyser Z, Overall RW, Nicola Z, Fabel K, Kempermann G, 2013. The α crystallin domain of small heat shock protein b8 (Hspb8) acts as survival and differentiation factor in adult hippocampal neurogenesis. *J Neurosci*, 33(13):5785-96

Rapino F, Jung M, Fulda S, 2014. BAG3 induction is required to mitigate proteotoxicity via selective autophagy following inhibition of constitutive protein degradation pathways. *Oncogene*, 33(13):1713-24

Rayner K, Chen YX, McNulty M, Simard T, Zhao X, Wells DJ, de Belleroche J, O'Brien ER, 2008. Extracellular release of the atheroprotective heat shock protein 27 is mediated by estrogen and competitively inhibits acLDL binding to scavenger receptor-A. *Circ Res*, 103(2):133-41

Rayner K, Sun J, Chen YX, McNulty M, Simard T, Zhao X, Wells DJ, de Belleroche J, O'Brien ER, 2009. Heat shock protein 27 protects against atherogenesis via an estrogen-dependent mechanism: role of selective estrogen receptor beta modulation. *Arterioscler Thromb Vasc Biol*, 29(11):1751-6

Reddy VS, Madala SK, Trinath J, Reddy GB, 2018. Extracellular small heat shock proteins: exosomal biogenesis and function. *Cell Stress Chaperones*, 23(3):441-454

Reilly MM, 2007. Sorting out the inherited neuropathies. *Practical Neurology*, 7: 93–105.

Rekas A, Adda CG, Andrew Aquilina J, Barnham KJ, Sunde M, Galatis D, Williamson NA, Masters CL, Anders RF, Robinson CV, Cappai R, Carver JA, 2004. Interaction of the molecular chaperone alphaB-crystallin with alpha-synuclein: effects on amyloid fibril formation and chaperone activity. *J Mol Biol*, 340(5):1167-83

Rhodes SJ, Konieczny SF, 1989. Identification of MRF4: a new member of the muscle regulatory factor gene family. *Genes & Development*, 3: 2050–2061.

Richter L, Flodman P, Barria von-Bischhoffshausen F, Burch D, Brown S, Nguyen L, Turner J, Spence MA, Bateman JB, 2008. Clinical variability of autosomal dominant cataract, microcornea and corneal opacity and novel mutation in the alpha A crystallin gene (CRYAA). *Am. J. Med. Genet*., 146A: 833-842

Ritossa F, 1962. A new puffing pattern induced by temperature shock and DNP in Drosophila. *Experientia*, 18:571–573

Roelofs MF, Boelens WC, Joosten LA, Abdollahi-Roodsaz S, Geurts J, Wunderink LU, Schreurs BW, van den Berg WB, Radstake TR, 2006. Identification of small heat shock protein B8 (HSP22) as a novel TLR4 ligand and potential involvement in the pathogenesis of rheumatoid arthritis. *J Immunol*, 176(11):7021-7

Rogalla T, Ehrnsperger M, Preville X, Kotlyarov A, Lutsch G, Ducasse C, Paul C, Wieske M, Arrigo AP, Buchner J, Gaestel M, 1999. Regulation of Hsp27 oligomerization, chaperone function, and protective activity against oxidative stress/tumor necrosis factor alpha by phosphorylation. *J Biol Chem*, 274(27):18947-56

Romano MF, Festa M, Pagliuca G, Lerose R, Bisogni R, Chiurazzi F, Storti G, Volpe S, Venuta S, Turco MC, Leone A, 2003. BAG3 protein controls B-chronic lymphocytic leukaemia cell apoptosis. *Cell Death Differ*, 10(3):383-5

Rossor AM, Kalmar B, Greensmith L, Reilly MM, 2011. The distal hereditary motor neuropathies. *J Neurol Neurosurg Psychiatry*, 83(1):6-14

Rusmini P, Cristofani R, Galbiati M, Cicardi ME, Meroni M, Ferrari V, Vezzoli G, Tedesco B, Messi E, Piccolella M, Carra S, Crippa V, Poletti A, 2017. The Role of the Heat Shock Protein B8 (HSPB8) in Motoneuron Diseases. *Front Mol Neurosci*, 10:176

Sala AJ, Bott LC, Morimoto RI, 2017. Shaping proteostasis at the cellular, tissue, and organismal level. *J Cell Biol*, 216(5):1231-1241

Sala D, Cunningham TJ, Stec MJ, Etxaniz U, Nicoletti C, Dall'Agnese A, Puri PL, Duester G, Latella L, Sacco A, 2019. The Stat3-Fam3a axis promotes muscle stem cell myogenic lineage progression by inducing mitochondrial respiration. *Nat Commun*, 10(1):1796

Salari S, Seibert T, Chen YX, Hu T, Shi C, Zhao X, Cuerrier CM, Raizman JE, O'Brien ER, 2013. Extracellular HSP27 acts as a signaling molecule to activate NF-κB in macrophages. *Cell Stress Chaperones*, 18(1):53-63

Schmitt E, Gehrmann M, Brunet M, Multhoff G, Garrido C, 2007. Intracellular and extracellular functions of heat shock proteins: repercussions in cancer therapy. *J Leukoc Biol*, 81(1):15-27

Schottmann G, Wagner C, Seifert F, Stenzel W, Schuelke M, 2016. MORC2 mutation causes severe spinal muscular atrophy-phenotype, cerebellar atrophy, and diaphragmatic paralysis. *Brain*, 139(Pt 12):e70

Schwartz H, Scroggins B, Zuehlke A, Kijima T, Beebe K, Mishra A, Neckers L, Prince T, 2015. Combined HSP90 and kinase inhibitor therapy: Insights from The Cancer Genome Atlas. *Cell Stress Chaperones*,729-41

Seidel K, Vinet J, Dunnen WF, Brunt ER, Meister M, Boncoraglio A, Zijlstra MP, Boddeke HW, Rüb U, Kampinga HH, Carra S, 2012. The HSPB8-BAG3 chaperone complex is upregulated in astrocytes in the human brain affected by protein aggregation diseases. *Neuropathol Appl Neurobiol*, 38(1):39-53

Selcen D, 2011. Myofibrillar myopathies. *Neuromuscul Disord*, 21(3):161-71

Senderek J, Bergmann C, Ramaekers VT, Nelis E, Bernert G, Makowski A, Züchner S, De Jonghe P, Rudnik-Schöneborn S, Zerres K, Schröder JM, 2003. Mutations in the ganglioside-induced differentiation-associated protein-1 (GDAP1) gene in intermediate type autosomal recessive Charcot-Marie-Tooth neuropathy. *Brain*, 126(Pt 3):642-9

Shatov VM, Weeks SD, Strelkov SV, and Gusev NB, 2018. The Role of the Arginine in the Conserved N-Terminal Domain RLFDQxFG Motif of Human Small Heat Shock Proteins HspB1, HspB4, HspB5, HspB6, and HspB8. *International Journal of Molecular Sciences*, 19(7): 2112.

Shen J, Li M, Min L, 2018. HSPB8 promotes cancer cell growth by activating the ERK-CREB pathway and is indicative of a poor prognosis in gastric cancer patients. *Oncol Rep*, 39(6):2978-2986

Shi CH, Song B, Luo HY, Mao CY, Shang DD, Cao Y, Sun SL, Wu J, Zhuang ZP, and Xu YM, 2015. Recessive hereditary motor and sensory neuropathy caused by IGHMBP2 gene mutation. *Neurology,* 85: 383-384

Shibayama-Imazu T., Okahashi I., Omata K., Nakajo S., Ochiai H., Nakai Y., Hama T., Nakamura Y., Nakaya K., 1993. Cell and tissue distribution and developmental change of neuron specific 14 kDa protein (phosphoneuroprotein 14). *Brain Research,* 622(1–2): 17-25

Shroff NP, Cherian-Shaw M, Bera S, and Abraham EC, 2000. Mutation of R116C Results in Highly Oligomerized αA-Crystallin with Modified Structure and Defective Chaperone-like Function. *Biochemistry*, 39(6): 1420–1426

Singh BN, Rao KS, Ramakrishna T, Rangaraj N, Rao CM, 2007. Association of alphaB-crystallin, a small heat shock protein, with actin: role in modulating actin filament dynamics in vivo. *J Mol Biol,* 366(3):756–767

Sinning A, Hübner CA, 2013. Minireview: pH and synaptic transmission. *FEBS Lett*, 587(13):1923-8

Sittler A, Lurz R, Lueder G, Priller J, Lehrach H, Hayer-Hartl MK, Hartl FU, Wanker EE, 2001. Geldanamycin activates a heat shock response and inhibits huntingtin aggregation in a cell culture model of Huntington's disease. *Hum Mol Genet*, 10(12):1307-15

Slingsby C, Clark AR, 2016. Structure and Action of Molecular Chaperones: Machines That Assist Protein Folding in the Cell. vol. 6. World Scientific, The small heat shock proteins family: assembly and binding functions: 161–203.

Sluchanko NN, Beelen S, Kulikova AA, Weeks SD, Antson AA, Gusev NB, Strelkov SV, 2017. Structural basis for the interaction of a human small heat shock protein with the 14-3-3 universal signaling regulator. *Structure,* 25:305–316

Smith CC, Lee KS, Li B, Laing JM, Hersl J, Shvartsbeyn M, Aurelian L, 2012. Restored expression of the atypical heat shock protein H11/HspB8 inhibits the growth of genetically diverse melanoma tumors through activation of novel TAK1-dependent death pathways. *Cell Death Dis*, 3(8):e371.

Solovei, I., Wang, A.S., Thanisch, K., Schmidt, C.S., Krebs, S., Zwerger, M., Cohen, T.V., Devys, D., Foisner, R., Peichl, L., 2013. LBR and lamin A/C sequentially tether peripheral heterochromatin and inversely regulate differentiation. *Cell,* 152: 584-598.

Sreedhar AS, Kalmár E, Csermely P, Shen YF, 2004. Hsp90 isoforms: functions, expression and clinical importance. *FEBS Lett*, 562(1-3):11-5

Sreekumar PG, Kannan R, Kitamura M, Spee C, Barron E, Ryan SJ, and Hinton DR, 2010. αB Crystallin Is Apically Secreted within Exosomes by Polarized Human Retinal Pigment Epithelium and Provides Neuroprotection to Adjacent Cells. *PLoS One*, 5(10): e12578.

Srivastava PK, Udono H, 1994. Heat shock protein-peptide complexes in cancer immunotherapy. *Curr Opin Immunol*, 6(5):728-32

Spillantini MG, Crowther RA, Jakes R, Hasegawa M, Goedert M, 1998. alpha-Synuclein in filamentous inclusions of Lewy bodies from Parkinson's disease and dementia with lewy bodies. *Proc Natl Acad Sci U S A*, 95(11):6469-73

Steinert PM, Steven AC, Roop DR, 1985. The molecular biology of intermediate filaments. *Cell*, 42(2):411-20

Stenoien DL, Cummings CJ, Adams HP, Mancini MG, Patel K, DeMartino GN, Marcelli M, Weigel NL, Mancini MA, 1999. Polyglutamine-expanded androgen receptors form aggregates that sequester heat shock proteins, proteasome components and SRC-1, and are suppressed by the HDJ-2 chaperone. *Hum Mol Genet*, 8(5):731-41

Stroud MJ, Banerjee I, Veevers J, and Chen J, 2014. Linker of Nucleoskeleton and Cytoskeleton Complex Proteins in Cardiac Structure, Function, and Disease. *Circulation Research*,114:538–548

Sudnitsyna MV, Mymrikov EV, Seit-Nebi AS, and Gusev NB, 2012. The role of intrinsically disordered regions in the structure and functioning of small heat shock proteins. *Current protein & peptide science,* 13: 76-85.

Sugiyama Y, Suzuki A, Kishikawa M, Akutsu R, Hirose T, Waye MMY, Tsui SKW, Yoshidai S, and Ohno S, 2000. Muscle Develops a Specific Form of Small Heat Shock Protein Complex Composed of MKBP/HSPB2 and HSPB3 during Myogenic Differentiation. *The Journal of Biological Chemistry*, 275(2): 1095–1104

Sui X, Li D, Qiu H, Gaussin V and Depre C, 2009. Activation of the bone morphogenetic protein receptor by H11 kinase/Hsp22 promotes cardiac cell growth and survival. *Circulation Research,* 104: 887–895.

Sun X, Fontaine JM, Rest JS, Shelden EA, Welsh MJ, Benndorf R, 2003. Interaction of Human HSP22 (HSPB8) with Other Small Heat Shock Proteins. *The Journal of Biological Chemistry*, 279: 2394-2402.

Sun Y, MacRae TH. Small heat shock proteins: molecular structure and chaperone function, 2005. *Cell Mol Life Sci*, 62(21):2460-76

Takayama S, Reed JC, Homma S, 2003. Heat-shock proteins as regulators of apoptosis. *Oncogene*, 22(56):9041-7

Tanguay RM, Hightower LE, 2015. The big book on small heat shock proteins vol 8. Heat shock proteins 8, Series Editors: Alexzander A.A. Asea, Stuart K. Calderwood edn. Springer

Tavaria M, Gabriele T, Kola I, Anderson RL, 1996. A hitchhiker's guide to the human Hsp70 family. Cell Stress *Chaperones*, 1(1):23-28

Thomas K, Engler AJ, Meyer GA, 2015. Extracellular matrix regulation in the muscle satellite cell niche. *Connect Tissue Res*, 56:1–8

Tjondro HC, Xi YB, Chen XJ, Su JT, Yan YB, 2016. Membrane insertion of αA-crystallin is oligomer-size dependent. *Biochem Biophys Res Commun*, 473(1):1-7

Tjondrokoesoemo A, Schips TG, Sargent MA, Vanhoutte D, Kanisicak O, Prasad V, Lin SC, Maillet M, Molkentin JD, 2016. Cathepsin S Contributes to the Pathogenesis of Muscular Dystrophy in Mice. *Journal of Biological Chemistry*, 291(19), 9920-8

Toivola DM, Strnad P, Habtezion A, Omary MB, 2010. Intermediate filaments take the heat as stress proteins. *Trends Cell Biol*, 20(2):79-91

Tue NT, Shimaji K, Tanaka N, Yamaguchi M, 2012. Effect of αB-crystallin on protein aggregation in Drosophila. *J Biomed Biotechnol*, 2012:252049

Tunggal P, Smyth N, Paulsson M, Ott MC, 2000. Laminins: structure and genetic regulation. *Microsc Res Tech*, 51(3):214-27

Ulbricht A, Gehlert S, Leciejewski B, Schiffer T, Bloch W, Höhfeld J, 2015. Induction and adaptation of chaperone-assisted selective autophagy CASA in response to resistance exercise in human skeletal muscle. *Autophagy*, 11(3):538-46

Ungelenk S, Moayed F, Ho CT, Grousl T, Scharf A, Mashaghi A, Tans S, Mayer MP, Mogk A, and Bukau B, 2016. Small heat shock proteins sequester misfolding proteins in nearnative conformation for cellular protection and efficient refolding. *Nat. Comm*, 7: 13673

Ungricht, R., and Kutay, U. (2017). Mechanisms and functions of nuclear envelope remodelling. *Nature reviews,* 18: 229-245.

Urciuolo A, Quarta M, Morbidoni V, Gattazzo F, Molon S, Grumati P, Montemurro F, Tedesco FS, Blaauw B, Cossu G, Vozzi G, Rando TA, Bonaldo P, 2013. Collagen VI regulates satellite cell self-renewal and muscle regeneration. *Nat Commun*, 4:1964

Van Montfort R, Slingsby C, Vierling E, 2001. Structure and function of the small heat shock protein/alpha-crystallin family of molecular chaperones. *Adv Protein Chem*, 59:105-56.

Vendredy L, Adriaenssens E, Timmerman V, 2020. Small heat shock proteins in neurodegenerative diseases. *Cell Stress and Chaperones,* 25: 679–699.

Vicart P, Caron A, Guicheney P, Li Z, Prévost MC, Faure A, Chateau D, Chapon F, Tomé F, Dupret JM, Paulin D, Fardeau M, 1998. A missense mutation in the alphaB-crystallin chaperone gene causes a desmin-related myopathy. *Nat Genet*, 20(1):92-5

Vleminckx V, Van Damme P, Goffin K, Delye H, Van Den Bosch L, Robberecht W, 2002. Upregulation of HSP27 in a transgenic model of ALS. *J Neuropathol Exp Neurol*, 61(11):968-74

Vos, M.J., Kanon, B., and Kampinga, H.H., 2009. HSPB7 is a SC35 speckle resident small heat shock protein. *Biochimica et biophysica acta,* 1793: 1343-1353.

Vos, M.J., Zijlstra, M.P., Kanon, B., van Waarde-Verhagen, M.A., Brunt, E.R., Oosterveld-Hut, H.M., Carra, S., Sibon, O.C., and Kampinga, H.H., 2010. HSPB7 is the most potent polyQ aggregation suppressor within the HSPB family of molecular chaperones. *Human molecular genetics*, 19:4677-4693.

Wallace GQ, and McNally EM, 2009. Mechanisms of muscle degeneration, regeneration, and repair in the muscular dystrophies. *Annu Rev Physiol* ,71: 37-57.

Walsh D, Li Z, Wu Y, and Nagata K, 1997. Heat shock and the role of the HSPs during neural plate induction in early mammalian CNS and brain development. *Cell. Mol. Life Sci*., 53: 198–211

Wang K, Spector A, 1996. alpha-crystallin stabilizes actin filaments and prevents cytochalasin-induced depolymerization in a phosphorylation-dependent manner. *Eur J Biochem*, 242(1):56-66

Wang L, Zhou L, Jiang P, Lu L, Chen X, Lan H, Guttridge DC, Sun H, Wang H, 2012. Loss of miR-29 in myoblasts contributes to dystrophic muscle pathogenesis. *Mol Ther*, 20(6):1222-33

Waudby CA, Knowles TP, Devlin GL, Skepper JN, Ecroyd H, Carver JA, Welland ME, Christodoulou J, Dobson CM, Meehan S, 2010. The interaction of alphaB-crystallin with mature alpha-synuclein amyloid fibrils inhibits their elongation. *Biophys J*, 98(5):843-51

Webster KA, 2003. Serine phosphorylation and suppression of apoptosis by the small heat shock protein alphaB-crystallin. *Circ Res*, 92(2):130-2

Wilhelmus MM, Boelens WC, Otte-Höller I, Kamps B, de Waal RM, Verbeek MM, 2006. Small heat shock proteins inhibit amyloid-beta protein aggregation and cerebrovascular amyloid-beta protein toxicity. *Brain Res*, 1089(1):67-78

Wong YC, Krainc D, 2017. α-synuclein toxicity in neurodegeneration: mechanism and therapeutic strategies. *Nat Med*, 23(2):1-13

Wyttenbach A, Sauvageot O, Carmichael J, Diaz-Latoud C, Arrigo AP, Rubinsztein DC, 2002. Heat shock protein 27 prevents cellular polyglutamine toxicity and suppresses the increase of reactive oxygen species caused by huntingtin. *Hum Mol Genet*, 11(9):1137-51

Yagami-Hiromasa T, Sato T, Kurisaki T, Kamijo K, Nabeshima Y, Fujisawa-Sehara A, 1995. A metalloprotease-disintegrin participating in myoblast fusion. *Nature*, 377(6550):652-6

Ye Q, Worman HJ, 1994. Primary structure analysis and lamin B and DNA binding of human LBR, an integral protein of the nuclear envelope inner membrane. *J Biol Chem*, 269(15):11306-11

Yin H, Price F, Rudnicki MA, 2013. Satellite cells and the muscle stem cell niche. *Physiol Rev*, 93(1):23-67

Zacksenhaus E, Jiang Z, Chung D, Marth JD, Phillips RA, Gallie BL, 1996. pRb controls proliferation, differentiation, and death of skeletal muscle cells and other lineages during embryogenesis. *Genes& Development*, 10(23):3051-64.

Zarranz JJ, Alegre J, Gómez-Esteban JC, Lezcano E, Ros R, Ampuero I, Vidal L, Hoenicka J, Rodriguez O, Atarés B, Llorens V, Gomez Tortosa E, del Ser T, Muñoz DG, de Yebenes JG, 2004. The new mutation, E46K, of alpha-synuclein causes Parkinson and Lewy body dementia. *Ann Neurol*, 55(2):164-73

Zeng Y, Feng H, Graner MW, Katsanis E, 2003. Tumor-derived, chaperone-rich cell lysate activates dendritic cells and elicits potent antitumor immunity. *Blood*, 101(11):4485-91

Zhang X, Wang X, Zhu H, Kranias EG, Tang Y, Peng T, Chang J, and Fan G, 2012. Hsp20 Functions as a Novel Cardiokine in Promoting Angiogenesis via Activation of VEGFR2. *PLoS One*, 7(3): e32765.

Zhou H, Li XM, Meinkoth J, Pittman RN, 2000. Akt regulates cell survival and apoptosis at a postmitochondrial level. *J Cell Biol*, 151(3):483-94

Zhu C.-H., Mouly V., Cooper R.N., Mamchaoui K., Bigot A., Shay J.W., Di Santo J.P., Butler-Browne G.S., Wright W.E, 2007. Cellular senescence in human myoblasts is overcome by human telomerase reverse transcriptase and cyclin-dependent kinase 4: consequences in aging muscle and therapeutic strategies for muscular dystrophies. *Aging Cell* 6:515-523

Zuehlke AD, Moses MA, Neckers L, 2018. Heat shock protein 90: its inhibition and function. *Philos Trans R Soc Lond B Biol Sci*, 373(1738):20160527